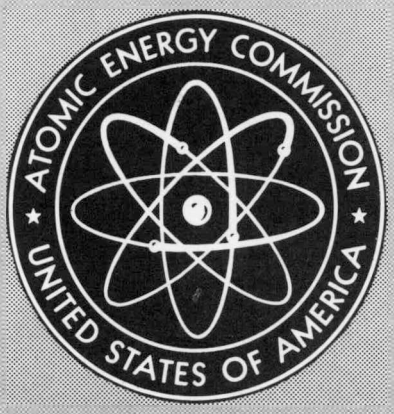

MND-M-1866

PM-1 REACTOR CORE FINAL DESIGN REPORT

By
R. O. Bagley
F. H. Cox
A. Carnasale
H. Vener

January 1962

Nuclear Division
Martin Company
Baltimore, Maryland

UNITED STATES ATOMIC ENERGY COMMISSION • DIVISION OF TECHNICAL INFORMATION

DISCLAIMER

MND-M-1866
REACTOR TECHNOLOGY

PM-1 Reactor Core
Final Design Report

January, 1962

Nuclear Division
Martin Company
Baltimore, Maryland

Report by: R. O. Bagley
F. H. Cox
A. Carnasale
H. Vener

Project Engineer:
Robert J. Akin

Blank Page

ABSTRACT

The PM-1 water cooled and moderated core contains 741 highly enriched stainless steel cermet tubular fuel elements and 90 lumped boron stainless steel burnable poison elements, and it is controlled by 6 Y-shaped europium titanate movable control rods. The core has a lifetime of 1.95 years when operated at its design power level of 9.37 mw of thermal energy. The control of the core is designed so that there is a positive shutdown margin at all times with either one rod stuck completely out of the core or with two rods stuck in the operating condition. The core power is removed by 2125 gpm of pressurized water at an average temperature of 463° F and pressure of 1300 psia. In reactors of this type, the core is stable with a negative temperature coefficient of approximately 2.5×10^{-4} $\Delta K/K/°F$.

Blank Page

FOREWORD

This report is submitted to the Atomic Energy Commission, Division of Reactor Development as an account of work performed under Contract AT(30-1)-2345. It contains the final design and analysis of the PM-1 reactor core.

In addition to the authors, the following have participated in this program:

P. A. Gilmore
R. A. Hoffmeister
L. I. Kopp
W. P. Kutz
D. Schweller

Blank Page

CONTENTS

CONTENTS (continued)

I. INTRODUCTION

This report presents and evaluates the final design of the reactor core for the PM-1 Nuclear Power Plant. The design criteria required a pressurized water cooled and moderated core with a two-year life at design power and a positive shutdown margin under all conditions with either one control rod stuck completely out or with two control rods stuck in the operating condition. A brief description of the core designed to satisfy these requirements is given here, together with a table of core characteristics. A detailed description of the core and its characteristics is contained in the body of the report. The results of supporting studies, tests and analytical techniques required to support the design effort are also included in an appendix.

The PM-1 reactor (refer to Drawing 372-210500) is designed to produce 9.37 mw of thermal energy. At this level, the entire PM-1 plant produces the required 1000 kw of net electric energy and 7 million Btu of heat energy.

The single-pass reactor operates at 1300 psia, with a mean coolant temperature of 463° F. Single inlet and outlet nozzles are located above the level of the core, providing an inherent safety feature in the event of a leak in the primary coolant system. The vessel internal structure consists of two major assemblies--the core shroud and the upper skirt assembly. The core shroud supports and aligns the core bundles. The upper skirt forms the vessel upper plenum and guides the control rods as they are withdrawn from the core.

Coolant flow entering the reactor is distributed around the vessel inside periphery by a plenum having an orificed plate on its underside. This plate distributes flow downward around the thermal shields to a plenum in the bottom of the vessel. Here the flow turns and flows upward through the core, which is located in the lower half of the vessel. Coolant leaving the core enters an upper vessel plenum from which it is again directed around the vessel perimeter and into the vessel outlet nozzle. Some of the flow from this upper plenum is directed toward the vessel head before leaving the vessel, in order to provide for head cooling.

The reactor core consists of seven individual fuel bundles containing a total of 741 fuel elements, 90 boron-stainless steel burnable poison elements and 18 dummy elements. All elements are in a triangular array of 0.665-inch pitch and have nominal diameters of approximately 1/2 inch. The fuel elements are tubular, containing an annular fuel section which is clad on its inner and outer surfaces. The fuel is a UO_2-stainless steel dispersion containing 28 wt % of 93% enriched UO_2.

Six identical truncated pie-shaped bundles make up the core periphery. These surround the small center bundle, which was designed to be replaced either with the core or to be removed and replaced through a port in the center of the reactor vessel head. This feature permits additional design flexibility for future experimentation.

The six control rods are of Y-blade configuration with blade widths of 3.5 inches and active absorber lengths of 32 inches. The absorber material is $Eu_2O_3 \cdot 2TiO_2$ dispersed in stainless steel which, in the finished control rod element, is equivalent to approximately 30 wt % Eu_2O_3.

All internal structural material is AISI Type 304 or 347 stainless steel modified to limit the cobalt and tantalum contents of the material.

The lifetime of the PM-1 core was determined both with and without control rods inserted. The more realistic calculation, which accounted for control rod withdrawal, indicated a lifetime of 17.33 mw-yr. To provide a check on the burnup calculation, the lifetime of the SM-1 core was calculated. The result was slightly conservative with respect to the reported value of the actual SM-1 lifetime. Therefore, the PM-1 core lifetime was corrected* to compensate for the conservatism. The resultant best estimate of the PM-1 core life is 18.2 mw-yr.

The PM-1 core has a large initial inventory of fuel which reflects itself in high initial reactivity. The high initial reactivity of the core is reduced through the use of discrete burnable poison in boron alloy stainless steel rods. The rods are 0.496 inch in diameter and contain 0.2794 wt % of natural boron. These rods initially control about 10% reactivity. The resultant initial clean reactivity of the PM-1 is 0.1327 at 68° F and 0.0908 at 463° F. The reactivity value at 68° F has been verified experimentally.

As in all designs, tolerances must be considered. The allowable 2% variation in fuel loading could result in an increase of reactivity of as much as 0.44%; thus exceeding the shutdown margin. In event of such a condition, adjustment is made by replacement of some center bundle fuel elements by dummy elements and/or poison rods. It has been determined analytically that this method is adequate. The final determination of shutdown margin is made with the fully assembled core and control rods in a "wet critical" test, which is a final proof test under experimentally controlled conditions.

---

*The correction factor is defined as

$$\frac{\text{Reported SM-1 life}}{\text{Calculated SM-1 life (unrodded)}} \times \frac{\text{PM-1 (unrodded)}}{\text{PM-1 (rodded)}} = \frac{15.0 \text{ mw-yr}}{14.5 \text{ mw-yr}} \times \frac{685 \text{ days}}{675 \text{ days}}$$

The reactivity of the PM-1 core is controlled through the use of six Y-shaped control rods located symmetrically in a ring. The control system has the capability of shutting down the reactor at any time with one control rod fully withdrawn or with two control rods at the operating six-rod bank level.

The six-rod bank reactivity worths calculated at both 68° F and 463° F, are 20.22% and 23.05%, respectively. The calculated six-rod bank worth versus insertion at 68° F was compared with experimental data. The agreement was excellent, lending credence to the calculated full insertion worth at 68° F.

The shutdown criteria for the PM-1 have been stated previously. Both conditions are met in the design core. The shutdown reactivity margin at 68° F for the condition of one rod fully withdrawn is 0.39%. With two rods stuck at the hot operating six-rod bank position (14.65 inches withdrawn), the shutdown reactivity margin at 68° F is 0.10%.

The reactivity of the PM-1 core decreases over life. As a result, the shutdown margins are a minimum for a clean core. This behavior allows a complete verification of shutdown margin in a "wet critical" test (see Appendix D).

The maximum peak-to-average power density in the PM-1 occurs at reactor startup. The value is 3.56, of which 1.95 and 1.83 are the axial and radial components, respectively. Shortly after startup, the peak-to-average power drops to about 3.42, due to control rod withdrawal necessitated by fission product buildup. The power peaking decreases nearly linearly over the life of the core to a value of 1.97 after 18.2 mw-yr of energy release.

The temperature coefficient was evaluated analytically at the beginning and end of core life at 68° F and 463° F, respectively. In each case, the control rods were at the critical bank position. The temperature coefficient is negative over the operating range of the reactor and decreases slightly with core life.

The 9.37 mw of heat developed in the PM-1 core is removed by increasing the temperature of pressurized coolant water from 447° to 479° F. The average flow rate inside each element is 1.20 gpm, and the average flow rate outside each element is 1.25 gpm. The average heat flux in the core is 71,200 Btu/hr ft^2. Local boiling (subcooled boiling) conditions exist in some high power regions of the core; however, adequate cooling is provided to preclude bulk boiling under all expected operating conditions.

The fundamental thermal criterion in the design of this core was that no bulk boiling of the primary loop shall occur. The "hot" channel, due to variations in channel flow rates and channel powers, will produce the maximum coolant outlet temperature. The BITE code and the results of the flow and power distribution tests were used to determine the hot channel. In determination of the maximum coolant temperature, consideration was also given to uncertainties due to manufacturing tolerances and imperfections in the analytical techniques by applying hot channel factors. An additional factor of 1.2 to the power generation was included, since accident studies indicate that the peak power increases almost 20% during certain plausible transients.

The following table lists the main characteristics and parameters of the core.

Design Data--PM-1 Reactor Core

1. Overall performance data:	
Reactor power, nominal (mw)	9.37
Reactor power, thermal design (mw)	10.4
Operating pressure, nominal (psia)	1300
Design pressure, structural (psig)	1485
Design pressure, thermal (psia)	1200
Core life, nominal (mw-yr)	18.2
2. Core design characteristics:	
Geometry--right circular cylinder (approx)	
Diameter (m)	
Core shroud, outside	23.6
Fuel element envelope	22.8
Equivalent	22.74
Length (m)	
Overall	33-1/4
Active	30
Structural material	Modified AISI Type 304 and 347

Moderator, coolant and reflector	Light water at 1300 psia and 463° F
U-235 inventory (kg)	29.14 ± 0.60
B-10 inventory (g)	32.16
U-235 burnup (kg)	9.0
3. Fuel element data:	
Type	Tubular, cermet
Number	741
Diameter (in.)	
Outside	0.506
Inside	0.417
Length (in.) overall	33-1/4
Total active	30
Clad thickness (in.)	
Average	0.0085
Minimum	0.0065
Meat thickness (in.)	0.0285
Clad material	AISI Type 347 stainless steel, modified, 0.01 wt % Co maximum and 0.03 wt % Co plus Ta maximum
Meat composition (wt %)	
UO_2	28
Type 304 stainless steel	72
Loading per tube (g)	
U-235	40.13 ± 0.80
4. Lumped poison rods:	
Type	Boron-stainless steel alloy rod, unclad
Diameter (in.)	0.470 - 0.500 varies to compensate for actual boron-loading obtained

Material--stainless steel	AISI Type 304, modified 0.01 wt % Co maximum and 0.03 wt % Co plus Ta maximum containing 0.27 wt % natural boron (nominal)
B-10 per rod (g)	0.383
Number	
Poison (30-in. length)	72
Poison (20-in. length)	18

5. Control rods:

Type	Y, cermet contained, europium titanate dispersed in stainless steel
Number	6
Length (absorbing) (in.)	32
Blade width (in.)	
Absorber	3.5
Total	3.875
Blade thickness (in.)	
Absorber	0.250
Clad thickness (in.)	0.030
Total	0.310
Clad material	AISI Type 347 stainless steel, modified, 0.05 wt % Co maximum and 0.15 wt % Co plus Ta maximum
Absorber material	Europium titanate Eu_2O_3, 2 TiO_2 dispersed in stainless steel (equivalent to 25 wt % europium metal)
Europium content of each blade (g)	
Average (per blade)	790
Maximum (per blade)	828
Minimum (per blade)	752

6. Fuel bundle data:	
Element pitch (in.)	0.665
Elements in peripheral bundle	
Fuel	121
Poison (30-in. length)	12
Poison (20-in. length)	3
Dummy	3
Elements in center bundle	
Fuel	15
Poison	0
Dummy	0
Structural rods	3
Control rods	
Peripheral bundle	1
Center bundle	0
7. Nuclear characteristics:	
Core reactivity (max) (%)	13.28
Control rod worth, 68° F (%)	
6-rod bank	-20.22
5-rod bank	-13.66
4-rod bank, minimum	-8.83
3-rod bank, alternating	-9.19
Minimum shutdown margin, 68° F (%)	
One rod completely withdrawn	0.38
Two rods at operating position	0.10
Core reactivity (initial) (%)	
At 68° F	13.28
At 463° F	9.08
Temperature coefficient	
Beginning of life at 68° F	-0.675×10^{-4}
At 463° F	-2.827×10^{-4}

End of life at 68° F	-0.650×10^{-4}
At 463° F	-2.433×10^{-4}
Burnup	
Peak U-235 (%)	61.7
Peak B-10 (%)	97.9
8. Heat transfer characteristics:	
Coolant flow rate (gpm)	2125
Coolant temperature (°F)	
Average	463
Inlet (full power)	447
Outlet (full power)	479
Maximum coolant temperatures (°F)	
Without hot channel factors	515
With hot channel factors	555
Surface temperatures, maximum (°F)	
Without hot channel factors	588
With hot channel factors	580
Flow rate (gpm)	
Inside fuel element	1.20
Flow ratio, flow inside element/total flow	0.51
Heat flux, Btu/hr-ft^2	
Average	71,200
Maximum, without hot channel factors	257,000
Maximum, with hot channel factors	366,000
Fraction of burnout heat flux	
Without hot channel factors	0.12
With hot channel factors	0.18

II. MECHANICAL DESIGN

This chapter describes the PM-1 reactor core and explains features of the design. In reading this section, reference should be made to the design drawings which are listed by title and number at the end of this chapter and included in the appendix of this report. Conclusions and results of supporting studies and tests that were conducted for this design are to be found in the appendix.

The shroud, which rests on the pressure vessel orifice plate, maintains the alignment of each fuel bundle relative to the vessel. The upper skirt assembly distributes the primary flow from the core to the exit plenum to minimize any radial flow perturbation within the core proper. A portion of this flow is also directed to the head for cooling. In addition, this assembly provides guidance for the control rods as they are withdrawn and supplies the necessary holddown force to each fuel bundle.

The overall reactor core structural installation (Drawing 372-2105002) shows the upper skirt and core shroud assemblies positioned within the pressure vessel. The core shroud (Drawing 372-2105009) is located axially and radially at its upper end by the pressure vessel's inlet orifice plate. This allows free downward thermal expansion of the shroud relative to the orifice plate. Two diametrically opposed guide bars welded onto the pressure vessel waterbox fit into slots in the core shroud flange. These guide bars bring the shroud into approximate angular alignment as the shroud is lowered into the vessel. Three dowel pins, located on the shroud, fit into slots on the orifice plate to provide the exact orientation of the shroud (and subsequently, the contained fuel bundles) relative to the pressure vessel and control drive mechanisms. Three such pins are provided to allow the shroud to sit level while rotating the shroud to locate the alignment slots during assembly. Improper positioning of the shroud is prevented by asymmetrical location of the pins.

The upper skirt assembly (Drawing 372-2105004) is supported on the core shroud upper flange. A heavy ring forms the lower bearing surface of the skirt assembly and contains three alignment slots which engage mating pins on the shroud flange. The ring also has an integrally machined pilot lip that centers the skirt radially on the shroud. Four integral pads at 90° intervals on the skirt upper plate locate its top radially within the throat of the pressure vessel. One of these pads is smaller than the remaining three. The smaller pad is used during refueling to angularly orient the skirt assembly as the assembly is lowered into position in the vessel. A double leaf spring, loaded against the pressure vessel head, supplies the holddown force through

the skirt and core shroud to the orifice plate. Supported by the core shroud, the skirt is free to expand thermally upward against this spring. The load of all the reactor core components plus the total spring holddown force is taken out at a single plane, the orifice plate.

To keep the overall systems activation to a minimum, some materials have their cobalt and tantalum contents limited. Because of the high surface area and neutron flux level within the core region, the fuel and poison elements have their cladding and dead end material compositions limited to 0.01 wt % cobalt and 0.03 wt % cobalt and tantalum. The remaining in-core structural stainless steel and that in the core shroud is limited to 0.05 wt % cobalt and 0.15 wt % cobalt and tantalum. The relatively larger average distance between the skirt assembly and the active core eliminated the need for such limitations in the skirt components. The material composition limits on the various components are specified on the applicable design drawings or specifications.

The basic PM-1 core is made up of six identical peripheral fuel bundles and one center bundle. The center bundle was designed into the system to permit easy substitution by an instrumented bundle (if desired) through a small access port in the vessel head.

A. CORE SHROUD

The core shroud (Drawing 372-2105009) rests upon the pressure vessel orifice plate with its primary function being to hold the fuel bundles and to position them relative to the control drive mechanisms located in the head of the pressure vessel. As a secondary function, it provides the first thermal shield and directs the primary coolant from the pressure vessel orifice plate to the core inlet. An alignment spider is incorporated integrally into the bottom of the shroud. Each of the six peripheral fuel bundles contained within the core rests directly upon this spider. Alignment of the bottom of each bundle is assured through the use of legs which fit into the accurately positioned holes in the spider. Although each bundle sits on three legs, to ease handling during remote assembly, only the two outermost are used for radial positioning. The centrally located hole is made slightly oversize to provide only the seat without accurately controlling the location. Bundle positioning at the top is accomplished by the fit of each bundle's alignment structure over two alignment pins located in the top flange of the core shroud. This flange also contains the alignment pins and seat used in positioning the skirt assembly and shroud relative to the orifice plate, as discussed previously. Each of these pins is pressed into place and is secured by a smaller lock pin. These lock pins are held mechanically and have their motion limited at assembly by adjoining components. The shroud flange has

two vertical slots at diametrically opposite positions on its outer diameter. During core insertion, these slots engage guide bars on the pressure vessel waterbox to prealign the shroud angularly as the shroud alignment pins approach their slots in the vessel orifice plate. These slots and the vessel guide bars assure positive angular orientation of the close-fit final alignment pins before they actually reach the orifice plate.

B. FUEL BUNDLES

The active core contained within the shroud consists of seven fuel bundles: one hexagon-shaped center bundle (Drawing 372-2105003) and six identical pie-shaped bundles located around the periphery (Drawing 372-2105010). Each of the peripheral bundles is individually held and positioned within the core shroud, as shown on the core installation drawing (Drawing 372-2105005). The center bundle, in turn, rests upon the lower grids of the peripheral bundles and is positioned within their supporting guide rail structure.

Each peripheral bundle is constructed basically from three control rod guide rails, an upper and lower grid, a guide alignment structure and the necessary core elements (fuel, poison and dummy). The control rod guides provide the fundamental structural connections for the bundle. They extend over the full length of the assembly and form a continuous track for the control rod wear pads. Positioning of the three guide rails relative to each other is achieved by a fit into the alignment structure at their top (Drawing 372-2105015) and through the lower grid at the bottom (Drawing 372-2105012). Sleeves thread over the portion of the guide rails which extend through the lower grid to lock it into place. These sleeves provide the seat upon which the bundle rests, as well as the required spacing to form a plenum between the grid and the alignment spider for flow redistribution. Each sleeve is mechanically locked into place by deforming its side wall at two places into corresponding grooves. A portion of the turned diameter on the guide rail extends through the sleeve to fit into the positioning holes in the core shroud alignment spider during assembly. Correct upper alignment is achieved through the alignment structure, which fits over two alignment pins in the core shroud flange, as discussed earlier. Thus, each control rod guide rail in a peripheral bundle is aligned at its top and bottom and the complete bundle is allowed free thermal expansion above its seat in the core shroud.

The guide rails fit through cutouts in the upper grid in a manner similar to the lower grid. The upper grid is located vertically by a shoulder on the guide rail and is secured by a sleeve fitting over the reduced portion of the guide rail which extends above the grid. When the alignment structure is locked into place at assembly, this sleeve

extend at three points from the center bundle lower grid to rest upon the peripheral bundle lower grids. The center bundle is free to expand axially upward from this point with top radial alignment being obtained by tabs bearing against the peripheral bundle upper grids. Three solid rods extend axially along the length of the center bundle to provide positioning for the pickup plate and the upper and lower grids. Each bar threads into the lower grid, captures the upper grid through the use of a sleeve and secures the pickup plate in place through the use of a special nut. This nut, which completely locks the assembly, is both encapsuled and prevented from rotating by the positive displacement of its housing into grooves in the nut. As will be discussed later, the upper skirt assembly applies a holddown force to the pickup plate of the center bundle and the guide rail alignment structure of each peripheral bundle.

C. SOURCE

The primary neutron source (Drawing 372-2105018) is located at the middle of the center bundle, where a core element has been displaced. Installation of the source into the center bundle will be made just prior to loading the core into the pressure vessel. Because of the relatively low source strength requirements, this operation is performed with two simple tools from a distance of approximately three feet. The source is lifted from the shipping cask and threaded into the upper grid with the source lifting tool. Positive locking into the upper grid by thread deformation is accomplished with the source locking tool. The source element is supported and aligned at the center bundle upper grid, with radial guidance (but free axial expansion) provided by the lower grid.

D. CORE ELEMENTS

Three types of core elements are included in each fuel bundle: fuel, poison and dummy. The general construction and dimensions of these elements are shown on Drawing 372-210501 while their locations within each fuel bundle are given on the bundle drawings. As mentioned previously, these elements have identical end construction to allow complete interchangeability.

The fuel element contains UO_2 dispersed in and clad with stainless steel. Its meat is nominally 0.0285 inch thick and it is sandwiched between cladding 0.008-inch thickness. Fabrication and testing are to the applicable design drawing, as referenced, and to PM-1-Type Reactor Fuel Element Specification MN-7891. When the element is assembled into a fuel bundle, the beginning of the active fuel region lies one inch

above the top surface of the lower grid. This distance provides for equalization of flow after it is orificed by the lower grid, and it also allows the diameter reduction of the tube end to start well away from the fuel-dead end interface.

Lumped burnable poison elements are substituted for fuel elements as required to provide the desired nuclear characteristics. These elements, which are unclad, contain natural boron alloyed in stainless steel. The poison length may be varied easily by the use of unpoisoned, tubular "dead ends" which are mechanically locked to the boron steel section. Two poison lengths are used in the PM-1 reactor. The 18 poison elements closest to the control rod centerlines contain boron steel only in the lower 20 inches of the 30-inch active core length. All other poison elements are the full active core length.

The use of an unclad poison element also offers a nuclear advantage in addition to the mechanical simplification realized. Normally the melting process for the boron-stainless steel cannot be controlled to provide a material composition tolerance much tighter than ±10% of the desired boron loading. With the unclad PM-1 element, the final machined diameter is varied slightly on the basis of the final material analysis to meet the prescribed loading with tolerances of approximately ±2%. These elements are manufactured to the referenced design drawing and to PM-1-Type Reactor Burnable Poison Element Specification MN-7892.

Dummy core elements are incorporated into each peripheral bundle to fill in at the core periphery where the basic triangular element pattern ends and thus reduce the total core flow requirements. These elements are tubular with swaged ends to fit the upper and lower grids in a manner identical to that of the fuel elements. A plug is entrapped within the tube to maximize the flow blockage. However, a small bleed is provided to eliminate a stagnant water area.

E. CONTROL ROD

The control rod (Drawing 372-2105016) utilizes a Y-shaped configuration to fit within the triangular core element pattern. Its poisoned region, consisting of europium titanate ($Eu_2O_3 \cdot 2TiO_2$ dispersed in stainless steel, is contained within cladding of nominal 0.030-inch thickness. Manufacture of this element is to the reference design drawing and to PM-1-Type Reactor Control Rod Specification MN-7893.

Each control rod is guided by wear pads contained on the lower edge of each blade and a wear cap located at its upper hub. This wear cap also integrally incorporates the pickup ball utilized in latching with the

control rod drive mechanism. The rod wear pads are contained within the three control rod guide rails that run the full length of each peripheral bundle. These pads provide the lower radial and overall angular alignment for the control rod. Upper alignment is obtained through the wear cap which is encaptured within the guide tube of the upper skirt assembly. This tube, which is split to fit over the control rod during rod withdrawal, interlocks with the guide alignment structure contained in each peripheral bundle. As discussed previously, the rod guide rails also terminate in this structure, thus providing a continuous structure for guidance and alignment. Both the wear cap and pads are made from hardened 17-4PH material to minimize wear between these areas and the guiding structure. The 17-4PH wear surfaces are hardened by a heat treatment process which ensures that the desired tensile strength and ductility are obtained without making the material susceptible to stress corrosion in the core operating environment.

F. UPPER SKIRT

The upper skirt assembly (Drawing 372-2105004) is both supported and positioned angularly by the core shroud. Its principal functions are to direct the primary flow after it exits from the active core region, to provide partial guidance to the control rods, and to provide the necessary holddown forces to the fuel bundles and the core shroud.

A series of 1-1/2-inch diameter holes is used to separate the fuel exit flow area from the single pressure vessel outlet pipe. These orifices provide sufficient pressure drop to prevent any local radial flow perturbations within the fuel region which might be caused by the single outlet.

The skirt assembly contains seven tubes which supply the holddown forces to the fuel bundles. Six split tubes are utilized for the peripheral bundles to provide guidance for the control rods, as previously discussed. A multifigured leaf spring (Drawing 372-2105017), deflected by the pressure head, simultaneously loads each individual tube and the skirt. Two such springs, operating in series, are used to provide maximum deflection while keeping the working stresses within allowable limits. As an extra precaution in the event of a failure, these springs are insulated from the primary system by the solid base plate and the raised section or fence at its periphery and at each holddown tube.

The center bundle holddown tube uses a sliding collar loaded by a completely enclosed spring to obtain the required loads. This tube bears against a plug extending downward from the center bundle access port located in the pressure vessel head. This design provides considerable versatility in that (1) the core may be refueled as a unit in the conventional manner, or (2) by means of a suitable locking tool,

the center fuel bundle, holddown tube and plug may be removed through the pressure vessel head as a single assembly. This latter is a desirable feature in that in-core instrumentation or irradiation test bundles may be inserted into the reactor without removing the pressure vessel head. This holddown tube also provides a positive flow of coolant to the vessel head by bypassing a portion of the primary flow around the main skirt orifices. Restrictions were also incorporated into each of the peripheral bundle tubes to maximize the center tube cooling flow. Although in opposition to this, an annular-type orifice was included at the radial support point between the skirt and the throat of the pressure vessel. This was necessary to reduce the hydrodynamic forces which tend to lift the skirt from its seat.

COMPONENT LIST AND SPECIFICATIONS

Martin Nuclear Specifications

MN-7890	PM-1 Reactor Core, Specification for
MN-7891	PM-1-Type Reactor Fuel Elements, Specification for
MN-7892	PM-1-Type Reactor Burnable Poison Elements, Specification for
MN-7893	PM-1-Type Reactor Control Rods, Specification for

DESIGN DRAWINGS

Title	Drawing Number
Reactor Assembly	372-2105000
Reactor Core Structural Installation	372-2105002
Core Installation	372-2105005
Center Bundle Assembly	372-2105003
Upper Skirt	372-2105004
Core Details--Center Bundle	372-2105006
Details, Holddown--Center Bundle	372-2105007
Shroud Assembly	372-2105009
Peripheral Bundle	372-2105010

Title	Drawing Number
Upper Grid	372-2105011
Lower Grid	372-2105012
Core Elements	372-2105013
Guide Rails	372-2105014
Lock Sleeve and Alignment Structure	372-2105015
Control Rod Assembly	372-2105016
Spring, Holddown--Upper Skirt	372-2105017
Source (primary)	372-2105018
Alignment Study	372-2105019
PM-1 Core Shroud, Center Bundle and Peripheral Bundle (envelope dimensions)	372-2105020

III. PHYSICS DESIGN

This chapter describes the physics of the PM-1 core. It is divided into several sections for ease of presentation. The first section discusses the core life and core reactivities; the second section discusses the control rods, their worths and shutdown margins; the third section discusses power distributions; the fourth section discusses temperature coefficients. Supporting data, test results, analytical techniques and intermediate calculations required to support the design are to be found in the appendix.

The core lifetime of the PM-1 was determined by two different but closely allied methods. One method consisted of performing both radial uniform and nonuniform burnup calculations, determining the reactivity defect between the two, then performing a nonuniform axial burnup with control rods and iterating on the positive value of the radial reactivity defect to determine the position of the rods with burnup. The other method involved performing both uniform and nonuniform axial burnup calculations, determining the reactivity defect between the two and applying it to a radial nonuniform burnup.

A. RADIAL UNIFORM AND NONUNIFORM BURNUP

The radial nonuniform burnup calculation was performed using the six core region configuration and the C_3-F_3 burnup program. The program performs a region-wise burnup, as described in the appendix. Time steps of 100 days were used. The three-group nuclear constants at time zero are tabulated in the appendix. The resulting core reactivity versus time with the reactor operating at a power level of 9.37 mw is shown in Fig. III-1.

The radial uniform burnup calculation was performed in a similar manner to the nonuniform burnup, except that the reactor core was homogenized into one region. The homogenization process causes the calculated reactivity to increase due to the displacement of materials to regions where they have a different worth. The increase in calculated reactivity is caused primarily be smearing out the boron in the LPR's; however, the steel in the rod guides, LPR's and fuel elements also makes a contribution. To reduce the homogenized core reactivity to that of the six-region core, burnable boron poison was added uniformly.

The three-group core constants used in the uniform burnup calculation are given in Table III-1.

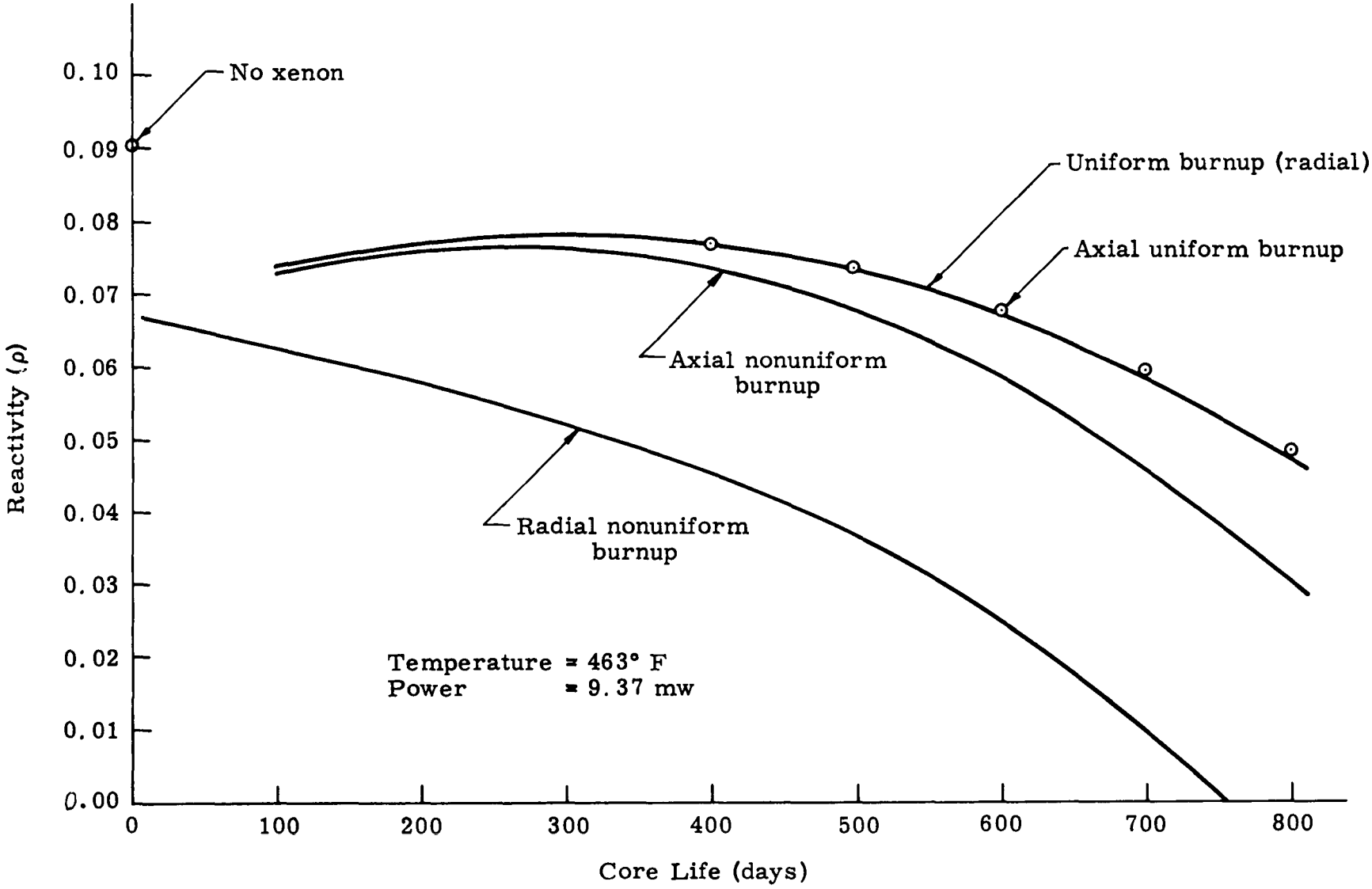

Fig. III-1. Uniform and Nonuniform Core Burnup Lifetimes (without rods)

TABLE III-1

Homogenized Core Constants (463° F, beginning of life)

Constants	Groups		
	1	2	3
B^2 (axial, cm^{-2})	1.92437×10^{-3}	2.29971×10^{-3}	2.40020×10^{-3}
D (cm)	1.85068×10^{0}	5.70307×10^{-1}	2.47739×10^{-1}
Σa^* (cm^{-1})	1.14928×10^{-3}	2.96948×10^{-2}	1.80890×10^{-1}
$\nu\Sigma_f$ (cm^{-1})	1.48811×10^{-3}	3.93176×10^{-2}	2.58534×10^{-1}
Σ_{SL} (cm^{-1})	5.67988×10^{-2}	4.86415×10^{-2}	

*Includes 4.8165×10^{18} atom/cc of B-10 to compensate for homogenization.

The resulting uniform core burnup reactivity versus full power operating time is shown in Fig. III-1. The difference in core reactivity between uniform and nonuniform radial burnup as a function of core life is presented in Fig. III-2. Due to the difficulty in reading curves precisely, the reactivity data is also presented in tabular form in Table III-2.

TABLE III-2

Radial Uniform and Nonuniform Burnup Reactivity Versus Core Life (463° F, 9.37 mw)

Days	ρ (uniform)	ρ (nonuniform)	$\Delta\rho$
0	0.09080*	0.09080*	0.00000
100	0.07346	0.06267	0.01079
200	0.07646	0.05789	0.01857
300	0.07744	0.05232	0.02512
400	0.07629	0.04540	0.03089
500	0.07290	0.03653	0.03637

*No xenon.

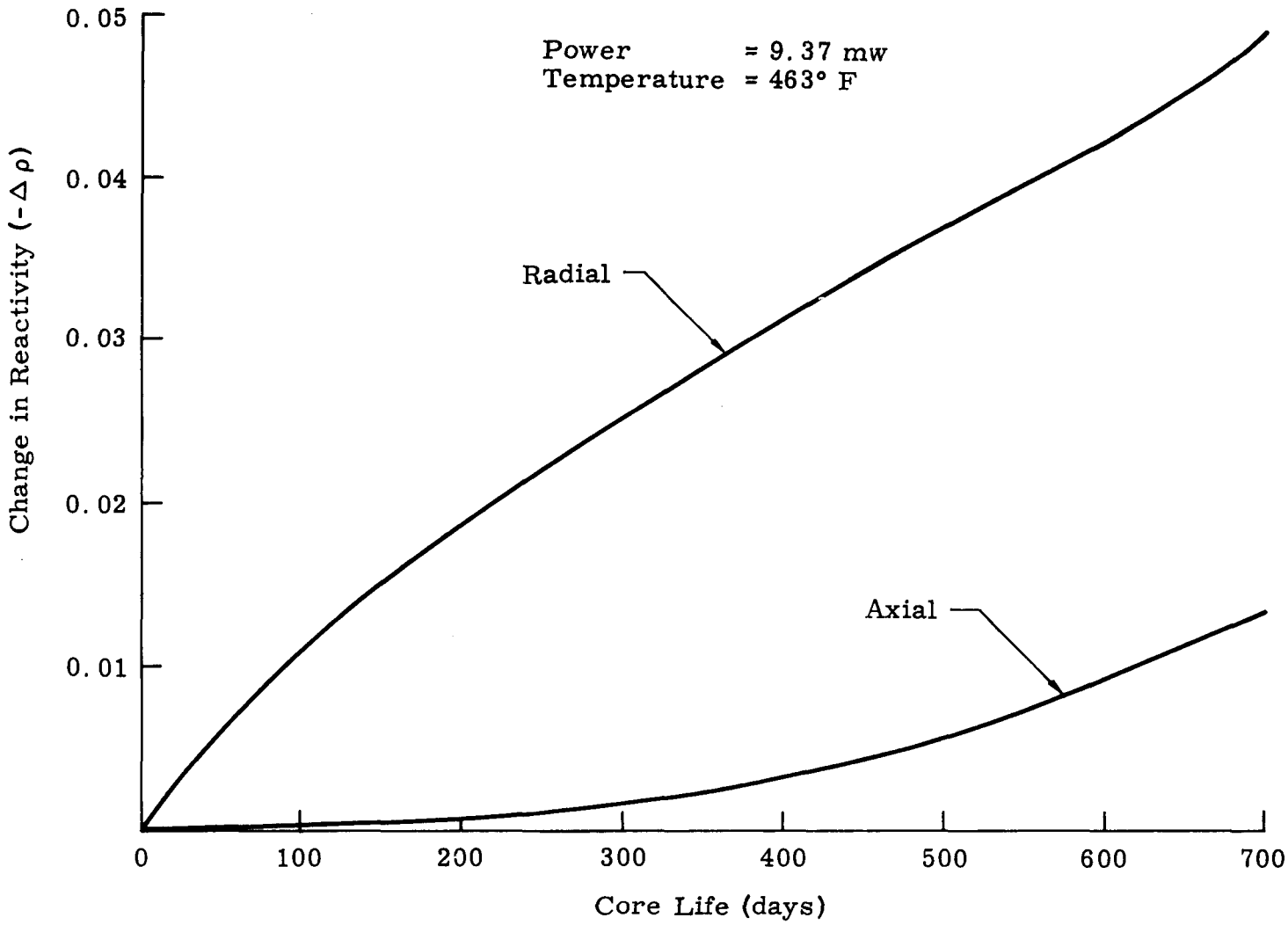

Fig. III-2. Reactivity Difference Between Uniform and Nonuniform Burnup Versus Core Life

TABLE III-2 (continued)

Days	ρ (uniform)	ρ (nonuniform)	$\Delta\rho$
600	0.06709	0.02506	0.04203
700	0.05863	0.01033	0.04830
800	0.04726	-0.00825	0.05551
900	0.03269		

*No xenon

B. AXIAL UNIFORM AND NONUNIFORM BURNUP

The axial uniform burnup calculation was performed in a manner similar to the radial uniform burnup. The same core constants were used as given in Table III-1, except the radial bucklings were used, which have values of 4.7844×10^{-3}, 5.7495×10^{-3}, 6.0092×10^{-3} cm^{-2} for the fast, epithermal and thermal groups, respectively.

The axial nonuniform burnup calculation with control rods withdrawn was performed in a manner identical to the uniform burnup except that the core was divided into 12 equally spaced axial regions. The initial constants used were identical to those given in Table III-1, except for the radial bucklings which are given above.

The resulting axial uniform and nonuniform burnup reactivity versus core life is shown in Fig. III-1. The difference between the two burnup reactivities versus core life is plotted in Fig. III-2. The data is also tabulated in Table III-3.

TABLE III-3

Axial Uniform and Nonuniform Burnup Reactivity Versus Core Life (463° F, 9.37 mw, no rods)

Days	ρ (uniform)	ρ (nonuniform)	$\Delta\rho$
0	0.09080	0.09080	0.00000
100	0.07350	0.07303	0.00047
200	0.07665	0.07597	0.00068
300	0.07779	0.07619	0.00160
400	0.07682	0.07354	0.00328

TABLE III-3 (continued)

Days	ρ (uniform)	ρ (nonuniform)	$\Delta\rho$
500	0.07360	0.06786	0.00574
600	0.06798	0.05893	0.00905
700	0.05972	0.04662	0.01310
800	0.04856	0.03074	0.01782
900	0.03423		

C. TOTAL NONUNIFORM BURNUP WITH CONTROL RODS

The axial nonuniform burnup with control rods was calculated by the "window shade" method. This method, which is used frequently, involves distributing a uniform poison over the rodded region of the core. For the present study, europium was used as the poison because it corresponds to the material in the control rods.

To burn out the core accurately, it is necessary to obtain the proper power generation split between the rodded and unrodded regions of the core. Also, the ratio of the thermal to epithermal worth of the poison should have the proper value. From the results of the PMZ-1 critical experiments, the necessary data concerning the control rods was available and is given in Table III-4.

TABLE III-4

Experimental Control Rod Data* (68° F)

Thermal/epithermal worth	3.06
Power (rodded)/power (total)	0.478
Critical bank position (in. withdrawn)	8.25

*Adjusted to account for the small difference between the experimental and the PM-1 cores.

To obtain agreement with the measured control rod data, it was necessary to perform a small parametric study in which the amount of poison and the thermal self-shielding of the poison were varied. The calculations were based on an axial two-core region (rodded and unrodded) model, using the F_3 program with the rods at the critical bank position. The poison was only allowed to effect the three-group absorption cross sections. The ratio of the epithermal to the fast cross

section of the poison was held constant. It had been determined previously from an eighteen-group, two-region diffusion theory cell calculation. The calculation was performed in slab geometry; one region was control rod material and the other, homogenized core material.

The results of the study to determine the proper values of the three-group poison cross sections are presented in Fig. III-3. The poison cross-section values which were used in the axial burnup calculation with control rods are given in Table III-5.

TABLE III-5

Poison Cross Sections Used in Window Shade Calculation

Group	Cross Section ($\Sigma\rho$)
1	3.646×10^{-5}
2	3.7055×10^{-3}
3	5.3778×10^{-2}

Although the use of the poison cross sections in Table III-5 forces agreement, the experimentally determined power split and thermal-to-epithermal rod worth do not provide a "just critical" condition with the control rods at the measured critical bank position. The reactivity bias* is caused by the inadequacy of the model to take into account such effects as changes in perpendicular buckling and smeared-out absorber. However, since the prime concern is to burn out the core properly, the reactivity bias is not of major importance, although it must be taken into account. The axial initial reactivity calculations without the rods inserted did not have any bias. Since it is felt that the bias is associated with the rodded region at the end of life, when the rods are completely withdrawn, it was assumed that there would not be any bias. Therefore, the bias was assumed to vary linearly with rod insertion, being zero when the rods are fully withdrawn.

The axial nonuniform burnup calculation was performed on a 12-region core, using a modified version of the C_3-F_3 program. This program varies the control rod bank position on a pointwise basis throughout the core life to obtain a desired reactivity which is not necessarily zero. The values of the reactivity which were iterated on during the burnup calculation were the sums of the biases discussed in the previous paragraph and the radial burnup reactivity defect plotted in Fig. III-2.

*Control rod reactivity bias is 1.406% ρ at 463° F.

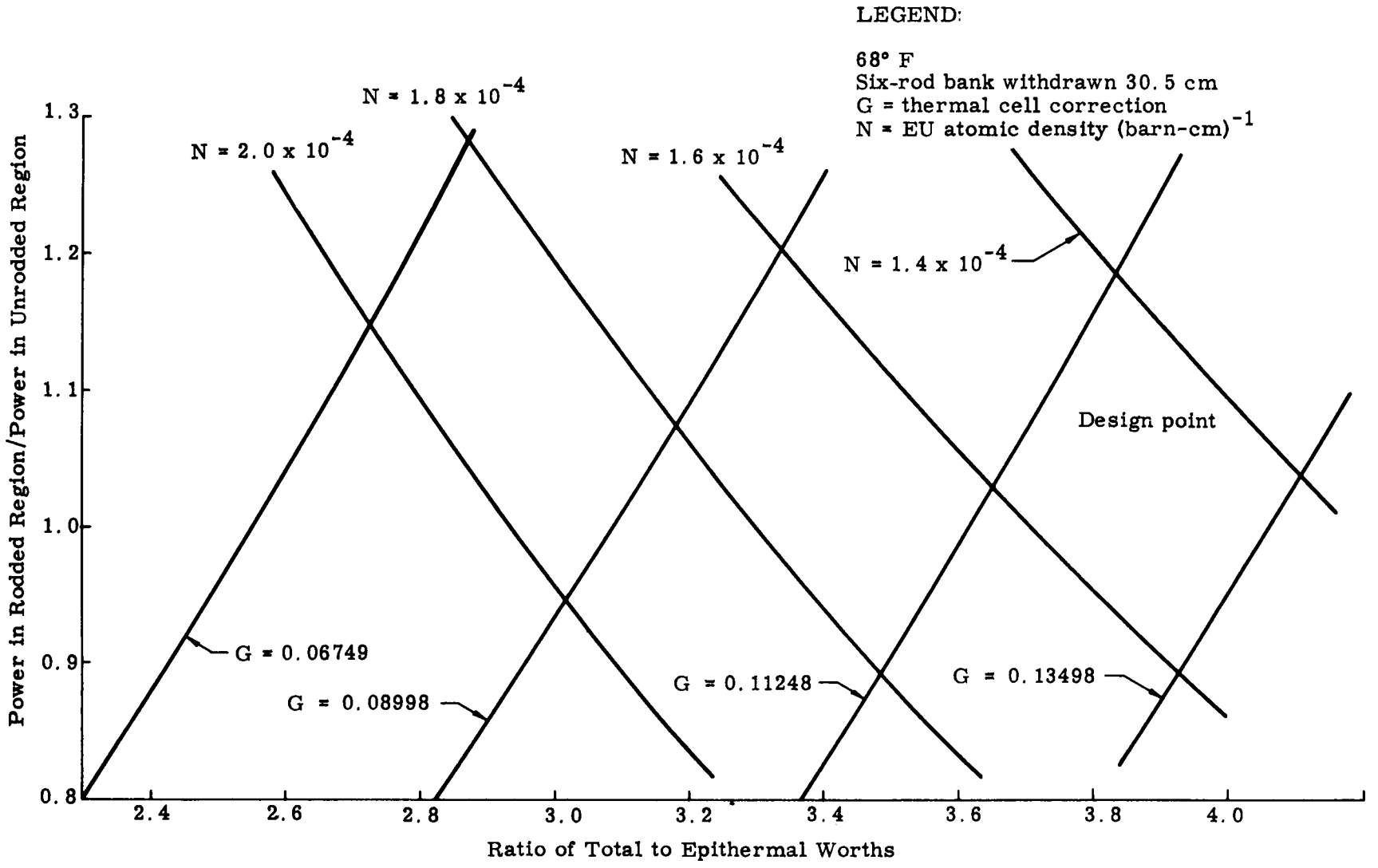

Fig. III-3. Cold Equivalent Europium Search for PM-1

The resulting core reactivity based on burnup with control rods is shown in Fig. III-4. The data is also tabulated in Table III-6. For comparison purposes, the nonuniform burnup core reactivity without control rods is also included in Fig. III-4. It can be seen that the calculation with control rods indicates a core life which is essentially the same as that obtained by a nonuniform burnup without control rods. However, the atom density distribution at the end of life is somewhat different.

TABLE III-6

Total Nonuniform Burnup Reactivity Versus
Core Life (463° F, 9.37 mw, rods at critical bank position)

Days	Reactivity
0	0.09094
100	0.06691
200	0.06175
300	0.05397
400	0.04281
500	0.02900
600	0.01209
700	-0.00661

D. EFFECT OF U-235 TOLERANCE LOADING

The effects of the ±2% U-235 loading tolerance per fuel element on the initial reactivity of the PM-1 was determined. The calculation was based on the six-region core geometry using the C_3-F_3 (linked) program. The resulting hot and cold initial reactivities are shown in Table III-7.

TABLE III-7

Initial Reactivity for Tolerance U-235 Loading

Δ U-235/Element	ρ (68° F)	Δ ρ (68° F)	ρ (463° F)	Δ ρ (463° F)
-2%	0.1282	-0.0045	0.0859	-0.0049
0	0.1327	0.0	0.0908	0.0
+2%	0.1371	0.0044	0.0955	0.0047

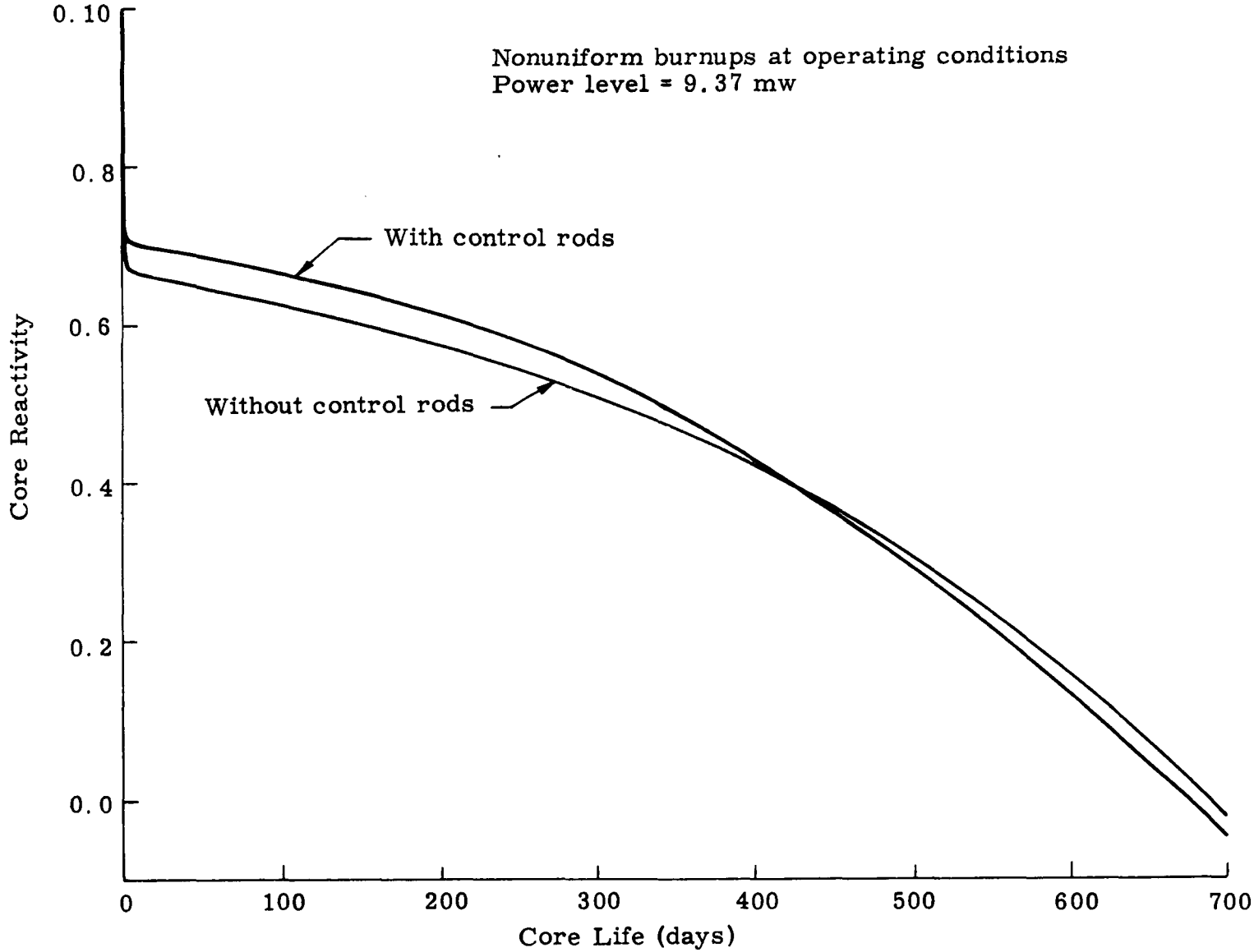

Fig. III-4. PM-1 Reactivity Throughout Core Life

E. INITIAL REACTIVITY WORTH OF CHANGES TO THE CENTER BUNDLE

The center bundle of the PM-1 core is composed of 19 elements. Three of these elements are 0.50-inch OD stainless steel rods required for structural purposes, 15 are fuel elements and the center location is occupied by a stainless steel tube containing the neutron source.

The worth in reactivity due to various changes made to the center bundle was determined both cold and hot. The changes were as follows:

(1) Three fuel tubes in the center bundle were replaced by:

  (a) Three lumped poison rods.

  (b) Three stainless steel rods.

  (c) Three stainless steel tubes.

(2) Six fuel tubes in the center bundle were replaced by:

  (a) Six lumped poison rods.

  (b) Six stainless steel rods.

  (c) Six stainless steel tubes.

Reactivity worth due to the center bundle changes is represented in tabular form in Table III-8.

TABLE III-8

Reactivity Worth of Changes in Center Bundle

Material Replacement	Fuel Elements Replaced	Cold (68° F) ρ	Cold (68° F) $\Delta\rho$	Hot (463° F) ρ	Hot (463° F) $\Delta\rho$
None	None	0.1327	0.0	0.0908	0.0
LPR	3	0.1250	-0.0077	0.0816	-0.0092
LPR	6	0.1195	-0.0132	0.0745	-0.0163
SS rods	3	0.1286	-0.0041	0.0860	-0.0048
SS rods	6	0.1250	-0.0077	0.0816	-0.0092
SS tubes	3	0.1304	-0.0023	0.0882	-0.0026
SS tubes	6	0.1275	-0.0052	0.0850	-0.0058

F. REACTIVITY WORTH OF LUMPED POISON RODS

A study was performed to determine the reactivity worth of the boron and stainless steel contained in the lumped poison rods. The purpose of the study was threefold: (1) to determine the worth of boron per rod in different regions of the core, (2) to indicate what magnitude of reactivity increase could be expected if steel rods were somehow inserted in place of LPR's, and (3) to show the overall reduction in reactivity due to the stainless steel in the rods. The six-region core configuration was used with the C_3-F_3 program. The boron in Regions 3, 4 and 5 was removed individually to determine the worth per region. The total boron in the three regions was then removed, and finally the stainless steel in the lumped poison rods was removed. The volume displaced by the steel was assumed to be replaced by inert material after removal of the rods. Thus, the volume fraction of water remained constant.

The results of the preceding study are shown in Table III-9. Referring to this table, it can be seen that the average worth of the boron in a lumped poison rod is slightly less than 0.1% in reactivity. However, it should be noted that the reactivity worth of the stainless steel is about 1/3 that of the boron. Since steel is a nonburnable poison, the results indicate that the use of a different carrier for the boron would be desirable. This point is discussed further under the section on core lifetime.

G. RELATIVE DISTRIBUTION OF U-235 AND B-10 DURING THE LIFE OF THE CORE

The burnup and buildup of the various isotopes in the core were calculated as a function of core lifetime during the nonuniform burnup study. The concentrations of the two most important isotopes, U-235 and B-10 have been converted to "fraction present" as a function of lifetime and position. The resulting distributions for both the radial and axial directions are shown plotted in Figs. III-5 through III-8.

The maximum burnup of the B-10 and U-235 was obtained from the data in the preceding figures by:

$$\beta(t)_{max} = 1 - \left\{\frac{\alpha(t)_{min}}{\alpha(t)_{avg}}\right\}_{axial} \left\{\alpha(t)_{min}\right\}_{radial} \qquad \text{(III-1)}$$

where

$\beta(t)$ = Fractional burnup

$\alpha(t)$ = Fraction remaining

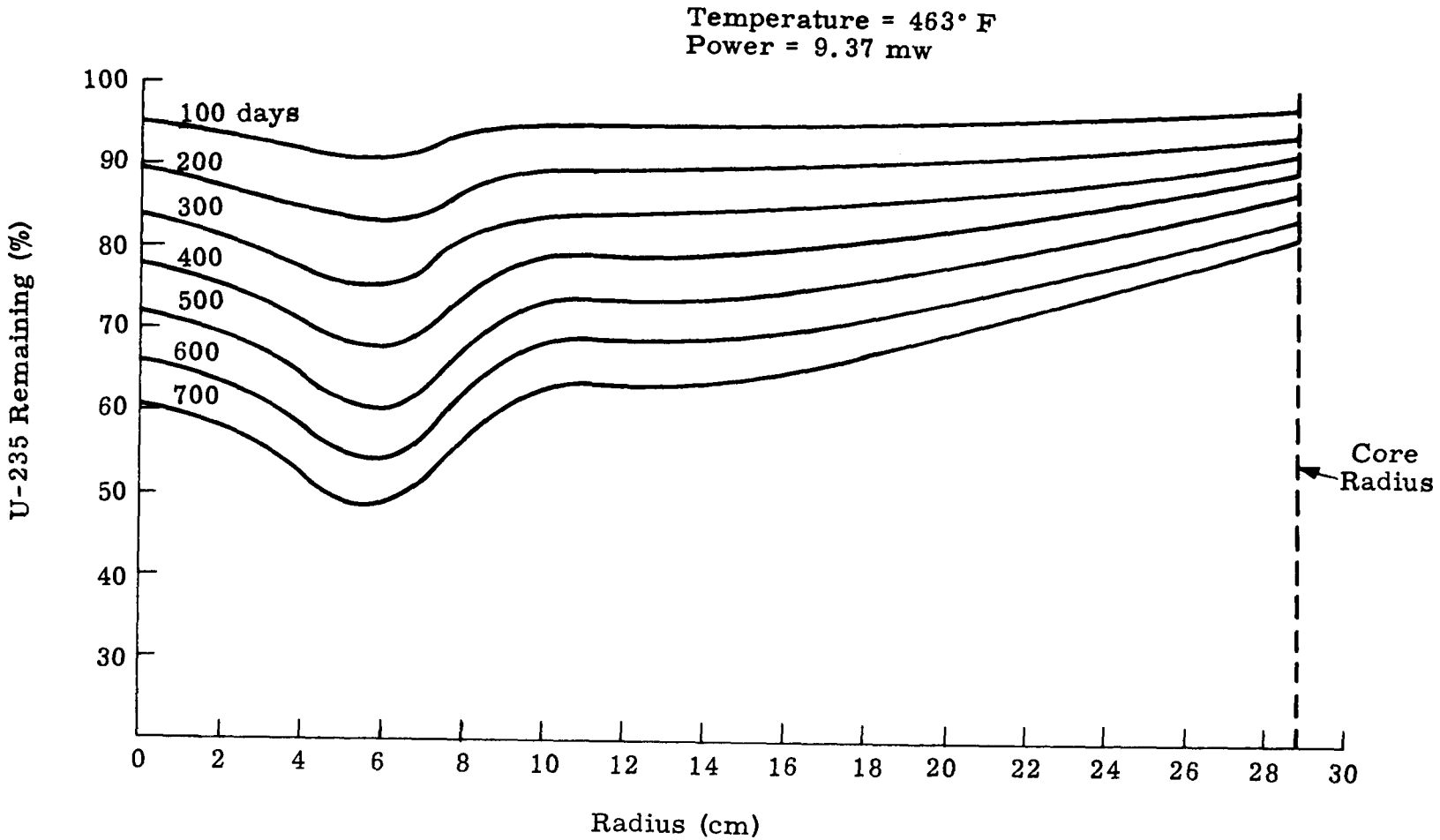

Fig. III-5. Radial U-235 Distribution Versus Core Life

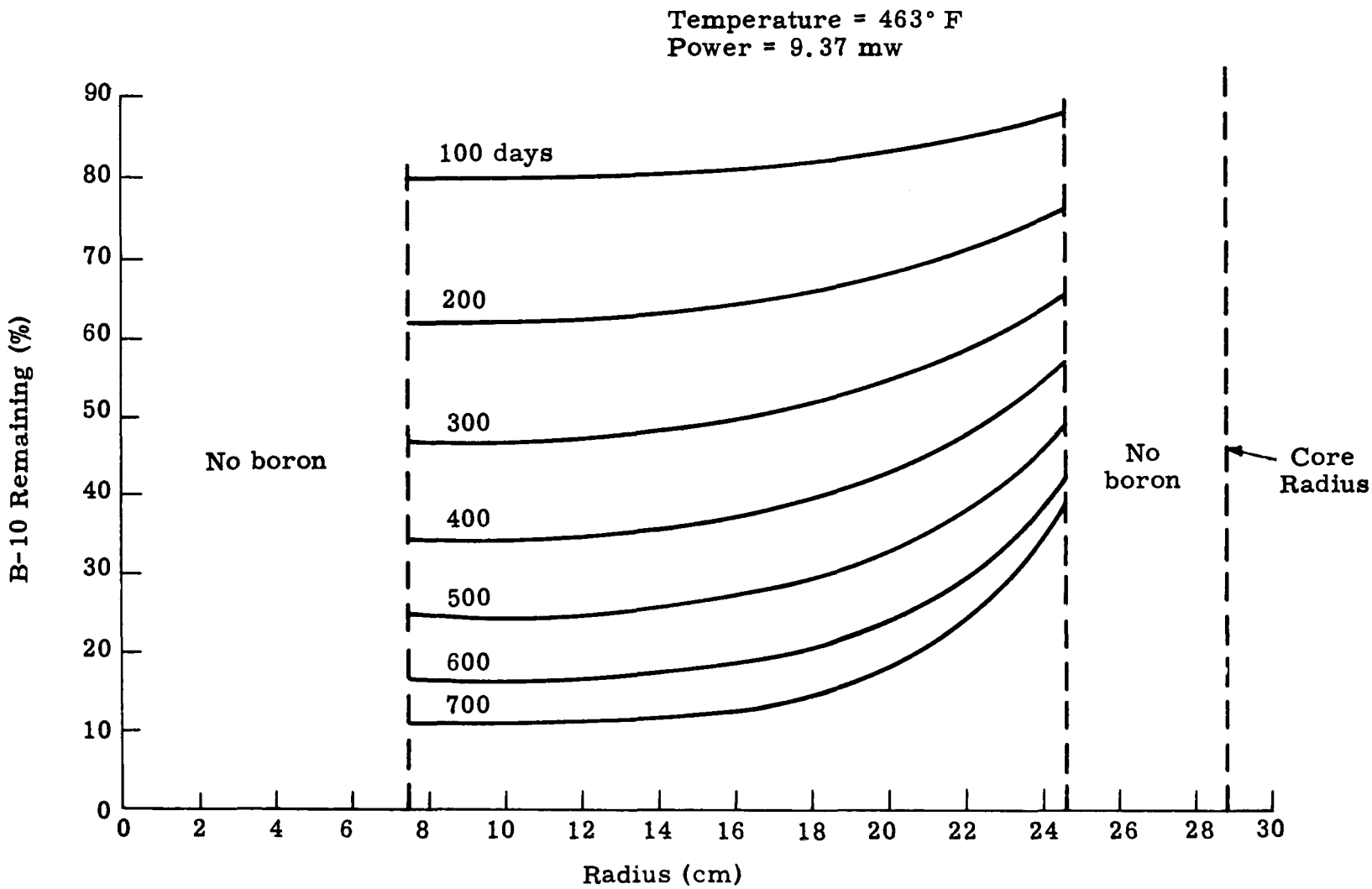

Fig. III-6. Radial Boron Distribution Versus Core Life

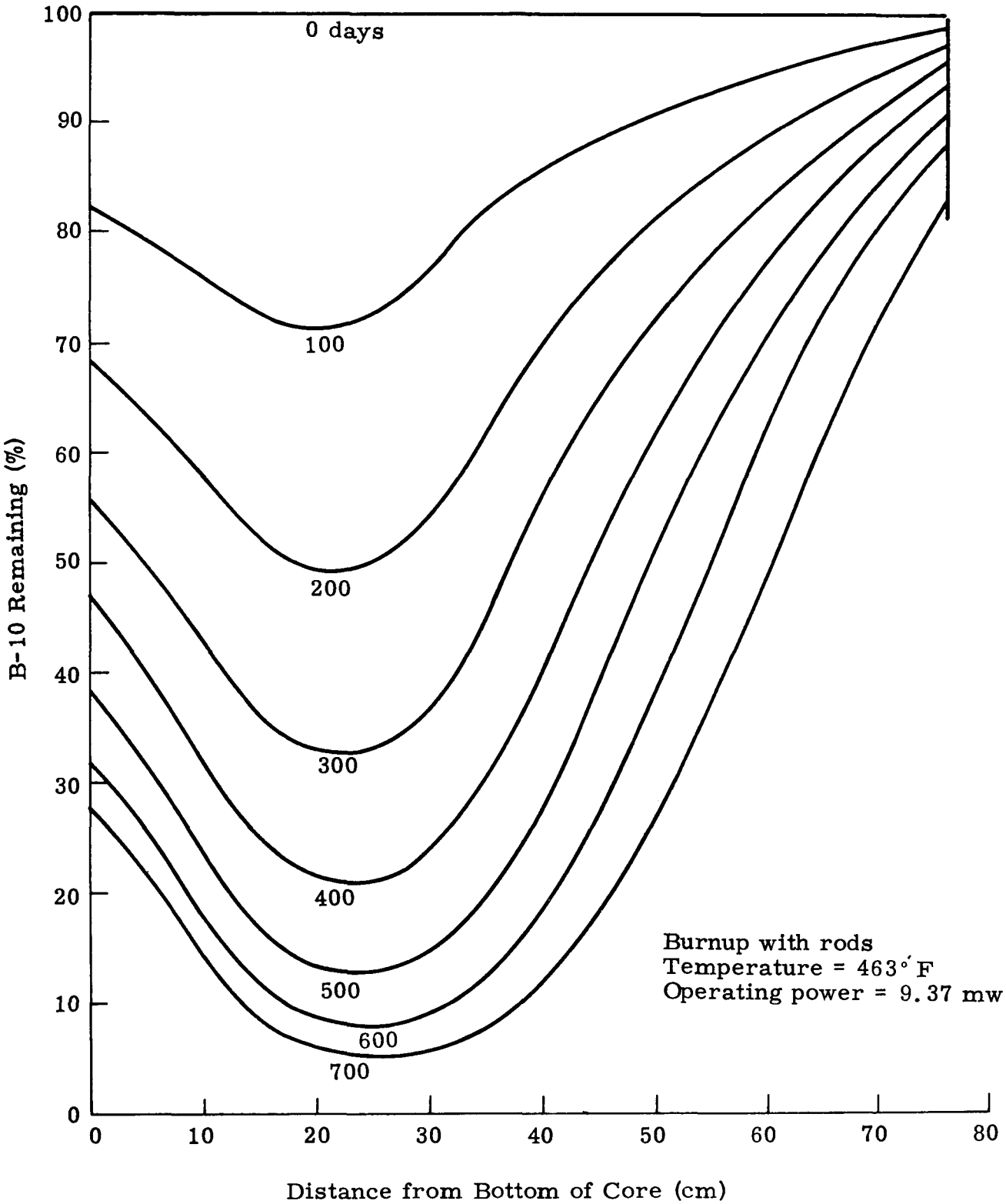

Fig. III-7. Axial Lumped Poison Burnup in PM-1

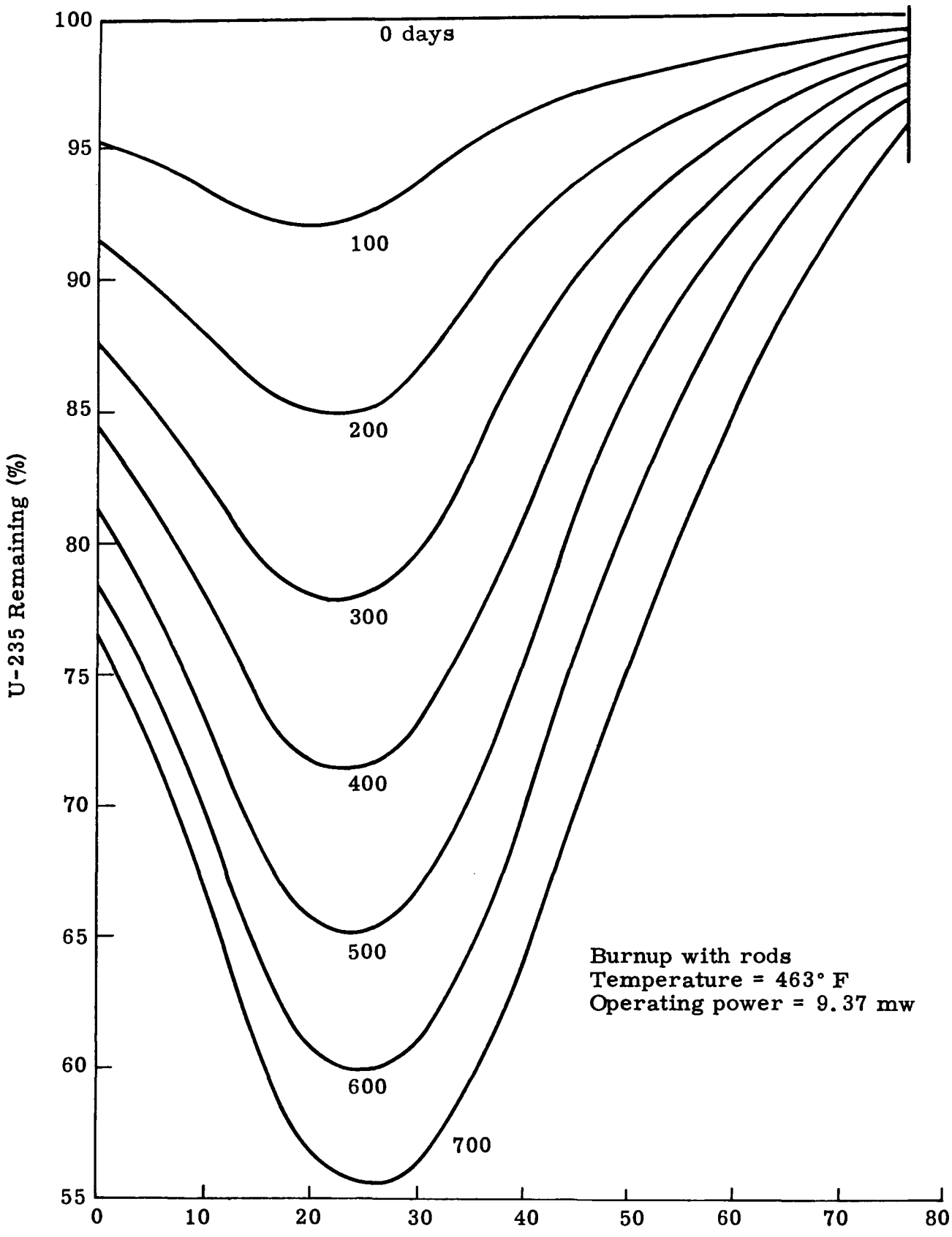

Fig. III-8. Axial Burnup of U-235 in PM-1

TABLE III-9

Reactivity Effect of Boron and Stainless Steel in Lumped Poison Rods

Material Removed	ρ (68° F)	$\Delta\rho$ (68° F)	ρ (463° F)	$\Delta\rho$ (463° F)	No. LPR's	$\Delta\rho$/LPR (68° F)	$\Delta\rho$/LPR (463° F)
Boron Region 3	0.15976	-0.02703	0.12226	-0.03146	24	-0.00113	-0.00131
Boron Region 4	0.16948	-0.03675	0.13292	-0.04212	30 + 18*	-0.00088	-0.00100
Boron Region 5	0.14261	-0.00988	0.10258	-0.01178	18	-0.00055	-0.00065
Boron Regions 3, 4 and 5	0.20266	-0.06996	0.17216	-0.08136	72 + 18*	-0.00083	-0.00097
Boron and SS Regions 3, 4 and 5	0.23330	-0.10057	0.19955	-0.10875	72 + 18*	-0.00120	-0.00129
None	0.13273	0.0	0.09080	0.0	72 + 18*		

* Indicates 2/3 length boron rod; remaining length SS
$\Delta\rho$ Indicates average reactivity change over region considered

The values of the maximum burnup after 675 days of core life are 97.9% and 61.7% for the B-10 and U-235, respectively.

H. XENON REACTIVITY WORTH

Xenon, due to its high cross section, short half life and relatively high production rate, is of particular concern over the life of the core. Therefore, it is treated in somewhat more detail than the remaining fission products.

1. Cold Reactivity, No Xenon (Early Life)

The maximum reactivities experienced in the PM-1 occur at the beginning of life, without xenon present. The stuck control rod criteria is such that the maximum reactivity caused by shutdown after a few days of operation is also important. Therefore, the cold (68° F) reactivity with no xenon present was calculated during the early portion of core life. The results are shown plotted in Fig. III-9 and are tabulated in Table III-10.

TABLE III-10

Cold Core Reactivity, No Xenon (68° F)

Days Burnup	ρ
0	0.13273
100	0.11960
200	0.11450
300	0.11014

2. Hot Reactivity, Xenon Buildup (Beginning of Life)

During the initial phase of the core life, the xenon concentration is built up rapidly, approaching its equilibrium value after about four days of full power operation.

The hot reactivity of the PM-1 core during the first few days of operation was calculated to follow the xenon buildup. By extrapolating back to time zero, the initial reactivity worth of equilibrium xenon can be obtained. The results are shown plotted in Fig. III-9 and are tabulated in Table III-11.

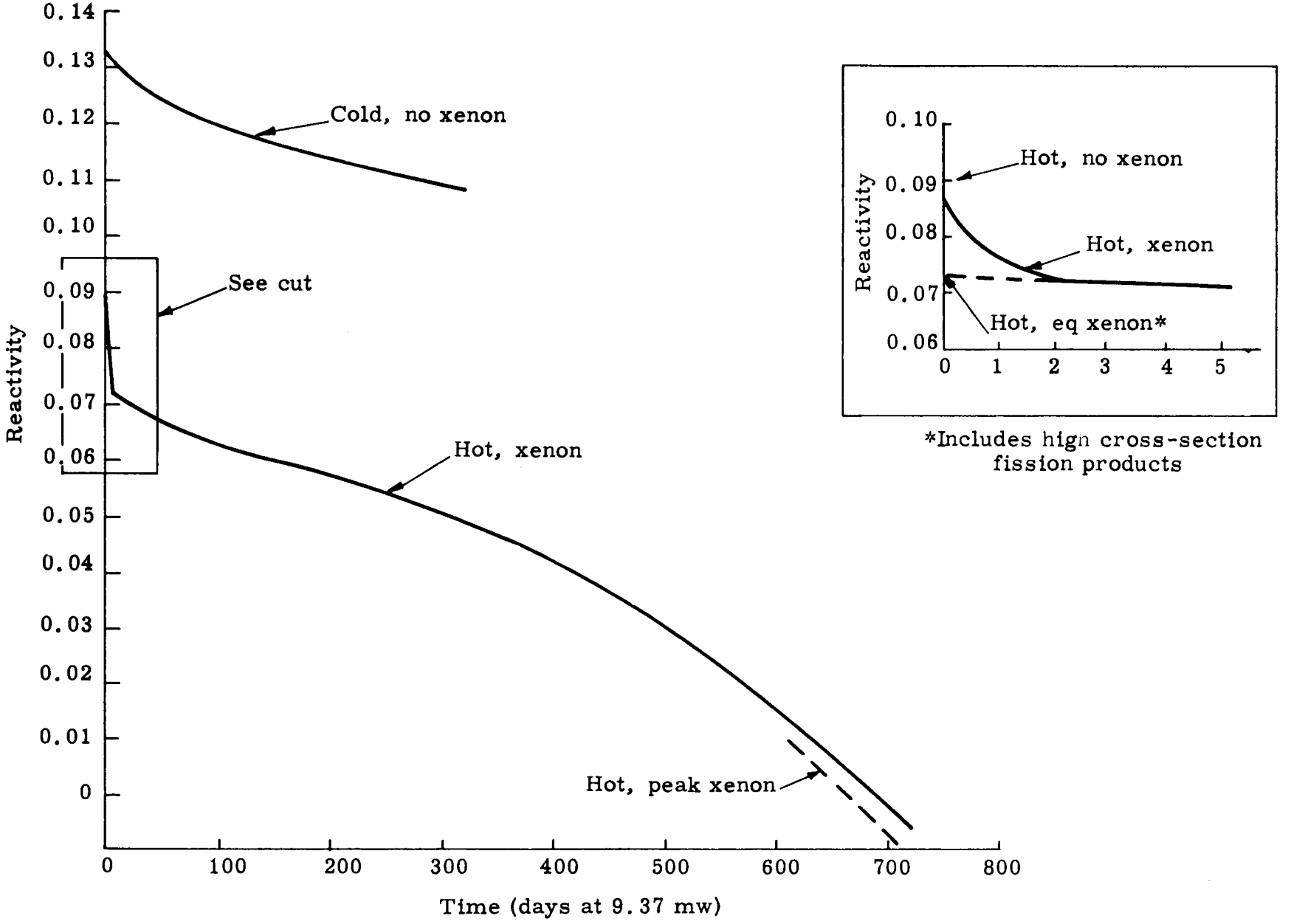

Fig. III-9. Xenon Reactivity Worth During Core Life--68° and 463° F

TABLE III-11

Reactivity During Xenon Buildup (463° F, 9.37 mw)

Hours	ρ
0 (no xenon)	0.09080
8	0.08561
24	0.07594
0 (equilibrium xenon)	0.07217

From the results in Table III-11, it can be seen that the worth of equilibrium xenon at time zero is 1.86% $\Delta\rho$.*

3. Hot Reactivity, Peak Xenon (End of Life)

When the reactor is shut down after sustained power operation, peak xenon builds, causing a temporary reduction in the core reactivity. If the shutdown occurs very near the end of core life, the loss in reactivity can prevent the reactor from being brought up to power until a portion of the xenon has decayed.

The peak xenon atom concentration was calculated for the PM-1 after 700 days of full power operation (end of life), by Eq. (III-2).

$$Xe_{max} = Xe_o \left(\frac{1 + \left[\frac{\lambda_1 + \lambda_2}{\lambda_1} \right] \cdot \frac{Xe_o}{I_o}}{\frac{\lambda_1}{\lambda_2}} \right)^{\frac{\lambda_2}{\lambda_1 - \lambda_2}} \cdot 1 - \left(\frac{\lambda_2}{\lambda_1} + \frac{I_o}{Xe_o} \right) \qquad \text{(III-2)}$$

and

$$I_o = \frac{\gamma_1}{\lambda_1} \cdot F_D$$

*Obtained by extrapolating data in Fig. III-9 back to zero time.

where:

Xe_{max} = Maximum Xe-135 atom density (at/cm^3)

Xe_o = Equilibrium Xe-135 atom density (at/cm^3)

I_o = Equilibrium I-135 atom density (at/cm^3)

F_D = Fission density before shutdown (fiss/cm^3-sec)

λ_1 = I-135 decay constant (2.87×10^{-5} sec^{-1})

λ_2 = Xe-135 decay constant (2.09×10^{-5} sec^{-1})

γ_1 = I-135 yield/fission (0.061 at/fiss)

γ_2 = Xe-135 yield/fission (0.002 at/fiss) (Value used in calculating Xe_o)

The reactivity worth of peak xenon above that for equilibrium, calculated after 700 days of core life is -0.460% $\Delta\rho$. This point is plotted on Fig. III-13 for comparison purposes.

4. Reactivity Worth of High Cross-Section Fission Products (End of Life)

The fission products utilized in the calculation of core lifetime are divided into two groups: the high cross-section and the low cross section fission products. The reactivity worth of the high cross-section fission products was calculated at the end of life (700 days) and found to be 0.891% ρ.

I. WORTH OF BORON AND STAINLESS STEEL IN LUMP POISON RODS (END OF LIFE)

The reactivity worth of the boron and stainless steel in the lumped poison rods at the beginning of life has been discussed. As the core is operated over its life, fuel and boron are depleted, resulting in a decrease of core blackness or overall neutron absorption characteristics. Since the steel in the LPR's does not burn out, it should contribute a larger fraction to core absorption at the end of life and thus be worth more in terms of reactivity. To determine its worth, the steel in the LPR's was removed after 700 days of operation and the increase in core reactivity calculated. The basic six-region core model, with all the fission products present, was used. The results are given in Table III-12.

In any core which contains a burnable poison material, the optimum condition at the end of life is to have burned all the poison and thus not have the core life shortned by residual neutron capture. Of course, this condition is unattainable, so the next best thing is to come as close to the optimum as possible. In Fig. III-6, it is shown that the percent of B-10 remaining after 700 days of operation varies between roughly 10% and 30%. Because of the relatively high concentration remaining, the B-10 reactivity worth at the end of life was analyzed. The results are shown in Table III-12.

TABLE III-12

Reactivity Worth of B-10 and Stainless Steel in the Lumped Poison Rods (463° F, 9.37 mw)

Material	$\Delta\rho$	Days
Stainless steel	0.03845	700
Boron-10	0.02521	700
Stainless steel	0.02739	0
Boron-10	0.08136	0

It is worthwhile to note that at the end of life the steel in the LPR's has a reactivity worth of over 150% of that of the boron. The data indicates that a substantial increase in core life could be obtained if the steel in the LPR's were reduced or eliminated.

J. REACTOR CONTROL

The analysis of the effect of control rods on the reactivity of a reactor is, in general, a fairly difficult problem; and the results usually contain a degree of uncertainty. However, in the PM-1, a series of critical experiments was performed on a core which was practically identical to the final design core. The control rod measurements which were made in these experiments were normalized to the present core and used as end points in the calculations. This technique lent considerable credence to the analytic results.

1. Measured Critical Rod Bank Position

Control rod bank evaluations were performed experimentally on the reference design mockup described in the appendix. The control rod configurations investigated are presented in Table III-13.

TABLE III-13

Control Rod Configuration Experimental Evaluations
(reference design mockup, 68° F)

Experiment No.	No. of Rods Withdrawn	No. of Rods in Critical Bank	Location of Critical Bank	Comments
1	5	1	Any one rod	Stuck rod condition
3	2	4	Adjacent rods	Stuck rod condition
4	1	5	Adjacent rods	Stuck rod condition
5	0	6	All rods	Operating condition
Experiment No.	**No. of Rods Inserted**	**No. of Rods in Critical Bank**	**Location of Inserted Rods**	**Comments**
6	1	5	Any one rod	Stuck rod condition
7	4	2	Adjacent rods	Stuck rod condition

The critical bank position was determined for each obtainable bank configuration. At each of the reactivity levels established during the measurements of critical bank position, the total core reactivity was evaluated.

The results of the study, corrected for the 0.14% reactivity difference between the mockup core and the final design core, are given in Figs. III-10 and III-11. The measurable critical bank positions and the total rod worths are tabulated in Tables III-14 and III-15, respectively.

TABLE III-14

Measured Critical Bank Positions
(normalized to final design core, 68° F)

Experiment No.	Bank Description	Critical Position (in. withdrawn)
4	5 rod bank--1 full out	3.90
5	6 rod bank	8.25
6	5 rod bank--1 full in	9.25
7	2 rod bank--4 full in	15.00

TABLE III-15

Measured Full Insertion Rod Reactivity Worth
(normalized to final design core, 68° F)

No. Rods Inserted	No. Rods Withdrawn	Worth (%ρ)
1	5	-2.37
3*	3	-9.19
4*	2	-8.83
5	1	-13.66

*Configuration as given in Table III-13.

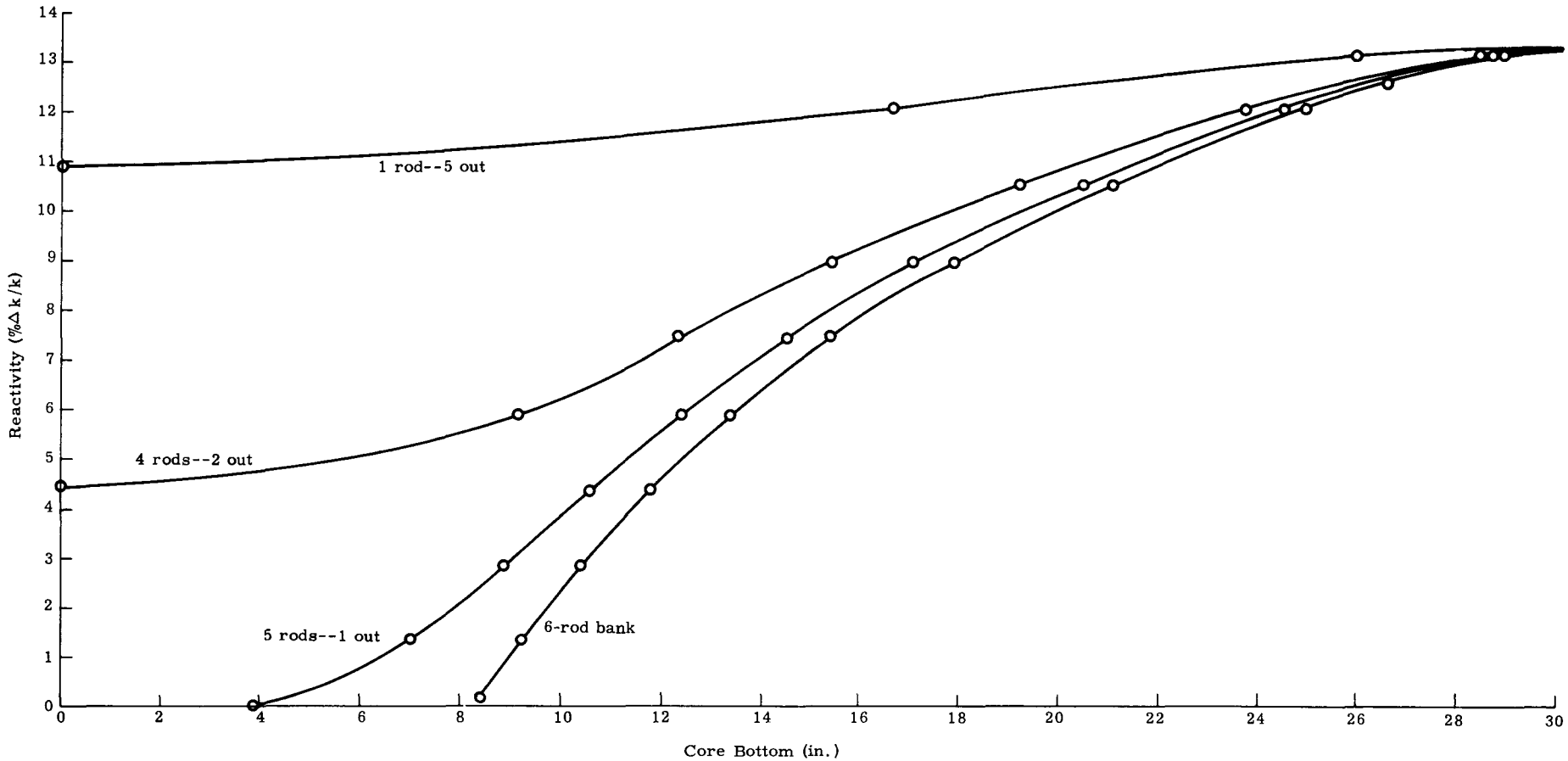

Fig. III-10. Experimental Rod Worth Versus Withdrawal for Banks with Rods Out--Reference Design Core

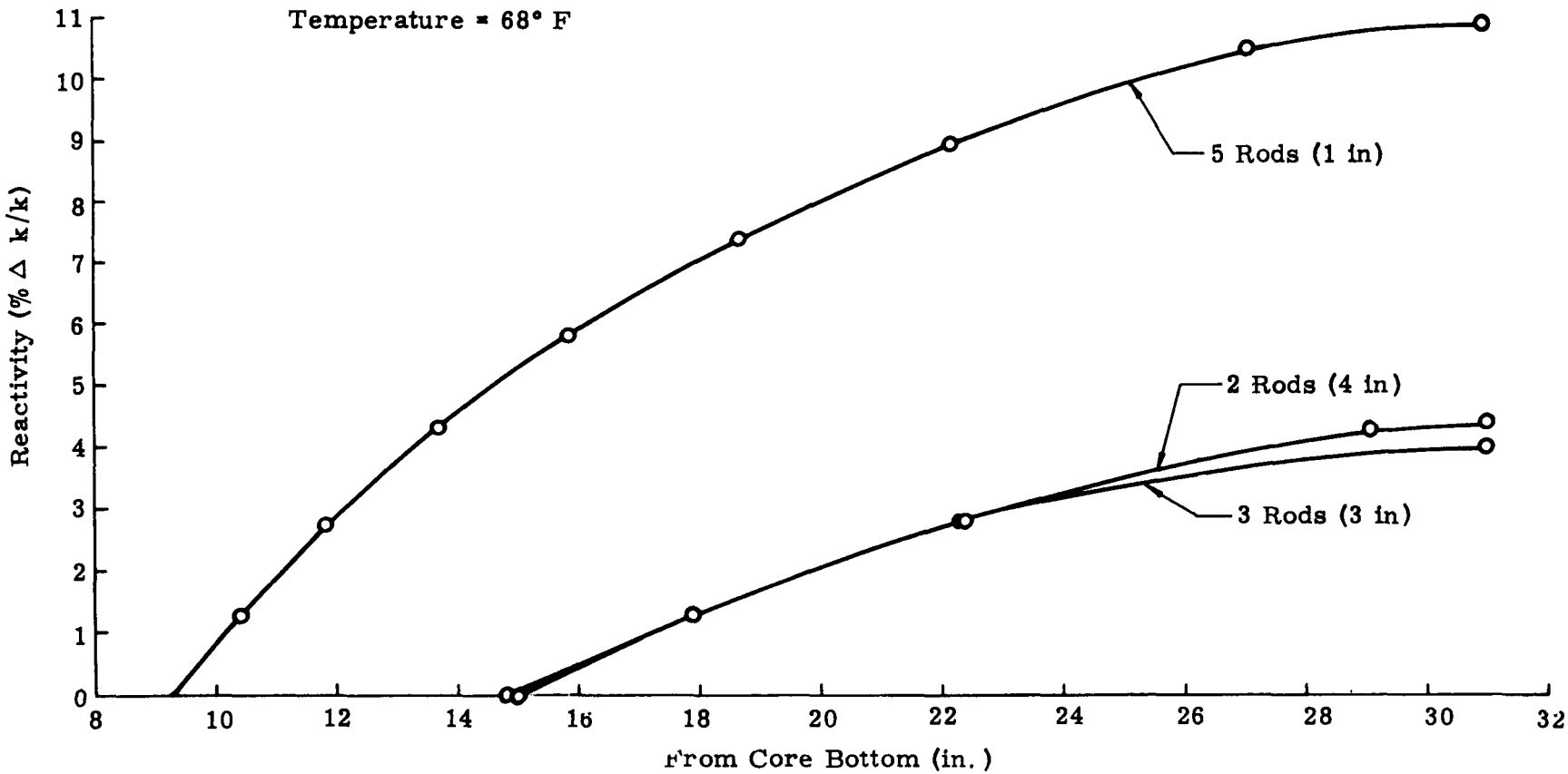

Fig. III-11. Experimental Rod Worth Versus Withdrawal for Banks with Rods Inserted--Temperature = 68° F

The data in Fig. III-10 and Table III-15 clearly show that the criterion of subcriticality with one rod stuck in the withdrawn position will be met. The shutdown margin of the five remaining rods is from full insertion to 3.9 inches withdrawn. The margin was measured by adding fuel to the core edge to increase the core reactivity so that the five-rod bank could be fully inserted. Period measurements from full insertion to 3.9 inches withdrawn showed the margin to be 0.38% reactivity.

2. Control Rod Worth Versus Insertion

The control rod worth as a function of six-rod bank position was calculated utilizing the "window shade" technique. The details of this calculation were described under "Total Nonuniform Burnup with Control Rods."

The calculation of the worth versus insertion at 463° F was performed in the same manner as for 68° F, except the worth of the rods at the hot critical bank position was increased by 0.45% reactivity over the cold rod worth at that position. The increase was necessary to compensate for the change in blackness of the core due to temperature. The magnitude of the increase was based on the change in the experimental rod worths of the two PMZ cores whose change in blackness gave them a difference in reactivity similar to the cold-to-hot change in reactivity of the PM-1. It was realized that the extrapolation was only approximate, so the results were checked using blackness theory and were found to be conservative.

The resulting rod worths versus insertion, both hot and cold, are presented in Fig. III-13. The fully inserted six-rod bank worths are given in Table III-16.

TABLE III-16

Six-Rod Bank Reactivity Worth, Fully Inserted

Temperature	% Reactivity
68° F	-20.22
463° F	-23.05

3. Comparison of Analytic and Measured Rod Worth Versus Insertion

Experimental rod worth from the critical six-rod bank position (8.25 inches withdrawn) to full withdrawal was obtained as outlined above for the PM-1 reference design core. An analytical rod worth-versus-insertion curve of the six-rod bank was obtained over the full

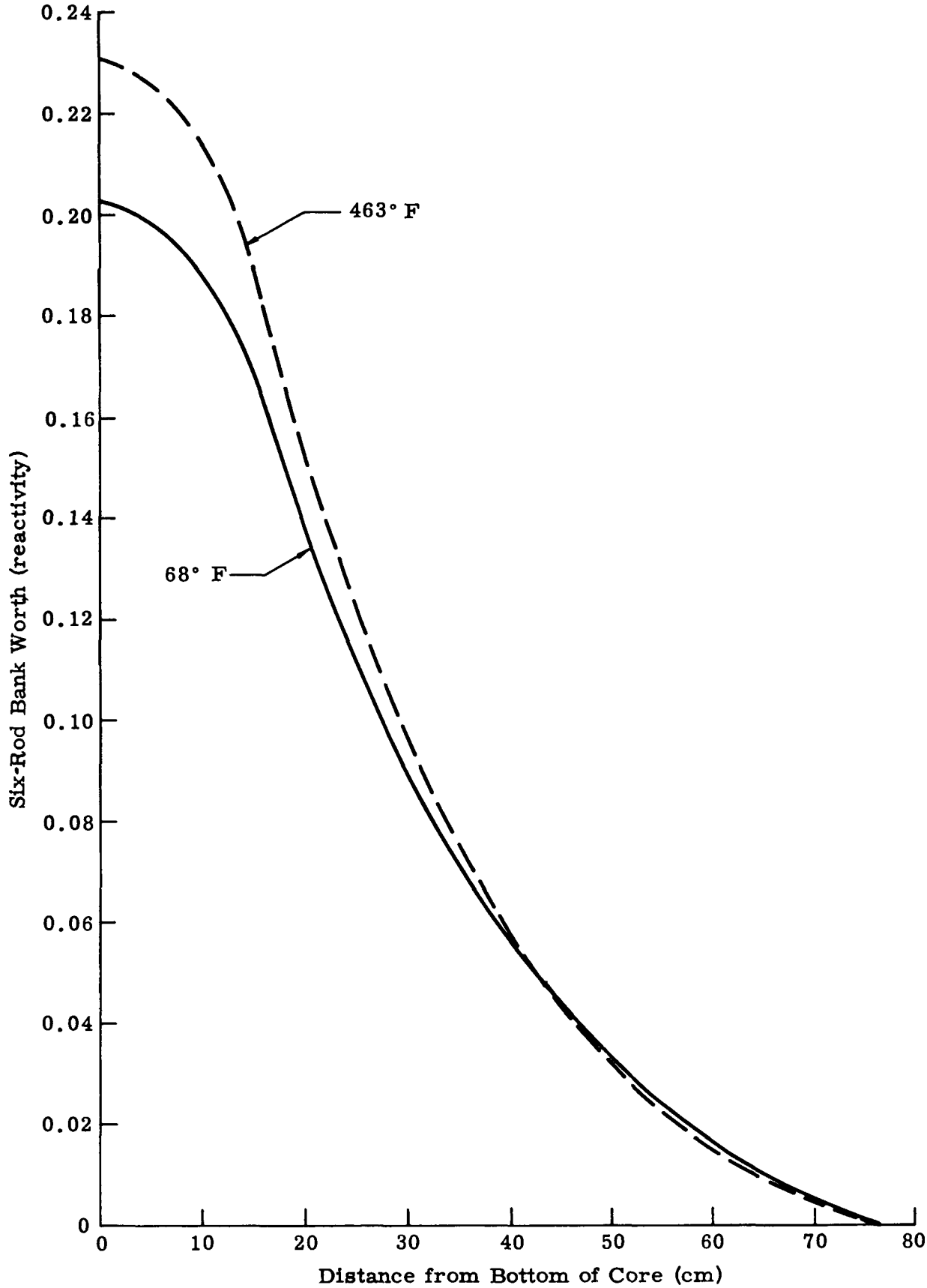

Fig. III-12. PM-1 Six-Rod Bank Worth as a Function of Distance Withdrawn from the Core Bottom

core length from a series of window shade calculations. The results are compared in Fig. III-13, which shows excellent agreement between analytical and experimental values over the measured portion of the bank.

4. Hot-to-Cold Rod Worth Change

In general, the worth of control rods increases as the temperature of the core is raised. The increase is due to a change in overall blackness of the core relative to that of the control rods. To gain a better insight into the magnitude of the change in rod worth with temperature, a series of calculations were performed utilizing Blackness Theory (Ref. 11).

The calculations consisted of determining the reactivity of a homogenized PM-1 core both with and without a 0.25-inch thick ring of europium absorber. * The ring was located at the radius of six inches from the center of the core to approximate the control rods. The calculations were performed using the diffusion theory program, F_3. The constants for the rod region were obtained from blackness theory and are given in Table III-17.

TABLE III-17

Blackness Theory Constants for a 0.25-Inch Slab

(30 wt % $Eu_2 O_3$ in SS)

Constants*	Temperature	
	68° F	463° F
Σ_1^a	1.9030×10^{-2}	1.9030×10^{-2}
Σ_2^a	6.6291×10^{-1}	6.3723×10^{-1}
Σ_3^a	2.4952	2.4615
D_1	9.5815×10^{-1}	9.5815×10^{-1}
D_2	2.0563×10^{-1}	2.1083×10^{-1}
D_3	4.7000×10^{-4}	1.8700×10^{-3}

* Based on one internal mesh point

---

* 30 wt % $Eu_2 O_3$ in stainless steel

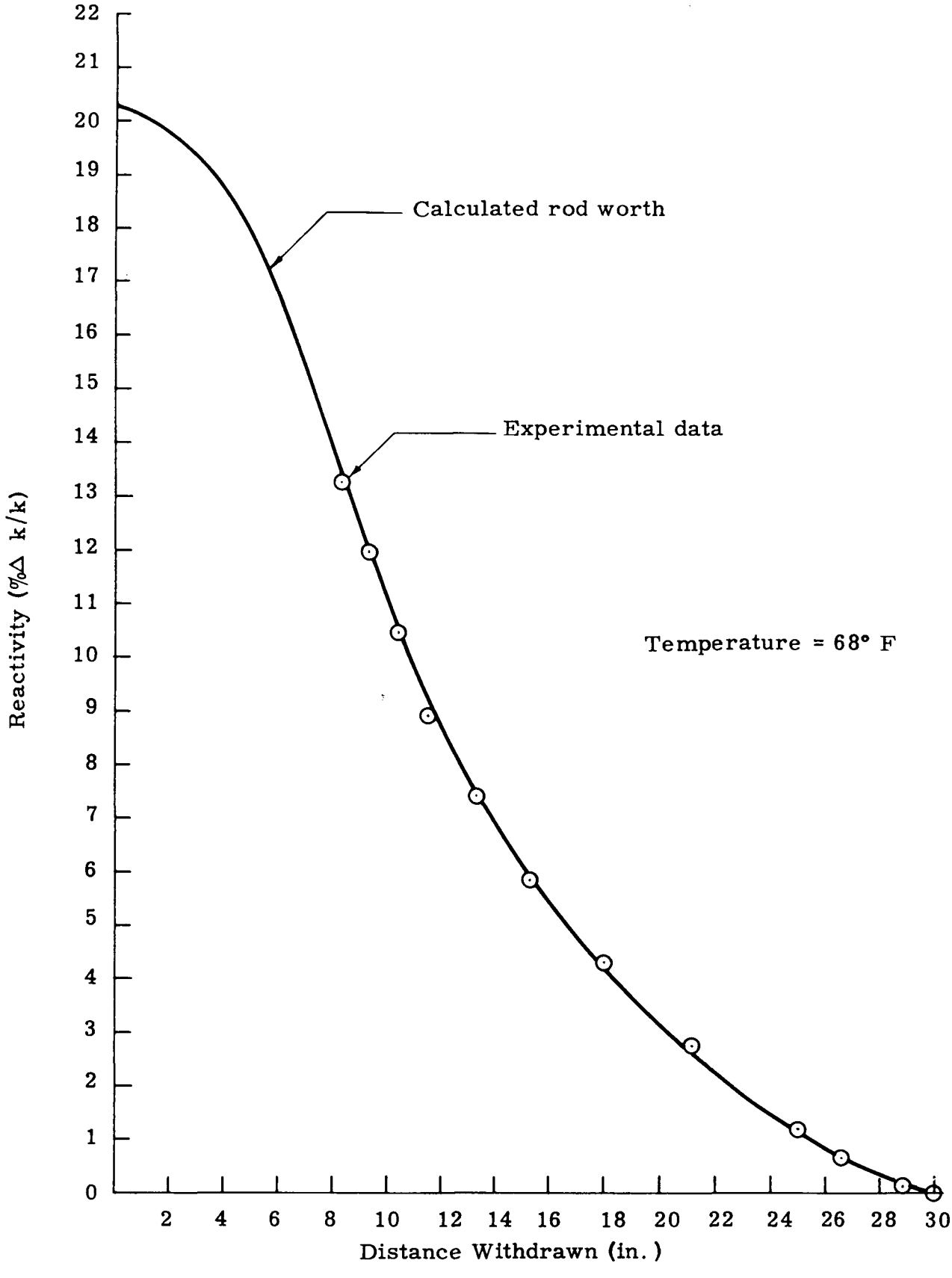

Fig. III-13. Comparison of Rod Worth Versus Withdrawal Distance for PM-1 Six-Rod Bank

The change in the worth of the absorber between 68° F and 463° F was inferred by determining the hot-to-cold change in core reactivity without the absorber and subtracting this from the hot-to-cold change with the absorber inserted. The worth of the absorber, hot and cold, and the percentage change is shown in Table III-18.

TABLE III-18

Worth of a $Eu_2 O_3$ Absorber Inserted in the PM-1 Core

Temperature (°F)	Reactivity
463	-0.1664
68	-0.1312
Hot to cold, $\Delta \rho$	-0.00355

The hot-to-cold change in reactivity worth of the europium ring, as shown in Table III-18, is 0.1% greater than that determined for the PM-1 with the control rods fully inserted. Although the results are not directly comparable, they tend to indicate that the hot worth of the PM-1 rods is probably conservative.

5. Critical Bank Position Versus Core Life

During the analysis of the axial nonuniform burnup with control rods, the withdrawal of the rods with core energy release was calculated. The above data has been plotted in Fig. III-14 in terms of six-rod bank insertion versus megawatt years. This information is of particular interest because it can be followed during the burnout of the operating reactor. Therefore, it gives an indication of the accuracy of the burnout calculation within the limitations imposed by errors in measuring the core energy release.

The initial hot critical six-rod bank position, both with and without equilibrium xenon, is given in Table III-19.

TABLE III-19

Initial Six-Rod Bank Position, 463° F

No xenon	30.5 cm withdrawn
Equilibrium xenon	37.2 cm withdrawn

The value of the initial bank position with equilibrium xenon was obtained by extrapolating back to time zero from the first time step in the burnup calculation.

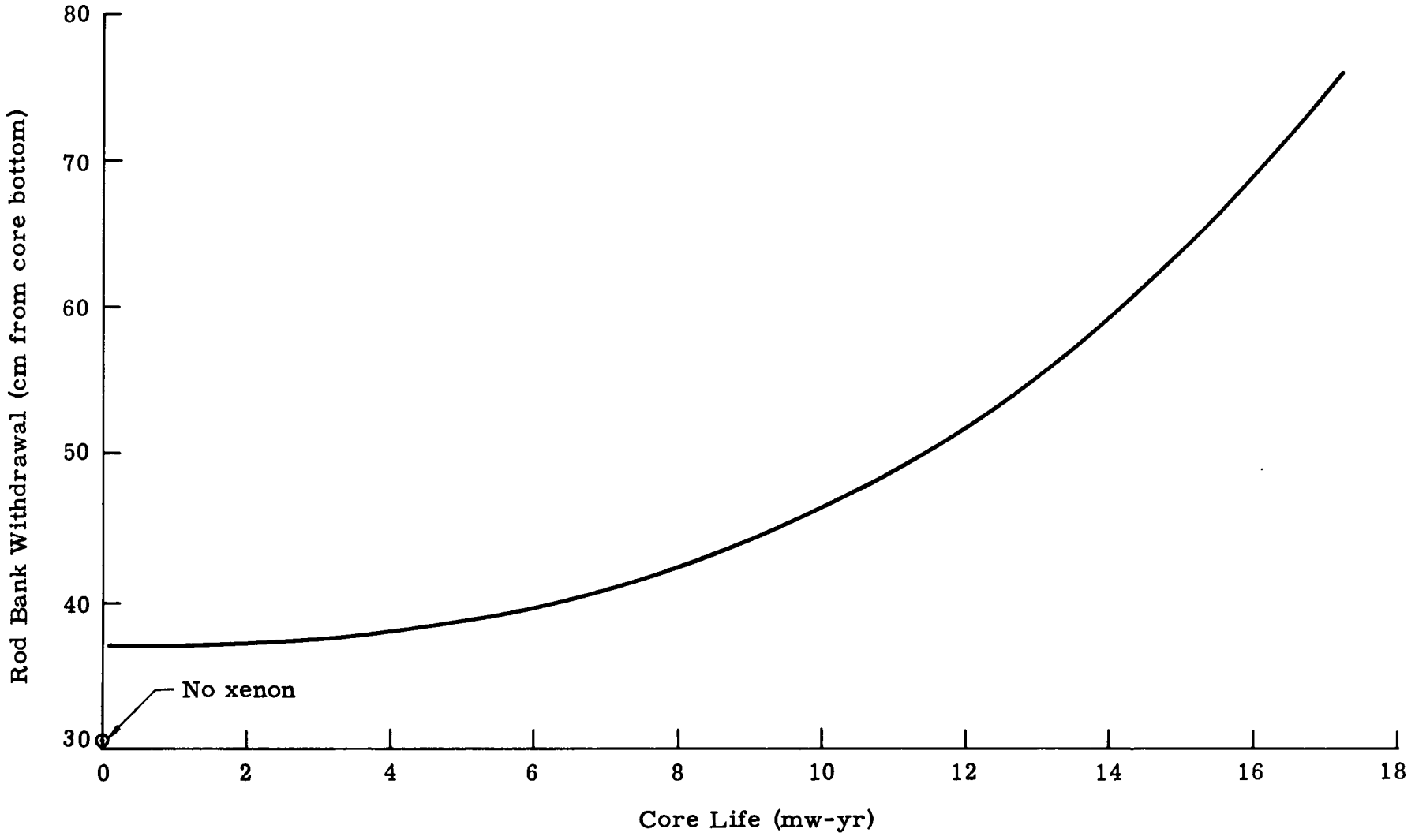

Fig. III-14. Six-Rod Bank Position Throughout Core Life of PM-1

6. Shutdown Reactivity Versus Life

The ability of the control system to meet the stuck rod requirements was evaluated by using experimental cold control rod worths and calculated reactivities as a function of life.

The one rod stuck out condition was evaluated by using the experimentally determined five-rod bank worth of 13.66%. The initial cold reactivity of 13.28% yields a shutdown margin for one rod stuck out of 0.38% at the beginning of life. The cold reactivity of the core as a function of life was obtained by recalculating the nonuniform depletion case with cold contents, no xenon, and equilibrium fission products at various times in life. Table III-20 summarizes the results obtained in this study. Figure III-15 shows these results graphically. From the results, it is quite clear that the condition of one rod stuck full out is met at all times in life with the least margin (0.38%) occurring at the beginning of life.

TABLE III-20

Cold Reactivity Shutdown Margin for One Rod Fully Withdrawn, 68° F

(five-rod bank worth, 0.1366 ρ)

Core Life (days)	Core Reactivity	$\Delta\rho$ (with life)	Shutdown Margin (ρ)
0	0.1328	0	-0.0038
100	0.1191	-0.0137	-0.0175
200	0.1138	-0.0190	-0.0228
300	0.1085	-0.0243	-0.0281

The shutdown margin for the two rods stuck condition is more complex, since the six-rod bank position for the operating conditions must be determined, as well as the cold no-xenon equilibrium fission product core reactivity, as a function of life. The most stringent rod pattern for this requirement is the maximum worth of two rods (minimum worth of four rods) which is obtained when the two rods are adjacent. This presents the largest uncontrolled region to the core with the most shadowing of the four-rod bank. This particular pattern was evaluated experimentally, as shown in Fig. III-11, and was used to determine the shutdown margin of the core for the two rod stuck condition. Table III-21 shows the results of the analysis, and Fig. III-15 shows these results graphically.

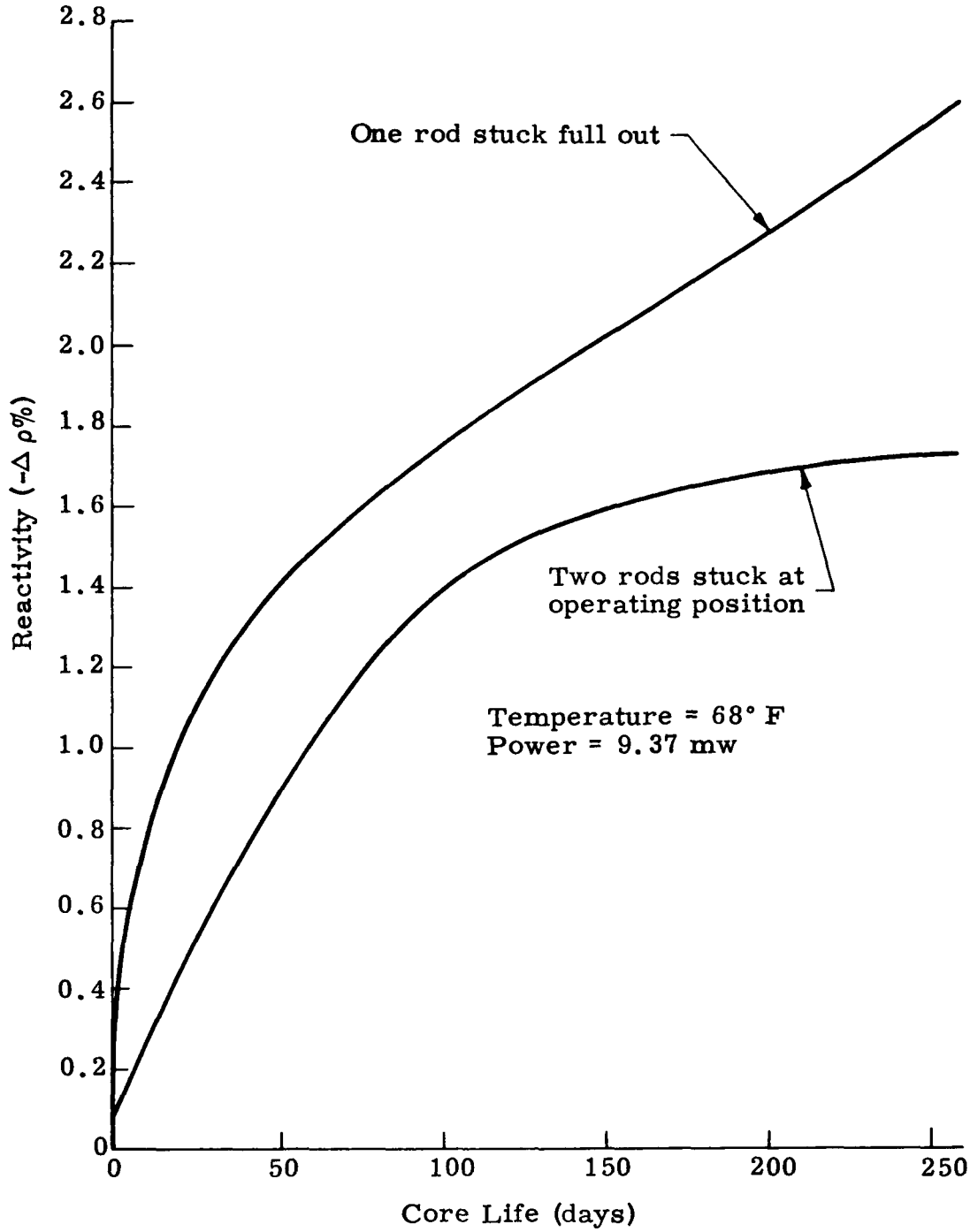

Fig. III-15. Minimum Shutdown Margin Versus Core Life

TABLE III-21

Cold Reactivity Shutdown Margin for Two Rods Stuck at the Operating Position, 68° F

Core Life (days)	Operating Bank Position (inches withdrawn)	Core Reactivity	Critical 2-Rod Bank Position, Four Rods Fully Inserted (inches withdrawn)	Shutdown Margin	
				Inches of the 2-Rod Bank	Reactivity of the 2-Rod Bank ($\Delta\rho$)
0	14.65	0.1328	14.98*	0.25	-0.0010
100	14.85	0.1191	17.90	3.05	-0.0140
200	15.35	0.1138	19.50	4.15	-0.0170
300	16.47	0.1085	20.90	4.43	-0.0170

* Experimental value

From the preceding table it is clear that, while the margin at the beginning of life (-0.10%) is small, it is negative and increases with life.

7. Effect of U-235 Tolerance on the Stuck Rod Criteria

The effect of an increase of 2% in the U-235 loading on the total core reactivity and life was evaluated in Table III-21.

In the present section, the effect of the 2% increase in U-235 loading on the ability to meet the stuck rod criteria is evaluated. Two assumptions were made in the following analysis: (1) the hot-to-cold reactivity change of the core with the increased loading is the same as that of the final design core, and (2) the rod worth is unchanged by the 2% increase in loading.

Using the above assumptions and the methods outlined in Section 6, it was found that the "one rod stuck full out" condition is not met at the beginning of life, but is met thereafter. The results are summarized in Table III-22 and plotted in Fig. III-16.

TABLE III-22

Shutdown Margin with 2% Increase in U-235 Loading

(one rod stuck full out, 68° F)

Core Life (days)	Core Reactivity (ρ)	Shutdown Margin (ρ)
0	0.1376	+0.0010
100	0.1242	-0.0124
200	0.1190	-0.0176
300	0.1139	-0.0227

The condition of two rods stuck at the operating bank position was treated as in Section 6. The results indicate that this shutdown criterion is not met at the beginning of life either, but it is met shortly thereafter. The results are tabulated in Table III-23 and are included on Fig. III-16. If this situation should occur, the initial reactivity will be decreased as described previously.

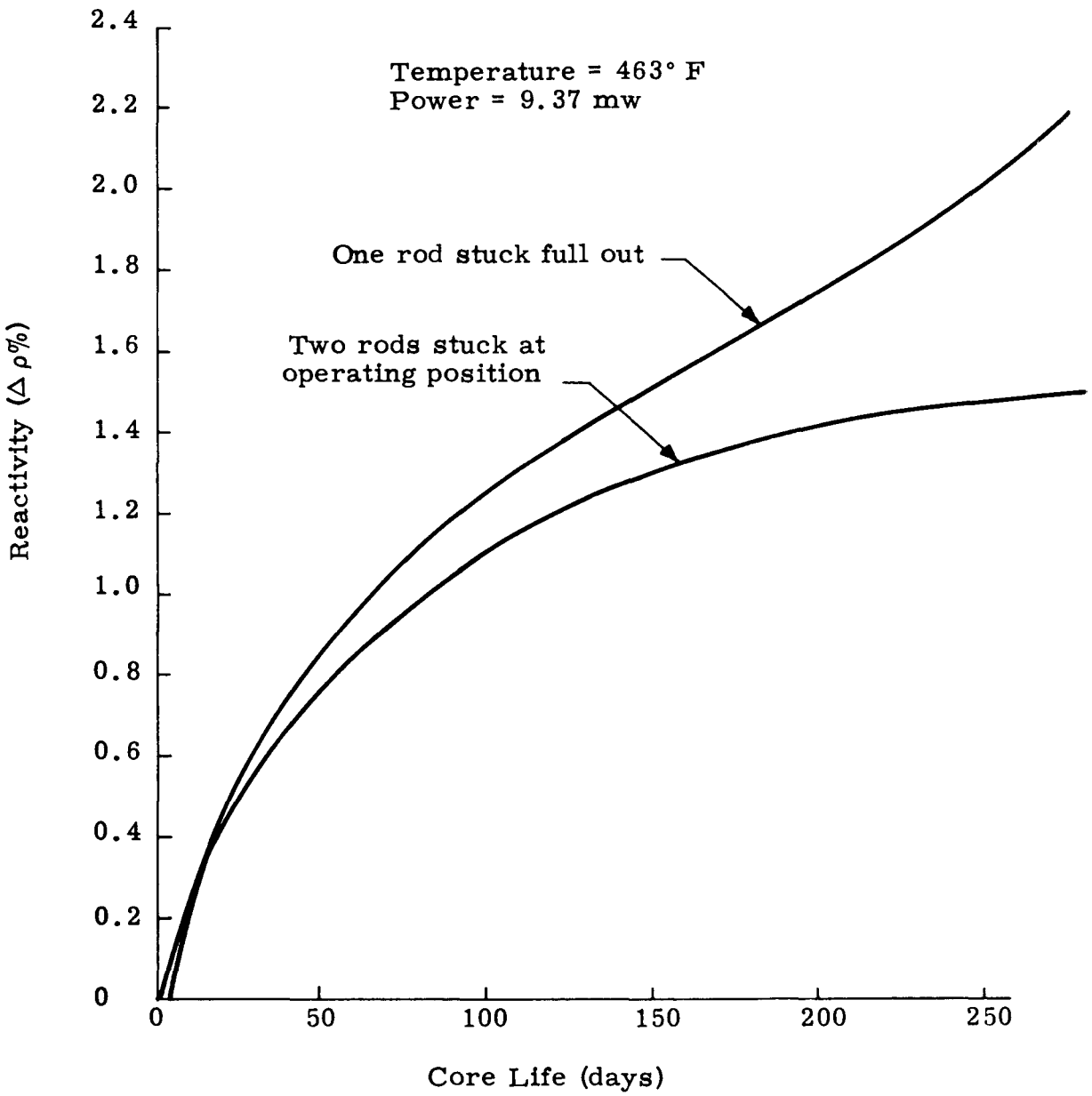

Fig. III-16. Minimum Shutdown Margin for a Two-Percent Increase in U-235 Loading Versus Core Life

TABLE III-23

Shutdown Margin with 2% Increase in U-235 Loading

(two rods stuck in operating position, 68° F)

Core Life (days)	Operating Bank Position	Core Reactivity Cold	Shutdown Margin
0	14.1	0.1376	+0.0010
100	14.3	0.1242	-0.0111
200	14.8	0.1190	-0.0143
300	15.8	0.1139	-0.0149

K. POWER DISTRIBUTIONS

1. Axial and Radial Power Distributions

The axial and radial power density distributions over the life of the PM-1 core were determined from the results of the nonuniform burnup calculation. The axial power distribution, which is plotted in Fig. III-17 for zero, 400 and 600 days of life, reflects the effect of control rod movement during the life of the core. The radial power distribution is shown in Fig. III-18 for zero, 400 and 700 days. Referring to this figure, it can be seen that the power level peaks at a radius of about 4 centimeters, then drops sharply to a low level and rises again to about a 7.5-centimeter radius. The low level of power density in this region is caused by the lack of fuel. The six inner control rod guides occupy most of the space. Since there is little fuel in this region, the neutron absorption is low and the neutron flux quite high. The high neutron flux overflows into the adjacent regions, causing the power to peak.

Axial power peaking occurs just below the end of the control rods and at the very bottom of the core.

a. Fast, epithermal and thermal power split

The PM-1 is usually referred to as a thermal reactor; however, like most compact heavily loaded cores, it has a large percentage of epithermal fissions.

The fractions of thermal, epithermal and fast fissions occurring over the life of the core are shown in Fig. III-19. The epithermal group, which extends from just above thermal to a lethargy of six, accounts for about 1/3 of all fissions. Fissions in the fast group account for less than two percent of the total, the remainder being thermal.

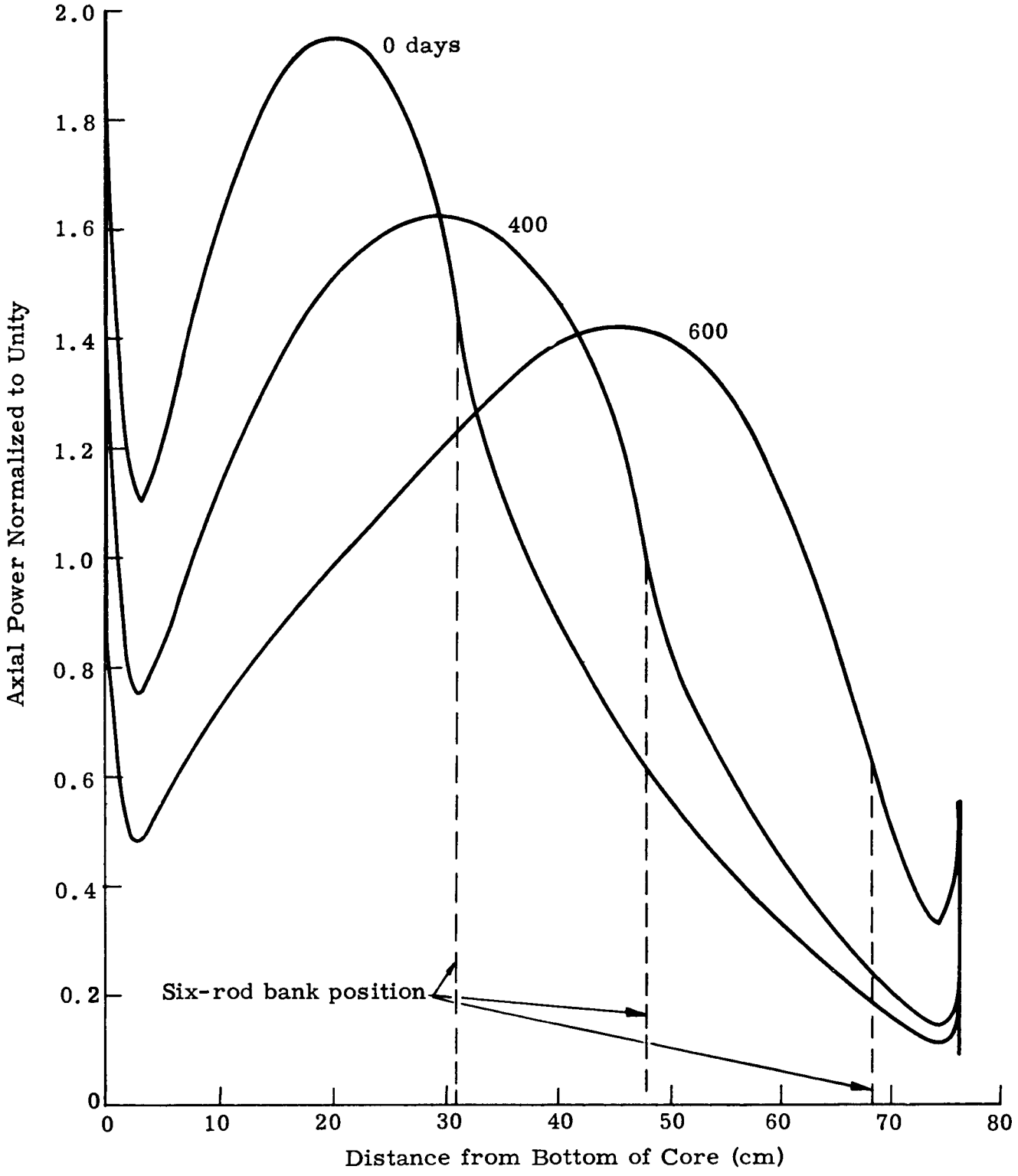

Fig. III-17. Axial Power Density Distribution in PM-1 Operating Conditions

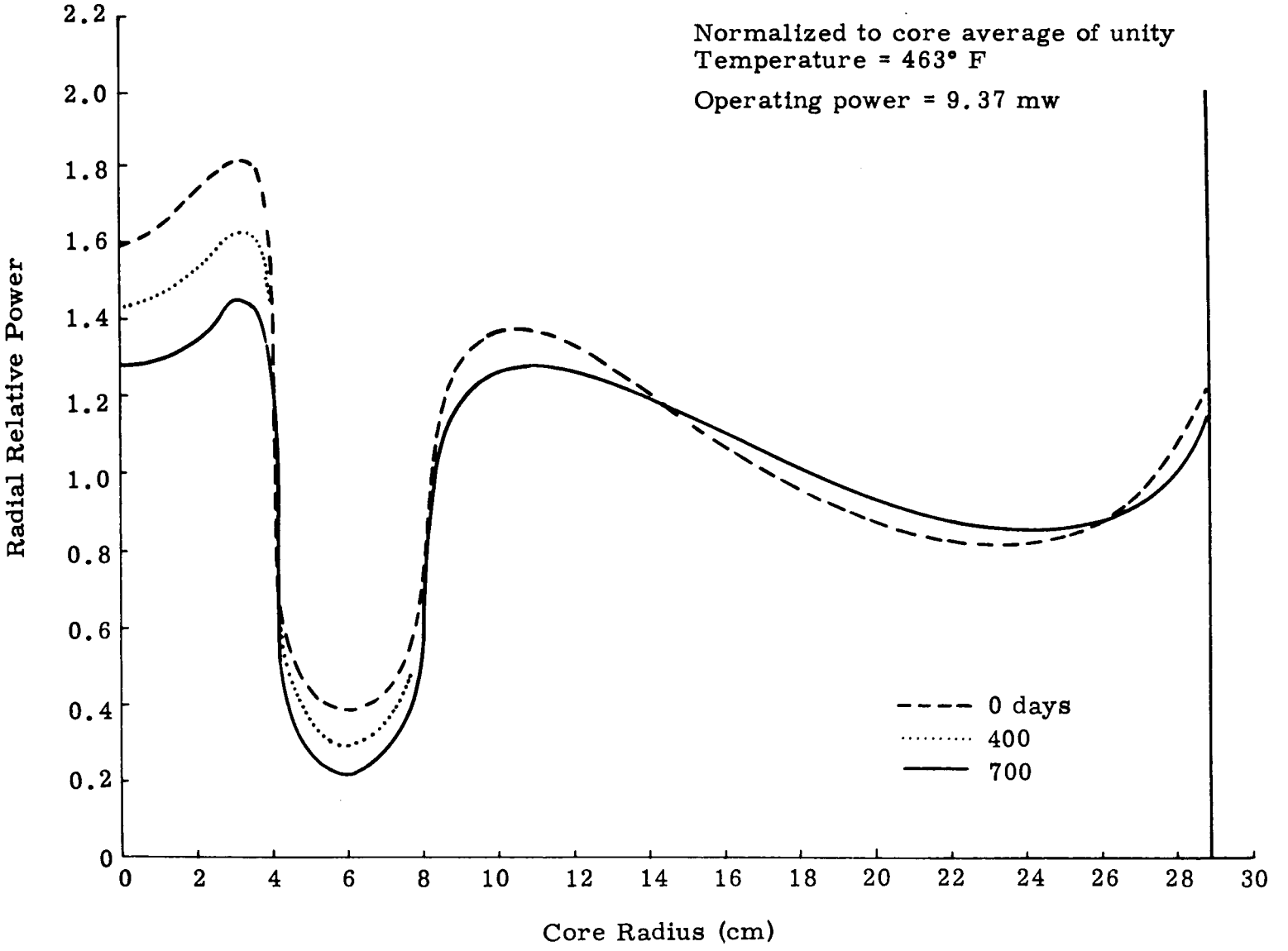

Fig. III-18. Radial Relative Power Distribution

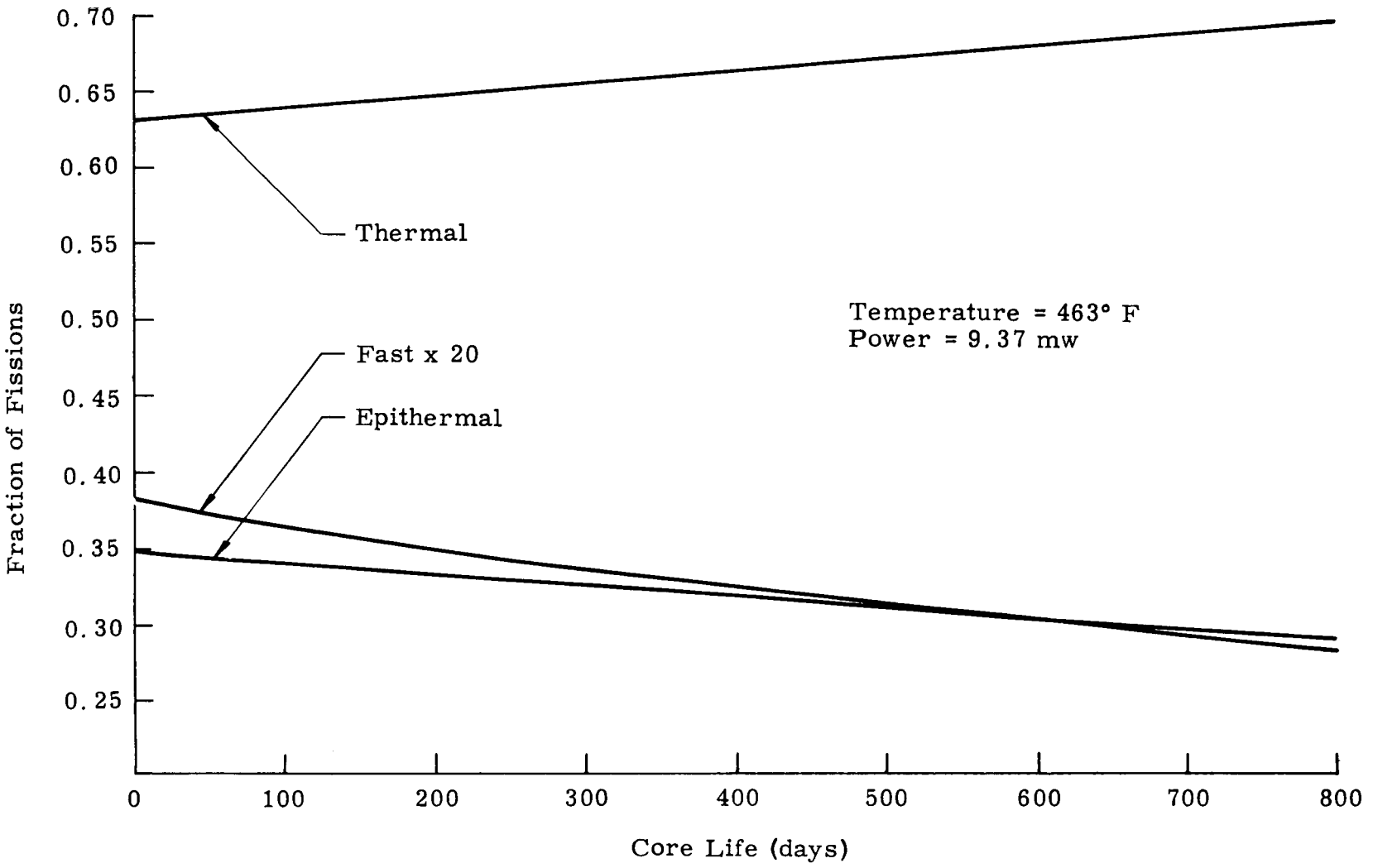

Fig. III-19. Three-Group Fission Fractions

b. Maximum-to-average power during burnup

The maximum-to-average power density occurring over the life of the core has been determined and is presented in Fig. III-20. The highest power peaks occur at the beginning of life. The axial and radial values are 1.95 and 1.83, respectively. The location of the power peak can be seen on the power distribution curves shown in Figs. III-17 and III-18.

c. Temperature coefficient

To assure that a reactor responds in a stable manner to changes in power level or to any change which affects the temperature of the core, it is necessary that the temperature coefficient be negative. The magnitude of the temperature coefficient is related to the speed of response. In general, for pressurized water reactors, a value of about 10^{-4} is very acceptable.

d. Temperature coefficient, beginning and end of life

The temperature coefficient of the PM-1 was evaluated at both the beginning and the end of core life (700 days). The calculations were based on axial geometry, using a 12-region core. The control rods were inserted to their critical bank position through use of the "window-shade" model, which has been described in previous sections. The actual calculations involved determining the core reactivity at 30° F above and below the operating temperature and then evaluating the temperature coefficient at the operating temperature from the change in reactivity with temperature.

The calculations were performed at 68° F and 463° F at the beginning and end of life (700 days). The results are presented in Table III-24.

TABLE III-24

Temperature Coefficient, Beginning and End of Life

Temperature (°F)	$\Delta\rho/\Delta T$(°F)
468, initial	-2.827×10^{-4}
468, end of life	-2.433×10^{-4}
68, initial	-0.675×10^{-4}
68, end of life	-0.650×10^{-4}

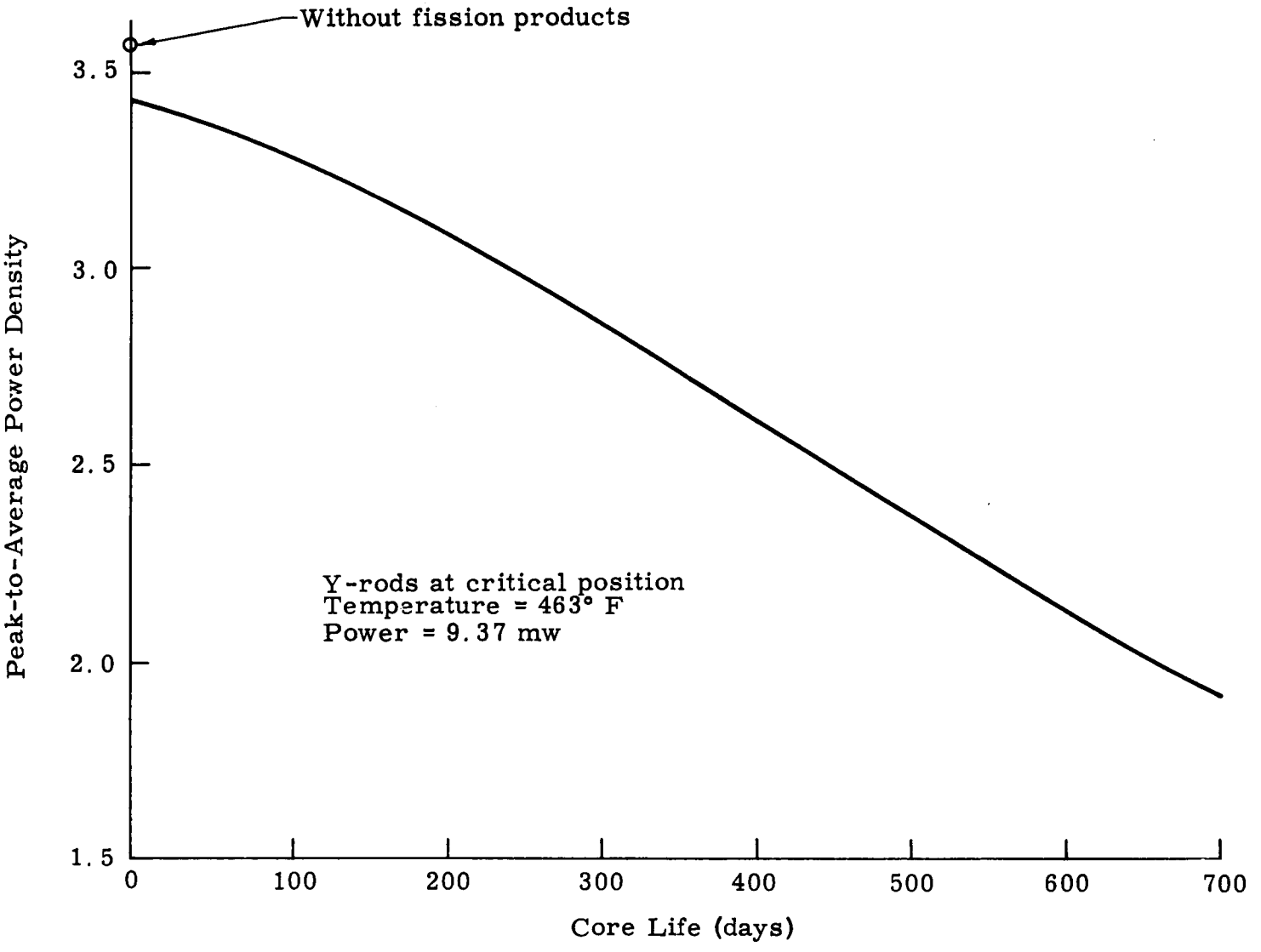

Fig. III-20. Overall Peak-to-Average Power Density for PM-1 Throughout Core Life

From the results in Table III-24, it is seen that the temperature coefficient is negative and slightly decreasing over the life of the core.

e. Measured temperature coefficient

The beginning-of-life temperature coefficient was determined experimentally for the PM-1 reference design core with the six-rod bank at the critical position. The temperature range covered by the experiments was from 77° to 158° F. The temperature coefficient was found to be linear and negative over the entire range. The resulting values for 77° and 158° F are shown in Table III-25. Figure III-21 shows the results obtained experimentally over the entire temperature range.

TABLE III-25

Measured Temperature Coefficients, Beginning of Life

Temperature (°F)	$\Delta\rho/\Delta T(°F)$
77	-0.44×10^{-4}
158	-1.20×10^{-4}

Comparing the calculated temperature coefficient at 68° F (Table III-24) with the measured values, it is seen that the calculated value is high and corresponds to that measured at about 100° F rather than 68° F.

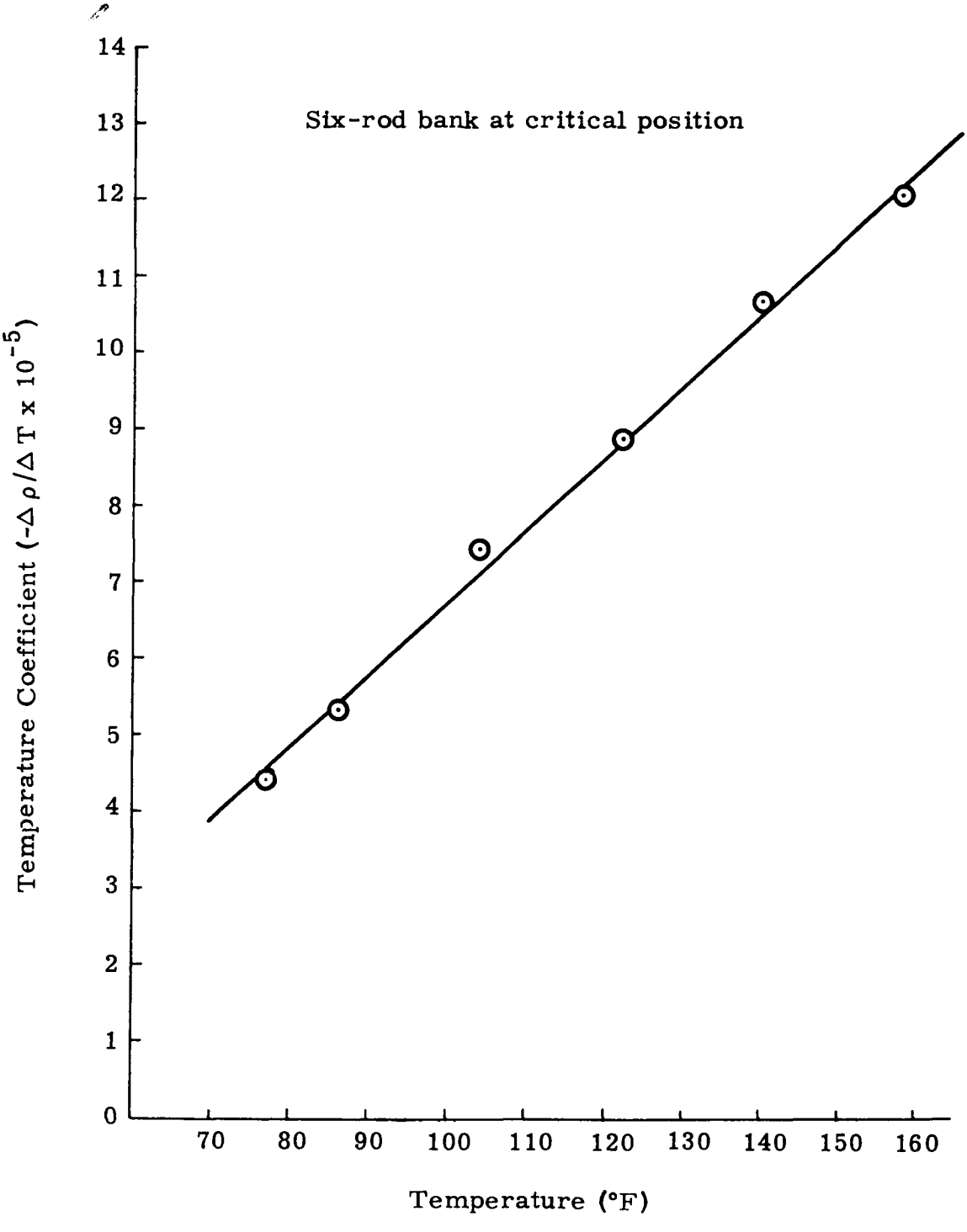

Fig. III-21. Measured Temperature Coefficient

Blank Page

IV. THERMAL AND HYDRAULIC DESIGN

This chapter describes the thermal and hydraulic design for the PM-1 core. Supporting data, test results and analytical techniques required to support the design are to be found in the appendix.

A. DESIGN CRITERIA

The fundamental thermal criteria in the design of this core are that no bulk boiling of the primary loop shall occur and that burnout heat flux shall not be exceeded. The former is found to impose the more severe limitation.

To preclude the existence of bulk boiling, the maximum coolant temperature must be lower than the saturation temperature corresponding to the minimum operating pressure. The pressurizer is designed to limit the minimum operating pressure to 1200 psia, corresponding to a saturation temperature of 567.2° F. Thus, the maximum coolant temperature, under all expected operating conditions, may not exceed 567.2° F.

B. SELECTION OF THE "HOT" CHANNEL

Due to variations in channel flow rates and channel powers, the selection of the "hot" channel, i.e., the channel with the highest exit coolant temperature, is not an intuitive process. Simplified hand calculations yielded sufficient information to reduce the selection to one of three possibilities, all of which lie in the high power region of the core. These were: the element producing the most power, the highest power-producing element in the "infinite" array, and the element receiving the least coolant flow. These elements, chosen on the basis of the full scale model flow test and the zero power test, are designated A, B and C, respectively, in Fig. IV-1. The power and flow rates in each of these elements appear in Table IV-1.

C. HOT CHANNEL FACTORS

In the determination of the maximum coolant temperature in the core, consideration must be given to uncertainties in power generation and flow rate due to manufacturing tolerances and imperfections in the analytical techniques. These effects are accounted for through the use of the hot channel factors F_q and F_b, which are applied as follows:

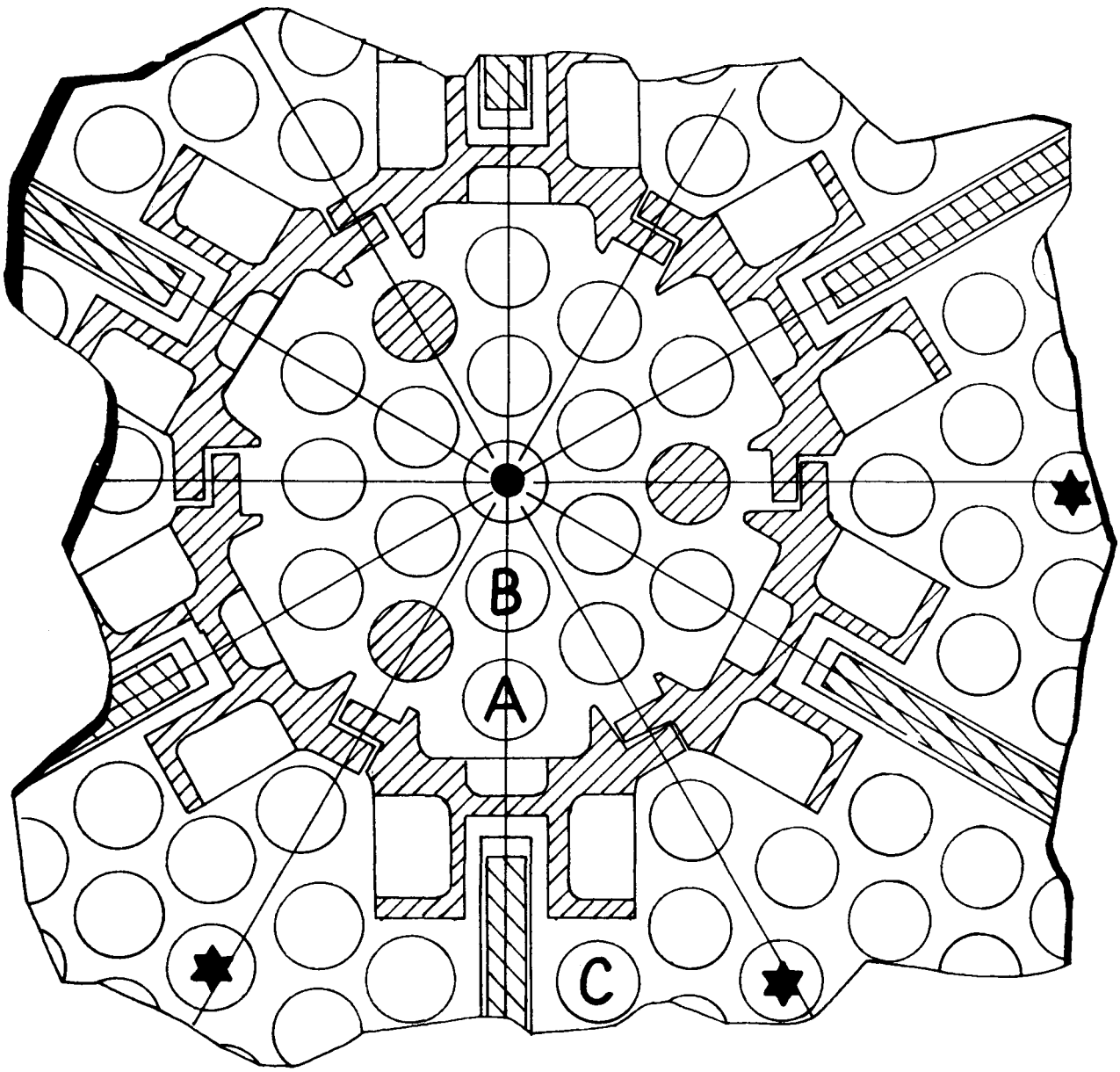

Fig. IV-1. Location of the Potentially Hot Fuel Elements

$$Q = F_q Q' \quad \text{(IV-1)}$$

$$W_i = W_i' / F_{bi} \quad \text{(IV-2)}$$

$$W_o = W_o' / F_{bo} \quad \text{(IV-3)}$$

where

Q = maximum power produced in element

W_i = minimum flow rate inside element

W_o = minimum flow rate outside element

F_q = hot channel factor to account for uncertainties in power generation

F_{bi} = hot channel factor to account for uncertainties in flow rate inside element

F_{bo} = hot channel factor to account for uncertainties in flow rate outside element

$'$ = denotes expected value of parameter without the hot channel factor

The uncertainties contributing to these hot channel factors are itemized in Table IV-2 (Ref. 7). Conservatism is maintained by assuming that all of these uncertainties act simultaneously in a detrimental fashion, i.e., the contributing factors are multiplied together to determine the resultant hot channel factor.

To preclude bulk boiling during plausible transients, an addition factor of 1.2 is applied to the power generation in the hot channel. This is based upon a reactor control system scram setting of 120% of full power.

D. RESULTS AND CONCLUSIONS

The three potentially "hot" elements (see Section B) and the average element were analyzed with the BITE code. It was found that the highest coolant temperature in the core occurred at the exits of the inside flow path of the element receiving the least flow (Element C of Fig. IV-1).

Axial distributions of the coolant and surface temperatures for the "average" and "hot" elements are shown in Figs. IV-2 and IV-3,

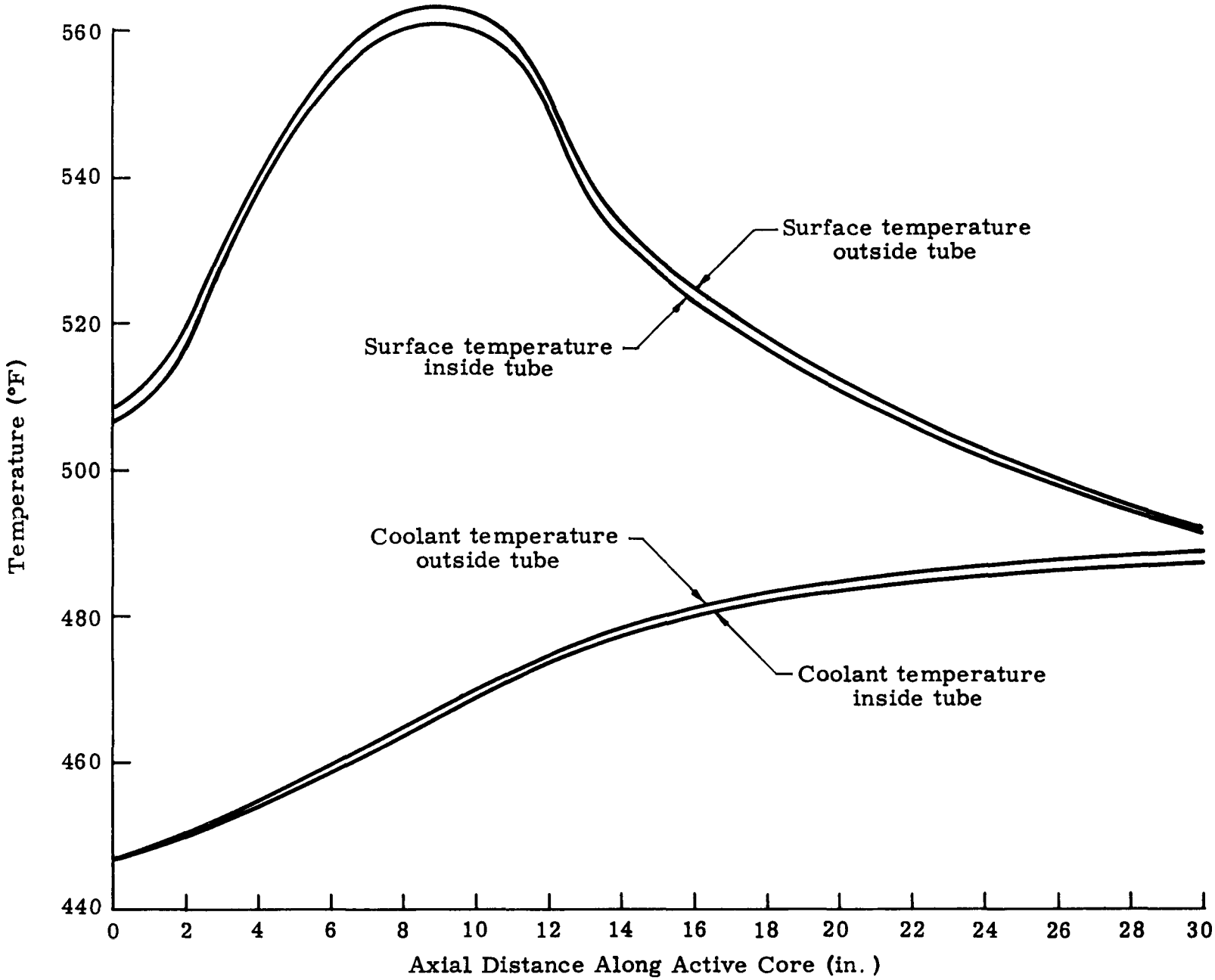

Fig. IV-2. Axial Temperature Distribution Hot Fuel Element

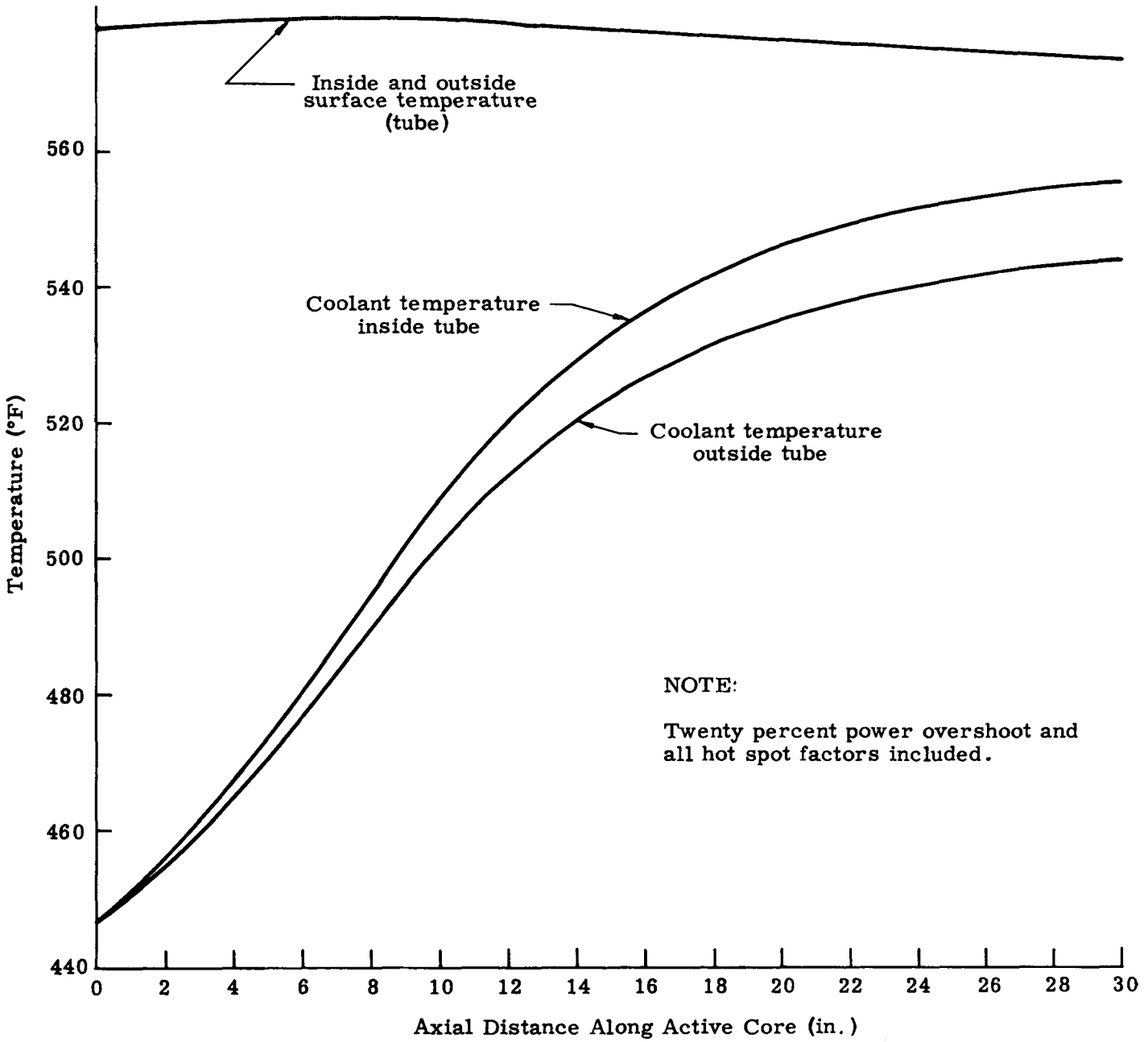

Fig. IV-3. Axial Temperature Distribution Hot Fuel Element

respectively. The nearest approach to burnout heat flux also occurred inside Element C, where the flux is 18.2% of the burnout flux. It should be noted that the "hot" element analyses incorporated both the hot channel factors and the 20% power overshoot condition.

The maximum coolant temperature in the core, under all anticipated operating conditions, is 555.3° F. This compares favorably with the allowable value of 567.2° F. By simple linear extrapolation,

$$\text{Allowable} = \frac{567.2 - 446.7 \times 9.37 \text{ mw(t)}}{555.3 - 446.7}$$

$$\text{Allowable} = 10.4 \text{ mw(t)},$$

it is apparent that the thermal aspect of this core would permit operation at a nominal operating power of 10.4 mw(t).

The hydraulic stability of the core is assured if, and only if, the pressure drop increases with respect to flow rate at all times for all of the channels (Ref. 8). This is certainly the case in all nonboiling channels. For the local boiling elements, an increase in flow rate tends to decrease the amount of local boiling, thereby decreasing the frictional pressure drop. However, the coolant temperature in these channels is decreased, and this raises the average coolant density. The latter effect results in an increased elevation head loss. Analyses, employing temperature-dependent coolant properties, have shown that the pressure drop decreasing effect of the local boiling is less significant than the pressure drop increasing effect of the density change (Ref. 9). Thus, the pressure drop increases monotonically with flow rate, and the core is hydraulically stable.

TABLE IV-1

Description of Potentially "Hot" Elements

Element Location (refer to Fig. IV-1)	Ratio of Power Produced In this Element to Power Produced in the Average Element	Measured Flow Rate Inside Element (gpm)	Measured Flow Rate Outside Element (gpm)	Maximum Exit Coolant Temperature	
				Without Hot Channel Factors (°F)	With Hot Channel Factors (°F)
A	1.83	1.131	3.250	510.6	546.9
B	1.40	1.075	1.395	501.1	531.7
C	1.77	1.208	1.205	515.2	555.3

TABLE IV-2

Hot Channel Factors

	F_q	F_{bi}	F_{bo}
Uncertainty in neutron flux distribution	1.10	--	--
Uncertainty in reactor power level	1.01	--	--
Variation in meat thickness	1.04	--	--
Variation in fuel concentration	1.02	--	--
Plenum chamber flow variations	--	1.07	1.07
Flow variation due to dimensional uncertainties	--	1.01	1.03
Resultant hot channel factor	1.18	1.08	1.10

APPENDIX A

MECHANICAL DESIGN STUDIES

During the design of the reactor core and associated in-vessel components, several general studies were accomplished in order to provide analytical support for pertinent phases of the mechanical, thermal and hydraulic design. These studies resulted in detailed reports, which are summarized below.

1. Stress Analysis Summary

The PM-1 core structure is primarily designed for the core dead weight and mechanical loads from the hold-down spring assembly. Thermal stress presents no problems, since the structure consists of thin sections, and thermal growth is allowed to take place without restraint. The structural components having significant stresses or deflections are discussed below.

a. Core shroud (Drawing 372-2105009)

The critical loading on the lower shroud occurs during lifting of the core (estimated weight of 1400 lb). Applying an ultimate load factor of 3 g, the resulting bending stress from eccentric loading around the circumference of the upper ring is approximately 8000 psi. The corresponding shear stress is negligible.

The lower alignment spider of the core shroud is designed to carry the dead weight of the fuel bundles plus half the total hold-down spring load. In the design of the spider, stiffness, rather than strength, was the primary concern. The estimated deflection along the inner ring of the spider is 0.014 inch. This deflection was considered in the overall design of the core and was found to be satisfactory.

b. Upper alignment structure (Drawing 372-2105015)

The bundle upper alignment structures were designed for the load from the hold-down spring assembly. Under the worst possible buildup of tolerances, the maximum spring load at each control rod is approximately 230 lb. The resulting bending stress and torsional shear stress are 8900 psi and 3200 psi, respectively. The corresponding maximum principal stress is 10,000 psi. The minimum allowable yield stress for Type 304 stainless steel at 500° F is 19,000 psi. It should be noted that the 19,000-psi allowable stress is the absolute minimum guaranteed under the ASTM specification, and typical expected properties of Type 304 would be significantly higher, resulting in an even greater margin of safety.

2. Fuel Element Deflection Thermally Induced

Possible fuel element bowing due to the neutron flux peaking in the control rod water gaps was investigated. It was found that the bowing under the worst expected condition would amount to less than 0.011 inch in the direction of the control rod blade. It was recognized that flux peaking in the control rod channel water gaps would cause an uneven circumferential power distribution in the adjacent fuel tubes. This uneven power distribution would obviously result in a similarly varying temperature distribution in the fuel element. The maximum thermal gradient would be along a tube diameter perpendicular to the control rod blade. Zero power tests verified that this gradient was greatest in the elements adjacent to the control rod blade, with the maximum circumferential distribution being ±23%. Due to the proximity of the control rod blade and adjacent fuel elements, a detailed analysis of fuel element thermal deflection was considered necessary.

Analysis of the extent of fuel element bowing required the following general steps:

(1) Determination of the most critical fuel element location and calculation of its temperature distribution in a vertical plane through the tube centerline and perpendicular to the control rod blade.

(2) Analysis of the PM-1 element as a fixed end, simply supported beam to determine the amount and direction of curvature resulting from the differential expansion induced by the calculated temperature variation along the tube.

(3) The effect of fuel tube-to-lower grid attachment on the calculated bowing.

The results of the above analysis showed that (1) maximum deflection of the critical element was 0.013 inch in the direction away from the control rod, and (2) the deflection toward the control rod would be less than 0.011 inch for the worst possible case. Bowing toward other fuel or poison elements is not critical from a thermal standpoint because of the nominal 0.159 clearance between the elements. In addition, this maximum bow exists above the control rod operating position, where power production is reduced to a low level. The maximum bow of 0.011 inch toward the control rod is not considered serious because.

(1) With the control rod displaced from its centerline by the amount of the clearance at the guide rails or guide tube, the nominal remaining clearance between control rod and fuel elements is at least 0.100 inch.

(2) The maximum bow toward the rod occurs only 7 inches above the lower end of the active core. This position is 5 inches below the control rods in the hot operating position at the start of core life. At the operating level of the control rods, there actually would be no deflection toward the rods.

For the maximum tube deflection of 0.013 inch, the end restraint imposed by the fixity of the lower grid causes a maximum bending stress of only 6500 psi.

Conclusions reached as a result of the thermal deflection analysis were:

(1) Bowing of the PM-1 fuel elements, due to an uneven circumferential temperature distribution, is not of sufficient magnitude to create alignment or wear problems between the bowed element and adjacent core components.

(2) Stress induced in the bowed element is low enough to preclude yielding or creep relaxation over the anticipated core life.

3. Fuel Element Vibration

Burgreen's analysis and experimental work at NDCA (Nucleonics, August 1959, p 78) showed that the amplitude and frequency of vibration of rods in parallel flow can be related to several physical constants which are known for the PM-1 core environment. Applying this method of analysis to the PM-1 fuel element, the maximum possible vibration amplitude found was 0.0001 inch. This amplitude is considered insignificant because:

(1) The nominal clearance between neighboring fuel elements is 0.165 inch.

(2) The induced bending stress in the tube is only 100 psi. This stress is not significant from a fatigue standpoint, because a cyclic stress of this level imposes virtually no limit on element lifetime.

(3) Successfully operating fuel rods in existing reactors indicated similar vibration amplitudes when evaluated by this method.

4. Fuel Element--Upper Grid Clearance

The sliding fit between fuel element and upper grid is necessary for differential thermal expansion of the fuel elements with respect to the surrounding bundle structure. Since the degree of corrosion of the surfaces around and in this sliding clearance fit is difficult to predict,

the necessity of using as large a clearance as possible to prevent seizing is apparent. However, alignment requirements and the necessity for restricting any vibration induced by coolant flow dictate as small a sliding clearance as can feasibly be maintained throughout the core life. The diametrical clearance of the PM-1 elements in the bundle upper grid is nominally 0.005 inch, with tolerances extending this to 0.002 to 0.008 inch.

Test samples of two sections of grid plate carrying 10 tubes with varying clearances in the plate were autoclaved in demineralized water at PM-1 operating temperature and pressure for 90 days. Checks on the condition of the samples were made every 30 days. No tubes showed evidence of binding or seizing after 90 days' exposure in the grid plates, even though tubes and plates had acquired the characteristic black oxide formation found on Type 304 stainless steel exposed to high temperature water.

Two tubes appeared to bind in the holes after 30 days, but these tubes were free again after 90 days' exposure.

The two seized tubes could be attributed largely to the poor water conditions and to the fact that it was a static autoclave test. No attempt was made to control either the pH or the oxygen content of the water during the test.

Under reactor conditions, this area of the grid is exposed to the primary coolant flow in a manner which would prohibit the formation of local, static water pockets and their attendant high corrosion rates. The small flow-induced vibration and the cyclic axial thermal growth of the elements are also expected to contribute to maintaining a "clean," free-sliding fit between tube and grid.

Seizure of the tube diameter in the grid from differential thermal expansion was investigated. To close even the minimum 0.002-inch diametrical clearance would require a difference of approximately 430° F between grid and tube operating temperatures. Even if the element dead end operated at centerline fuel temperatures, a differential of 120° F could not be attained.

The possibility of interference between the swaged portion of the upper end of the fuel element and the lower surface of the upper grid due to axial thermal growth of the fuel element was investigated. The maximum axial differential expansion between the hottest fuel element and the adjacent core structure was conservatively calculated to be 0.050 inch. Since the tapered portion of the fuel element upper end is at least 0.154 inch below the upper grid at assembly, no interference from thermal expansion would occur, even under the worst transient conditions.

5. Alignment

An overall alignment study (Drawing 372-2105019) of the reactor vessel and core components was completed to verify that the final assembly would provide complete freedom of movement for the control rods over their total length of travel, even under "worst case" cumulative tolerance conditions. It is, of course, realized that the probability that all components will have their extreme manufacturing tolerances additive in the most unfavorable manner is quite remote.

The results of the study were drawn to scale on the referenced drawing, and the following results were obtained from the information:

(1) The nominal expected operating clearance between a control rod blade and the adjacent upper grid is 0.163 inch. The running clearance between the control rod guide cap and the guide tube is a nominal 0.062 inch, so the control rod would still be 0.1 inch away from the upper grid and the fuel elements even with the guide cap fully deflected to one side of the guide tube.

Assuming maximum control rod displacement and "worst case" manufacturing and assembly tolerances of all core components, a minimum clearance of 0.024 inch between a control rod blade and the adjacent upper grid would result.

(2) The maximum possible mismatch between the control drive mechanism rod latch and the control rod pickup ball centerline at the moment before latching is 0.202 inch. The latch is designed to pick up a ball as much as 0.250 inch off center.

The alignment study showed that, for the proper combination of the approximately 30 variable tolerances, some drive mechanism shaft deflection could be induced by relative misalignment of the mechanism and control rod. This deflection could approach a maximum of approximately 1/16 inch at the fully extended shaft length and would reduce to zero as the control rod is withdrawn from the core. Since the drive mechanism shaft is actually a split bundle of four shaft segments, calculations verified that the 50-inch shaft (extended length) could easily absorb the 1/16-inch shaft deflection with a negligible bearing reaction.

To provide additional verification of the flexural properties of the drive mechanism shaft, the prototype actuator was tested at Martin Marietta to determine allowable shaft deflection that would still permit reliable operation of the control rod. These tests indicated that the small deflection possible in the PM-1 core would not adversely affect the operation of the control drive mechanism.

Conclusions drawn from the alignment study and the drive mechanism tests were:

(1) There are no significant alignment problems anticipated or demonstrated that would adversely affect normal control rod extraction and insertion.

(2) A control rod operating in its guide rails would have no opportunity to contact the structural components or a neighboring fuel element.

APPENDIX B

PHYSICS SUPPORTING DATA

In preparing the physics design of the PM-1 core, various analytical techniques, experimental studies and intermediate studies were performed. For the sake of clarity, these have all been assembled in this appendix.

1. Analytical Techniques

a. Neutron diffusion calculations (few-group)

In general, the core reactivity and spatial neutron flux distributions were obtained from a three-group, multiregion, one-dimensional diffusion calculation. The basic equation is

$$\left(\left[\Sigma_i^a (r) + \Sigma_i^r (r) + D_i (r)\, B_i^2 \right] \phi_i (r) - \nabla \cdot \left[D_i (r)\, \nabla\, \phi_i (r) \right] = S_i (r) \right)_{i=1}^{3} \qquad \text{(B-1)}$$

where the source is defined as,

$$S_i (r) = \frac{\chi_i}{\lambda} \cdot \sum_{i=1}^{3} \nu\, \Sigma_i^f (r)\, \phi_i (r) + \Sigma_{i-1}^r (r)\, \phi_{i-1} (r)$$

The symbols are defined as follows:

B^2 = perpendicular buckling

Σ = neutron cross section for absorption, degradation or fission, as noted by superscript

ϕ = neutron flux

D = diffusion coefficient

χ = fraction of fission neutrons born in group i

ν = neutrons produced per fission

λ = eigenvalue

i = group index.

Equation (B-1) has been programmed for a digital computer and is designated as program F_3. A more detailed description of the computer code is given in (Ref. 1).

b. Neutron transport calculation (few-group)

To obtain a more accurate representation of the neutron leakage, the core reactivity was obtained for some specific calculations from a three-group, multiregion, one-dimensional transport calculation. The calculation employed the S_n approximation to the transport equation as described in (Ref. 2). The basic equation is

$$\sqrt{1 - \mu^2} \cdot \left(\cos \phi \frac{\partial N}{\partial r} - \frac{1}{r} \sin \phi \frac{\partial N}{\partial \phi}\right) + \Sigma N = S(r) \qquad \text{(B-2)}$$

where the symbols are defined as:

Σ = total transport cross section, including in-group scattering, leakage and degradation

N = angular flux

S = source, including fission, scattering and degradation

ϕ = angular variable in the plane perpendicular to the cylinder

μ = cosine of scattering angle relative to the polar axis of the cylinder.

For details on the derivation and numerical solution of Eq (B-2), see Ref. 2.

The above transport equation has been programmed for a digital computer and is incorporated in a larger computer code designated SYNFAR (Ref. 3). The code is written to utilize up to 8th order approximation to the transport equation in cylindrical geometry and a 16th order approximation in slab geometry. It also has provision for performing a two-dimensional synthesis by iterating on the buckling to obtain a consistent value of K_{eff}.

c. Dynamic reactivity calculation

Reactivity values based on experimental period measurements and on the in-hour equation cannot be compared with static reactivity calculations. This incompatibility is caused by the relative effectiveness

of delayed neutrons due to the difference in their spectrum compared to that of prompt neutrons. However, the experimental reactivity can be compared with dynamic reactivity calculations. The dynamic reactivity equations for P_1 and S_n were obtained by modifying the static equations of Sections and by the method developed by Gross and Marable (Ref. 4). The terms,

$$w\,\phi/v \text{ and } w\,N/v$$

were added to the left side of the P_1 and S_n equations, respectively, i.e., Eq (B-1) and (B-2)

where

w = inverse stable period

v = velocity.

The fission source spectrum, normalized to unity, was modified as follows,

$$X_d(u, \omega) = X_s(u) + \frac{1}{\alpha(\omega)} \cdot \sum_{i=1}^{6} \left(\left[X_s(u) - X_i(u) \right] \cdot \frac{\beta_i \omega}{\omega + \lambda_i} \right) \qquad \text{(B-3)}$$

where

$$\alpha(\omega) = 1 - \sum_{i=1}^{6} \frac{\omega\,\beta_i}{\omega + \lambda_i}$$

X_s = static prompt plus delayed spectrum

X_i = spectrum of delayed group i

β_i = neutron fraction of delayed group i

λ_i = decay constant of precursors of group i.

The preceding modifications to the diffusion and transport equations have been included in the SYNFAR computer program (Ref. 2).

d. Calculation of fast, epithermal and thermal group constants

The fast and epithermal nuclear constants were determined by a multigroup (19 groups) slowing down calculation based on "Modified Age Theory" (Ref. 5). The neutron balance condition is written as

$$\Sigma(E)\,\phi(E)\,dE = S(E)\,dE + M(E)\,dE \qquad \text{(B-4)}$$

where

$\Sigma(E)$ = total cross section including scattering absorption and leakage

$\phi(E)$ = neutron flux per unit energy at E

$S(E)$ = fission source per unit energy at E

$M(E)$ = neutrons moderated to energy E per unit energy.

The neutron flux is eliminated from Eq (B-4), and it is solved in terms of slowing down. The analytic expression for the slowing down is:

$$\frac{dq}{du} = \frac{\xi\,\Sigma_s\,(S(u) + q(u))}{\xi\,\Sigma_s + \Sigma_a + DB^2} - q(u). \qquad \text{(B-5)}$$

After the slowing down distribution as a function of lethargy is determined, the neutron flux spectrum is obtained from

$$\phi(u) = \frac{q(u) + S(u)}{\xi\,\Sigma_s + \Sigma_a + DB^2} \qquad \text{(B-6)}$$

where the symbols in Eqs (B-5) and (B-6) are defined as:

$\phi(u)$ = neutron flux per unit lethargy

$q(u)$ = slowing down per unit lethargy

$S(u)$ = source neutrons per unit lethargy

ξ = log energy decrement

u = lethargy

D = diffusion coefficient

The diffusion coefficient is represented by the expression

$$D = \frac{1}{3\,(\gamma\,[\Sigma_a + \Sigma_s] + \Sigma_m - \Sigma_s)} \qquad \text{(B-7)}$$

The term γ is a transport correction, which is set equal to unity if the constants are to be used in a transport calculation.

The fast and epithermal group cross sections are obtained by flux weighting the multigroup cross sections.

$$\Sigma_i = \int_{u_1}^{u_2} \Sigma_i(u)\,\phi(u)\,du \Big/ \int_{u_1}^{u_2} \phi(u)\,du \qquad \text{(B-8)}$$

The thermal neutron cross sections were evaluated over a Maxwellian spectrum at an effective hardened temperature. The effective temperature was calculated from (Ref. 6).

$$T_{eff} = T_o \left(1.0 + 0.75 \cdot \frac{\Sigma_a(kT)}{\xi\,\Sigma_s}\right)^2 \qquad \text{(B-9)}$$

where T_o is the thermal temperature in °K, Σ_a is evaluated at energy kT, and $\xi\Sigma_s$ is the last epithermal energy level.

The preceding equations, which are used to obtain the three-group nuclear constants, have been programmed for a digital computer which is given the designation of program C_3. The program has been linked with both the three-group diffusion and three-group transport calculations.

The multigroup lethargy levels and cross sections used in the calculations are given in Tables B-1 through B-8.

e. The reflector savings and/or buckling calculations

The reflector savings and buckling were determined by two methods:

(1) The consistent K_{eff} method which involved performing both axial and radial one-dimensional diffusion or transport calculations and iterating on the reflector savings to obtain a consistent K_{eff}.

(2) The average regional buckling method, which consists of integrating the gradient of the flux (angular fluxes in transport theory) over the surface of the core.

TABLE B-1

Multigroup U-235 Cross Sections

Designation	Formula	Code	Density
CF 235 URAN	U235 CFINE	-1.0820	0.00000
Atomic Number	Atomic Weight	XI	1-S
92.00000	235.11750	1.00000	0.00000

Cross Sections

Level	Lethargy	Sigma Scatter	Xi Sigma Scatter	Sigma Transport	Sigma Absorption
1	0.000	3.4374614	0.6763955	0.6910081	2.3352148
2	0.500	5.1834738	3.2801998	2.3465369	1.7129494
3	1.000	6.2512301	4.0615421	3.4982190	1.4451706
4	1.500	5.7645340	2.6008012	3.3766386	1.5123018
5	2.000	5.1522307	1.7468553	3.2729288	1.4681921
6	2.500	5.3590515	1.6220368	3.7601081	1.3968770
7	3.000	6.1992431	1.3476928	4.6034080	1.4404724
8	3.500	7.4234471	1.0129796	5.8534204	1.6239860
9	4.000	9.2629858	0.8042408	8.1910087	2.1108953
10	6.000	10.352577	0.0985557	10.245376	3.7301160
11	8.000	10.199984	0.0872915	10.170812	7.3692298
12	10.000	13.149161	0.1125305	13.111553	21.010643
13	12.000	21.319517	0.1824524	21.258541	54.873752
14	14.000	10.675002	0.0913567	10.644471	79.567306
15	15.500	11.171581	0.0956064	11.139630	35.867774
16	16.500	12.644239	0.1082094	12.608076	85.865986
17	17.500	13.656149	0.1168693	13.617092	221.39245
18	18.500	14.209185	0.1216022	14.168546	326.47052
19	19.795	14.427859	0.1234730	14.386597	520.62417
3000	17.675	14.000000	0.1198000	13.960000	214.20000
2500	17.831	14.000000	0.1198000	13.960000	234.80000
2000	18.016	14.000000	0.1198000	13.960000	260.70000
1500	18.243	14.000000	0.1198000	13.960000	294.60000
1000	18.537	14.000000	0.1198000	13.960000	343.40000
500	18.957	14.000000	0.1198000	13.960000	429.40000
68	19.555	14.000000	0.1198000	13.960000	600.39998

TABLE B-1 (continued)

Designation	Formula	Code	Density
CF 235 URAN	U235 CF INE	-1.0820	0.00000

Level	Lethargy	Mu Sigma Fission	Fission Spectrum
1	0.000	6.9925210	0.0000000
2	0.500	4.5403728	0.0000000
3	1.000	3.6345988	0.0000000
4	1.500	3.6462461	0.0000000
5	2.000	3.4146576	0.0000000
6	2.500	3.1485105	0.0000000
7	3.000	3.1571243	0.0000000
8	3.500	3.4727327	0.0000000
9	4.000	4.3411736	0.0000000
10	6.000	7.2096283	0.0000000
11	8.000	13.321375	0.0000000
12	10.000	35.433343	0.0000000
13	12.000	88.213590	0.0000000
14	14.000	116.75076	0.0000000
15	15.500	67.543470	0.0000000
16	16.500	180.91095	0.0000000
17	17.500	454.13146	0.0000000
18	18.500	684.54809	0.0000000
19	19.795	1085.1309	0.0000000
3000	17.675	436.80000	0.0000000
2500	17.831	478.80000	0.0000000
2000	18.016	532.10000	0.0000000
1500	18.243	602.60000	0.0000000
1000	18.537	705.60000	0.0000000
500	18.957	886.89999	0.0000000
68	19.555	1242.0000	0.0000000

TABLE B-2

Multigroup U-238 Cross Sections

Designation	Formula	Code	Density
CF 238 URAN	U238 CFINE	-1.0840	0.00000
Atomic Number	Atomic Weight	Xi	1-S
92.00000	238.12520	1.00000	0.00000

Cross Sections

Level	Lethargy	Sigma Scatter	Xi Sigma Scatter	Sigma Transport	Sigma Absorption
0	0.000	4.8740267	6.6944607	3.0368882	1.0150000
1	0.500	6.2302029	5.8982034	3.1788638	0.7200939
2	1.000	7.1895432	4.5505559	3.3670933	0.5822751
3	1.500	6.6943703	3.2884843	3.7677715	0.5990790
4	2.000	6.5530605	2.3073481	4.4849035	0.2665853
5	2.500	6.9065034	1.3932751	5.0202868	0.1523061
6	3.000	8.0344107	0.7122479	6.1540152	0.1270516
7	3.500	9.3166157	0.3632919	7.5274119	0.1369370
8	4.000	11.472360	0.1656840	10.174524	0.2397217
9	6.000	13.264913	0.1138595	13.129704	0.4704326
10	8.000	14.298487	0.1201073	14.258450	1.1110579
11	10.000	23.668785	0.1988178	23.602509	6.0971205
12	12.000	56.919174	0.4781211	56.759800	37.908871
13	14.000	24.137062	0.2027513	24.069479	111.31363
14	15.500	7.9855257	0.0670784	7.9631663	0.5335789
15	16.500	8.2824273	0.0695724	8.2592366	0.5906141
16	17.500	8.3449018	0.0700972	8.3215362	0.8863046
17	18.500	8.3663111	0.0702770	8.3428853	1.4152286
18	19.795	8.3502400	0.0701420	8.3268591	2.0570701
3000	17.675	8.6575999	0.0727238	8.6333586	0.9525000
2500	17.831	8.6163000	0.0723769	8.5921743	1.0298000
2000	18.016	8.5649999	0.0719460	8.5410179	1.1296000
1500	18.243	8.4957999	0.0713647	8.4720116	1.2656000
1000	18.537	8.3967999	0.0705331	8.3732888	1.4664000
500	18.957	8.2340000	0.0691656	8.2109447	1.8085000
68	19.555	7.9182000	0.0665129	7.8960289	2.4389000

TABLE B-2 (continued)

Designation	Formula	Code	Density
CF 238 URAN	U238 CF INE	-1.0840	0.00000

Level	Lethargy	Nu Sigma Fission	Fission Spectrum
0	0.000	3.7597239	0.0000000
1	0.500	2.4032950	0.0000000
2	1.000	1.6843074	0.0000000
3	1.500	1.5529864	0.0000000
4	2.000	0.4584836	0.0000000
5	2.500	0.0190008	0.0000000
6	3.000	0.0004298	0.0000000
7	3.500	0.0000000	0.0000000
8	4.000	0.0000000	0.0000000
9	6.000	0.0000000	0.0000000
10	8.000	0.0000000	0.0000000
11	10.000	0.0000000	0.0000000
12	12.000	0.0000000	0.0000000
13	14.000	0.0000000	0.0000000
14	15.500	0.0000000	0.0000000
15	16.500	0.0000000	0.0000000
16	17.500	0.0000000	0.0000000
17	18.500	0.0000000	0.0000000
18	19.795	0.0000000	0.0000000
3000	17.675	0.0000000	0.0000000
2500	17.831	0.0000000	0.0000000
2000	18.016	0.0000000	0.0000000
1500	18.243	0.0000000	0.0000000
1000	18.537	0.0000000	0.0000000
500	18.957	0.0000000	0.0000000
68	19.555	0.0000000	0.0000000

TABLE B-3

Multigroup Oxygen Cross Sections

Designation	Formula	Code	Density
CF Oxygen	0 CFINE	3.6010	0.00000
Atomic Number	Atomic Weight	XI	1-B
8.00000	16.00400	0.12090	0.95800

Cross Sections

Level	Lethargy	Sigma Scatter	Xi Sigma Scatter	Sigma Transport	Sigma Absorption
0	0.000	0.9265122	0.4342565	0.7044189	0.2505446
1	0.500	1.2480409	0.2392801	1.0225726	0.1639934
2	1.000	2.1944859	0.2321665	1.7079913	0.0263153
3	1.500	1.3575250	0.2089150	1.2629528	0.0000000
4	2.000	2.7172039	0.4169699	2.6028992	0.0000000
5	2.500	4.0768085	0.6247430	3.8266198	0.0000000
6	3.000	6.6930606	0.8152686	5.1178707	0.0000000
7	3.500	3.7219412	0.5910943	3.8983901	0.0000000
8	4.000	3.4242966	0.4142240	3.2828068	0.0000001
9	6.000	3.4770600	0.4203765	3.3310234	0.0000002
10	8.000	3.7663525	0.4553520	3.6081659	0.0000006
11	10.000	3.7999963	0.4594196	3.6403962	0.0000016
12	12.000	3.7999956	0.4594194	3.6403961	0.0000042
13	14.000	3.7999889	0.4594187	3.6403894	0.0000107
14	15.500	3.7999776	0.4594173	3.6403785	0.0000223
15	16.500	3.7999610	0.4594153	3.6403626	0.0000389
16	17.500	3.7999357	0.4594122	3.6403384	0.0000641
17	18.500	3.8513539	0.4656287	3.6895970	0.0001058
18	19.795	4.0342926	0.4877460	3.8648524	0.0001550
3000	17.675	3.7624000	0.4548742	3.6043791	0.0000700
2500	17.831	3.7747000	0.4563612	3.6161626	0.0000700
2000	18.016	3.7931000	0.4585858	3.6337898	0.0000800
1500	18.243	3.8217000	0.4620435	3.6611885	0.0000900
1000	18.537	3.8699000	0.4678709	3.7073642	0.0001100
500	18.957	3.9634000	0.4791751	3.7969371	0.0001300
68	19.555	4.1623999	0.5032341	3.9875791	0.0001800

TABLE B-4

Multigroup SS-304 Cross Sections

Designation	Formula	Code	Density
CF 304 SS	CF 304 SS	4.1520	7.94000

Composition

Code	3.3010	4.0020	4.1020
Designation	of carbon	CF iron	CF nickel
Weight		0.714200	0.095000
Fraction	0.000800		

Code	4.2020
Designation	of chromium
Weight	
Fraction	0.190000

CF SS304

Level	Lethargy	Sigma Scatter	XI Sigma Scatter	Sigma Transport	Sigma Absorption
0	0.000	0.282322	0.286407	0.141157	0.001419
1	0.500	0.313261	0.262345	0.157981	0.001575
2	1.000	0.305017	0.212968	0.200323	0.001533
3	1.500	0.269231	0.138661	0.209048	0.001353
4	2.000	0.242328	0.063515	0.200450	0.001216
5	2.500	0.242635	0.030815	0.204045	0.001208
6	3.000	0.289813	0.019407	0.259242	0.001453
7	3.500	0.272747	0.009546	0.236502	0.001368
8	4.000	0.471531	0.016805	0.457955	0.002046
9	6.000	0.818129	0.029390	0.808252	0.004063
10	8.000	1.256303	0.045036	1.241170	0.005218
11	10.000	0.834456	0.029976	0.824379	0.002278
12	12.000	0.902051	0.032390	0.891164	0.005663
13	14.000	0.897666	0.032234	0.886831	0.013646
14	15.500	0.890925	0.031994	0.880171	0.029035
15	16.500	0.882050	0.031677	0.871403	0.049240
16	17.500	0.876468	0.031479	0.865888	0.080418
17	18.500	0.864004	0.031035	0.853568	0.132047
18	19.795	0.855370	0.030721	0.845037	0.192781
3000	17.675	0.869091	0.030867	0.858676	0.085396
2500	17.831	0.869393	0.030880	0.858974	0.092441
2000	18.016	0.869237	0.030875	0.858822	0.101531
1500	18.243	0.868392	0.030846	0.858004	0.113590
1000	18.537	0.867001	0.030796	0.856611	0.132172
500	18.957	0.865711	0.030751	0.855367	0.162794
68	19.555	0.863765	0.030677	0.853418	0.221774

TABLE B-5

Multigroup Boron-10 Cross Sections

Designation	Formula	Code	Density
CF 10 Boron	B-10 CFINE	8.0210	0.00000
Atomic Number	Atomic Weight	XI	1-B
5.00000	10.01612	0.00000	0.00000

Cross Sections

Level	Lethargy	Sigma Scatter	XI Sigma Scatter	Sigma Transport	Sigma Absorption
0	0.000	2.079054	0.9694629	0.8934764	0.001179
1	0.500	1.731479	0.8620323	1.0003378	0.001647
2	1.000	1.898694	0.7051461	1.0854042	0.036662
3	1.500	1.940459	0.5470276	1.0968336	0.259121
4	2.000	2.222853	0.4415455	1.2149479	0.247331
5	2.500	3.079442	0.5359558	2.3583194	0.313209
6	3.000	3.558259	0.6539903	3.4214214	0.629752
7	3.500	5.009459	0.7030258	3.7549426	0.898985
8	4.000	3.969926	0.5453959	2.9130231	1.837100
9	6.000	0.999988	0.2907177	1.5527569	4.468368
10	8.000	0.608084	0.2773495	1.4813558	11.533301
11	10.000	3.9508978	0.6937771	3.7055456	31.529204
12	12.000	4.0000000	0.7023995	3.7515986	85.739193
13	14.000	4.0000000	0.7024000	3.7516000	216.7589
14	15.500	4.0000000	0.7024000	3.7516002	451.8750
15	16.500	4.0000000	0.7023999	3.7515998	788.3194
16	17.500	4.0000000	0.7024000	3.7515999	1299.814
17	18.500	4.0000000	0.7024000	3.7515999	2143.239
18	19.795	4.0000000	0.7037634	3.7510732	3143.066
3000	17.675	4.0000000	0.7552000	3.7312000	1388.9000
2500	17.831	4.0000000	0.7552000	3.7312000	1501.7000
2000	18.016	4.0000000	0.7552000	3.7312000	1647.2000
1500	18.243	4.0000000	0.7552000	3.7312000	1845.5000
1000	18.537	4.0000000	0.7552000	3.7312000	2138.3000
500	18.957	4.0000000	0.7552000	3.7312000	2637.1000
68	19.555	4.0000000	0.7552000	3.7312000	3556.4000

TABLE B-6

Multigroup Slag Cross Sections

Designation	Formula	Code	Density
Slag	Slag	9.0000	0.00000
Atomic Number	Atomic Weight	XI	1-B
0.00000	235.11700	0.00000	0.00000

Cross Sections

Level	Lethargy	Sigma Scatter	XI Sigma Scatter	Sigma Transport	Sigma Absorption
0	0.000	0.0000000	0.0000000	0.0000000	0.0060000
1	0.500	0.0000000	0.0000000	0.0000000	0.0235000
2	1.000	0.0000000	0.0000000	0.0000000	0.0465000
3	1.500	0.0000000	0.0000000	0.0000000	0.0695000
4	2.000	0.0000000	0.0000000	0.0000000	0.0920000
5	2.500	0.0000000	0.0000000	0.0000000	0.1165800
6	3.000	0.0000000	0.0000000	0.0000000	0.1435000
7	3.500	0.0000000	0.0000000	0.0000000	0.1705000
8	4.000	0.0000000	0.0000000	0.0000000	0.2227932
9	6.000	0.0000000	0.0000000	0.0000000	0.4211325
10	8.000	0.0000000	0.0000000	0.0000000	1.6250000
11	10.000	0.0000000	0.0000000	0.0000000	7.0283390
12	12.000	0.0000000	0.0000000	0.0000000	22.537875
13	14.000	0.0000000	0.0000000	0.0000000	42.590582
14	15.500	0.0000000	0.0000000	0.0000000	32.851332
15	16.500	0.0000000	0.0000000	0.0000000	14.859245
16	17.500	0.0000000	0.0000000	0.0000000	15.980321
17	18.500	0.0000000	0.0000000	0.0000000	27.408326
18	19.795	0.0000000	0.0000000	0.0000000	42.596197
3000	17.675	0.0000000	0.0000000	0.0000000	18.048666
2500	17.831	0.0000000	0.0000000	0.0000000	19.024478
2000	18.016	0.0000000	0.0000000	0.0000000	20.577173
1500	18.243	0.0000000	0.0000000	0.0000000	22.922639
1000	18.537	0.0000000	0.0000000	0.0000000	26.524411
500	18.957	0.0000000	0.0000000	0.0000000	32.704353
68	19.555	0.0000000	0.0000000	0.0000000	44.097605

TABLE B-7

Multigroup Xe-135 Cross Sections

Designation	Formula	Code	Density
CF 135 Xenon	CF Xe 135	8.6010	0.00000
Atomic Number	Atomic Weight	XI	1-B
54.00000	134.95000	0.00000	0.00000

Cross Sections

Level	Lethargy	Sigma Scatter	XI Sigma Scatter	Sigma Transport	Sigma Absorption
0	0.000	4.6888320	4.3737525	1.7120412	0.0052639
1	0.500	4.6186875	4.4117042	2.5957216	0.0064765
2	1.000	5.2306638	4.4159474	3.1601389	0.0084975
3	1.500	6.5604843	3.7698022	3.4311806	0.0111738
4	2.000	7.2736731	2.6320066	4.0364805	0.0146672
5	2.500	7.4594834	1.2804293	5.2907375	0.0193330
6	3.000	7.4787897	0.5025002	5.5053765	0.0256356
7	3.500	7.4840171	0.2316186	5.9604051	0.0340942
8	4.000	7.5290931	0.1339775	7.0767743	0.0555902
9	6.000	8.1750412	0.1250781	8.1333482	0.1413984
10	8.000	8.6062756	0.1316760	8.5623833	0.4121033
11	10.000	8.2756726	0.1266178	8.2334652	1.2584392
12	12.000	8.4404134	0.1291383	8.3973682	3.9953981
13	14.000	71.322224	1.0912300	70.958475	22.865817
14	15.500	1043.6990	15.968595	1038.3761	827.93378
15	16.500	9755.8055	149.26382	9706.0505	12832.087
16	17.500	94853.821	1451.2635	94370.067	216891.02
17	18.500	558803.13	8549.6880	555953.23	1966054.1
18	19.795	519767.31	7948.6067	517117.39	2489305.4
3000	17.675	119040.00	1771.3152	118444.80	567200.00
2500	17.831	143120.00	2129.6256	142404.40	697660.00
2000	18.016	175070.00	2605.0416	174194.65	878160.00
1500	18.243	217980.00	3243.5424	216890.10	1135900.0
1000	18.537	274720.00	4087.8336	273346.40	1513900.0
500	18.957	339220.00	5047.5936	337523.90	2062000.0
68	19.555	353430.00	5259.0383	351662.85	2623400.0

TABLE B-8

Multigroup Water Cross Sections

Designation	Formula	Code	Density
CF Water	CF H20	2.512	0.99800

Composition

Code	2.512	3.601
Designation	CF END H	CF Oxygen
Weight Fraction	0.1119005	0.8880995

Cross Sections

Level	Lethargy	Sigma Scatter	Xi Sigma Scatter	Sigma Transport	Sigma Absorption
0	0.000	0.100601	0.084175	0.046704	0.008362
1	0.500	0.136012	0.102350	0.065537	0.005474
2	1.000	0.206682	0.141200	0.101422	0.000880
3	1.500	0.226492	0.188163	0.102464	0.000002
4	2.000	0.327534	0.250776	0.165710	0.000002
5	2.500	0.452968	0.337773	0.233199	0.000004
6	3.000	0.636019	0.439876	0.308162	0.000005
7	3.500	0.652842	0.548365	0.306074	0.000006
8	4.000	0.886138	0.785692	0.366503	0.000010
9	6.000	1.263230	1.161230	0.493059	0.000023
10	8.000	1.446180	1.335690	0.559996	0.000063
11	10.000	1.461440	1.349960	0.565778	0.000172
12	12.000	1.461140	1.349660	0.565680	0.000469
13	14.000	1.468150	1.356670	0.568013	0.001185
14	15.500	1.505350	1.393880	0.580398	0.002471
15	16.500	1.543040	1.337700	0.660645	0.004312
16	17.500	1.858110	1.435540	0.919276	0.007109
17	18.500	2.368599	1.461774	1.431200	0.011722
18	19.795	2.919055	1.417512	2.035157	0.017160
3000	17.675	1.903505	1.420723	0.993237	0.007630
2500	17.831	1.973993	1.431452	1.057701	0.008251
2000	18.016	2.065060	1.444920	1.142710	0.009056
1500	18.243	2.185620	1.458760	1.257360	0.010122
1000	18.537	2.364570	1.472580	1.434150	0.011759
500	18.957	2.646200	1.480760	1.721500	0.014429
68	19.555	3.158120	1.487740	2.249960	0.019540

f. Consistent K_{eff} method of obtaining buckling

In the three-group formulation, the neutron multiplication can be defined as:

$$K_{eff} = \sum_{n=1}^{3} k_n \cdot \frac{1 - p_n}{p_o} \cdot \prod_{j=1}^{n} \frac{p_{j-1}}{M_j} \qquad \text{(B-10)}$$

where

p = resonance escape probability

k = multiplication factor (infinite)

M = inverse nonleakage probability

n = group index.

The inverse nonleakage probability is calculated from the equation

$$M_j = 1 + L_j^2 \left[\left(\frac{\pi}{H + 2\Delta H + 2\delta_{\lambda_j}} \right)^2 + \frac{4.81}{D + 2\Delta R + 2\delta_{\lambda_j}} \right]^2 \qquad \text{(B-11)}$$

where

L^2 = slowing down or diffusion length

$\Delta H, \Delta R$ = axial or radial reflector savings

δ_λ = extrapolation distance.

The core reflector savings were determined by assuming an axial reflector savings (ΔH), and using this value in a few-group multiregion radial core calculation of K_{eff}. Equation (B-10) was then solved for ΔR using core constants, K_{eff} and the assumed ΔH. The radial reflector savings (ΔR) are then used in an axial core calculation, and the resulting K_{eff} used to solve for a new value of ΔH. The procedure is then repeated until consistent values of ΔH and ΔR are obtained which yield identical results for K_{eff} in either axial or radial one-dimensional core calculations. The final value of reflector savings were then used to determine the buckling.

g. Buckling from the flux shape

The few-group bucklings for use in transport calculations were obtained from the few-group transport angular flux shape. The average buckling can be represented by integrating the Laplacian over the region.

$$\overline{B}_r = \frac{\int_V \nabla \cdot \nabla \phi_r \, dV}{\int_V \phi_r \, dV} \qquad \text{(B-12)}$$

By applying the Divergence Theorem, the buckling can be expressed in terms of the gradient of the flux integrated over the region surface.

$$\overline{B}_r = \frac{\oint_S \nabla \phi_r \, dS}{\int_V \phi_r \, dV} \qquad \text{(B-13)}$$

The above method, which is incorporated in the SYNFAR (Ref. 3) computer code, was used only with transport theory fluxes because of the inherent error in diffusion theory fluxes near boundaries.

h. Fine-flux calculations

The fine-flux calculations are to be distinguished from gross or overall flux calculations in that they are performed to obtain the detailed spatial neutron flux distribution in small regions where relatively large flux perturbations occur. Since the regions are generally small both physically and in terms of mean free path, diffusion theory is not applicable and transport theory is required.

The calculations of the fine flux were based on the use of the S_n approximation to the transport equation as discussed in Section b. Equation was used in a one-group model, with the neutron source distribution as an input quantity. Because of the discrepancies involved in the zero flux gradient boundary condition in cylindrical geometry transport theory, all calculations were set up so that a zero flux boundary condition was applicable.

i. Core burnup calculations

The core burnup and lifetime calculations were based on a region-by-region, one-dimensional, three-group depletion calculation.

The few-group diffusion program F_3, discussed above, was used to obtain the average three-group neutron flux in each of the reactor core regions. The average fluxes were then used to deplete the burnable materials in each region over a time increment which was usually taken to be 100 days. The atom concentrations remaining in each region at the end of each time increment were then used to evaluate a new set of three-group nuclear constants. These new constants were used to obtain a new flux distribution, and the procedure was repeated until the core became subcritical.

Buildup and/or depletion was allowed for B-10, U-235, U-238 (and chain), Xe-135 and fission products.

The fission products were separated into two types; those with low cross sections and those with high cross sections. Multigroup cross sections for the stable, low cross-section fission products were obtained from Ref. 7 and are identified as SLAG. These are presented in Table B-6.

The fission yields and thermal cross sections of the high cross section fission products were obtained from Ref. 8 and are shown in Table B-9. With the exception of xenon, which was treated exactly, the concentrations were assumed to be at equilibrium after the first time step (100 days).

The burnup of B-10 and U-235 was also reflected in the values of the applied cell corrections, which were varied with core lifetime.

TABLE B-9

High Cross-Section Fission Product Isotopes (Ref. 8)

Isotope	σ_{abs} (68° F)	Yield/Fission (%)	Half Life
Xe-135	27.2×10^5	6.3	9.2 h
Sm-149	4.08×10^4	1.13	Stable
Sm-151	1.24×10^4	0.45	80 Y
Gd-155	5.62×10^4	0.03	Stable
Eu-155	1.40×10^4	0.03	1.9 Y
Cd-113	2.00×10^4	0.01	Stable
Gd-157	2.42×10^5	0.0078	Stable

2. Cell Corrections

The local flux distribution in the PM-1 is perturbed quite severely due to the heterogeneous nature of the core. To account for this phenomenon in the homogenization of various core materials, it was necessary to perform a series of fine flux calculations. These calculations then yielded cell corrections which were applied to the atom densities of the appropriate materials.

Since the core is composed primarily of fuel elements, the representative neutron flux in the core would be that in a fuel element cell. Therefore, all cell corrections were based on the ratio of the average flux in a given material to the average flux in a fuel element cell.

The cell correction calculations were based on the method described above (fine-flux calculation), and consisted of surrounding the cell to be analyzed with homogenized core material. The source was given a zero order Bessel function radial distribution and weighted by the volume fraction of moderator in each region. A zero flux gradient boundary condition was imposed at the center of the cell, and at the outer boundary, the flux was forced to zero.

The object of using the above geometry and boundary conditions was to avoid the use of a zero-current boundary condition at the outer radius of the cell. In cylindrical geometry, this condition yields cell corrections which are consistently low (Ref. 9).

Thermal neutron spectrum hardening was included in all cell calculations by evaluating the thermal cross sections over a Maxwell-Boltzmann neutron distribution at an effective hardened neutron temperature obtained from Eq (B-4).

a. Thermal and epithermal cell corrections

The cell correction calculations for the LPR's were extended to include the lower five epithermal energy groups (to lethargy 15.5), as well as the thermal energy group. Each group was treated as a separate one-group calculation. In the epithermal calculations, the neutron absorption term was modified to include removal by neutron slowing down, and in-group scattering was allowed.

The configuration for the LPR cell calculation consisted of a lump poison rod at the center, with its associated water, surrounded by a homogeneous cell-corrected mixture of five fuel elements. The cell was then surrounded by homogeneous core material as described above and shown in Fig. B-1. The ratio of one lumped poison rod to five fuel elements was used because it approximates the true ratio in that portion of the core in which the LPR's are located.

The results of LPR cell calculations for the beginning of life are shown in Table B-10, stainless steel rods are also included, as they are LPR's with zero weight percent boron.

TABLE B-10

Beginning-of-Life Cell Corrections for Lumped Poison Rods

	Cell Correction ($\bar{\phi}_i / \bar{\phi}_{FE}$)			
	68° F		463° F	
Energy Groups	0 wt % B	0.27 wt % B	0 wt % B	0.27 wt % B
15	0.9706	0.8858	0.9686	0.8850
16	0.9631	0.8250	0.9616	0.8253
17	0.9626	0.7519	0.9617	0.7536
18	0.9408	0.6389	0.9411	0.6423
19	0.9273	0.5532	0.9406	0.6232
68° F *	0.9451	0.5215		
436° F **			0.9574	0.6104

The thermal fine-flux distribution through the lumped poison cell is shown in Fig. B-2

*68° F corresponds to an effective temperature of 259° F
**463° F corresponds to an effective temperature of 779° F

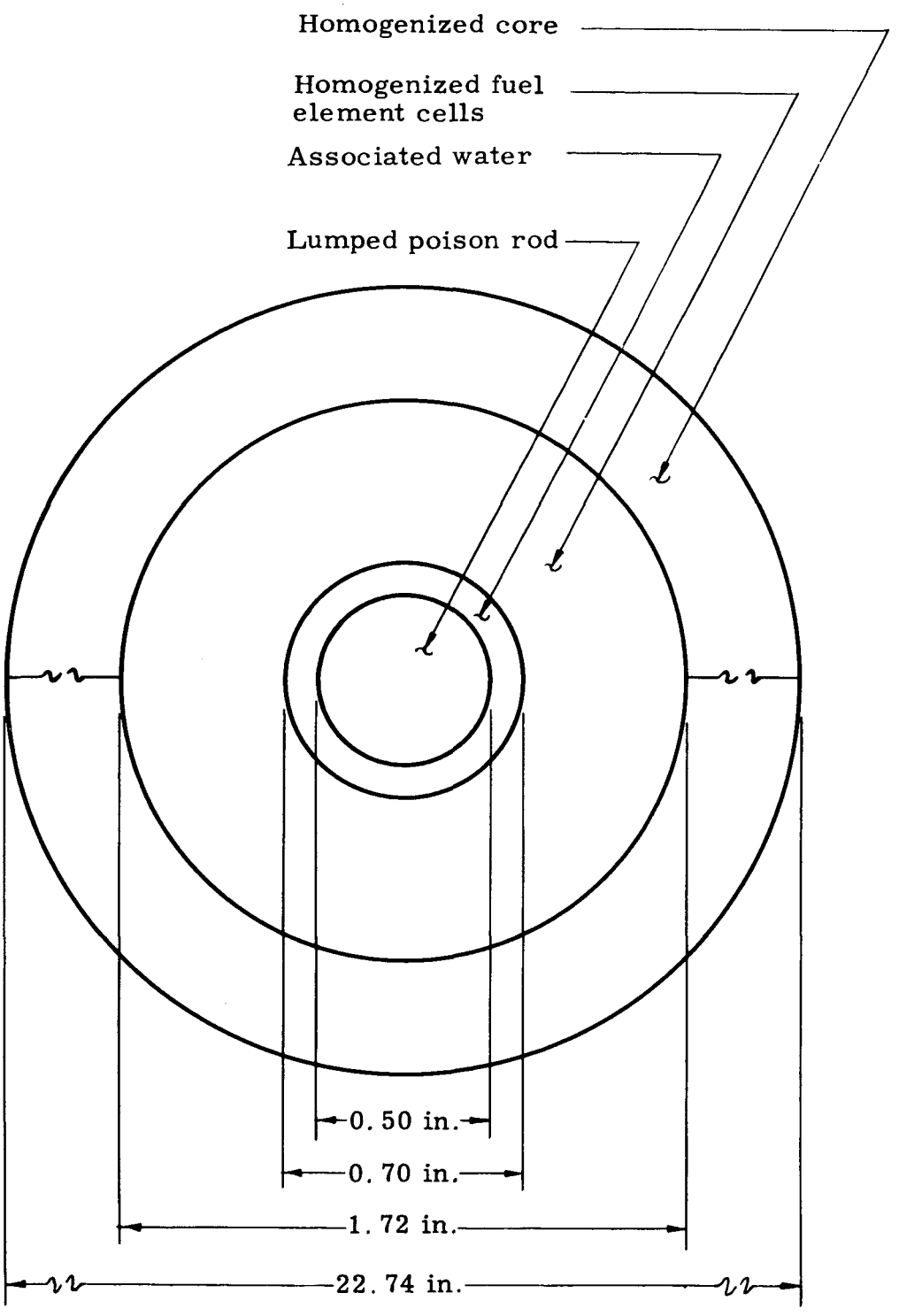

Fig. B-1. Lumped Poison Rod Cell

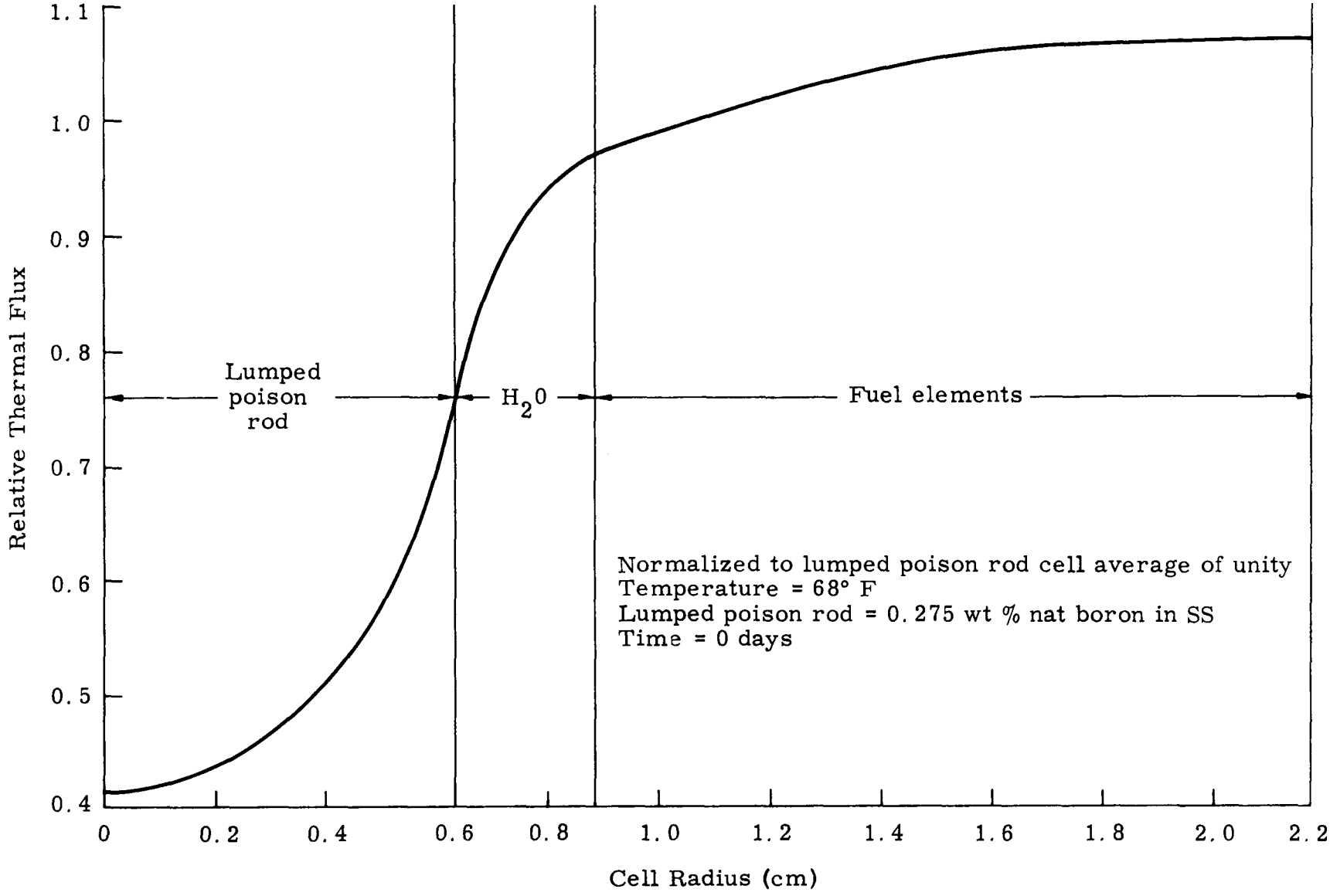

Fig. B-2. Relative Thermal Flux Distribution in Lumped Poison Rod Cell

b. Cell corrections versus burnup

During operation of the PM-1, the boron in the lumped poison rods is depleted, causing a change in the neutron absorption properties of the rods. The result is a change in the cell correction with core burnup and a corresponding change in the rate of boron depletion. In order to account for this change, cell calculations were based on conditions existing at the end of core life (about 700 days).

The conditions, which were based on the results of previous burnup calculations, are that when the boron is 81% depleted, the average fuel burnup is 29%. Using the above data, cell calculations were made in which both the boron and uranium were partially depleted. The results of the calculation are shown in Table B-11.

TABLE B-11

End-of-Life Cell Corrections for Lumped Poison Rods
(N(t)/No (U-235) = 0.71, N(t)/No(B-10) = 0.192)

	Cell Corrections $(\bar{\phi}_1/\bar{\phi}_{FE})$			
	68° F		463° F	
Energy Groups	700 Days	100% Burnup**	700 Days	100% Burnup**
15	0.9564	0.9748	0.9546	0.9728
16	0.9341	0.9643	0.9320	0.9615
17	0.9088	0.9560	0.9075	0.9537
18	0.8544	0.9287	0.8545	0.9270
19	0.8062	0.9043	0.8455	0.9236
68° F*	0.7963	0.9097		
463° F*			0.8448	0.9295

The data presented in Table B-11 for 700 days of reactor operation was combined with the data in Table B-10 (0.27 wt % B) and fitted, at each energy level, with the expression

$$g(t) = \frac{1}{h + \gamma (1 - \beta_B(t)} \qquad \text{(B-14)}$$

*Evaluated at an effective temperature of 259° F and 779° F, respectively.
**Extrapolated to 100% boron burnup.

where

$g(t)$ = cell correction (with time)

$\gamma = \frac{1}{\beta(700)} \left(\frac{1}{g(0)} - \frac{1}{g(700)} \right)$

$\beta_B(t)$= fractional burnup of boron (days)

$h = \frac{1}{g(0)} - \gamma$

Equation (B-14) was used to obtain the variation in the LPR cell correction as a function of burnup of boron. The resulting cell corrections are shown in Figs. B-3 and B-4.

The stainless steel in the lumped poison rods is subjected to the same neutron flux depression as the boron, so it was given the same cell correction. However, stainless steel in other portions of the core was treated differently, i.e., steel in the fuel elements was given the cell correction obtained from a fuel cell calculation.

c. Lumped poison rod cell corrections--comparison with experiment

A definitive series of experiments to determine the effects of lumped poison rods has been performed at the Martin Marietta critical facility. The experiments consisted of a series of repeating cells containing one lumped poison rod surrounded by six fuel tubes. The lumped poison rods studied were from 0.3 to 0.5 inch in diameter and from 0 wt % (stainless steel rods) to 0.84 wt % natural boron in stainless steel.

Thermal fine-flux distributions were measured for each core through the central cell, using 1/16-inch diameter by 0.002-inch thick 10% dysprosium in aluminum foils. The measurements were made through a 1/16-inch hole in the lumped poison rod, through the water channel between the lumped poison rod and the fuel tube, and inside the inner fuel tube water hole. Measurements in the water were effected by a plastic foil holder with a 1/16-inch hole drilled through it. In both the lumped poison rod and plastic foil holder, slugs 1/16 inch in diameter by 1/16 inch long of either lumped poison rod material or plastic were used to space the foils and provide a constant cross section of the particular material.

Figure B-5 shows the results obtained for two different runs for the 0.5-inch diameter, 0.27 wt % boron rod similar to that used in the PM-1 core. The computed accuracy for an individual data point is approximately ±2%. The observed spread in data points was also found to be ±2%. The errors are primarily due to counting statistics, foil positioning and normalization.

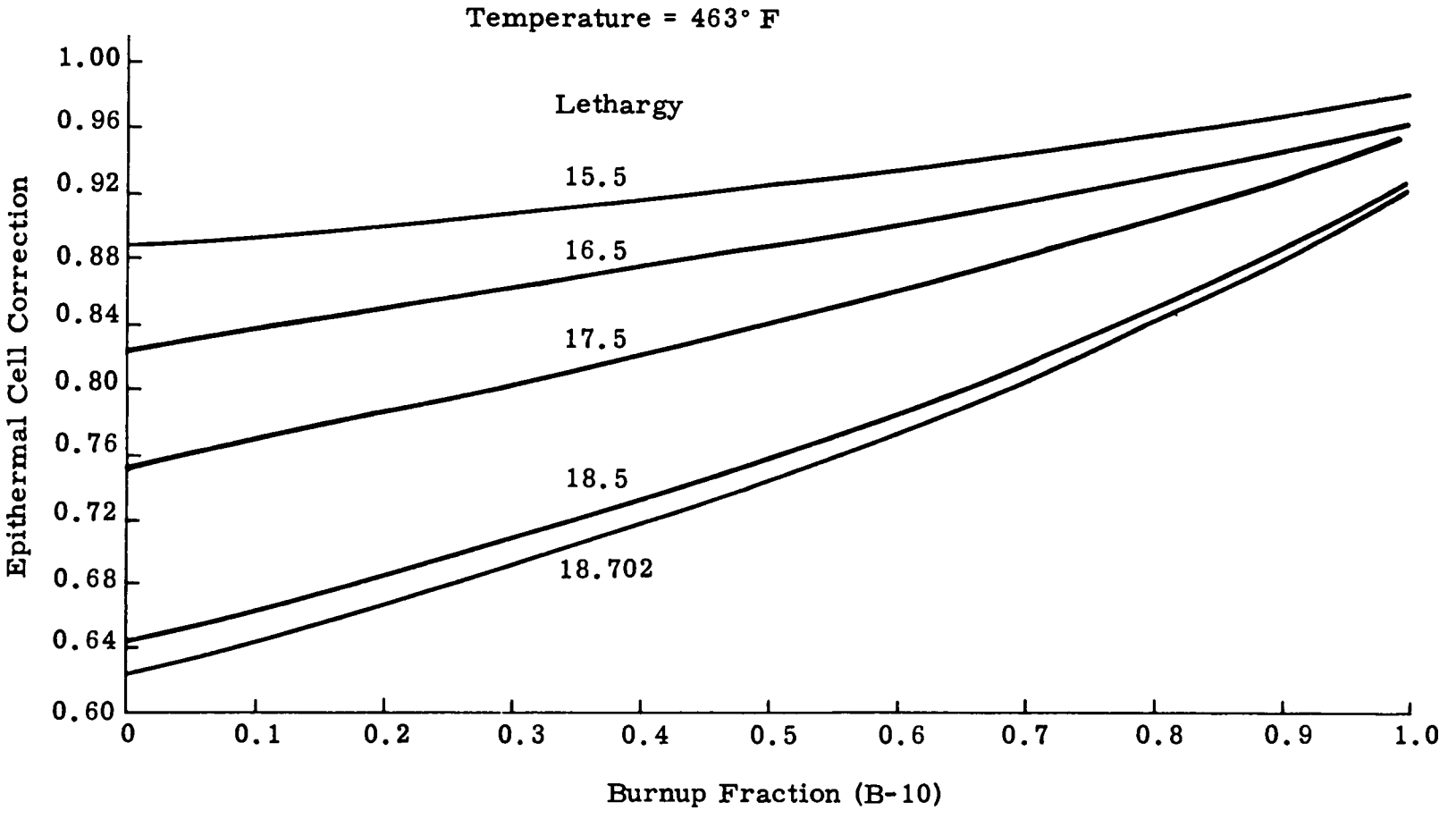

Fig. B-3. Lumped Poison Rod Epithermal Cell Correction Versus B-10 Burnout

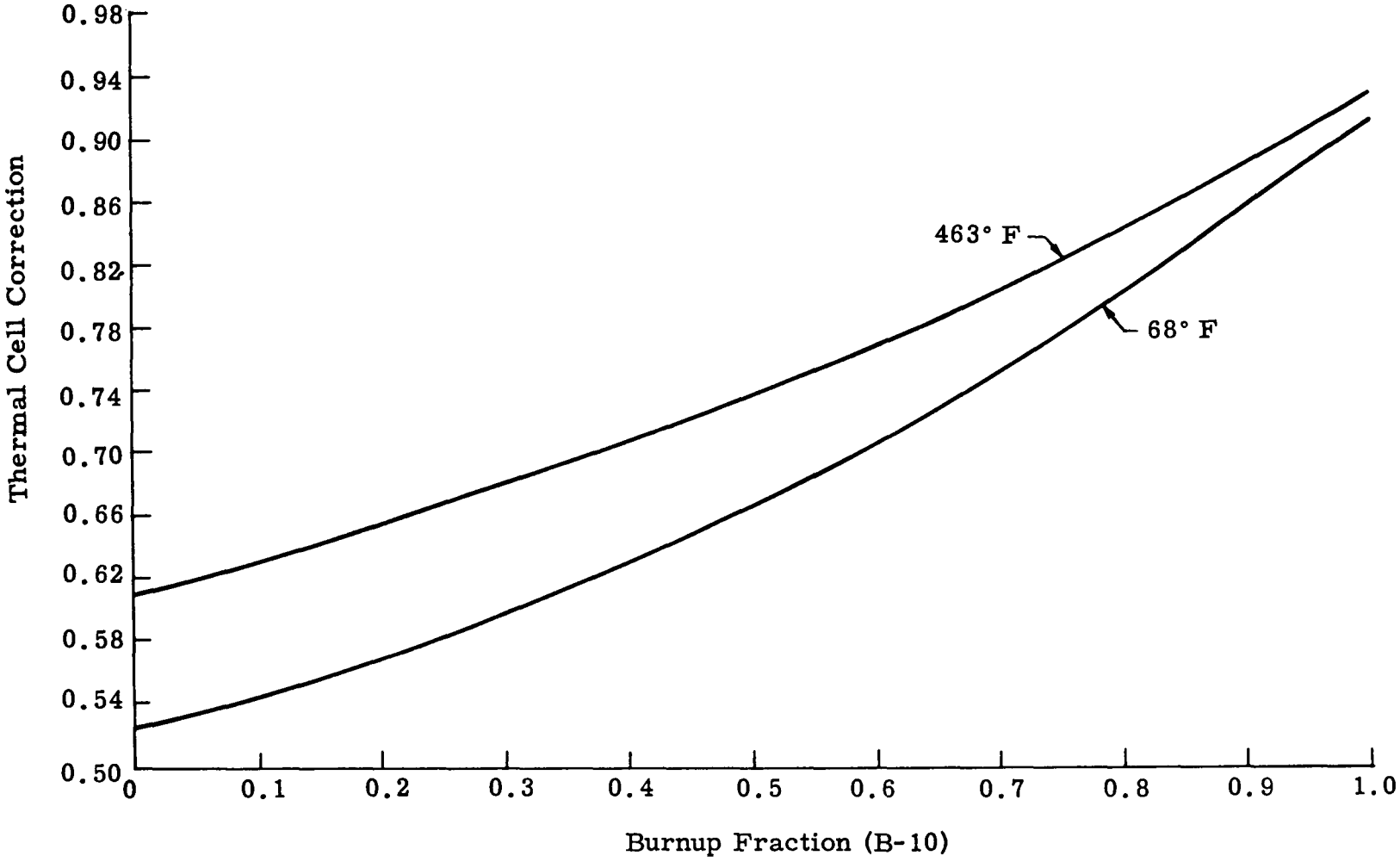

Fig. B-4. Lumped Poison Rod Thermal Cell Correction Versus B-10 Burnup

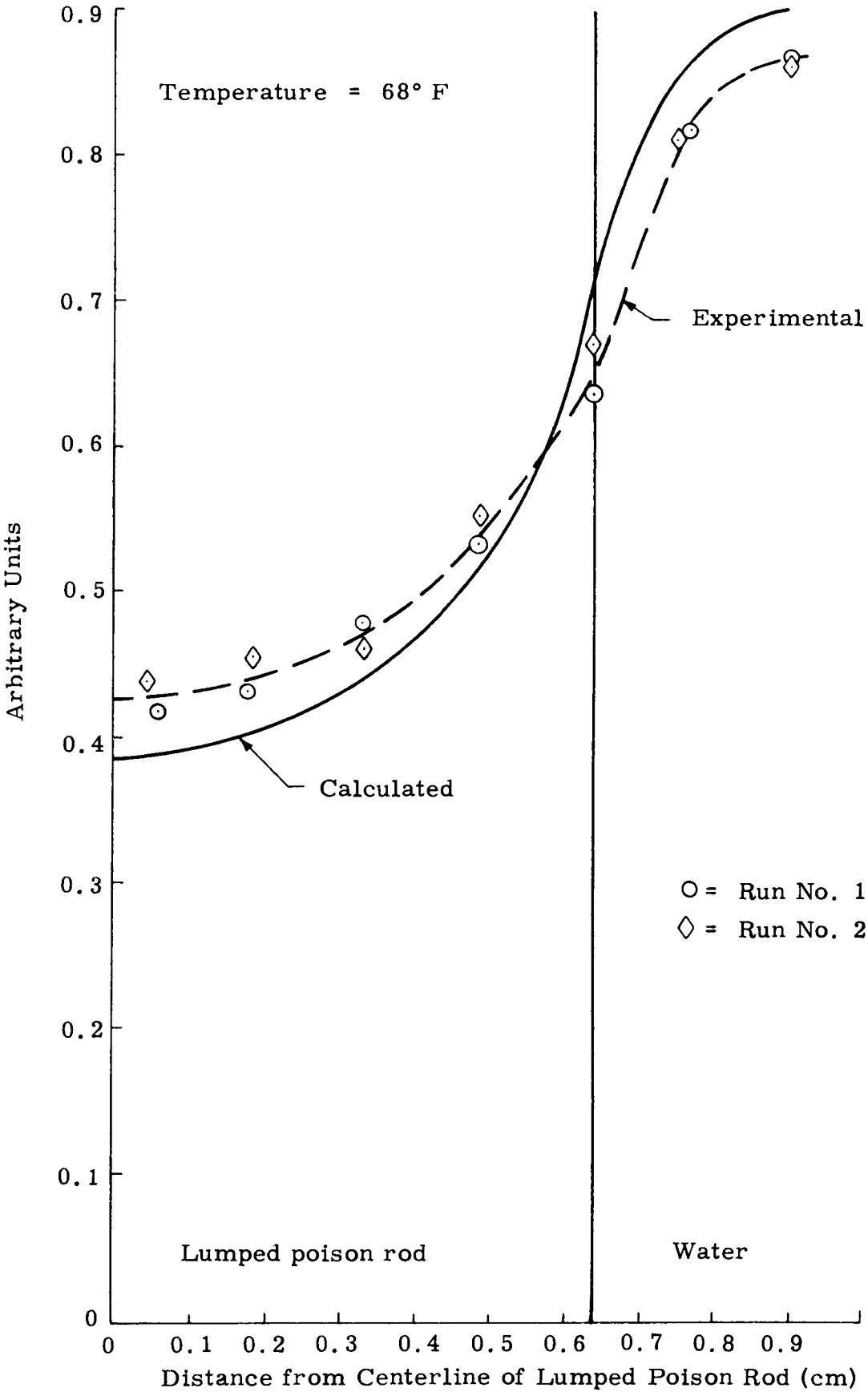

Fig. B-5. Comparison Between Experimental and Calculated Fine Flux Distributions Through a 0.27 wt % Lumped Poison Rod--Temperature = 68° F

Figure B-5 also contains the results of a SYNFAR S-6 transport calculation. The analytical model consisted of a lumped poison rod region, water region, fuel-bearing region and the homogenized core region as described previously. Experimental and analytical values were normalized so that the areas under the two curves are equal. A comparison of the two curves shows a steeper analytic flux gradient, yielding a maximum difference of about 9% between the two curves. The difference is believed to be caused by increased spectrum hardening in the lumped poison rod relative to that used in the calculation. The calculation was based on an average core hardening and, thus, did not account for differences between the spectrum in the water and that in the rod.

The relative average flux in the lumped poison rod in the experimental measurement was found to be about 0.50 compared to 0.46 determined analytically. However, the net effect on core reactivity would be very small. Spectrum hardening would reduce the cross section, whereas higher flux would increase the cell correction; thus, the product would remain nearly constant.

d. Thermal cell corrections for fuel elements

The cell correction calculation for the fuel elements was performed for the thermal neutron energy group only. Preliminary calculations have shown that epithermal corrections approach unity.

The configuration for the fuel element cell calculation was that of a cylindrical core having a fuel element at the center, with its associated water, surrounded by homogeneous core material. This is shown in Fig. B-6.

The results of the fuel element cell calculations for the beginning of life are given in Table B-12.

TABLE B-12

Beginning of Life Cell Corrections for Fuel Elements

	Cell Corrections	
Material	68° F*	463° F*
UO_2	0.8288	0.8772
SS	0.8494	0.8928
H_2O	1.0316	1.0225

*68° F and 463° F correspond to effective temperatures of 259° F and 779° F, respectively.

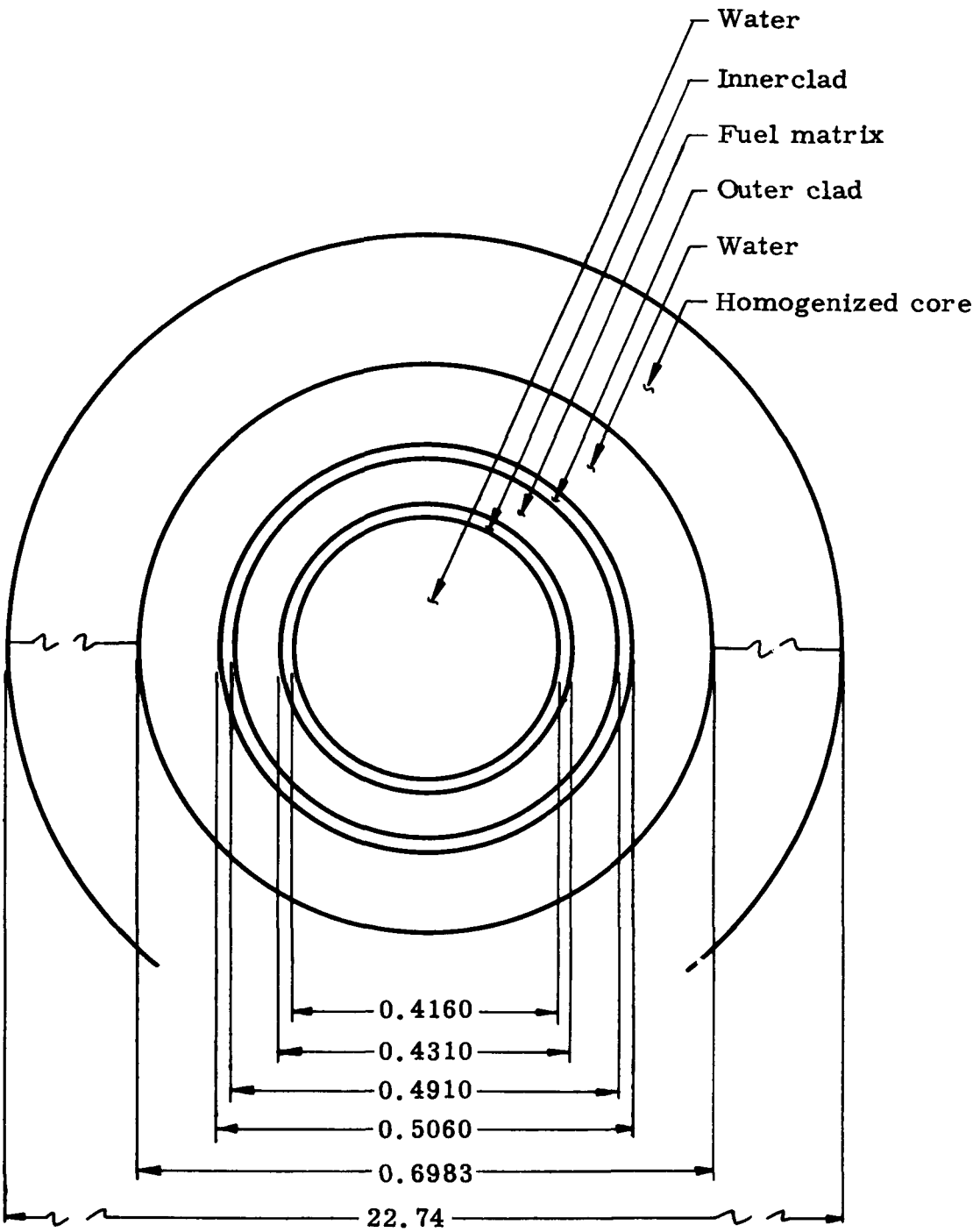

Fig. B-6. Fuel Element Cell

The cell corrections are based on an average neutron flux of one in a fuel element cell. The values for SS are based on the average volume weighted flux in the steel in the matrix and in both the inner and outer clad. The values for water are based on the volume weighted average flux in both water regions.

The fine-flux distribution through the fuel element cell is shown in Fig. B-7.

e. Cell correction versus burnup

As the fuel is depleted with lifetime, the cell corrections for the materials in the fuel cell increase. Since the fuel element walls are relatively thin, it was assumed that when the uranium is completely removed, the cell corrections are unity. On this basis, the fuel element cell corrections as a function of uranium burnup were fitted with

$$g(t) = \frac{1}{1 + \gamma (1 - \beta_{25}(t)} \qquad \text{(B-15)}$$

where

$$\gamma = \frac{1}{g(o)} - 1$$

$\beta_{25}(t)$ = fractional burnup of U-235

The cell corrections obtained from Eq (B-15) as a function of fuel burnup are presented in Figs. B-8 and B-9 for 68° F and 463° F, respectively.

f. Effect of U-235 loading tolerance

The manufacturing tolerance on the U-235 loading per fuel element allows a difference of ±2% from the nominal loading. Fuel element cell corrections were determined for the end points of the tolerance through use of the time-dependent cell correction formulas, Eq (B-15). Both hot and cold cell corrections were determined by setting the burnup, β_{25}, in Eq (B-15) equal to ±0.02. The results are given in Table B-13.

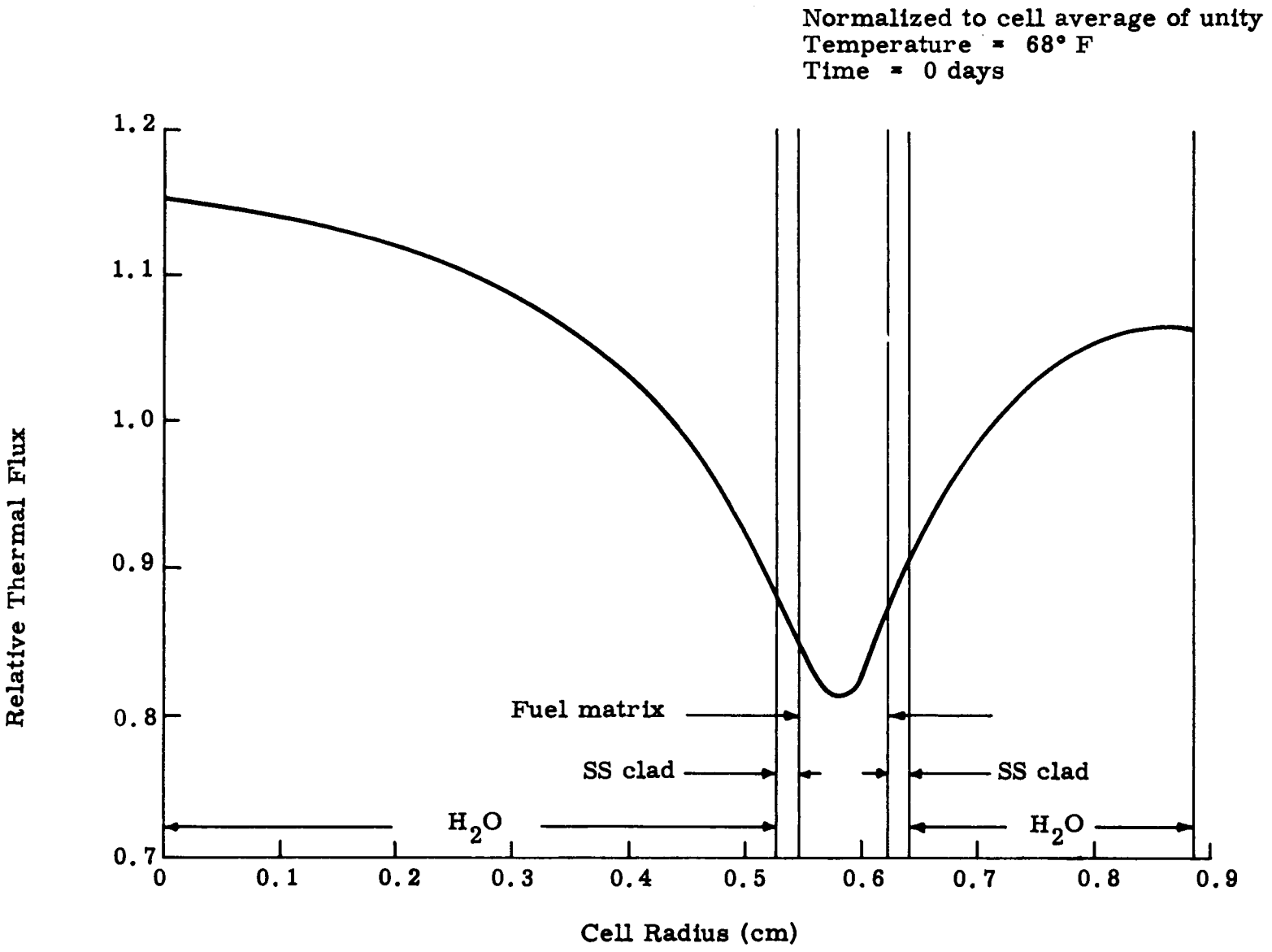

Fig. B-7. Relative Thermal Flux Distribution in a Fuel Element Cell

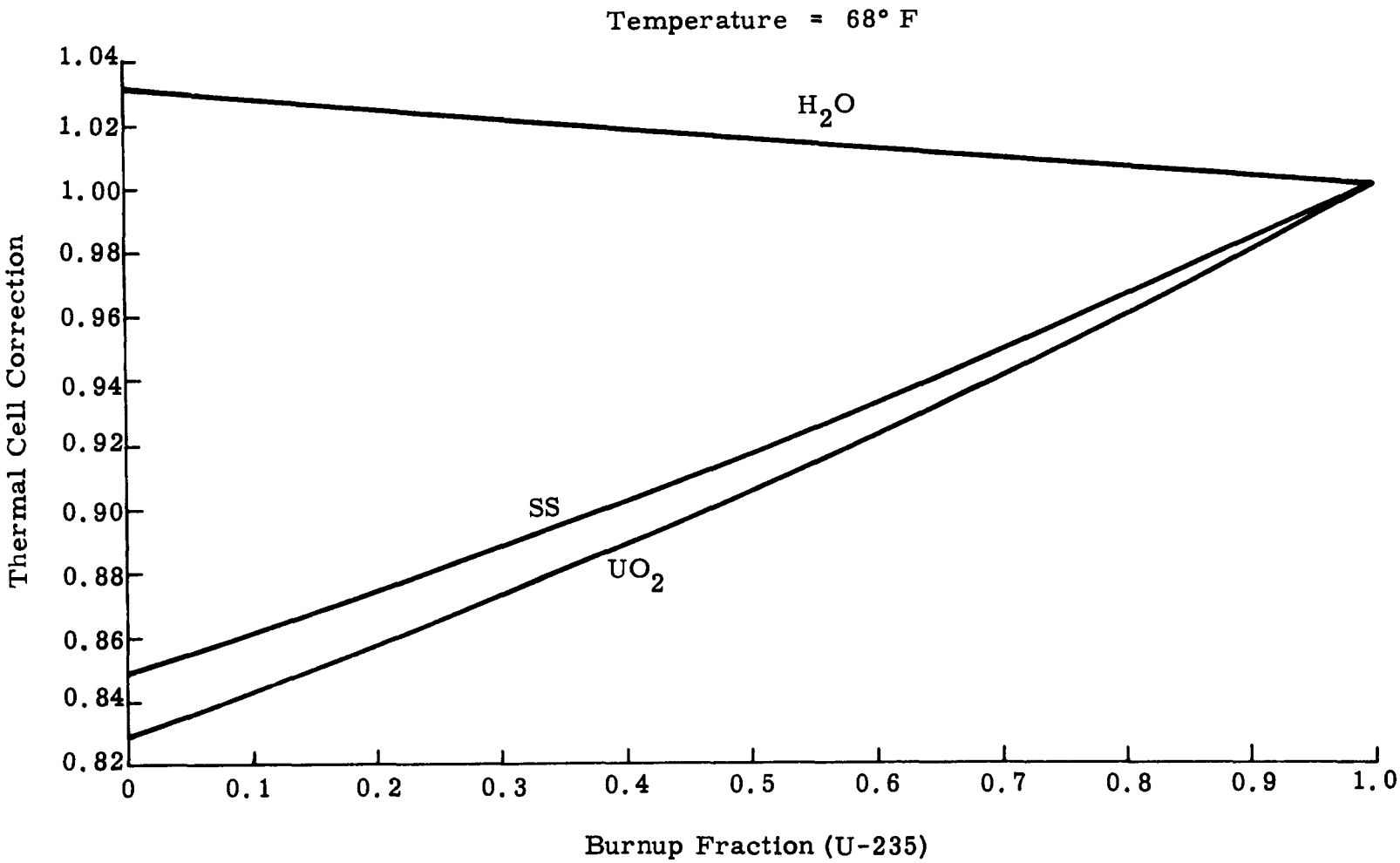

Fig. B-8. Fuel Cell Thermal Cell Correction Versus U-235 Burnup

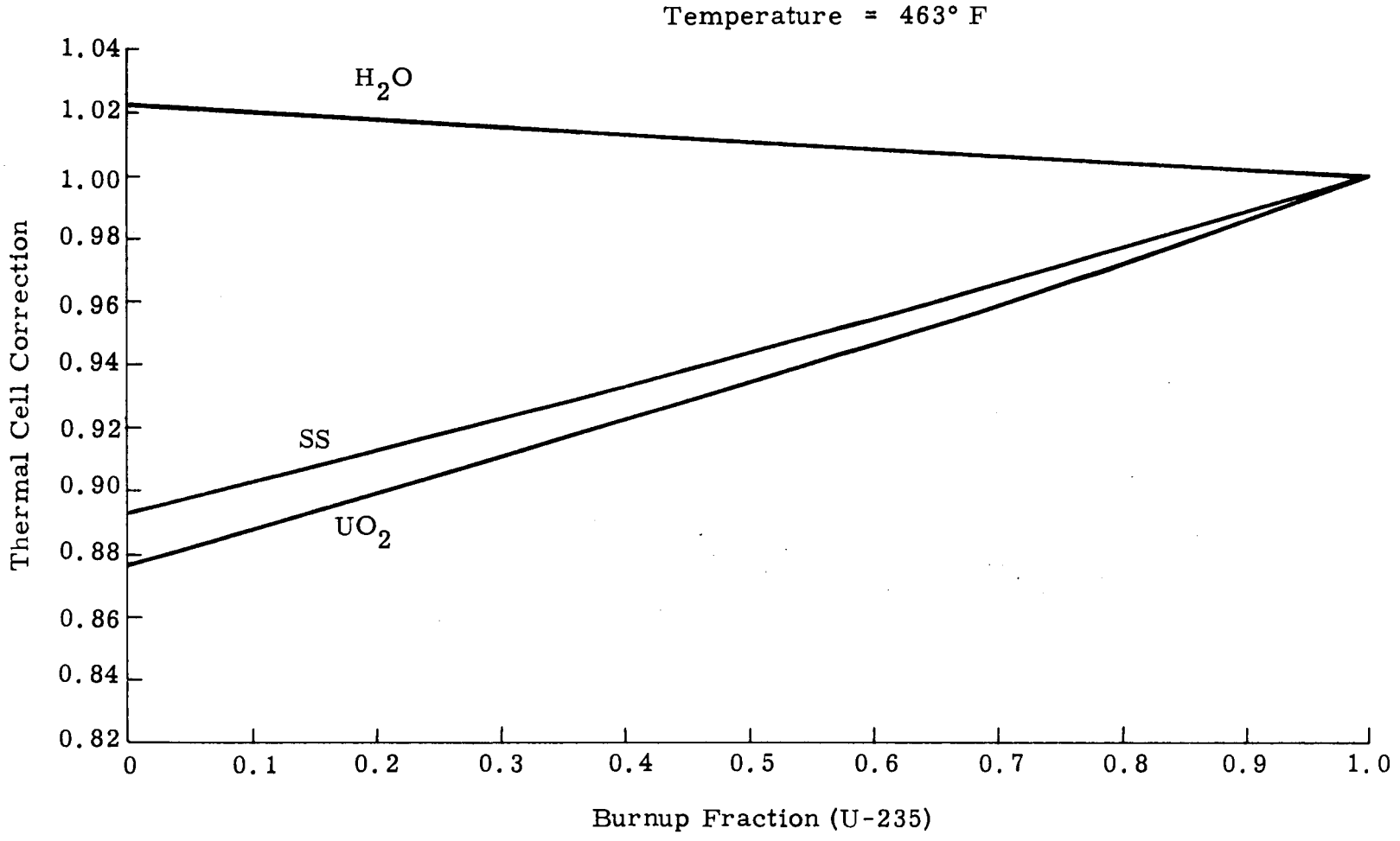

Fig. B-9. Fuel Cell Thermal Cell Correction Versus U-235 Burnup

TABLE B-13

Fuel Element Cell Corrections for Tolerance U-235 Loading

		Cold (68° F)			Hot (463° F)*		
U-235	Fuel Loading (gm U-235/FE)	$g(UO_2)$	g(SS)	$g(H_2O)$	$g(UO_2)$	g(SS)	$g(H_2O)$
-2%	39.32885	0.8316	0.8520	1.0309	0.8794	0.8947	1.0220
0	40.13148	0.8288	0.8494	1.0316	0.8772	0.8928	1.0225
+2%	40.93411	0.8260	0.8468	0.0322	0.8750	0.8909	1.0230

g. Comparison of analytical and experimental results

In the series of experiments described above, measurements were made of the fine-flux distribution through a fuel tube water hole and at both the inner and outer surfaces of the tube. No measurements were made through the matrix of the fuel tube because of the difficulties involved in mocking up the meat and clad structure. While the measurements are not directly compatible with the analytical results, due to the differences in geometry, they do serve to indicate whether general agreement exists. The measurements were made using plastic holders with 1/16-inch diameter by 0.002 inch thick 10% dysprosium-aluminum foils. The accuracy of the experimental data is ±2%. The analytical and experimental results are shown in Fig. B-10, with the normalization accomplished by equating the areas under the curves in the inner fuel tube water hole. The data shows good agreement (approximately ±5%) in the water, and therefore lends credence to the resultant flux shapes within the fuel tube.

3. Reactivity Determinations and Lifetime Calculations

a. Reflector savings and buckling

The PM-1 axial and radial three-group reflector savings and bucklings were obtained by the consistent K_{eff} method. The three-group core constants for use in the above calculation were calculated by the multigroup slowing down code, program C_3. The constants for the reflector regions, which include water, stainless steel and dead ends, were also determined by C_3; however, the core neutron energy spectrum was used as a source rather than a fission spectrum.

*68° F and 463° F correspond, respectively, to effective temperatures of 259° F and 779° F.

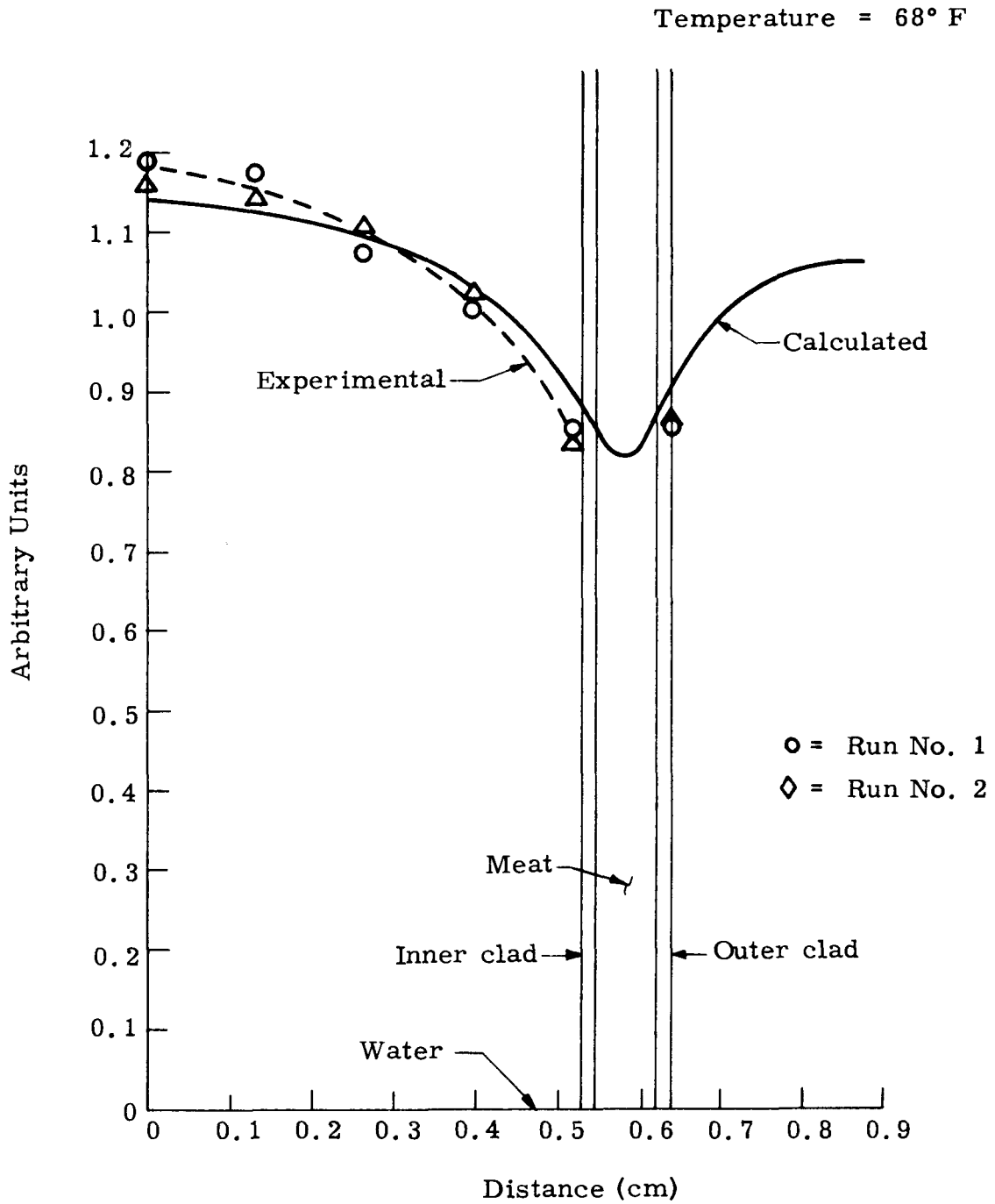

Fig. B-10. Comparison Between Experimental and Calculated Fine Flux Distributions Through a Fuel Tube Cell

The thermal neutron constants were evaluated at an effective temperature to account for spectrum hardening.

The resulting reflector constants are shown in Table B-14.

The geometrical configuration used to calculate the buckling consisted of a homogenized core region, and

(1) In the axial direction, a region containing stainless steel and water (dead ends) and a water region.

(2) In the radial direction, a water reflector plus a series of four stainless steel regions with water in between.

The axial and radial reflector savings, buckling and extrapolation length obtained using the reflector constants shown in Table B-14 and the geometries listed above are given in Table B-15.

b. Radial six-region core reactivity

The radial composition of the PM-1 reactor core is extremely heterogeneous. The lumped poison rods are not distributed evenly, but tend to be clustered in about 67% of the core. This means that the relative concentration of fuel elements in these areas is reduced. Fairly massive pieces of stainless steel used for control rod guides also displace fuel elements and further contribute to the nonuniformity of the core. Therefore, in order to analyze the core with a reasonable degree of accuracy, it is necessary to use a multiregion radial model.

A good approximation to the radial core geometry can be obtained by using a six-region core model. The six-region core model was adopted and used in all the radial calculations, except where a one-region core was required because of other considerations. A diagram showing the core regions and the number of elements in each region is presented in Fig. B-11. The volume fraction and atom densities of the materials initially present in each region are given in Table B-16.

The initial reactivity of the PM-1 was calculated, using program C_3 to obtain regionwise group constants and program F_3 to perform the three-group multiregion diffusion calculation. The moderation calculation tends to underestimate the neutron age and thus, the core leakage. Therefore, the perpendicular core buckling was modified through a change in core height to normalize the calculated initial core reactivity to that measured experimentally.* The resulting hot and cold initial reactivities are given in Table B-17.

*The reactivity bias was 1.8% ρ

TABLE B-14

Three-Group Reflector Constants
Based on Core Neutron Source Spectrum

Material	Water		Stainless Steel		Dead Ends	
Temp (°F)	68	463	68	463	68	463
T_{eff} (°F)	78.4	476.8	268	663	106.9	522.4
D1	1.39434E&0	1.67686E&0	8.71515E-1	8.73629E-1	1.26475E&0	1.44793E&0
D2	3.49779E-1	4.81423E-1	3.60331E-1	3.62217E-1	3.47447E-1	4.47879E-1
D3	1.46850E-1	2.31459E-1	3.18812E-1	3.30601E-1	1.67731E-1	2.51273E-1
Σ_{a_1}	1.33326E-4	1.04026E-4	2.37670E-3	2.37273E-3	4.74483E-4	4.57578E-4
Σ_{a_2}	9.10810E-3	5.68113E-3	4.91786E-2	4.28148E-2	2.58666E-2	1.89203E-2
Σ_{a_3}	1.95390E-2	1.19930E-2	1.89584E-1	1.50968E-1	5.64905E-2	4.01953E-2
Σ_{SL_1}	1.76689E-1	1.45343E-1	6.49535E-3	6.47579E-3	1.49476E-1	1.23696E-1
Σ_{SL_2}	4.04133E-1	3.37521E-1	3.91771E-3	4.37203E-3	3.22809E-1	2.69716E-1

TABLE B-15

PM-1 Reflector Savings, Buckling and Extrapolation Length

	68° F		463° F	
	Radial	Axial	Radial	Axial
B_1^2	4.4835×10^{-3}	1.3083×10^{-3}	4.0876×10^{-3}	1.2245×10^{-3}
B_2^2	5.2366×10^{-3}	1.4863×10^{-3}	4.8410×10^{-3}	1.4097×10^{-3}
B_1^2	5.4601×10^{-3}	1.5377×10^{-3}	5.0410×10^{-3}	1.4576×10^{-3}
$\Delta D/2$, $\Delta H/2$ (CM)	3.3116	1.6000	4.4666	2.5150
$\delta\lambda_1$ (CM)	3.7283		4.2732	
$\delta\lambda_2$ (CM)	1.0447		1.2210	
$\delta\lambda_3$ (CM)	0.3574		0.5280	

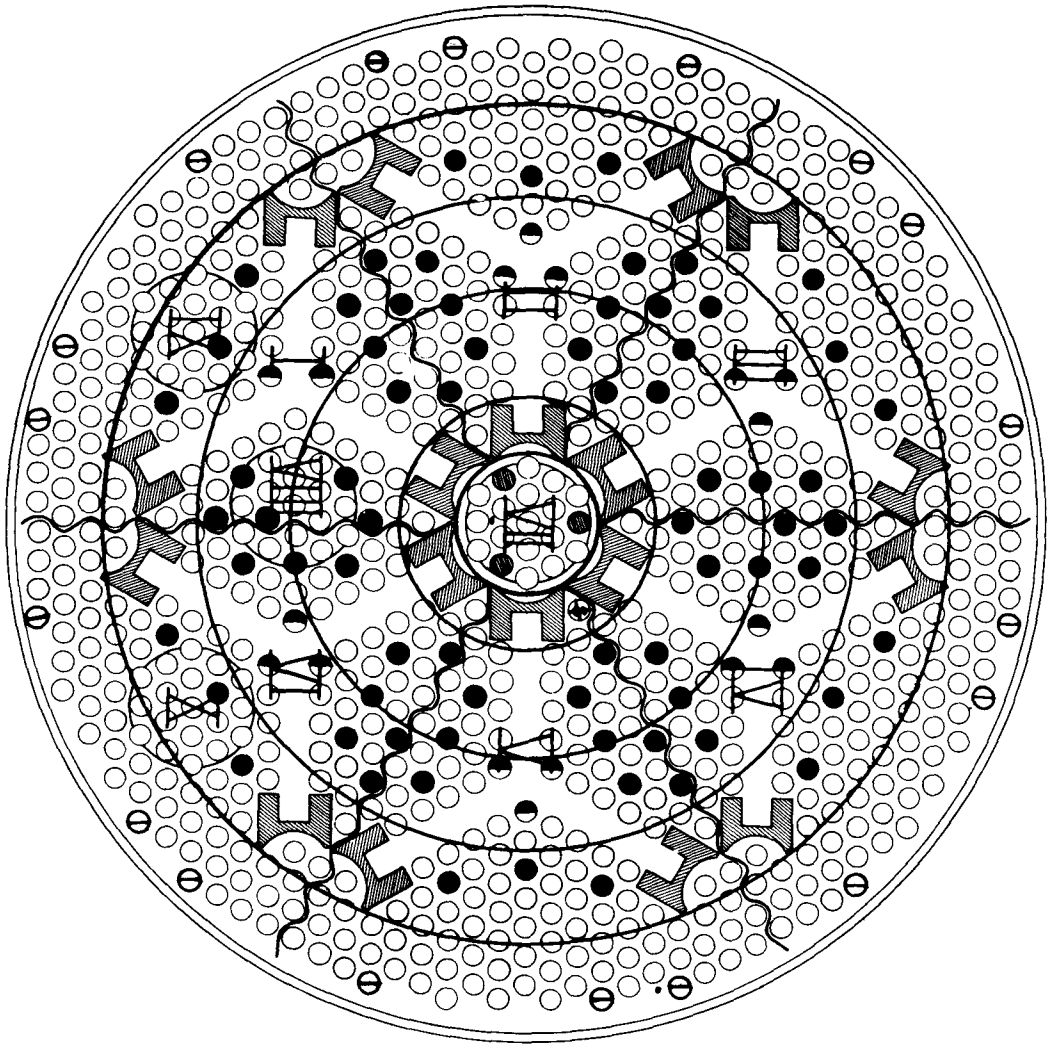

Region	1	2	3	4	5	6
○ Fuel element	15	6	126	156	180	258
Lumped poison rods						
● Full length	0	0	24	30	18	0
◓ 2/3 length	0	0	0	18	0	0
◙ Stainless steel rods (center bundle structure)	3	0	0	0	0	0
⊖ Stainless steel tubes	1	0	0	0	0	0
Control rod guides	0	6	0	0	12	0
⊕ Source	0	1	0	0	0	0

Fig. B-11. Radial Six-Region Core Configuration

TABLE B-16

Regional Volume Fractions (\F) and Atomic Densities (N) for the Component Materials of the PM-1 Core

	Core	Region 1	Region 2	Region 3	Region 4	Region 5	Region 6
Volume fraction UO_2	1.65648×10^{-2}	1.73655×10^{-2}	2.82732×10^{-3}	1.73891×10^{-2}	1.43246×10^{-2}	1.52864×10^{-2}	2.17979×10^{-2}
Atomic density U-235	3.81580×10^{20}	4.00023×10^{20}	6.51290×10^{19}	4.00568×10^{20}	3.29976×10^{20}	3.52132×10^{20}	5.02126×10^{20}
Atomic density U-238	2.78406×10^{19}	2.91862×10^{19}	4.75190×10^{18}	2.92260×10^{19}	2.40755×10^{19}	2.56920×10^{19}	3.66358×10^{19}
Atomic density Oxygen	8.18840×10^{20}	8.58420×10^{20}	1.39762×10^{20}	8.59589×10^{20}	7.08103×10^{20}	7.55645×10^{20}	1.07752×10^{21}
Volume fraction SS1*	1.00673×10^{-1}	1.02731×10^{-1}	1.67259×10^{-2}	1.02870×10^{-1}	8.47417×10^{-2}	9.04314×10^{-2}	1.39076×10^{-1}
Volume fraction SS2**	3.92149×10^{-2}	7.51191×10^{-2}	2.65349×10^{-1}	0	0	9.56437×10^{-2}	0
Volume fraction SS3***	4.11502×10^{-2}	0	0	7.10094×10^{-2}	8.63485×10^{-2}	3.27720×10^{-2}	0
N B-10	9.70267×10^{18}	0	0	1.71144×10^{19}	1.99275×10^{19}	7.89858×10^{18}	0
Volume fraction H_2O (68° F)	7.97678×10^{-1}	8.00213×10^{-1}	7.14354×10^{-1}	8.03524×10^{-1}	8.10081×10^{-1}	7.61553×10^{-1}	8.33389×10^{-1}
Volume fraction H_2O (463° F)****	6.51208×10^{-1}	6.53278×10^{-1}	5.83184×10^{-1}	6.55981×10^{-1}	6.61334×10^{-1}	6.21717×10^{-1}	6.80362×10^{-1}
Volume fraction/region	1.0	0.01931	0.04744	0.16198	0.24345	0.26323	0.26459
Volume (CC)/region	1.99642×10^{5}	3.8550×10^{3}	9.4710×10^{3}	32.3380×10^{3}	48.6028×10^{3}	52.5518×10^{3}	52.8233×10^{3}

*SS1 includes SS in the fuel elements and SS tubes
**SS2 includes SS in the SS rods and control rod guides
***SS3 includes SS in the lumped poison rods
****Effective volume fraction accounts for thermal expansion

TABLE B-17

PM-1 Initial Core Reactivities

T (°F)	Reactivity
68	0.13273
463	0.09080

The three-group, six-region core constants used to obtain the above reactivities are listed in Table B-18.

c. Reactivity versus stable period

To utilize the results of the PM-1 critical experiments (PMZ-1), it was necessary to convert the period measurements to reactivities. To perform the conversion properly, the difference in the energy spectrum of delayed neutrons relative to prompt neutrons must be considered. Delayed neutrons are born at a somewhat lower energy than prompt neutrons; thus, their fast constants are different, particularly the neutron age. If we define

$$\frac{K^{i}_{eff}}{K^{s}_{eff}} \equiv \gamma_i \qquad \text{(B-16)}$$

where:

K^{i}_{eff} = multiplication based on a delayed spectrum, i

K^{s}_{eff} = multiplication based on regular prompt plus delayed spectrum,

then the conversion from period to reactivity can be represented by weighting the delayed fraction, β_i, by γ_i. Thus,

$$\rho_s = \frac{\ell^* \omega}{K^{s}_{eff}} + \sum_i \frac{\gamma_i \beta_i}{\omega + \lambda_i} \qquad \text{(B-17)}$$

where:

ℓ^* = neutron lifetime

ρ_s = static reactivity

TABLE B-18

Regional 3-Group Constants for the PM-1 Core
Beginning of Life (68° F)

				Cross Sections		
Region	Group	Axial Buckling	Diffusion Coefficient	Sigma Absorption	Nu Sigma Fission	Sigma Slowing Down
1	1	2.09143E-03	1.62833E-00	1.20993E-03	1.56031E-03	6.89377E-02
	2	2.46096E-03	4.88357E-01	3.33531E-02	5.11342E-02	5.81148E-02
	3	2.57138E-03	1.66632E-01	2.15548E-01	3.53471E-01	
2	1	2.09143E-03	1.54298E-00	7.44291E-04	2.54269E-04	6.43796E-02
	2	2.46096E-03	4.65232E-01	1.43939E-02	9.81165E-03	6.09976E-02
	3	2.57138E-03	1.76309E-01	9.86454E-02	6.23950E-02	
3	1	2.09143E-03	1.63300E-00	1.20617E-03	1.56239E-03	6.91013E-02
	2	2.46096E-03	4.89553E-01	3.33524E-02	5.12792E-02	5.84256E-02
	3	2.57138E-03	1.66254E-01	2.15308E-01	3.54278E-01	
4	1	2.09143E-03	1.63763E-00	1.07913E-03	1.28705E-03	6.95334E-02
	2	2.46096E-03	4.90120E-01	2.94768E-02	4.40059E-02	6.12195E-02
	3	2.57138E-03	1.64990E-01	1.89148E-01	2.98482E-01	
5	1	2.09143E-03	1.59150E-00	1.17343E-03	1.37391E-03	6.68228E-02
	2	2.46096E-03	4.79283E-01	3.10490E-02	4.52865E-02	5.57357E-02
	3	2.57138E-03	1.71419E-01	2.02583E-01	3.11945E-01	
6	1	2.09143E-03	1.66440E-00	1.34544E-03	1.95810E-03	7.06162E-02
	2	2.46096E-03	4.97558E-01	3.84223E-02	6.20053E-02	5.84767E-02
	3	2.57138E-03	1.63233E-01	2.47361E-01	4.35282E-01	

TABLE B-18 (continued)

Regional 3-Group Constants for the PM-1 Core
Beginning of Life (463° F)

				Cross Sections		
Region	Group	Axial Buckling	Diffusion Coefficient	Sigma Absorption	Nu Sigma Fission	Sigma Slowing Down
1	1	1.92437E-03	1.85443E-00	1.16549E-03	1.56000E-03	5.69005E-02
	2	2.29971E-03	5.71125E-01	2.78736E-02	4.22068E-02	5.00238E-02
	3	2.40020E-03	2.45829E-01	1.66006E-01	2.75097E-01	
2	1	1.92437E-03	1.72405E-00	7.08182E-04	2.54291E-04	5.34475E-02
	2	2.29971E-03	5.34220E-01	1.15919E-02	7.98052E-03	5.22408E-02
	3	2.40020E-03	2.57893E-01	7.34901E-02	4.82517E-02	
3	1	1.92437E-03	1.86106E-00	1.17593E-03	1.56205E-03	5.70151E-02
	2	2.29971E-03	5.73620E-01	3.07180E-02	4.10144E-02	4.85541E-02
	3	2.40020E-03	2.48749E-01	1.83744E-01	2.70954E-01	
4	1	1.92437E-03	1.86897E-00	1.05063E-03	1.28676E-03	5.73565E-02
	2	2.29971E-03	5.76091E-01	2.79938E-02	3.48453E-02	5.04503E-02
	3	2.40020E-03	2.48944E-01	1.66465E-01	2.27270E-01	
5	1	1.92437E-03	1.79660E-00	1.13969E-03	1.37378E-03	5.52869E-02
	2	2.29971E-03	5.55059E-01	2.72571E-02	3.68009E-02	4.71673E-02
	3	2.40020E-03	2.51986E-01	1.64180E-01	2.40731E-01	
6	1	1.92437E-03	1.91087E-00	1.29760E-03	1.95755E-03	5.81477E-02
	2	2.29971E-03	5.86945E-01	3.22658E-02	5.13087E-02	5.03580E-02
	3	2.40020E-03	2.41968E-01	1.91420E-01	3.39261E-01	

The dynamic reactivity calculation, which was described before, takes into account the effect of delayed neutrons when the reactor is on a stable period. Thus, the relationship between inverse stable period and dynamic reactivity is

$$\rho_d = \frac{\ell^* w}{K^d_{eff}} + \sum_i \frac{\beta_i}{w + \lambda_i} \qquad \text{(B-18)}$$

where:

ρ_d = dynamic reactivity

Experiment measurements are usually made on a relatively long stable period, so the first term on the right side of both Eqs. (B-17 and B-18) is negligible. Therefore, the average weighting factor, $\bar{\gamma}$, is

$$\frac{\rho_s}{\rho_d} = \frac{\sum_i \frac{\gamma_i \beta_i}{w + \lambda_i}}{\sum_i \frac{\beta_i}{w + \lambda_i}} = \bar{\gamma} \qquad \text{(B-19)}$$

The dynamic and static reactivity were calculated for the PM-1 cold core poisoned out to near critical with europium. The calculation was based on a two-dimensional synthesis which iterated on the buckling. The S_2 approximation was used in the axial direction and S_4 in the radial direction. The extreme detail used in the calculation is required for determination of the small difference between ρ_s and ρ_d, which is caused primarily by differences in neutron leakage. The results are given in Table B-19.

TABLE B-19

Results of Static and Dynamic Reactivity Calculation
(Core Poisoned Out with Eu, 68° F)

ρ_d	=	0.00415
ρ_s	=	0.00467
$\bar{\gamma}$	=	1.125
$\sum_i \beta_{i_{eff}}$	=	0.0072
ℓ^*	=	8.9×10^{-6}

By using the above delayed neutron weighting factor ($\bar{\gamma}$) and the delayed neutrón data given in Table B-20, the reactivity versus period was calculated for periods of 10 to 200 seconds. The results are shown in Fig. B-12.

TABLE B-20

Delayed Neutron Data (Ref. 10)

Delayed Group (i)	Decay Constant (λ_i)	Delay Fraction (β_i)
1	1.24×10^{-2}	2.112×10^{-4}
2	3.05×10^{-2}	1.402×10^{-3}
3	1.11×10^{-1}	1.255×10^{-3}
4	3.01×10^{-1}	2.528×10^{-3}
5	1.13	7.360×10^{-4}
6	3.00	2.680×10^{-4}

d. Comparison of experimental and analytical reactivities

The total reactivity of the reference design core was determined experimentally. The reference design core differs slightly from the experimental mockup in that the clad thickness is increased by 1-1/2 mils, and the weight of U-235 is increased by 0.794 gram per fuel element. Table B-21 summarizes the major differences in the two cores.

TABLE B-21

Differences in Experimental and Final Design Core

	Experimental Core	Final Design Core
UO_2 per active element	47.989 gm	48.958 gm
U-235 per active element	39.337 gm	40.131 gm
U-235 total core	29.1 kg	29.7 kg
Stainless steel per active element	192.044 gm	209.631 gm
Volume of water per active fuel cell	158.567 cm^3	156.237 cm^3

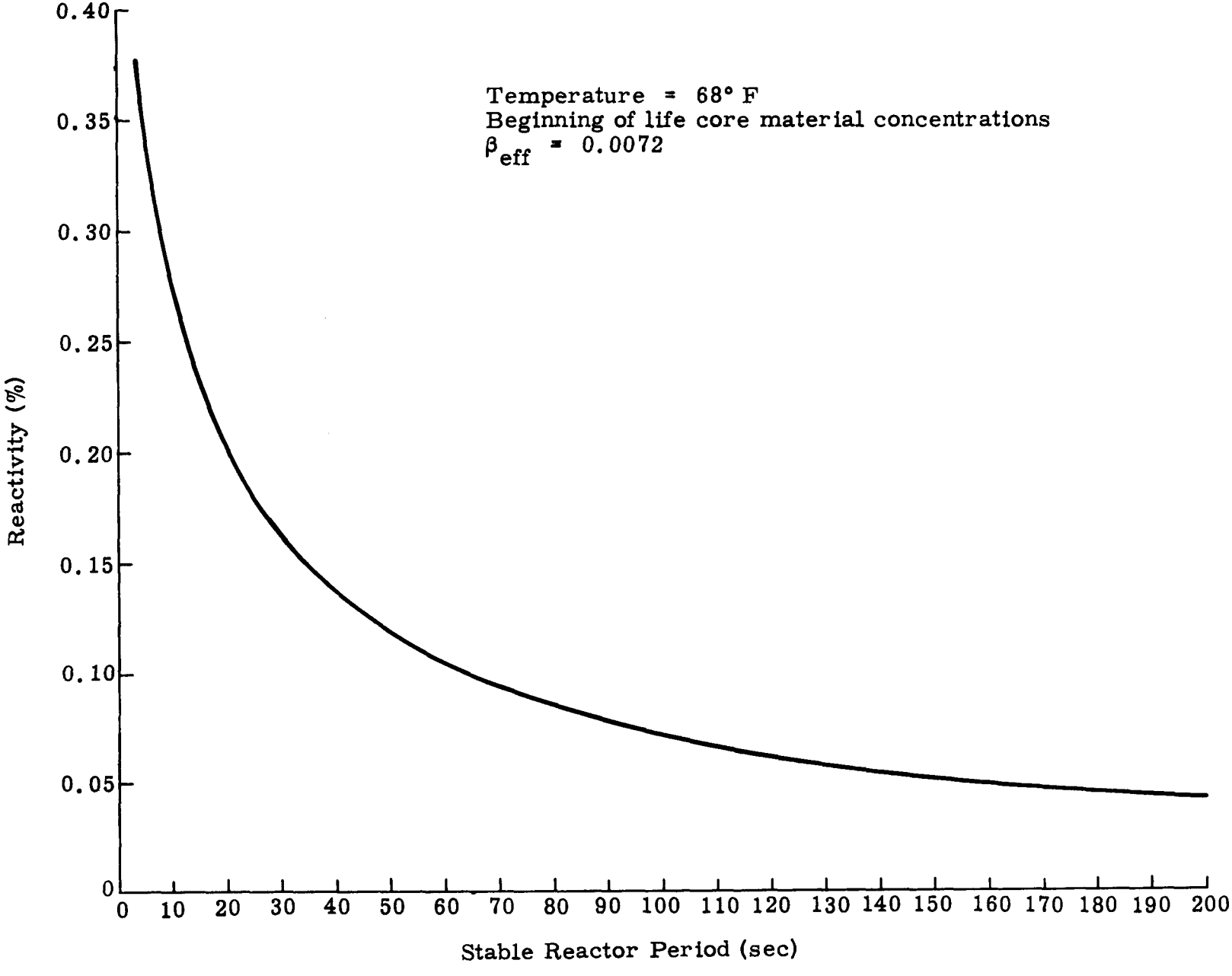

Fig. B-12. PM-1 Reactivity Versus Stable Reactor Period

The total core reactivity was determined experimentally by the poison substitution method. Boron plastic strips, uniformly distributed throughout the core by inserting them in the fuel tube water holes, were used to poison out the core. The resultant reactivity for the reference design mockup was 13.42 ± 0.41% ΔK/K. An analytical evaluation of the differences in the mockup fuel element and design fuel element, as shown in Table B-21, result in a decrease in the experimental total reactivity of 0.14% ΔK/K or a corrected reactivity of 13.28 ± 0.41% ΔK/K. The total reactivity determined analytically was found to be 13.273% ΔK/K. *

e. Reactivity versus boron strip loading

The reactivity measurements carried out at the Martin Marietta critical facility were performed with the reactor near critical. The gross reactivity of the core is several orders of magnitude larger than that which is measured incrementally by boron strip addition. It is usually assumed that the reactivity worth per boron strip is independent of the number of strips in the core. Since the measured values of reactivity are used in several areas of this report, it was deemed necessary to check the above assumption analytically.

A comparison was made of the thermal flux depression in a typical fuel element with that in an element containing a boron polyethylene strip. The strip contained 5.09 wt % boron, which is equivalent to 0.491 gram of natural boron per strip per 30 inches of length. S_6 cell corrections were computed by the homogenized core method by mocking up a boron strip into an equivalent cylinder at the center of the fuel tube. Cell corrections for the fuel element with and without the boron are given in Table B-22. The thermal flux distribution through both fuel elements is shown in Fig. B-13.

---

*This value was obtained by correcting the perpendicular buckling to account for the 1.8% ρ bias.

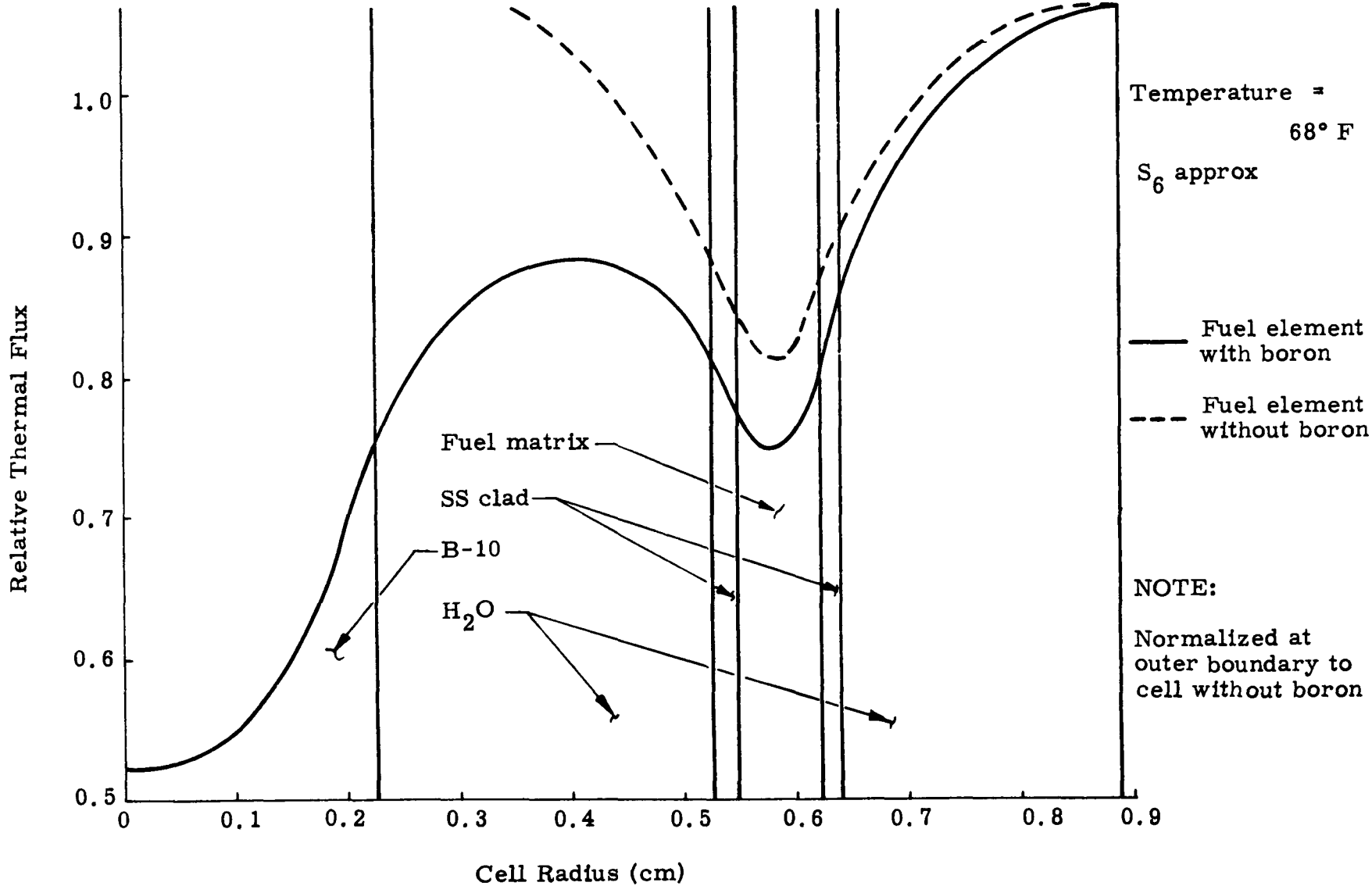

Fig. B-13. Calculated Thermal Flux Distribution Through a Fuel Element Cell with a Boron Strip Inserted

TABLE B-22

Fuel Element Cell Correction with and Without Plastic Boron Strip at Center of Cell (68° F)

Without Strip ($\overline{\phi}_i / \overline{\phi}_{FE}$)	With Strip ($\overline{\phi}_i$)*
(UO_2) = 0.8288	(B) = 0.6177
(SS) = 0.8494	(UO_2) = 0.7741
(H_2O) = 1.0316	(SS) = 0.7942
	(H_2O) = 0.9509

Several radial six-region core calculations were made with varying amounts of boron added to the core regions in which the boron polyethylene strips are placed during the reactivity measurements. The amount of boron added to each region was assumed to be proportional to the number of fuel elements in the various regions. The reactivity and number of strips per region for the cases of 0, 200, 400 and 600 total strips in the core are given in Table B-23.

TABLE B-23

Reactivity and Boron Strip Load for the PM-1 (68° F)

		Strips per Region					
Total Strips	Reactivity	1	2	3	4	5	6
0	0.13273	0	0	0	0	0	0
200	0.08671	4	2	34	42	48	70
400	0.04353	8	4	68	84	96	140
600	-0.00254	12	6	102	126	144	210

A plot of initial cold reactivity versus number of boron strips in the core, based on the preceding analysis, is shown in Fig. B-14. From the results shown in Fig. B-14, it can be seen that the assumption of a linear change in reactivity with boron strip loading is valid.

*Flux normalized at outer boundary of cell to that of a fuel element cell without the plastic boron strip inserted.

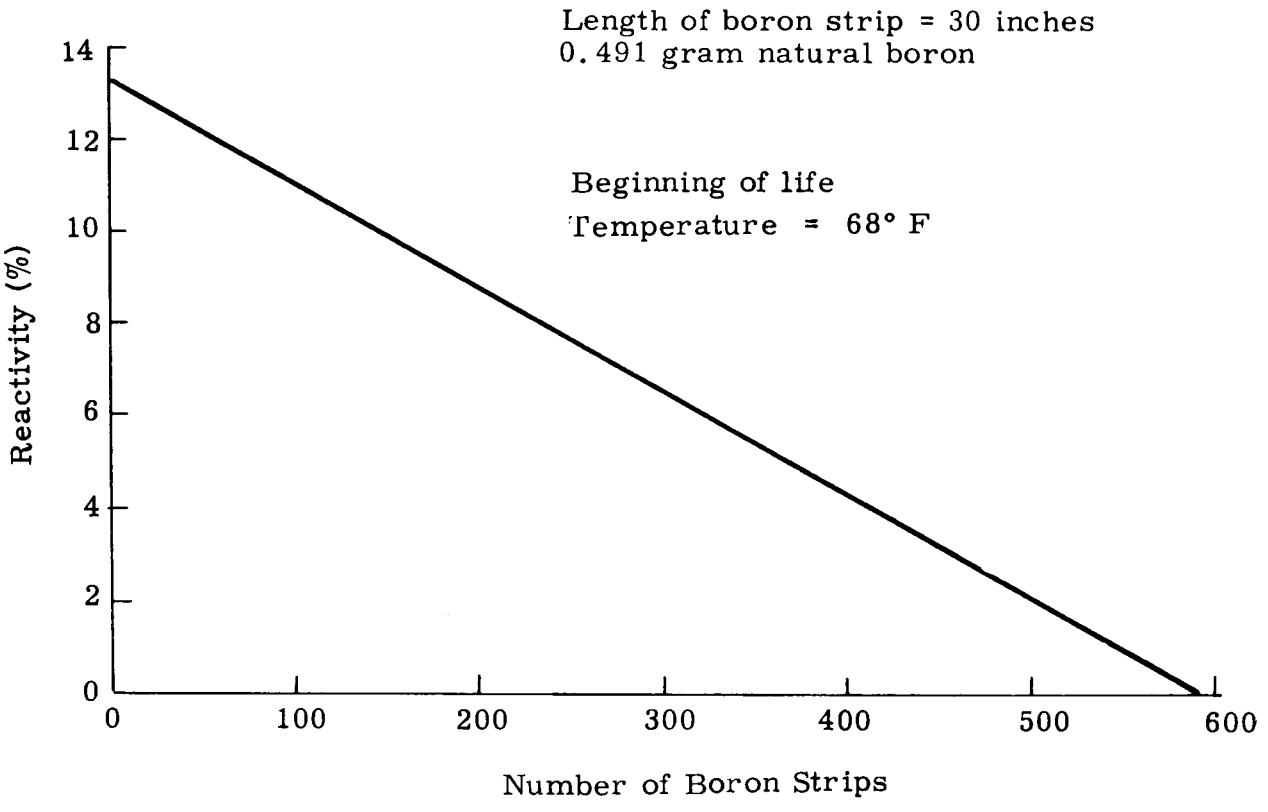

Fig. B-14. Calculated Reactivity Versus Boron Strip Loading

f. Fission, flux and slowing-down spectrum

The moderation program utilized in the analysis of the PM-1 performs a 19-group slowing-down calculation. From the results of the slowing-down calculation, the constants for the fast and epithermal groups are obtained. Therefore, it seems pertinent that the 19-group flux and slowing-down distribution should be available. These are presented in Figs. B-15 and B-16.

The multigroup fission spectrum is presented in Fig. B-17 to show the effect of lethargy on the fission distribution.

All three of the above curves are based on 463° F and end-of-life (700 days) conditions. The data was obtained using the properties of core region five, as this is typical of the whole core.

g. Comparison with SM-1 burnup

To check the accuracy of the cross sections and methods used to calculate the PM-1 core lifetime, it was felt that the lifetime of an existing burned-out core should be calculated. Since the SM-1 core is similar in many respects to the PM-1, it was decided that this core would serve as an excellent check on our capability to predict core lifetime.

The material concentrations of the SM-1 that were used in the calculation are given in Table B-24.

TABLE B-24

Material Concentrations in the SM-1

UO_2 (kg)	27.54
U-235 (kg)	22.50
B_4C (gm)	114.71
B-10 (gm)	15.75
SS (kg)	208.92
H_2O (kg)	111.08

The cell corrections used in the calculation were obtained from a two-dimensional synthesis of an SM-1 fuel element. An S_6 approximation in slab geometry was used. The resulting cell corrections, normalized to an average flux of one in the fuel element cell, for the beginning of life, are presented in Table B-25.

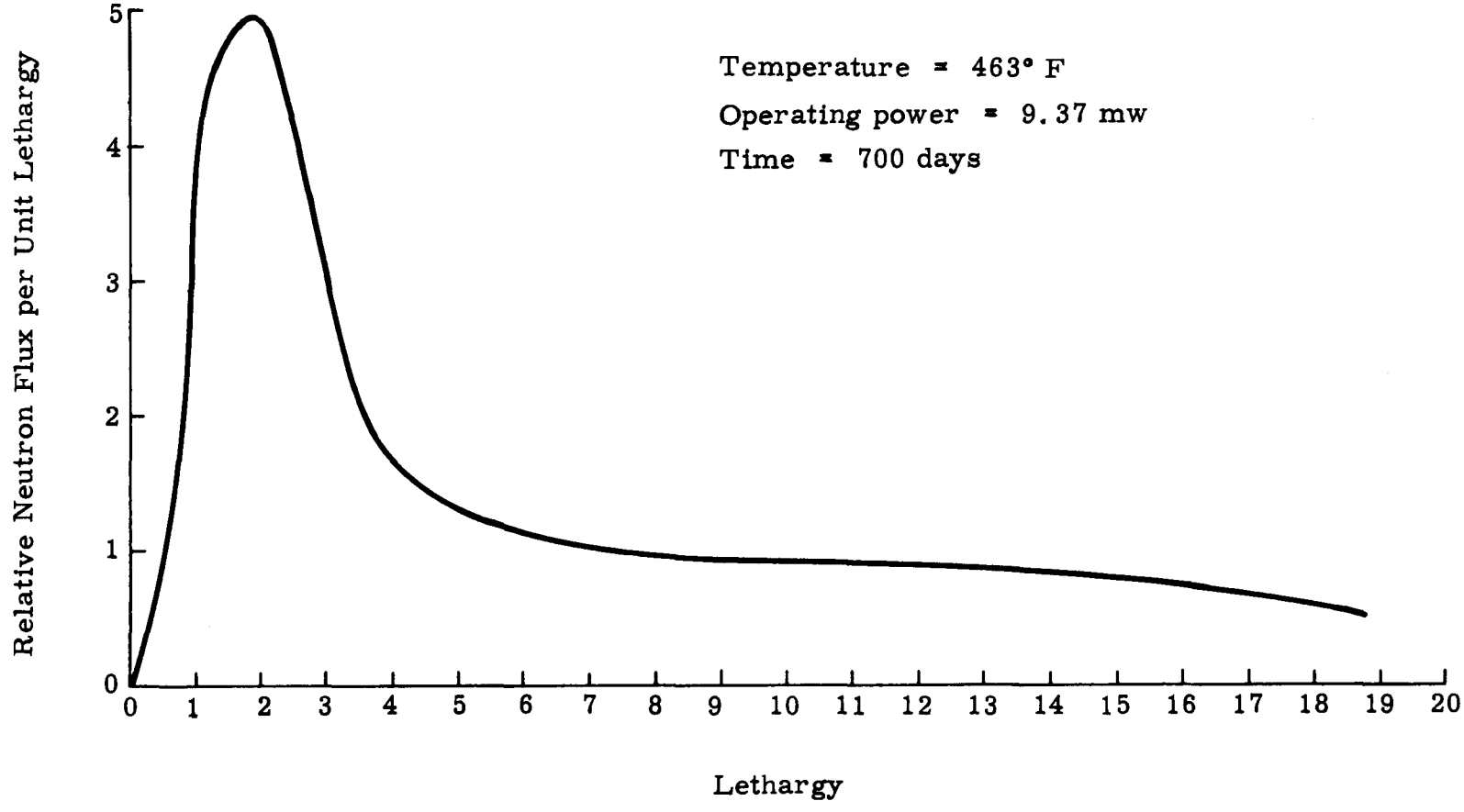

Fig. B-15. Neutron Flux Spectrum Versus Lethargy

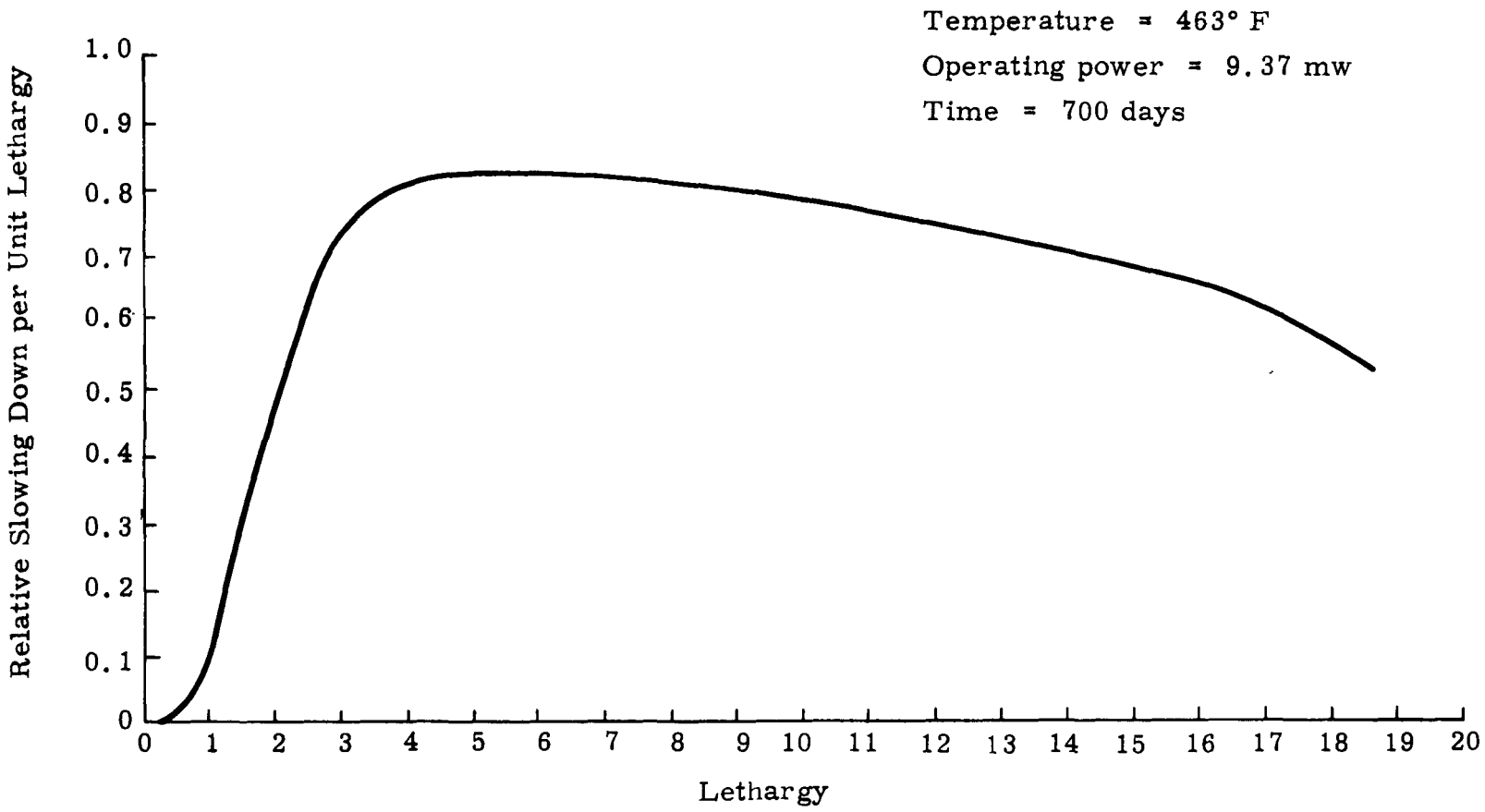

Fig. B-16. Slowing Down Spectrum Versus Lethargy

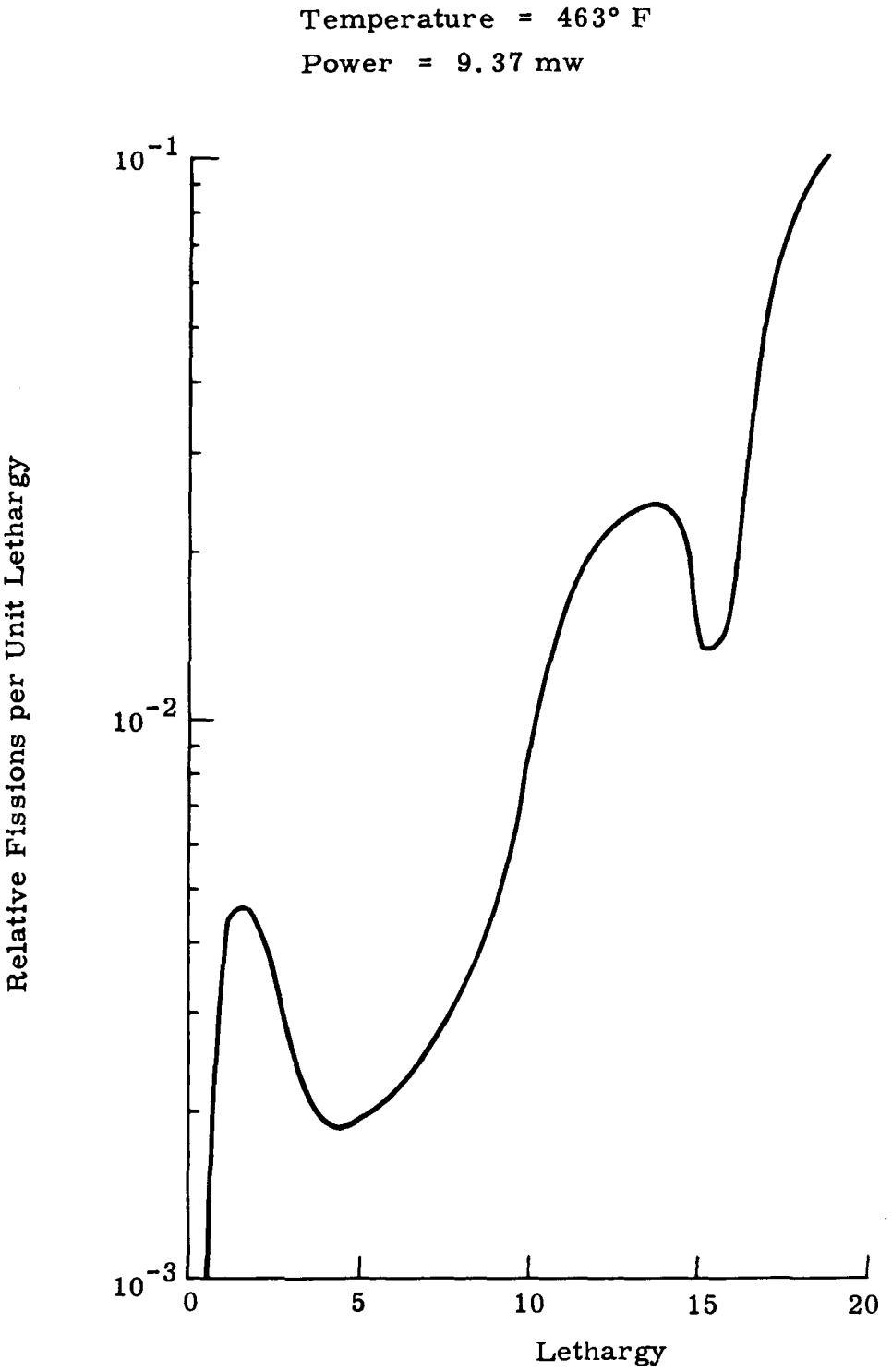

Fig. B-17. PM-1 Fission Spectrum 700 Days

TABLE B-25

SM-1 Thermal Cell Corrections, Beginning of Life (440° F)
(Normalized to an Average Cell Flux of Unity)

Material	Cell Correction
UO_2	0.8945
SS	1.0972
H_2O	1.0015

The SM-1 core lifetime was calculated in the axial and radial directions with both uniform and nonuniform burnup. Control rods were not included in the calculation because their net effect on core life is small and, therefore, was not considered necessary for comparative purposes. The total nonuniform core life was obtained by subtracting the axial nonuniform burnup reactivity defect from the radial nonuniform burnup reactivity. The results of the calculations are shown in Fig. B-18 as plots of lifetime versus core reactivity. The final SM-1 core life was calculated to be 14.52 mw-yr.* This compares very favorably with the extrapolated actual core life of 15 mw-yr reported in APAE 65. The difference between the actual and calculated core life indicates that the analysis is conservative by about 3%. If this factor is applied to the PM-1 core life, it would yield an increase of about 32 days.

*Normalized to an initial hot reactivity of 10.37% (APAE 42)

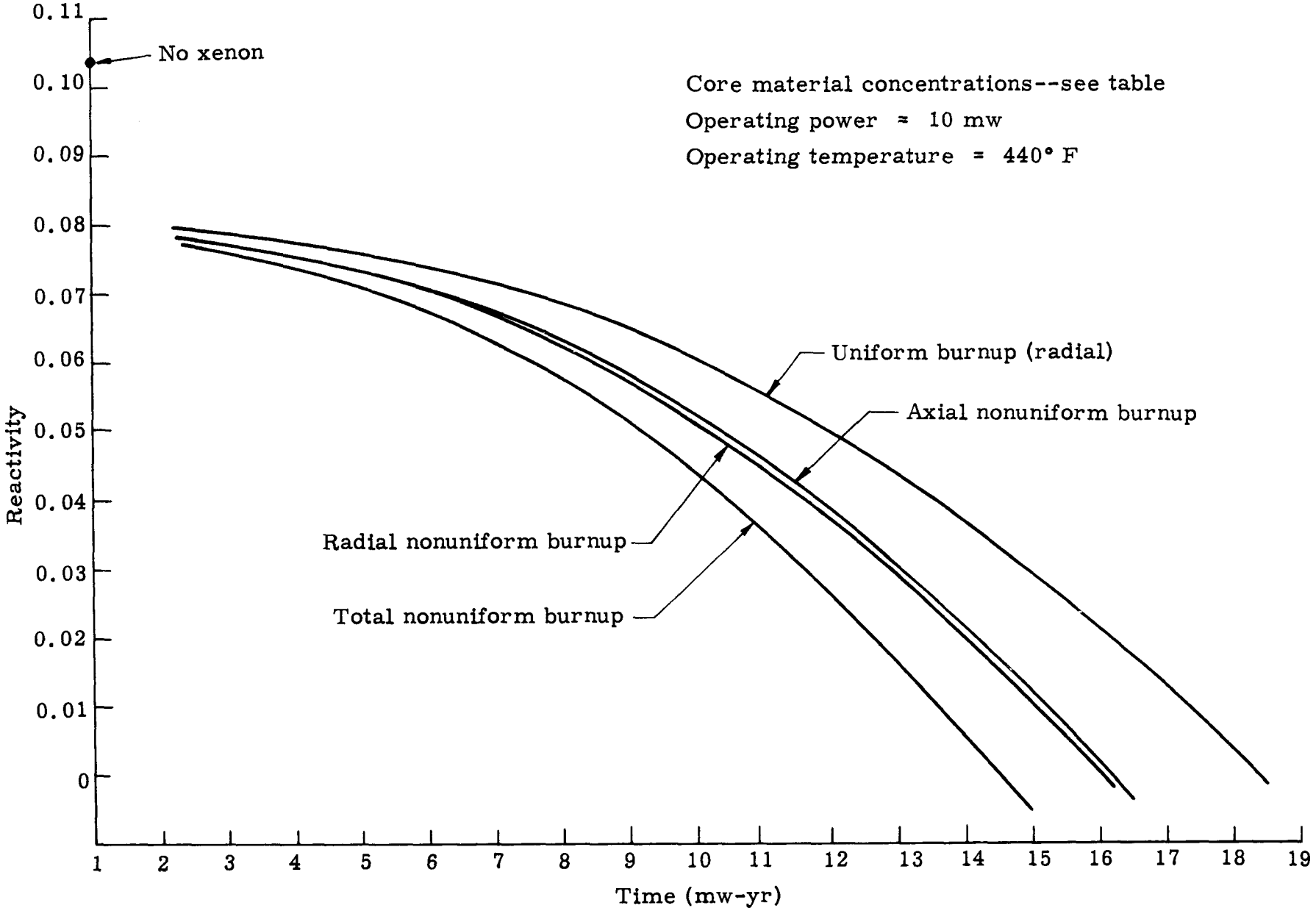

Fig. B-18. PM-1 Uniform and Nonuniform Core Lifetime

REFERENCES FOR APPENDIX B

(1) Keppler, J. G. and Orr, W. L., "A Three-Group Diffusion Calculation (Program F_3)," XDC July 18, 1958.

(2) Carlson, B., "Numerical Solutions of Transient and Steady-State Neutron Transport Problems," LA-2260, October 29, 1959.

(3) Frederick, D. H., "APWRC-SYNFAR, A. FORTRAN-II Program for Two-Dimensional Static or Dynamic Synthesis, Using P_1 or S_2 to S_{16} DSN Flux or Adjoint in Slab, Cylindrical or Spherical Geometry," MND-C-2460, January 20, 1961.

(4) Gross, E. E. and Marable, J. H., "Static and Dynamic Multiplication Factors and Their Relations to the Inhour Equations," Nuclear Science and Engineering,7, 281-291, 1960.

(5) Olsen, T. M., "Theory and Basic Equations of Program C," MND-E-1413, June 1958.

(6) Deutsch, R. W., "Computing 3-Group Constants for Neutron Diffusion," Nucleonics, 15, 47-51, 1957.

(7) Breslauer, S. K., XDC 60-1-144, 1959.

(8) Nephew, E. A., ORNL-2869, 1960.

(9) Thie, J. A., "Failure of Neutron Transport Approximations in Small Cells in Cylindrical Geometry," Nuclear Science and Engineering, 9, 286-287, 1961.

(10) Keepin, G. R., Wimett, T. F., and Ziegler, R. K. "Delayed Neutrons from Fissionable Isotopes of Uranium, Plutonium and Thorium," Physical Revision, 107, No. 4, 1044, 1957.

(11) Henry, A. F., "A Theoretical Method for Determining the Worth of Control Rods," WAPD-218, August, 1959.

Blank Page

APPENDIX C

THERMAL AND HYDRAULIC SUPPORTING DATA

In preparing the thermal and hydraulic design, analytical techniques were developed, experimental programs were conducted and supporting studies were performed.

1. Analytical Techniques

All steady-state thermal and hydraulic analyses of the fuel elements were performed with BITE, an IBM-7090 machine program.

BITE (Boiling in Tubular Elements) may be used for the analysis of tubular elements operating in any combination of the nonboiling, local boiling and bulk boiling regimes. The required input data include: element and orifice dimensions, coolant inlet conditions, flow distribution, radial and axial power distribution. Among the output data are axial distributions, both inside and outside the element, of: coolant temperature, quality, void fraction, slip ratio, pressure, surface temperature, heat flux and burnout heat flux.

Calculations of wall superheat in local boiling are based upon the Jens and Lottes correlation; local boiling friction factors are determined by means of the Martin Marietta correlation; and burnout heat fluxes are obtained from the -33% line of the Griffith correlation.

2. Experimental Programs

The experiments pertaining to the thermal and hydraulic design of the core are the full scale model flow test, heat transfer and burnout tests, and the zero power test.

a. Full Scale Model Flow Test

Core flow distributions were obtained by hydraulic testing of a full scale model of the reactor (Ref. 1). Using water at 100° F as the circulating medium, distributions were obtained with the control rods fully inserted at flow rates of 1750, 2125 and 2900 gpm, and, with the control rods fully withdrawn, at 2125 gpm. Actual operating conditions involve a mean coolant temperature of 463° F. It has been shown that the flow distribution is relatively insensitive to Reynolds number (within the turbulent range); hence, application of the experimental data is justified.

Analysis of the test data indicated that the measured flow allocation in the core was very close to that predicted (a maximum negative deviation of 7% was anticipated). No appreciable circumferential variations were observed; however, significant variations in velocity occurred in the radial direction. In this regard, the core may be divided into three areas: peripheral elements, elements above the lower alignment spider, and all remaining elements.

The average flow rate inside the three rows of tubes adjacent to the peripheral boundary was found to be 5.7% lower than the measured core average, with a maximum negative deviation of 13%. Since this is a relatively low power region of the core, a reduction in flow rate is desirable, as it provides additional coolant for the higher power regions.

The flow rates in the tubes above the outer region of the lower alignment spider were found to be somewhat lower than the core average. The results of a series of flow blockage tests were employed to demonstrate that this flow rate reduction was, in fact, due to the presence of the spider. Once again, the power density in this region of the core is relatively low; hence, adequate heat removal capacity is available.

Only one tube in the remainder of the core had a flow rate less than the anticipated minimum. The flow rate in this tube was 8.6% lower than the measured core average. Structural members below the core could account for this deviation.

b. Heat transfer tests

A series of experiments was performed to determine the thermal and hydraulic characteristics of tubular fuel elements in local boiling operation (Ref. 2). Single-tube test sections, with flow inside the tube only, were employed throughout. The ranges of local boiling parameters investigated were: pressure, 800 to 1500 psia; flow rate, 1.2 to 9.0 gpm; heat flux, 0.1×10^6 to 1.3×10^6 Btu/hr-ft^2; and inlet coolant temperature, 445° F.

The measured values of wall superheat were consistently higher than those predicted by the Jens and Lottes correlation (Ref. 3)

$$\Delta T_{SAT} = 1.9 \left(\frac{q}{10^6}\right)^{1/4} \exp\left(\frac{-P}{900}\right) \qquad \text{(C-1)}$$

where

ΔT_{SAT} = difference between surface temperature and saturation temperature, °F

q = heat flux, Btu/hr-ft^2

P = pressure, psia

These differences were not sufficiently large to warrant modification of the relationship.

Local boiling friction factor data were correlated by

$$f/f_{iso} = a + bj + cN_{Re} \qquad (C\text{-}2)$$

and

$$j = \frac{N_{Nu}}{N_{Re}\, N_{Pr}^{2/3}} \qquad (C\text{-}3)$$

where

f/f_{iso} = ratio of local boiling friction factor to isothermal friction factor

a, b, c = pressure-dependent constants

j = dimensionless heat transfer factor

N_{Re} = Reynolds number

N_{Nu} = Nusselt number

N_{Pr} = Prandtl number

c. Burnout tests

Local boiling burnout data was obtained with a single-tube test section, having coolant flow both inside and outside of an electrically heated tube (Ref. 4). To obtain the high heat fluxes required to achieve burnout conditions, it was essential that the dimensions of the test section tube differ from those of the actual PM-1 element. The tube dimensions were: 0.457-inch inside diameter, 0.416-inch outside diameter, and a 15-inch long section of stainless steel with a 4-inch nickel "A" extension. The outer diameter of the annular flow path was 0.688 inch.

The ranges of the parameters investigated were: flow ratio (ratio of flow inside tube to total flow rate), 0.43 to 0.56; pressure, 1100 and 1300 psia; mass flux, 4.2×10^5 to 15.0×10^5 lb/hr-ft^2; and outlet subcooling, 20° to 165° F. It was found that the resultant burnout data agreed favorably with the -33% line of the Griffith correlation (Ref. 5).

d. Zero power tests

The zero power testing of the PM-1 core has been reported in detail (Ref. 6). Insofar as the core thermal analysis is concerned, the items of interest are the radial and axial power distributions.

3. Supporting Studies

Several thermal and hydraulic analyses have been performed in support of the core design. Of particular interest in this area are the analyses of operational transients, scram conditions and decay heat removal.

a. Operational transients

The reactor coolant system was simulated on an analog computer. Various transient maneuvers were executed to determine that which caused the most severe thermal problems. This was determined to be an instantaneous closing of the main steam valve while operating at full power. Control rods were assumed to be locked in place and power to the primary coolant pump was cut off instantaneously (a natural convection flow of 3% of rated flow was assumed). Computer traces of reactor power and average reactor coolant temperature, as functions of time, are shown in Fig. C-1. The pressurizer safety valve set point is 1500 psia, which is adequate to assure that bulk boiling of the primary coolant does not take place.

b. Scram conditions and decay heat removal

The PM-1 control system is designed so that a reactor scram is always accompanied by a primary coolant pump scram. This safeguard reduces the magnitude of the thermal shock to the fuel elements and prevents, by means of an interlock, inadvertent withdrawal of the control rods.

Insofar as the heat removal aspects of a scram are concerned, an analog computer study has shown that the afterheat removal capacity is more than adequate. This study is described below.

After a reactor scram, core heat is produced by two means, i.e., fission decay and fission product decay. The former was determined

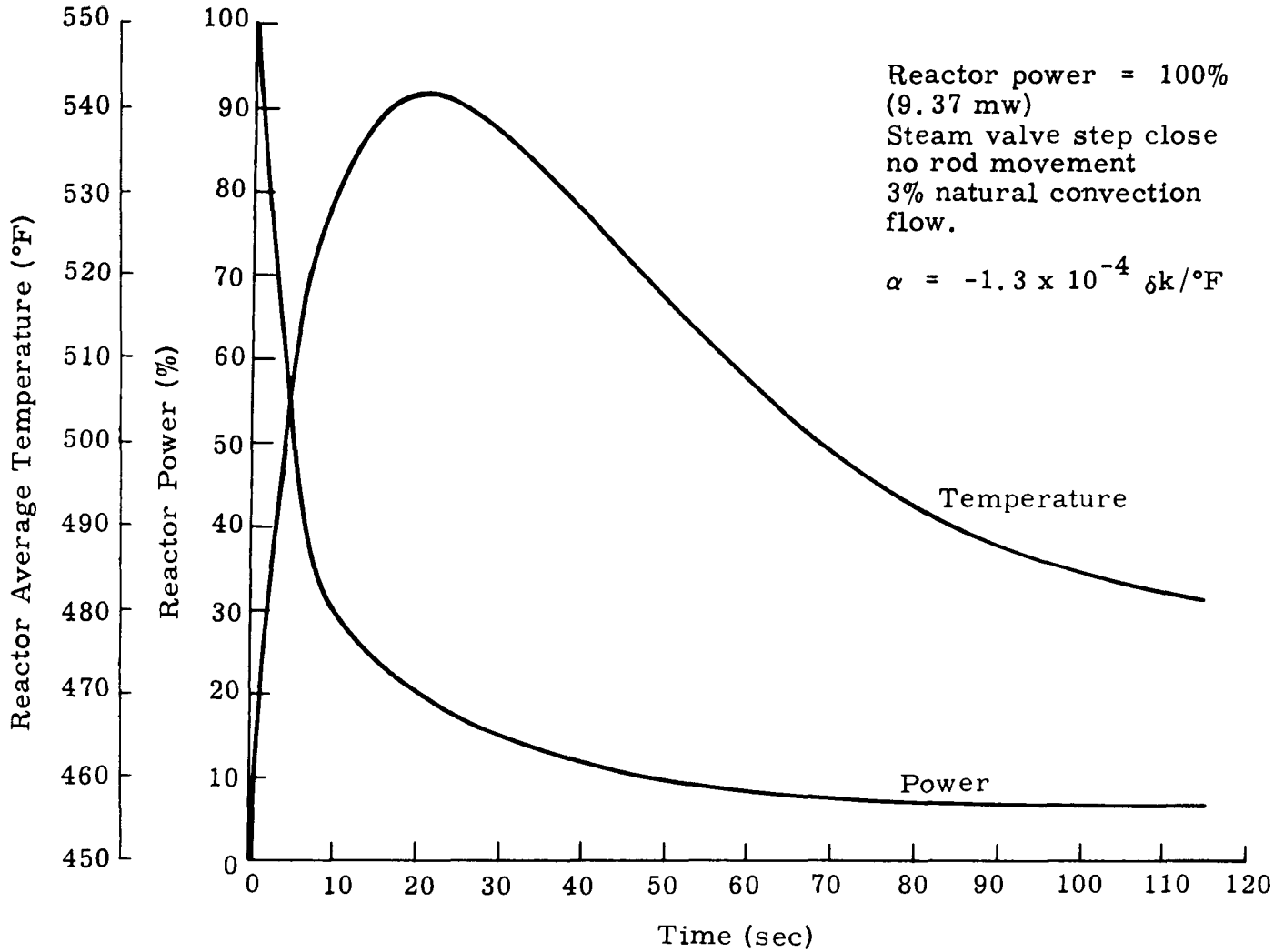

Fig. C-1. Reactor Power and Average Reactor Coolant Temperature as a Function of Time

from a two-delay-group analog model of the reactor kinetics. This is shown as Curve A in Fig. C-2. The fission product decay source, shown as Curve B, was determined through the use of an IBM-7090 code which computes the inventory and energy release of the fission products as functions of time. Curve C is the total heat production rate (the sum of Curves A and B), and Curve D is the analog computer simulation of Curve C.

An equation describing the flow after pump cutoff was derived and incorporated in the simulation of the power plant (Ref. 10).

$$\frac{d}{dt}\left(\frac{w}{w_o}\right) = \frac{g}{\sum_{j=1}^{N} \frac{L_j}{A_j}}\left[\Delta P_o + \sum_{i=1}^{3} \rho_i Z_i - k_1 w_o^2 \left(\frac{w}{w_o}\right)^2 - k_2 w^{1.8}\left(\frac{w}{w_o}\right)^{1.8}\right] \qquad \text{(C-4)}$$

where

w = flow rate

w_o = initial flow rate

L_j = length of the jth section of the primary loop

A_j = cross-sectional area of the jth section of the primary loop

ΔP_o = initial pump head

ρ = density

Z = elevation

K_1, K_2 = constants

Subscripts 1,2 and 3 refer to hot leg, cold leg and core, respectively. The flow coastdown obtained from the simulation is plotted in Fig. C-3. Curve A depicts this coastdown, neglecting the effects of natural con-

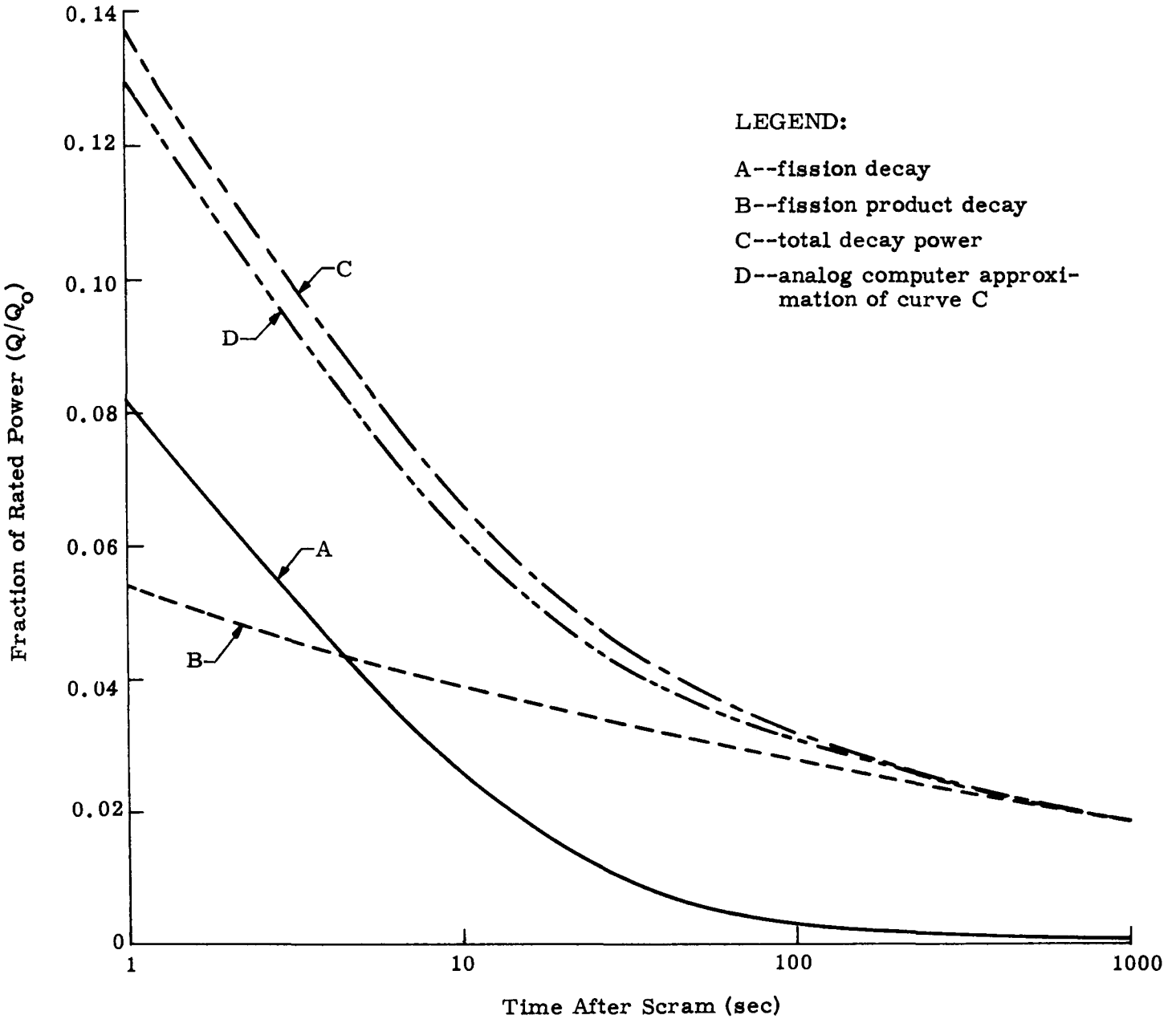

Fig. C-2. PM-1 Reactor Afterheat

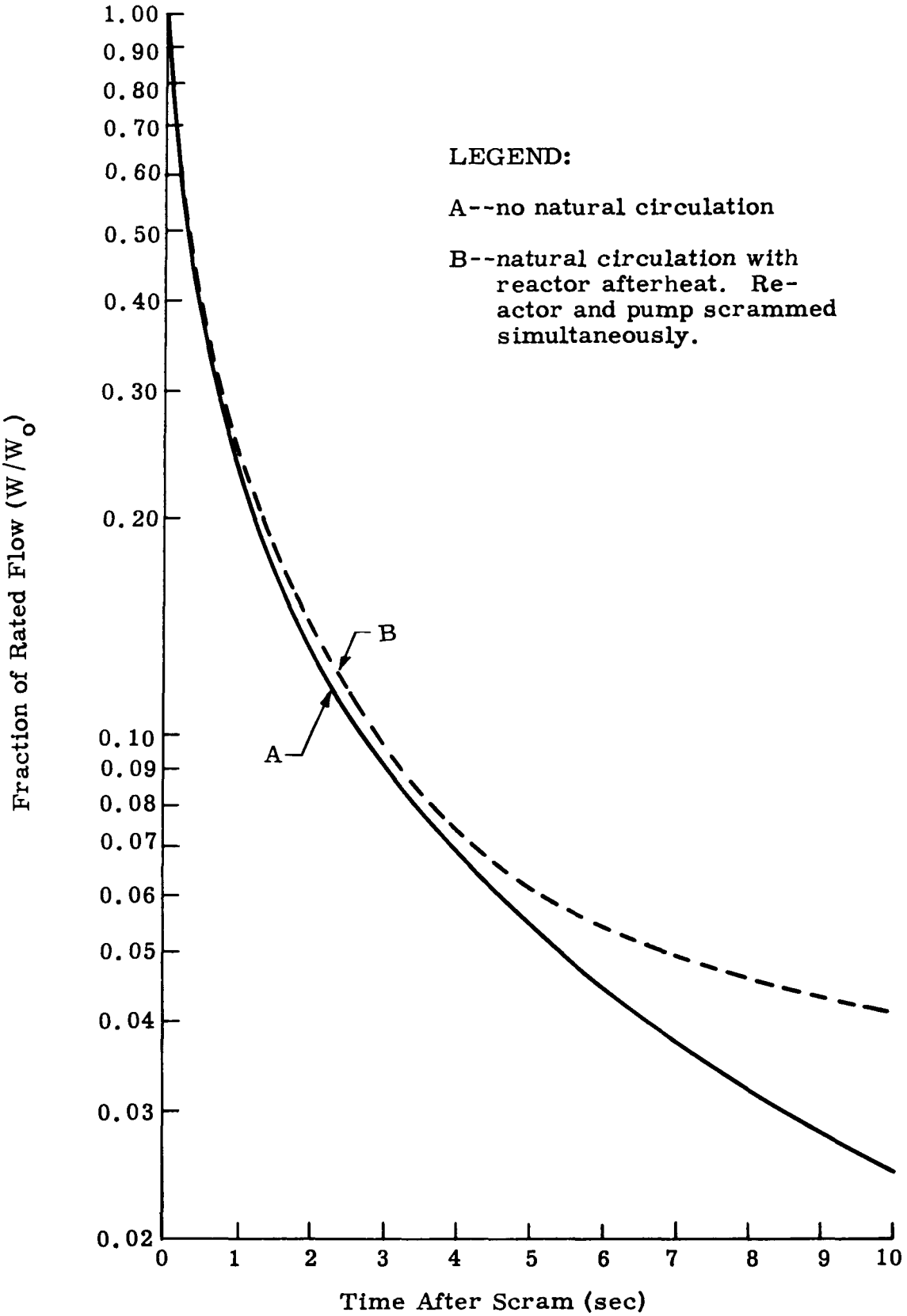

Fig. C-3. PM-1 Flow Coastdown

vection, viz., the $\sum_{i=1}^{3} \rho_i Z_i$ term in Eq (C-1). Curve B is obtained when this effect is included.

Evaluation of the power production in the hot channel was based upon a power factor of 2.72, viz. The power produced in the hot channel is 2.72 times that in the average channel. Results of the Zero Power Test indicate that the value of this factor is 2.16; hence, an additional factor of conservatism has been included. A series of runs was performed to determine the hot channel outlet temperature for the loss-of-flow scram. In the low flow region (flow less than 10% of normal), the pressure drop through the reactor channels is almost entirely due to the elevation head loss. Since the pressure drop across all channels must be equal, the flow in each channel tends to be proportional to the power production in that channel. For this reason, the exit coolant temperatures of all channels are very nearly equal and the concept of a hot channel is not applicable. The maximum coolant temperature is plotted as a function of scram set point (fraction of rated flow) and instrumentation time constant in Fig. C-4.

The loss-of-flow scram point is set at 90% of power to the pump, which corresponds to approximately 96% of rated flow; and the time constant of the instrumentation is only a few milliseconds. Thus, from Fig. C-4, with ($W/W_o = 0.96$, $\tau = 0$), it can be seen that the maximum coolant temperature is 543° F. This compares favorably with the 567.2° F boiling point of 1200-psia water. It may, therefore, be concluded that bulk boiling will not occur under these conditions; hence, the core is thermally safe.

Adequate heat removal capacity is available in event of an extended shutdown period. Two methods of dissipating decay heat are:

(1) Through the steam generator and main condenser, using secondary system water. This method is employed during initial cooldown.

(2) Through the coolant purification demineralizer cooler, where the shield water serves as the heat sink. This method is used after initial cooldown is accomplished. The system has an 85-kw capacity.

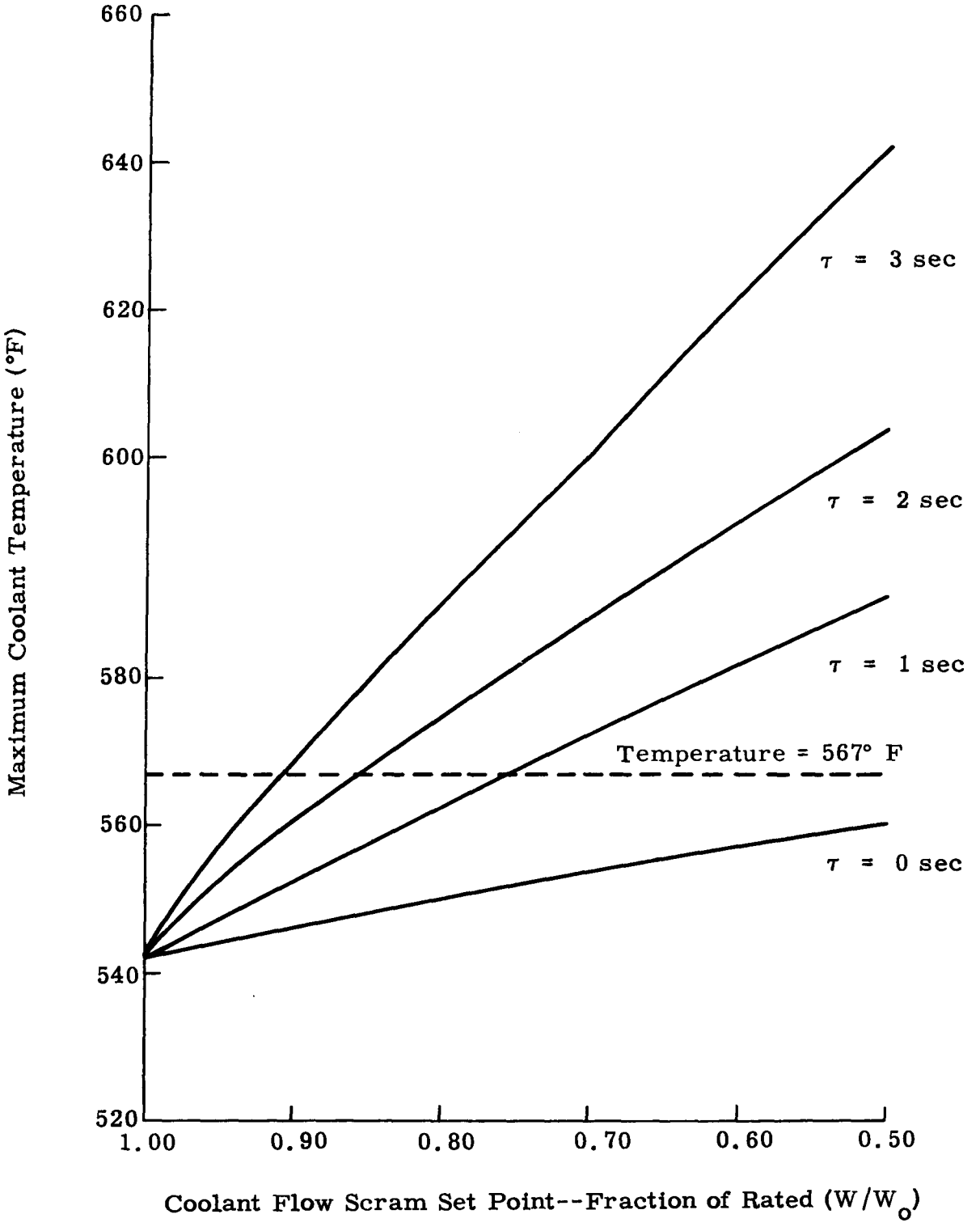

Fig. C-4. Maximum Coolant Temperature After Scram

REFERENCES FOR
APPENDIX C

(1) "Reactor Flow Studies, Full Scale Model Flow Test," MND-M-1859, June 1961.

(2) "Local Boiling Heat Transfer Tests, Single Tube Heat Transfer and Pressure Drop Tests," MND-MD-2539, July 1961.

(3) Jens, W. H. and Lottes, P. A., "Analysis of Heat Transfer, Burnout, Pressure Drop and Density Data for High Pressure Water," ANL 4627, May 1951.

(4) "Local Boiling Heat Transfer Tests, Single Tube Burnout Tests," MND-MD-2540, July 1961.

(5) Griffith, P., "The Correlation of Nucleate Boiling Burnout Data," ASME Paper No. 57-HT-21, Penna. State Univ. Joint ASME-A.I.Ch.E. Heat Transfer Conference, August 1957.

(6) "PM-1 Critical Experiments and Zero Power Testing," MND-M-1858, June 1961.

(7) "PM-1 Nuclear Power Plant Program, Third Quarterly Progress Report, 1 September to 30 November 1959," MND-M-1814, p III-76.

(8) Carnesale, A., "Hydraulic Stability in Heated Parallel Channels," MS Thesis, Drexel Institute of Technology, June 1961.

(9) "PM-1 Nuclear Power Plant Program, Second Quarterly Progress Report, 1 June to 31 August 1959," MND-M-1813, p III-34.

(10) "PM-1 Nuclear Power Plant Program, Fourth Quarterly Progress Report, 1 December 1959 to 29 February 1960," MND-M-1815, p III-1.

(11) "Spent Fuel Shipping Cask for PM-1 and PM-3A Nuclear Power Plants, Hazards Summary Evaluation," MND-M-1856, May 1961.

Blank Page

APPENDIX D

PRESHIPMENT WET CRITICAL TESTS

A series of zero power tests, referred to as Wet Critical Tests, was performed with the PM-1 core to demonstrate the achievement of several design characteristics in the as-built core. These properties are concerned with safety and operating characteristics of the core and include:

(1) Assurance that the core is subcritical when flooded with all control rods inserted.

(2) The ability of the core to meet stuck rod criteria.

(3) Achievement of the design lifetime as indicated by the initial cold, clean reactivity.

(4) The similarity between the PM-1 and the PMZ (development) cores.

Extensive measurements of flux and power distribution, temperature coefficient and other core characteristics have been performed in the PMZ core, which is a zero power experimental assembly. * The similarity between the experimental and PM-1 core is established so that this data may be attributed to either core.

Table D-1 summarizes the results of the Wet Critical Tests and includes PMZ-based predicted results. Control rod and bundle worths presented are the average deviations from the most reactive rod or bundle in that core. The critical five-rod bank data is for the case of minimum shutdown. All data were adjusted to 20° C.

---

*MND-M-1858

TABLE D-1

Summary of Wet Critical Test Results

	Predicted	PM-1
Average deviation relative bundle worth (% Δ K/K)	--	-0.074
Average deviation relative rod worth (% Δ K/K)	--	-0.014
Critical 6-rod bank (inches withdrawn)	8.15	8.59
Critical 5 rods--1 rod full out (inches withdrawn)	3.08	5.25
Critical 2 rods--4 rods full in (inches withdrawn)	14.53	15.37
Shutdown margin--1 stuck rod (% Δ K/K)	-0.21	-0.73
Total core reactivity (% Δ K/K)	12.87	12.32

The PM-1 core differs from the PMZ core primarily in fuel element size and U-235 loading. The dimensions and loading of these fuel elements are listed in Table D-2 below.

TABLE D-2

Comparison Between PM-1 and PMZ Fuel Elements

	PM-1	PMZ
Outer diameter, in.	0.507	0.500
Inner diameter, in.	0.417	0.416
Cladding thickness, in.	0.008	0.006
Meat thickness, in.	0.028	0.030
Active length, in.	30.14	30.14
U-235 loading, gm	40.43	39.34

Conclusions reached as a result of the Wet Critical Tests are:

(1) The PM-1 core (with control rods fully inserted) is subcritical when flooded.

(2) With one rod stuck full out, the core is shut down by -0.73% $\Delta K/K$.

(3) From the critical positions of two adjacent rods with four rods in, the two stuck rod shutdown margin may be calculated.

(4) The similarity of the PM-1 and PMZ cores was demonstrated.

(5) The adequacy of the PM sources was demonstrated.

The data in this appendix indicates that the differences in the fuel and stainless steel content of the fuel tubes are largely self-compensating with respect to total core reactivity. Furthermore, data developed in the experimental assembly* indicate that the small differences listed above have a negligible effect on such parameters as temperature coefficient of reactivity and power distribution. Finally, the data presented here indicate that sufficient shutdown is available in the rods of the PM-1 core to assure operating safety under conditions of the most stringent "stuck rods" requirement.

The PM-1 core Wet Critical Tests were conducted in Test Cell 1 of the Martin Marietta Critical Experiments Facility using the PMZ assembly** with minor modifications. The assembly is shown in Fig. D-1. The PM-1 core shroud was installed on the PMZ core support stand. Both the inner and outer PMZ thermal shield mockups were located in their proper positions. These were required, since they increase the reactivity of the core by 1.83% $\Delta K/K$. Special turnbuckle brackets were installed to assure that the core shroud was held rigidly in place. The only control rods used were the six PM-1 rods. To drive these rods, four nonscrammable Teleflex actuators were used. In two adjacent locations (Core Locations I and VI, Fig. D-2) the rods were driven by scrammable Lear actuators. Appropriate interlocks were associated with the Lear actuators to assure that a minimum of 2% $\Delta K/K$ was always available for fast shutdown. The use of only two scrammable actuators imposed limitations on performance of the tests, but did not prevent any required test from being conducted.

---

*MND-M-1858.

**Described in MND-M-1858, "PM Critical Experiments and Zero Power Testing."

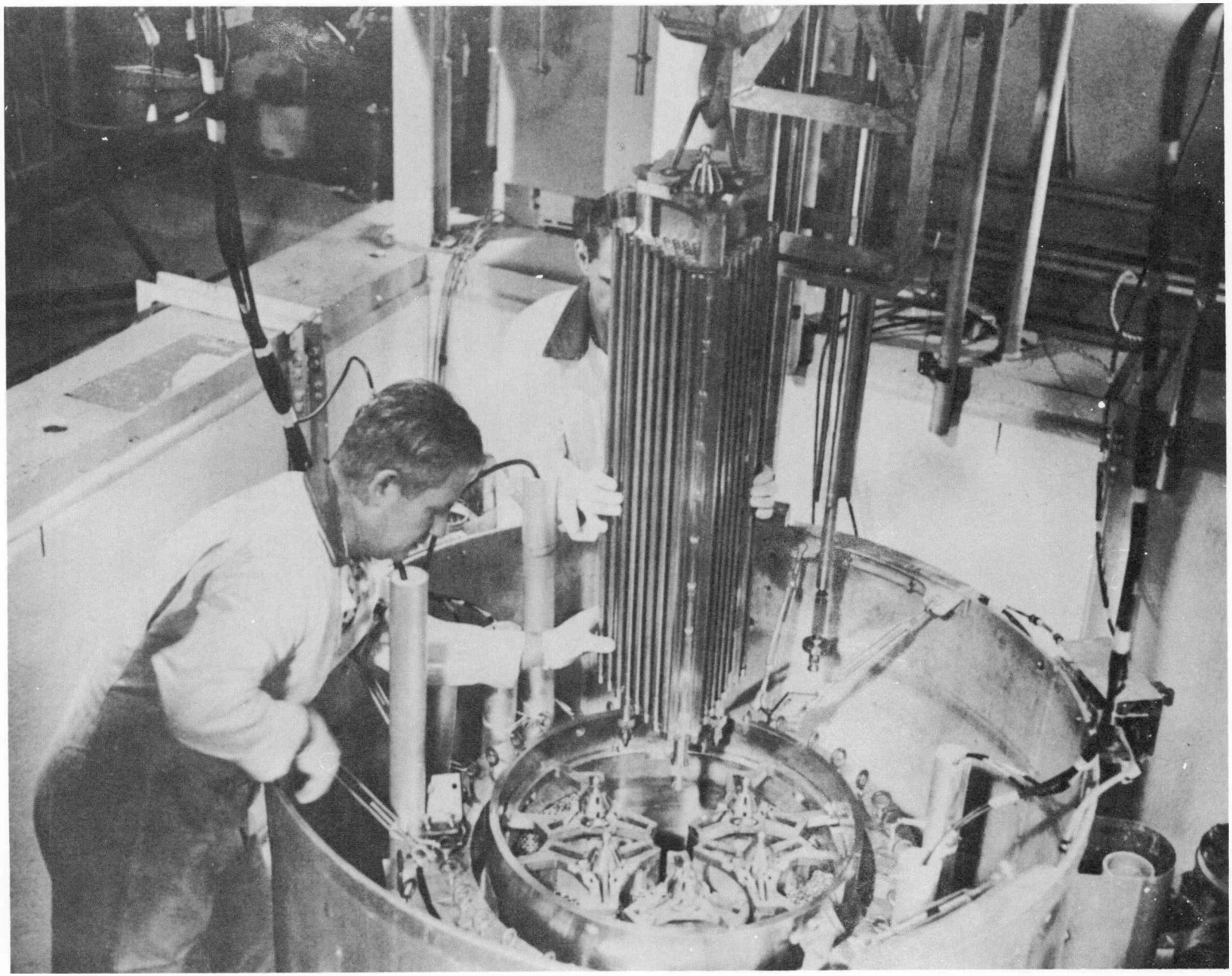

Fig. D-1. PMZ Assembly in Test Cell One in Critical Experiment Facility

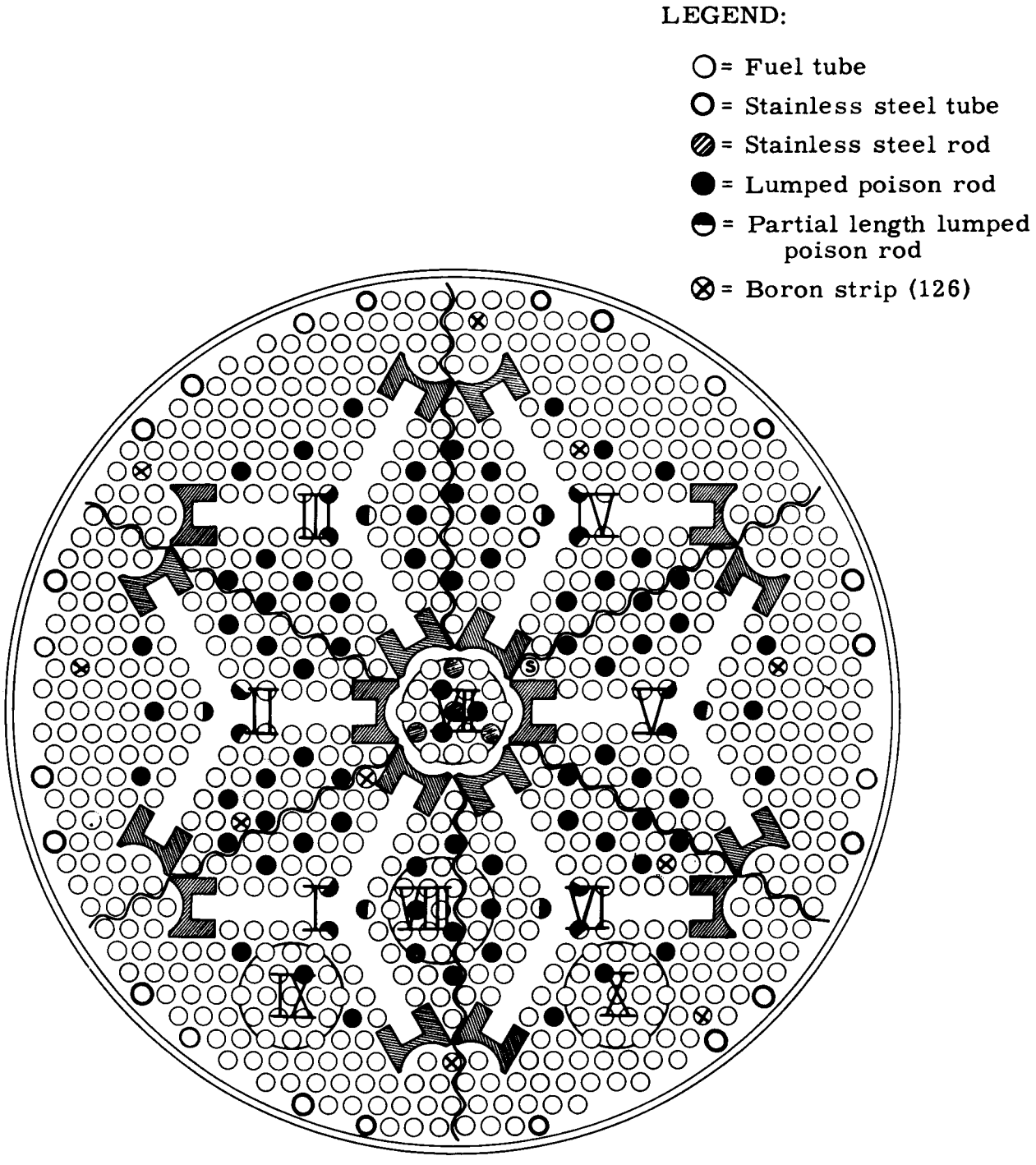

Fig. D-2. Strip Configuration for Rod Evaluation

The boron polyethylene strips, used to assure nuclear safety of the fuel bundles during the cleaning process after fabrication, were in each fuel tube when the fuel bundles were delivered to the critical facility. These strips were 0.25 inch square and 32 inches long and contained 10% natural boron by weight. The strips were positioned in the fuel tubes so that the lower end of each strip was located at the bottom plane of the core. These strips were not only removed experimentally to assure a safe approach to criticality, but were also used to poison the core for the evaluation measurements made during the tests.

The measurements made in the Wet Critical Test Program consisted of determining the deviations in relative worth of the individual bundles for each core, the deviations in relative worth of the individual control rods for each core, and the following critical rod bank positions for each core:

(1) Critical six-rod bank position.

(2) Critical five-rod bank position with one rod fully withdrawn.

(3) Critical position of two adjacent rods with the remaining four rods fully inserted.

In addition, miscellaneous measurements were made. One was the evaluation of the boron polyethylene strips. The other was an evaluation to determine that the PM sources are sufficiently strong that they will produce a minimum of five counts per second on the PM startup channels.

All reactivities presented in this appendix are based on an effective delayed neutron fraction of 0.0069. This value was obtained from the latest reactivity-versus-stable reactor period calculations for the PM-1 core.

1. Bundle and Rod Evaluation

The relative reactivity worths of the bundles and the control rods in each core were determined so that rods and bundles could be matched to maximize shutdown margins under the stuck rod conditions and to ensure that the most stringent shutdown cases were tested.

a. Relative bundle evaluation

The deviations in relative bundle worths were obtained by peaking the neutron flux into the bundle being evaluated to maximize differences and then measuring relative reactivity on the control rod opposite the bundle being evaluated. Peaking the flux into the test bundle depressed

the flux in the measuring rod bundle, thus increasing the sensitivity of the measurement (maximum rod motion per unit change in reactivity). The flux was peaked into the test bundle by poisoning the remaining bundles with a uniform distribution of boron polyethylene strips. Criticality was established with five rods fully withdrawn and the sixth rod (in the bundle opposite the one being evaluated) partially withdrawn. Thus, the relative reactivity worth of the bundle was determined by the position at criticality of the sixth rod. The relative rod positions were translated into reactivity by period evaluation. For these measurements, six PMZ control rods were used. In previous work, the differences in reactivity worths of these rods were found to be extremely small in comparison to the reactivity differences between fuel bundles.

The reactivity differences had been magnified by peaking the flux into the bundle being evaluated. From data obtained in the PMZ-1 program*, it was determined that peaked reactivity worths under similar conditions to those of this study were approximately 1.5 times the unpeaked worth.

Table D-3 presents the worths of the bundles of each core relative to the most reactive bundle in that core. Also listed are the average variations from the most reactive bundle, both in the peaked flux condition and corrected to the unpeaked condition, as described above.

TABLE D-3

Relative Bundle Worths

Bundle	Reactivity Difference (% Δ K/K)
1	-0.065
2	-0.110
3	-0.154
4	-0.175
5	-0.164
6	--
Average	-0.111
Average (unpeaked)	-0.074

*MND-M-1858, "PM Critical Experiments and Zero Power Testing."

In considering the deviations in relative worth of the bundles, it should be recognized that the deviations shown in Table D-3 are very small, representing less than 0.5% of the total worth of the bundle. This assumes that 1/6 of the K_{eff} of the core (1.1474, based on PMZ-1 data) is contributed by each bundle.

b. Relative rod evaluation

The relative reactivity worths of the control rods for each core were obtained by fully inserting each rod successively in the same location in the core and evaluating the reactivity worths on a PMZ rod in the opposite bundle. The four remaining rod locations were occupied by PMZ rods. In each case, the rod was located in the core so that the poison was one inch above the top of the bottom grid at full insertion. This located the bottom of the poison in the same plane as the bottom of the active core. The poison location used for the rod was the average of the locations of poison in the three blades of the rod. The location of the poison in each blade was determined by X-rays as the distance from the end of the blade to the furthest extremity of the poison within the blade.

The measurement was performed with the rod being measured fully inserted and the evaluation made on the opposite rod. This approach was taken to assure evaluation of the total rod and to increase the sensitivity of the measurement by using a rod in the minimum flux region for the evaluation.

To establish criticality with one rod (the rod being measured) fully inserted, the opposite rod partially inserted and the remaining rods fully withdrawn, the core was uniformly poisoned with 126 boron polyethylene strips (21 per bundle) as shown in Fig. D-2. The relative worths of the rods being evaluated were seen as differences in position of the opposite rod. These differences were related to reactivity by period evaluations.

The worths of the rods in each core relative to the most effective rod in that core are presented in Table D-4, which also shows the average variation from the strongest rod.

The average deviation from the most effective rod represents less than 1% of the worth of the rod, which was found in the PMZ-1 program to be 2.27% $\Delta K/K$.

TABLE D-4

Relative Rod Worths

Rod	Reactivity Difference (% Δ K/K)
15	-0.012
16	-0.027
18	-0.012
19	-0.016
20	-0.018
22	--
Average	-0.014

c. Bundle-rod matching

To maximize the four-rod shutdown margin under the two stuck rods condition, the bundles and rods were matched in the order of their relative worths, i.e., the most effective rod with the strongest bundle, etc. Although the differences in the reactivity associated with individual bundles are seen to be too small to produce a significant amount of flux tilting, a core configuration was chosen which alternates bundles of high and low reactivity. Table D-5 shows the bundle and rod configurations for the core. The configuration shown is relative, since the position of Location I in the pressure vessel is arbitrary.

TABLE D-5

Bundle and Rod Configurations for Shipment

Location	Bundle	Rod
I	6	22
II	3	19
III	2	18
IV	5	16
V	1	15
VI	4	20
Spare	7	21

Figure D-3 shows the configurations of the PM-1 core. Included in this figure are bundle location, rod location and the blade orientation for each rod.

2. Critical Bank Positions

Critical positions were determined for three different rod bank configurations. The critical position of the six-rod bank gives an approximate measure of total core reactivity. With one rod fully withdrawn, the critical position of the remaining five rods yields a measure of the shutdown margin for the condition of one rod stuck full out of the core. The critical position of two adjacent rods with the remaining rods fully inserted presents the reference point from which the shutdown margin with two rods stuck in the operating position may be calculated.

For the critical bank position measurements, the two most reactive bundle-rod combinations, as described in Section 1c, were located under the adjacent scrammable Lear actuators. The two weakest bundle-rod combinations were on the opposite side of the core. This permitted the evaluation of the shutdown margin for either of the two worst conditions of one rod stuck full out and for the worst two-stuck-rod condition. All rods were adjusted so that the bottom of the poison was in the bottom plane of the active core, as described in Section 1b.

Table D-6 presents the bundle-rod orientation which was used for the critical bank position determinations. Locations I and VI were the adjacent bundles under the scrammable Lear actuators.

TABLE D-6

Bundle and Rod Configurations for Critical Bank Position Determinations

Location	Bundle	Rod
I	1	15
II	2	18
III	3	19
IV	4	20
V	5	16
VI	6	22

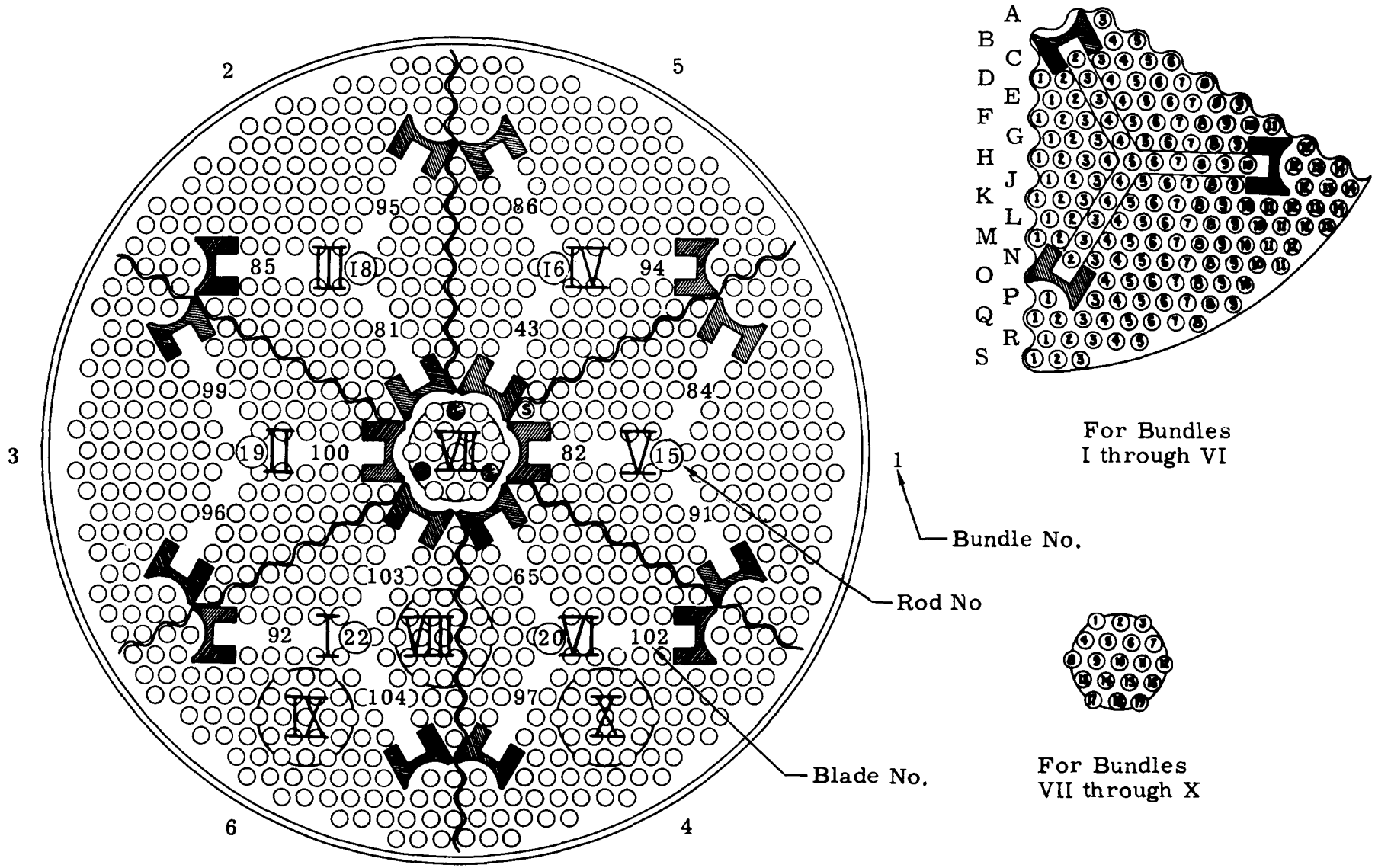

Fig. D-3. Bundle, Rod and Blade Orientation--PM-1 Core

Table D-7 presents the critical bank positions as measured at the temperatures indicated for each core studied, including spare bundles. The spare bundle was evaluated by replacing simultaneously the bundle in Location I and the center bundle with the respective spare bundles and determining the critical bank positions. Only the critical 5-rod bank with one rod out and the critical 2-rod bank with 4 in were required to demonstrate that the core with spare bundles would meet the stuck rod requirements.

Critical positions are presented in Table D-7 as inches withdrawn from the zero position, defined in Section 1b.

The shutdown margins and reactivities were obtained from PMZ-1 data, as described below.

TABLE D-7

Critical Bank Positions (in.)

	Predicted	PM-1	Spare
Temperature (°C)	20.0	13.7	13.4
Critical 6 rods	8.15	8.55	8.58
Critical 5 rods	3.08		
Rod I out		5.10	4.96
Rod VI out		5.26	
Rod in Position I		15	21
Rod in Position VI		22	
Critical 2 rods	14.53	15.27	15.13
Shutdown margin for worst case of 1 stuck rod (% Δ K/K)	-0.21	-0.73	-0.68
Total core reactivity (% Δ K/K)	12.87	12.37	

In Table D-8, the bank positions and reactivities have been corrected to 20° C, using the temperature coefficient of -0.0079% ΔK/K per degree centigrade observed in the temperature range of 20° to 30° C in the PMZ-1 program.

TABLE D-8

Critical Bank Positions Corrected to 20° C (in.)

	Predicted	PM-1	Spare
Critical 6 rods	8.15	8.59	8.62
Critical 5 rods	3.08		
Rod I out		5.25	5.11
Rod VI out		5.41	
Rod in Position I		15	21
Rod in Position VI		22	
Critical 2 rods	14.53	15.37	15.23
Shutdown margin for 1 stuck rod (% Δ K/K)	-0.21	-0.78	-0.73
Total core reactivity (% Δ K/K)	12.87	12.32	

The shutdown margins and reactivities presented in Tables D-7 and D-8 were based on extrapolations of data obtained in the PMZ-1 program. In the PMZ studies, it was demonstrated that control rod worth was not appreciably affected by minor changes in material composition of the core. The material differences between the PMZ and PM cores were sufficiently small that the PMZ-1 data can be used for the extrapolation considered herein. In the PMZ-1 with one rod fully withdrawn, criticality was established with the remaining five rods withdrawn to 3.17 inches. This represented a shutdown margin of -0.23% Δ K/K. The shutdown margins shown in Tables D-7 and D-8 were obtained by determining the reactivity difference between the five-rod bank at 3.17 inches and at the measured position for each of the PM cores, using the PMZ-1 curve for the worth of five rods with one rod fully withdrawn. The shutdown margin presented is the sum of this difference and -0.23% Δ K/K. The total reactivity of the PMZ-1 core was 12.85% Δ K/K, with the critical six-rod bank at 8.17 inches withdrawn. Total reactivities shown in Tables D-7 and D-8 were obtained by subtracting from 12.85% the reactivity differences between 8.17 inches and the measured critical six-rod bank positions for the PM cores, using the six-rod bank worth curve from PMZ-1.

3. Miscellaneous Measurements

a. Boron polyethylene strip evaluation

As described in the beginning of this appendix, all cores were delivered to the critical facility with a boron polyethylene strip in each

fuel tube. These strips were removed experimentally to assure a safe approach to criticality and were used to poison the core for the bundle and rod worth evaluations.

The boron strips were removed incrementally from each core, using the standard multiplication technique in which inverse multiplication is plotted as a function of number of strips removed to predict the safe next incremental removal. The strips removed for each increment were uniformly distributed throughout the core. The end point of the strip removal for each core was the appropriate strip loading for the evaluation which followed. In the case of the first core studied, this end point was with all strips removed.

As an aid in determining strip distribution requirements for the various evaluations that were made, the reactivity worth of an average boron polyethylene strip was measured. Because of the heavy boron loading in the strips, they were sufficiently "black" that the differences in strip worth were a function of location in the core only. The strips were evaluated by locating 10 strips uniformly in the core, as shown in Fig. D-4. The worth of the 10 strips was determined by period evaluation. From this measurement, the worth of an average strip was determined to be 0.064% $\Delta K/K$. This is slightly less than 3 times the worth (average of 0.024% $\Delta K/K$) of the strips used in the PMZ program.

From the strip evaluation data combined with the inverse multiplication data obtained during the strip removal, it was determined that 175 uniformly distributed strips were required to control the reactivity of the core with all control rods out at 20° C. A total of 300 uniformly distributed strips would maintain the core 8% $\Delta K/K$ subcritical with no control rods in the core. Thus, a core with 300 uniformly distributed strips and six control rods fully inserted would have a K_{eff} of approximately 0.8.

b. PM source evaluation

To determine whether the PM sources will be adequate to produce a minimum of five counts per second on the PM startup channels at initial startup, an evaluation was obtained in the wet critical assembly with operating conditions mocked up as closely as practical. Figure D-5 shows the location of the startup chamber with respect to the source and core for both the PM systems and the wet critical assembly mockup. As Fig. D-5 indicates, the only difference between the geometries of the PM and wet critical systems was the material between the pressure vessel and the chamber. The wet critical mockup had 9 inches of water instead of the fiberglas, 5 inches of lead and 2-1/4 inches of water in the PM system. Since the attenuation of neutrons

LEGEND:

- ○ = Fuel tube
- ○ = Stainless steel tube
- ○ = Stainless steel rod
- ● = Lumped poison rod
- ◒ = Partial length lumped poison rod
- ⊗ = Boron strip (10)

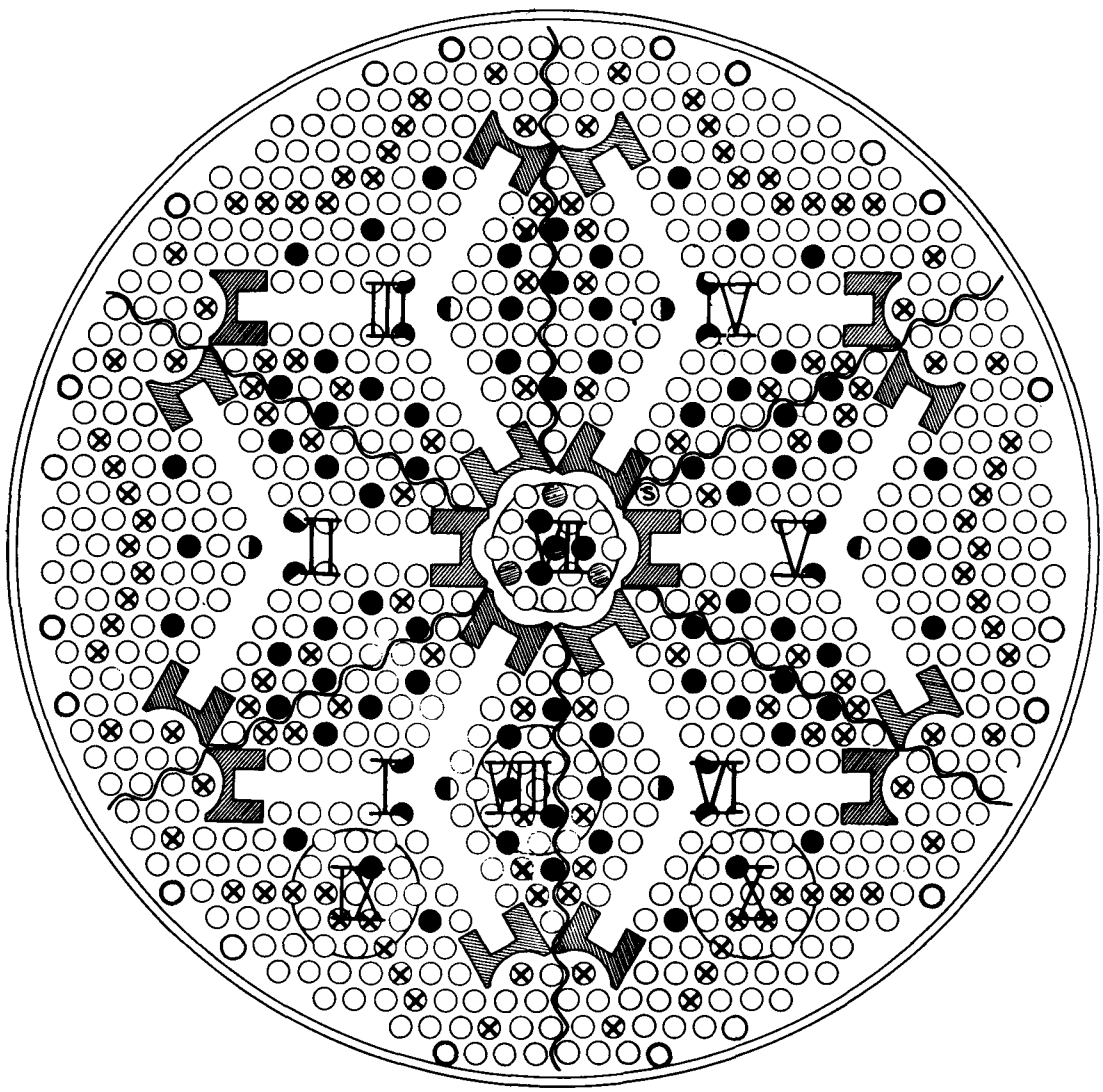

Fig. D-4. PM Core Configuration Showing Location of 10 Sample Boron Strips

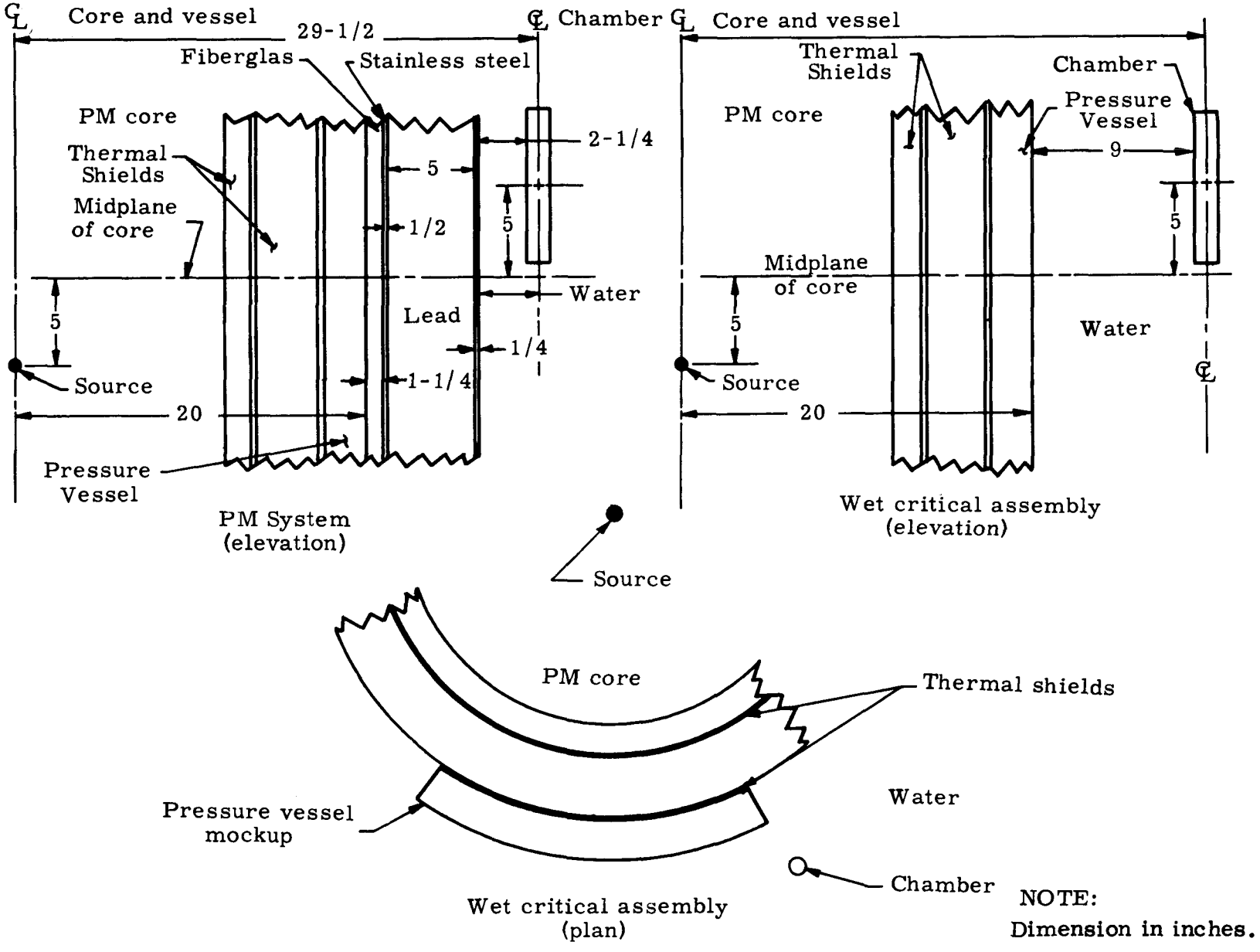

Fig. D-5. Source and Chamber Location for PM-1 and Wet Critical Assemblies

is greater in water than in lead, measurements in the wet critical mockup would be more pessimistic than the actual case. In addition, the lead is primarily a gamma ray shield for the chamber, and at the initial startup, there will be negligible gamma present. The measurement was made using a Po-Be source with a strength of approximately 1.4 curies, compared to 30 curies for the PM sources. The difference in source strength was therefore a factor of 21, assuming the same efficiency for the two sources.

For the measurement, a BF_3 proportional counter from a PM startup channel was used with the instrumentation from PMZ Channel 2. If a proportional counter is operated on its plateau, the efficiency of the channel will be independent of the electronics which follow the chamber. The operating plateau for the system used was measured to extend from 2200 to 2500 volts. The test was run with the chamber operated at 2300 volts.

Measurements were made in a PM core with six PMZ control rods and no boron strips. Since previous measurements had demonstrated that the PMZ rods differed from the PM rods by less than 2% of the total worth, the use of the PMZ rods did not prejudice the results of this measurement. The background count rate was measured with the PMZ source in the storage pig, which resulted in a higher than normal background count rate (15.1 counts per second). To reduce counting statistics, each measurement was made for sufficient time to produce a minimum of 10,000 counts.

With the test source installed in the core (and the PMZ source in the storage pig), measurements were made with all rods fully inserted and with the two rods on scrammable Lear actuators (the rods located between the source and the PM chamber) withdrawn to 10.25 and 12.50 inches. The reason for using different rod positions was to demonstrate that adequate count rates would be seen at startup and to show that the chamber would see multiplication as the control rods were withdrawn. Table D-9 presents the measured count rates after subtracting background and the anticipated count rates for the PM source for the various positions of the two control rods with the other four rods fully inserted. The anticipated PM count rates were obtained, using the factor of 21 difference between the sources described above.

TABLE D-9

Source Count Rates

Rod Position (inches withdrawn)	Measured Count Rates (counts per second)	Anticipated PM Count Rates (counts per second)
In	10.5	220
10.25	27	570
12.50	57	1200

Table D-9 demonstrates that the PM sources will be adequate to produce more than the minimum required count rate at startup and to permit the PM chambers to see multiplication. The differences in count rates presented in Table D-9 were verified by comparable differences seen on the PMZ startup channel.

4. Water Samples

To assure that the PM cores were not contaminated by the water of the PMZ systems, samples of the water were chemically analyzed periodically throughout the program. The purpose of the analyses was not to demonstrate that the PMZ water met the specifications of reactor grade water. Specifications for reactor grade water are based on operation at elevated temperatures for extended periods of time. The wet critical tests were performed with water below 20° C. Each core was blown dry prior to packaging for shipment. Thus, the requirements for the PMZ water were that it not exceed the reactor grade water specifications by more than a factor of about 10.

Table D-10 presents the results of the chemical analyses of the PMZ water at significant times throughout the Wet Critical Test program. Specifications for reactor grade water are included for reference.

TABLE D-10

Water Analysis

	Reactor Grade Water	Sample 4	Sample 9
Time	--	Initial run	After final run
P_h	6.8	6.9	6.1
Resistivity (Ω)	≥500,000	2,600,000	121,000
Chlorine ions (ppm)	≤0.1	0.2	0.25
Boron (ppm)	*	none detected	none detected
Suspended solids (ppm)	≤2	--	0.7
Dissolved solids (ppm)	≤0.5	--	1.1
Total solids (ppm)	≤2.5	0.15	1.8

*Boron content was not a reactor grade water specification. It was included in the analysis to detect any contamination resulting from use of the boron polyethylene strips.

ENGINEERING DRAWINGS

Blank Page

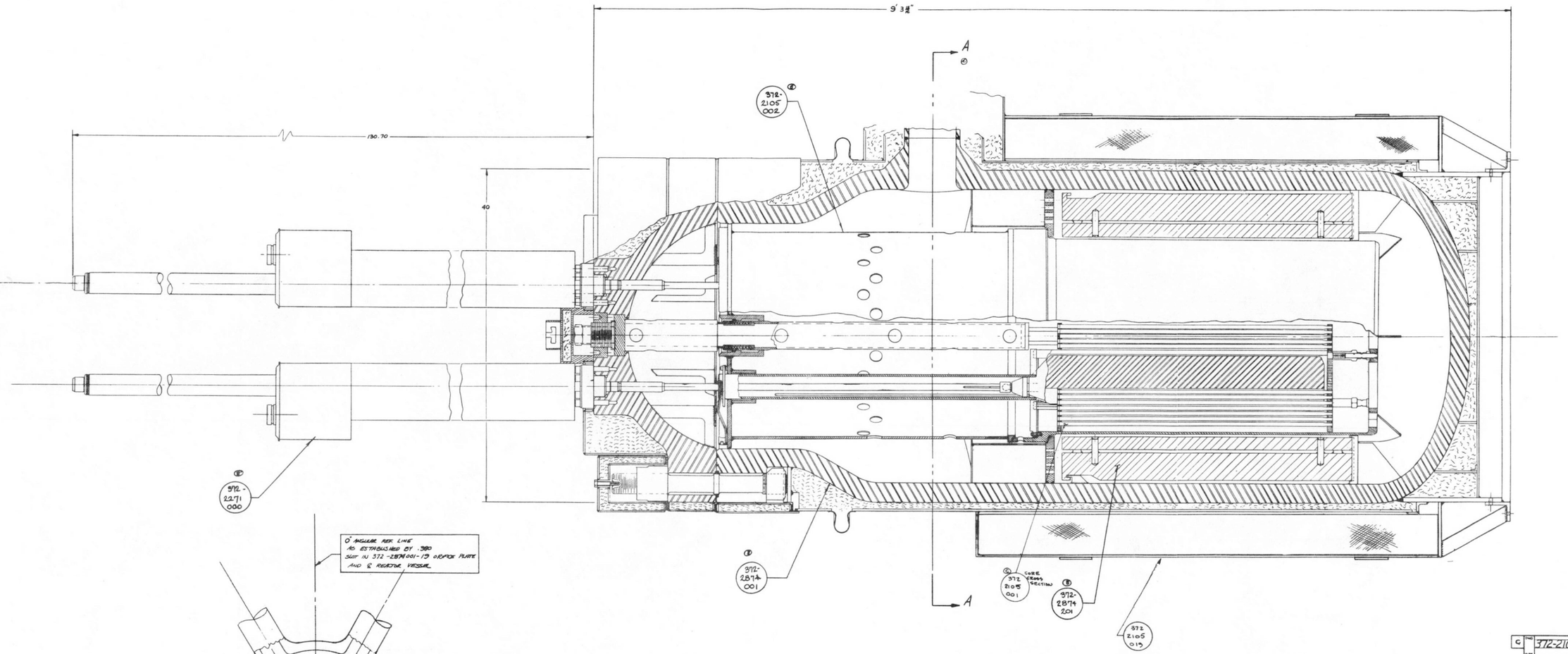

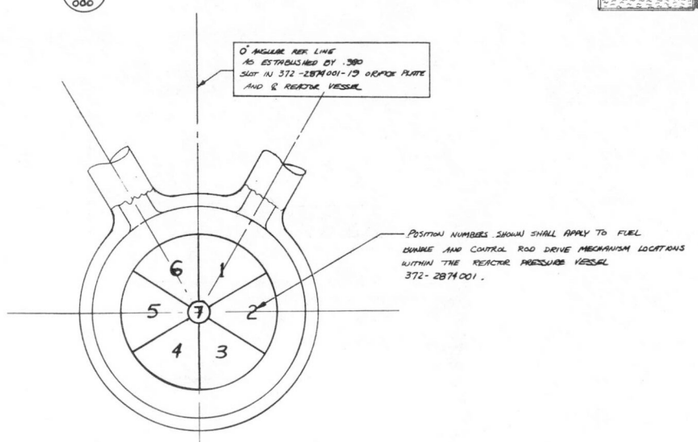

VIEW A-A

NOT TO SCALE

372-2105000 C

1	372-2108 019	REACTOR CORE ALIGNMENT STUDY					C
1	372-2874 201	REACTOR VESSEL LOAD SHIELDING		KNAPP MILLS			C
1	372-2874001	REACTOR VESSEL		A.O. SMITH			C
1	372-2871 000	CONTROL ROD ASS'Y		TAPCO			C
1	372-2105 005	INSTALLATION, REACTOR CORE STRUCTURE					C
1	372-2105 001	REACTOR CORE CROSS-SECT.					C
BASIC	PART NO.	DESCRIPTION	STOCK SIZE	MATERIAL SPECIFICATION		FINISH	

CALC BY | DASH NUMBER | 372-2000 001 | NEXT ASSY | USED ON | APPLICATION

REACTOR ASSEMBLY

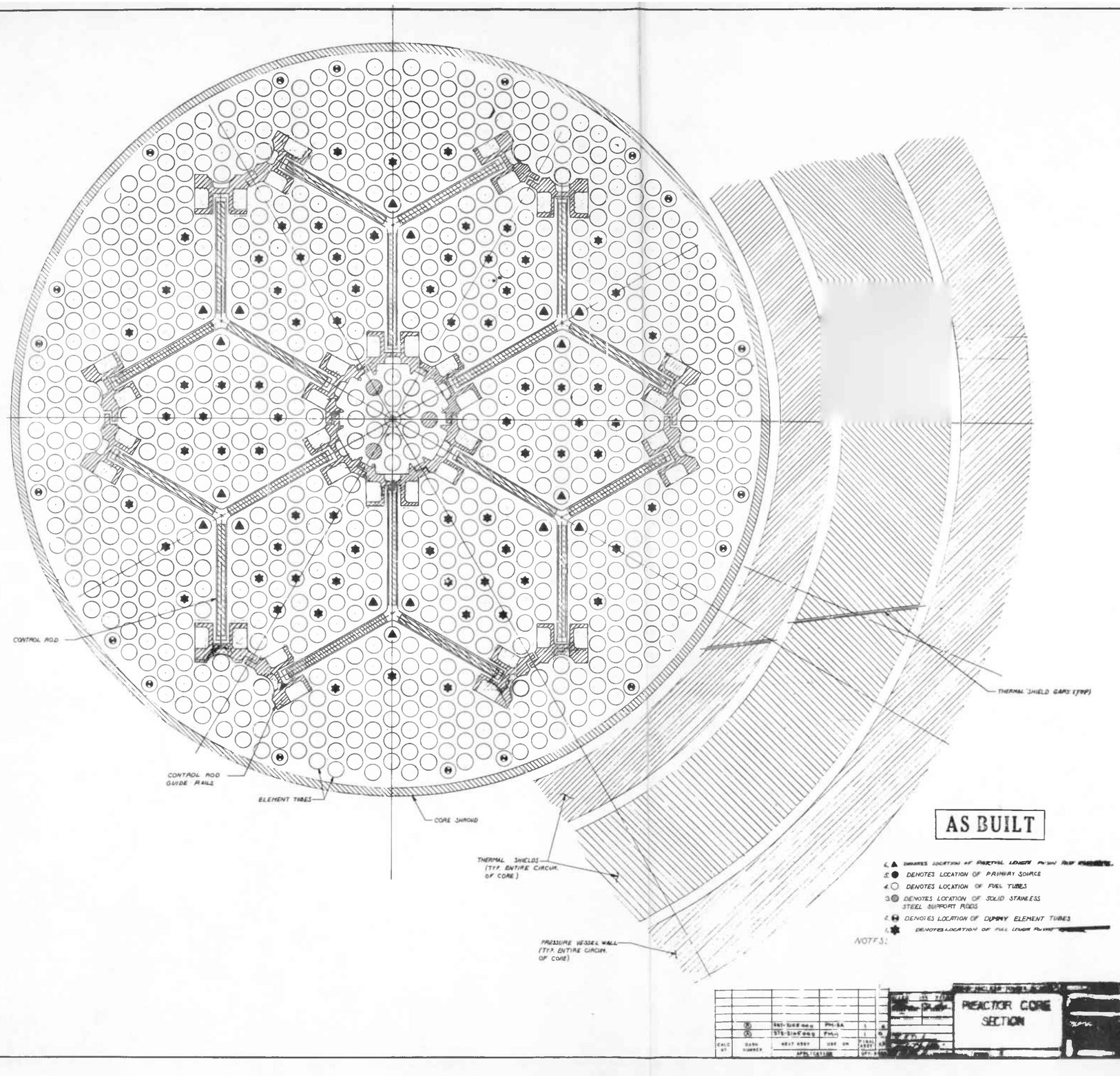
CONTROL ROD
CONTROL ROD GUIDE RAILS
ELEMENT TUBES
CORE SHROUD
THERMAL SHIELDS (TYP. ENTIRE CIRCUM. OF CORE)
PRESSURE VESSEL WALL (TYP. ENTIRE CIRCUM. OF CORE)
THERMAL SHIELD GAPS (TYP)
AS BUILT
DENOTES LOCATION OF PRIMARY SOURCE
DENOTES LOCATION OF FUEL TUBES
DENOTES LOCATION OF SOLID STAINLESS STEEL SUPPORT RODS
DENOTES LOCATION OF DUMMY ELEMENT TUBES
NOTES:
REACTOR CORE SECTION

REVISIONS					
ZONE	SYM	DESCRIPTION	DATE	APPROVAL
1/0	A1	REVISED NOTE 1 & 2		
6/0	A2	1.250±.040 WAS ±.050		
5/E	A3	RELOCATED HOLES TO AGREE WITH DETAIL		
6/C	A4	372-2105004-9 WAS 372-2105004		
6/C	A5	36.125 WAS 35.125	4/15/60	H. STRAUSS
5/A	B1	DELETED 372-2105004-11 FROM 5/A, 1 PLCS	9/61	
7/E	C1	REVISED CENTER GUIDE PICTURE	APPROVED	
6/A	D1	ADDED PM3A USAGE (1st ASSY.)	6-1-62	J. LEONARD
3/E	D2	REMOVED GUIDE SPRING AND SUPPORT	6-19-62	

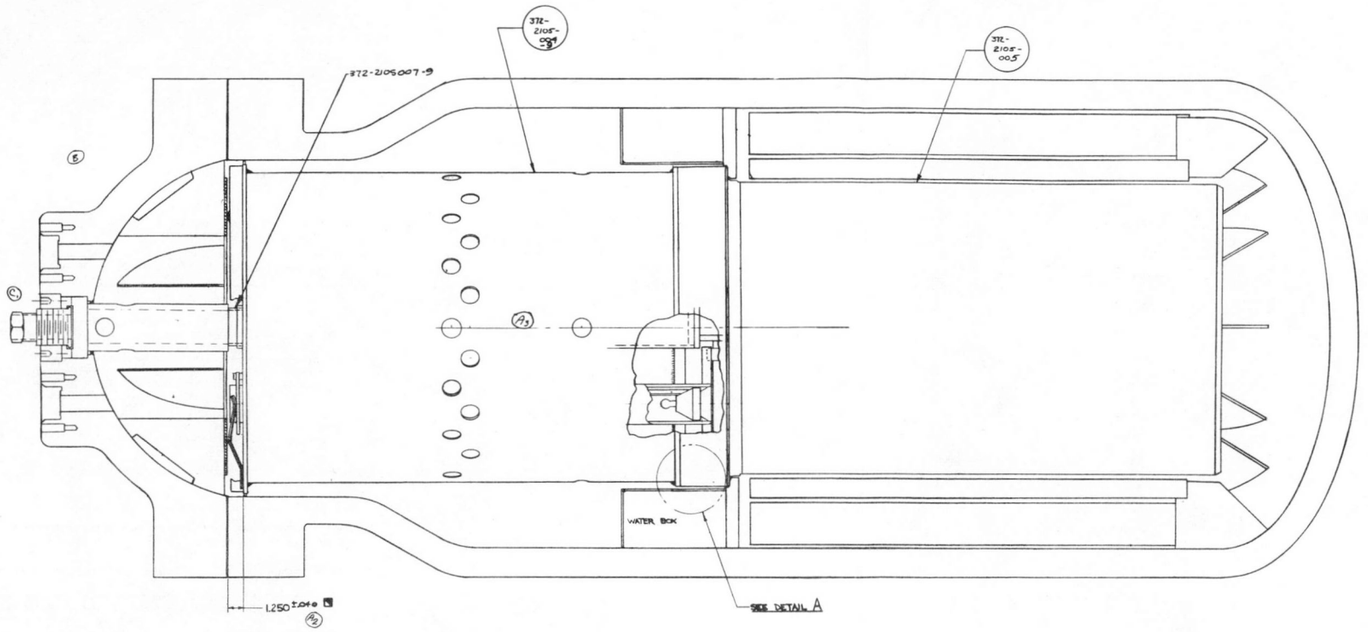

4. DEVIATIONS FROM INDICATED DIM., TOLERANCES, AND/OR NOTE 3 SHALL BE REPORTED TO NUCLEAR ENGINEERING.

3. THE ONLY PROTRUSIONS ALLOWED ABOVE VESSEL FLANGE FACE LEVEL WHEN REACTOR CORE STRUCTURE ASSY IS COMPLETE ARE THOSE BY THE HOLD DOWN SPRING 372-2105007 AND CENTER BUNDLE HOLD DOWN STRUCTURE 372-2105007-9

(A2) INDICATED DIM SHALL BE CHECKED AT 4 EQUAL SPACES AROUND VESSEL FLANGE FACE PERIMETRY AFTER SKIRT ASSY 372-2105004-9 IS INSTALLED.

(A1) INDICATED DIM SHALL BE CHECKED AT 4 EQUAL SPACES AROUND SURFACE SHOWN AFTER CORE INSTL. 372-2105005 IS IN PLACE AND BEFORE SKIRT ASSY. IS LOWERED INTO VESSEL.

NOTES:

APPROVED BY AEC
25 APRIL 1960

QUANTITY	PART NO.	DESCRIPTION	STOCK SIZE	MATERIAL OR VENDOR	MATERIAL SPECIFICATION	FINISH
1	372-2105005	CORE INSTL.				
1	372-2105004-9	UPPER SKIRT ASS'Y				

LIST OF MATERIAL

PM-1 NUCLEAR POWER PLANT

CONTRACT: AT(30-1)-2345

INSTALLATION, REACTOR CORE STRUCTURE

PM-1 REACTOR CORE

THE MARTIN COMPANY
BALTIMORE, MARYLAND
NUCLEAR DIVISION

SCALE 1/4 FULL

372-2105002

AS BUILT

372-075109
372-075107 372-075106

372-075103 372-075100

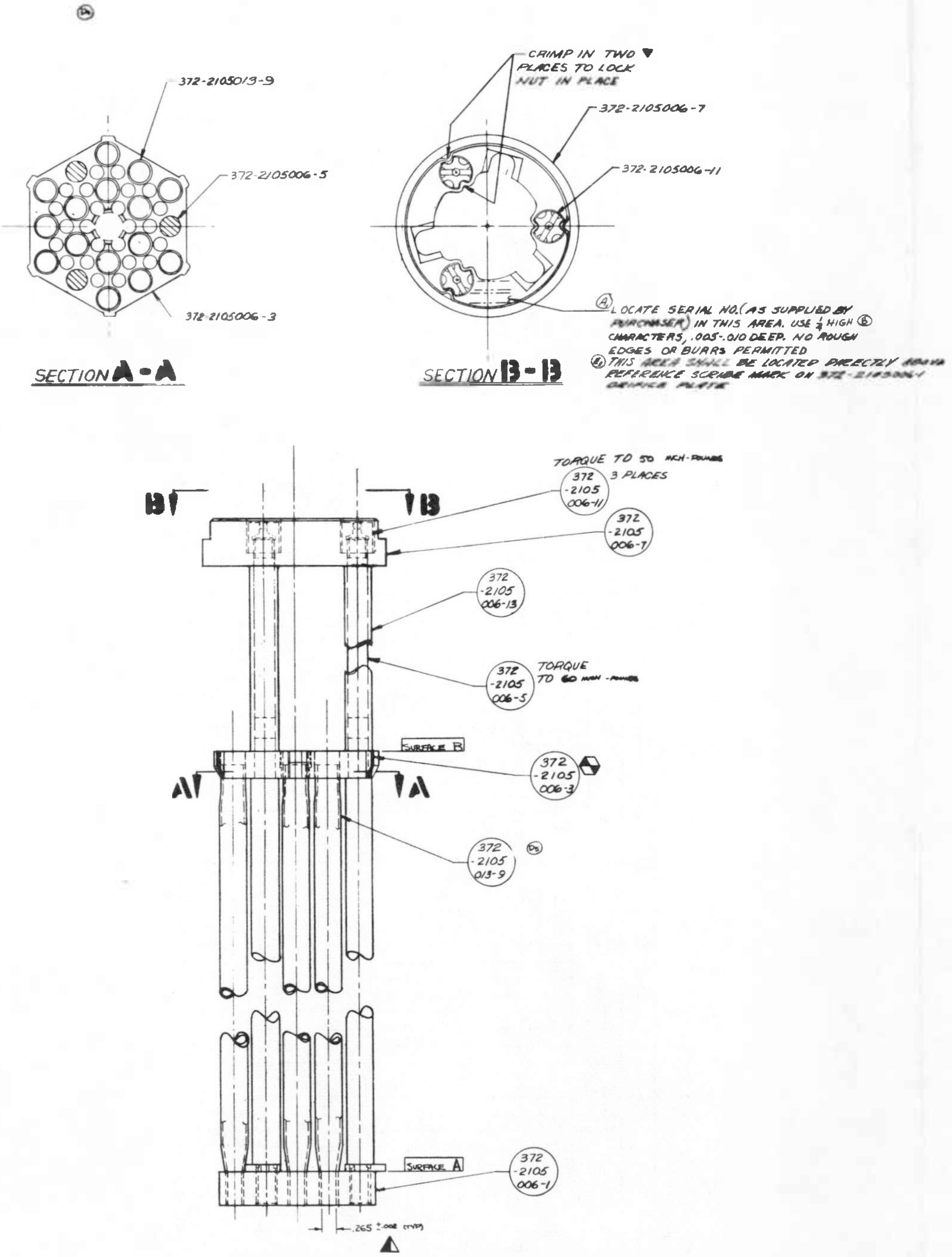

9. ▲ DUMMY SOURCE MAY BE REQUIRED WHEN ORDERING. SEE NOTE (SEC. 3-E) DWG. 372-2105005

8. NO METAL STAMPS OR MARKINGS SHALL BE PERMITTED ON ANY SECTION UNLESS NOTED OR SPECIAL PRIOR APPROVAL HAS BEEN OBTAINED FROM THE PURCHASER.

7. LUBRICATE THREADS WITH COLLOIDAL GRAPHITE (DISPERSED IN ALCOHOL OR PURE WATER) AS MFG. BY APPROVED VENDORS.

6. ▲ CORE ELEMENTS (372-2105013-9) SHALL BE EXPANDED INTO LOWER GRID (372-2105006-3) BY A PROCESS, AS APPROVED BY THE PURCHASER, WHICH WILL PROVIDE THE FOLLOWING:

a) AN INSIDE DIA. OF .265 [illegible]
b) A MINIMUM OF 300 LBS FORCE REQUIRED TO PULL THE ELEMENT FROM THE GRID.
c) SHARP EDGES AT THE INLET I.D., MAX R .005, [illegible]
d) LINE TO LINE CONTACT OVER A MINIMUM OF 80% OF THE TOTAL EXPANDED AREA WITH A MAX GAP OF .001 ALLOWED IN THE VOID REGION.
(e) [illegible] FIXITY OF THE ELEMENT TO LOWER GRID JOINT

5. THE CENTER HOLES AT SURFACES A & B SHALL ESTABLISH THE ASSEMBLY ℄. THIS ℄ SHALL BE ⊥ SURFACE A WITHIN .015 MEASURED AT SURFACE B. HOLE PATTERNS AT SURFACES A & B SHALL BE IN ANGULAR ALIGNMENT ABOUT ASSY ℄ WITHIN 1/2°. SURFACE B SHALL BE ∥ SURFACE A WITHIN .010.

4. ALL FUEL TUBES SHALL HAVE .002-.008 TOTAL FREE LATERAL MOTION AT -3 GRID PLATE LEVEL AFTER FINAL ASSEMBLY.

3. MANUFACTURING SHALL BE IN ACCORDANCE WITH MARTIN SPECIFICATION MN-7890

2. ▼ THE -7 PICKUP PLATE SHALL BE DEFORMED INWARD (6 PLCS AS INDICATED) A MINIMUM OF .063 INCHES USING A STAINLESS STEEL ROD (300 SERIES ALLOY) OF 1/8 MIN DIA. THE RESULTING DEFORMATION SHALL NOT LOOSEN THE -11 NUT NOR SHALL THERE BE ANY EVIDENCE OF CRACKING IN THE PICKUP PLATE.

NOTES:

APPROVED BY AEC 25 APRIL 1960

E 372-2105003

Quantity	Part No.	Description	Stock Size	Material or Vendor
		LUBRICANT	SEE NOTE 7	DAG 154 (OR EQUIV)
▲	372-2105013-11	DUMMY SOURCE		
45	372-2105013-9	FUEL TUBE		
3	372-2105006-13	SPACER		
3	-11	NUT		
1	-7	PICK UP PLATE		
3	-5	SUPPORT ROD		
1	-3	GRID PLATE		
1	372-2105006-1	ORIFICE PLATE		

AS BUILT

Part Number	Next Assy	Used On
372-2105003	372-2105005	PM-1

PM-1 NUCLEAR POWER PLANT

CONTRACT AT(30-1)

CENTER BUNDLE ASS'Y

PM-1 REACTOR CORE

SCALE 1/1

THE MARTIN COMPANY
BALTIMORE, MARYLAND
NUCLEAR DIVISION

E 372-2105003

PLAN VIEW

DETAIL "C"

DETAIL "E"

SCALE: 1/1
TYP 2 PLACES

DETAIL-17

A There Shall Be No Evidence Of Cracking After Bending.

DETAIL-5

B-B

SLOT TYP 3 PLACES

DETAIL-15

A-A

SLOT TYP 3 PLACES

DETAIL-13

DETAIL-11

ALL DIM CONCENTRIC WITHIN .020 T.I.R.

DETAIL -3

SCALE: 1/8

D-D

DETAIL -7

DETAIL -1

DETAIL "D"

TYP 6 PLACES

DETAIL "B"

(-17 OMITTED FOR CLARITY)

-29 ASSY

E-E

DETAIL "A"

C-C

APPROVED BY AEC
25 APRIL 1960

AS BUILT

QTY	PART NUMBER	NEXT ASSY	USED ON	REV	QTY REQD	DESCRIPTION	STOCK SIZE	MATERIAL OR VENDOR	MATERIAL SPECIFICATION	FINISH
						LUBRICANT	SEE NOTE 11	DAG-154 (OR EQUIV)		
						PIN		DAG-154 (OR EQUIV)		
6	D14-1250									
2	372-2105017					SPRING				
1	372-2105007-9					HOLD-DOWN TUBE				
1					-17	RETAINER	.063 X 1 7/8 X 83	5/5 SHEET	ASTM 304 or 347	
1					-15	TUBE		5/5 TUBING		
1					-13	FLANGE	5 DIA. x 2	5/5 ROUND BAR		
6					-11	BEARING	4 DIA. x 3 7/8	5/5 ROUND BAR		
1					-7	BEARING	5 DIA x 6	5/5 ROUND BAR		
1					-5	RING		5/5 PLATE		
1					-3	PLATE	1/4 x 28 DIA	5/5 PLATE		
1					-1	CYLINDER	24 7/8 - 8 TO 8 1/16 DIA	5/5 PLATE	ASTM 304 or 347	
6					-29	GUIDE TUBE ASSY				NONE
1					-19	CYLINDER ASSY				NONE
						SKIRT ASSY				NONE

LIST OF MATERIAL

CALC BY	PART NUMBER	NEXT ASSY	USED ON	REV	QTY REQD
	372-2105004-9	372-2105002	PM-1	1	0
	372-2105004-7	372-2105002	PM-1		

APPLICATION

INTERCHANGEABILITY STATUS
INTERCHANGEABLE
REPLACEABLE
UNCONTROLLED

DIMENSIONS ARE IN INCHES. DIMENSIONS ARE AFTER PLATING. TOLERANCES ON: FRACTIONS ± 1/32 DECIMALS ± .005 ANGLES ± 1/2° NOTED
RMS FINISH 125 EXCEPT AS NOTED

MATERIAL SPECIFICATIONS: AISI 4130 SHEET PER MIL-S-18729 (ORD) TYPE II CLASS 1 OR 2 ANNEALED PER MIL-H-6875 (SHIPS) OR NORMALIZED PER MIL-H-6875 (SHIPS) OR AMS 6350 (SHEET) OR AMS 6355 (PLATE) OR AMS 6370 (BAR) OR AMS 6371 (FORGING) OR AMS 6372 (TUBING) OR AMS 6373 (WELDING WIRE)

DM-1 NUCLEAR POWER PLANT CONTRACT: AT(30-1)-2346

UPPER SKIRT ASSY.
PM-1 REACTOR CORE

THE MARTIN COMPANY
BALTIMORE, MARYLAND
NUCLEAR DIVISION

SCALE 1/8 NOTED

E 372-2105004 SHEET 1 OF 2

E 372-2105004 SHEET 1 OF 2

E 372-2105004 SHEET 2 OF 2

1020 SITE AREA

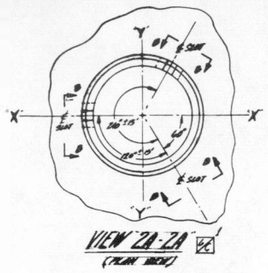

VIEW ZA-ZA
(PLAN VIEW)

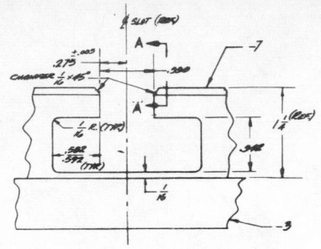

VIEW B-B (TYP 3 PLCS)
SCALE: 2/1

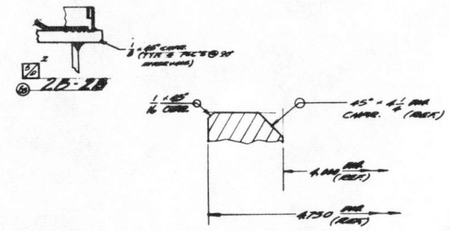

A A
SCALE: 2/1

2B-2B

ZONE	REV	DESCRIPTION	DATE	APPROVAL
	LAW	PER CHG. CHART 74	6-7-66	Coulombe
	AA	(SHEET 2A) SHEET 2A, 0.375 ± .005 DIA. (SHEET 2) AT SECTION 'B'		
	BA	(SHEET 2A) SHEET 2A, 0.375 ± .005 DIA. AT 8 PLACES EQUALLY SPACED ON 7.500 DIA. B.C.		
	BT	(SHEET 2)		
	BC	(SHEET 2)		
	BC	(SHEET 2)		
	BD	(SHEET 2)		
	AF	(SHEET 2)		
	Same	(SHEET 2)		
	AGC	(SHEET 2)		
	CM	(SHEET 2)	12-1-67	J.A. Hamilton
	BD	(SHEET 2)		
		(SHEET 2)		

372-7105004
SHEET 2 OF 2

372-7105004
SHEET 3 OF 3

AS BUILT

UPPER SKIRT ASSY
THIN FLEXURE CORE

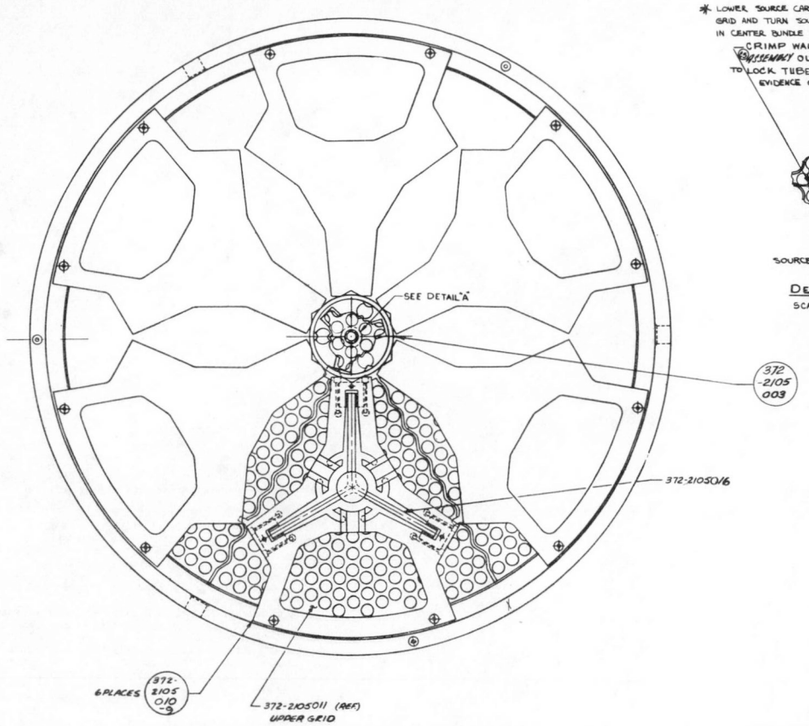

CORE SEGMENT INSTL.
TYPICAL 6 PLACES
(1 PLACE SHOWN)

* LOWER SOURCE CAREFULLY INTO PLACE. FIT INTO BOTTOM GRID AND TURN SOURCE UNTIL SHOULDER ON SOURCE BOTTOMS IN CENTER BUNDLE UPPER GRID. TORQUE TO 10 IN-LBS. (A3)
CRIMP WALL OF SOURCE ASSEMBLY OUT, IN 2 PLCS., A MIN OF .010 TO LOCK TUBE IN PLACE. THERE SHALL BE NO VISUAL EVIDENCE OF CRACKING AFTER DEFORMATION.

▲ THIS SOURCE TO BE USED FOR INITIAL CORE LOADING ONLY. FOR SUBSEQUENT CORE LOADS OR INDIVIDUAL CENTER BUNDLE REPLACEMENT, INSERT DUMMY SOURCE 372-2105018-11. (23)

372 2105 0185 (2) (A)

SOURCE INSTALLATION

DETAIL "A"
SCALE 1/1

CAUTION: DO NOT ASSEMBLE CORE UNLESS CONTROL RODS (OR EQUIV.) ARE SUITABLY LOCKED IN PLACE. (24)

(A4) 3. NO METAL STAMPS OR MARKINGS SHALL BE PERMITTED ON ANY SECTIONS UNLESS NOTED OR SPECIFIC PRIOR APPROVAL HAS BEEN OBTAINED FROM PURCHASER.

(A3) 2. ASSEMBLY SEQUENCE: AFTER FINAL CLEANING & INSPECTION OF COMPONENTS; PICK UP EACH BUNDLE SO THAT IT HANGS VERTICALLY & LOWER SLOWLY OVER TRUE POSITION.
a. INSERT 3 PERIPHERAL BUNDLES IN ALTERNATE POSITIONS
b. LOWER EACH OF REMAINING 3 BUNDLES, INTERLOCK CONTROL ROD GUIDE RAIL TABS & INSERT BUNDLE INTO SHROUD.
c. ALIGN & INSERT CENTER BUNDLE
d. REVIEW CHECK DIMENSIONS TO INSURE PROPER ASSEMBLY
(23)(24) 1. SOURCE ASSEMBLY TO BE INSTALLED AT SITE PER ASSY - DISASSEMBLY ASSEMBLY INSTRUCTIONS
1. ▣ DIM. INDICATED SHALL BE CHECKED AT ASSY TO INSURE PROPER FIT OF PERIPHERAL BUNDLES INTO CORE SHROUD. DEVIATIONS SHALL BE REPORTED TO NUCLEAR ENGINEERING.

NOTES:

CHANGE NOTICE DATE	CHANGE NOTICE SYM	ZONE	SYM	DESCRIPTION	DATE	APPROVAL
		5/C	A,	1.25±.060 WAS 1.25±.070		
9/60	1135	1/D	A4	ADDED NOTE 2 & CAUTION NOTE		
		A/E	B3	WAS - TORQUE TO 30 IN-LBS		
		7-G	A4	TOLERANCE WAS ±.057	11/1/60	
9/60	1177	3-E	B1	ADDED HOLD NOTE	11 Aug 60	TW Cox
		3-E	B1	ADDED NOTE 3		
		6-C	B3	1.075 WAS 1.070		
		5/D	B4	5 PLCS. WAS 3 PLCS		
4/61	1/61	1/D	C1	ADDED PARTS LISTAGE	6-2-61	Compton
		7-E	C2	WAS 372-2105018-1	6-2-61	J
		8-C	C3	WAS 372-2105016-3	6-2-61	Compton
		7-C	C4	WAS 4.938 ± .047	6-5-61	Compton
		4-C	C5	NOTE REVISED "SOURCE CAPSULE" TO "FUEL RODS" AT DETAIL "A"	6-5-61	Compton
		5/D	C6	(2) ADDED "MUST BE UTILIZED IN CONJUNCTION WITH ASSY DWG. 372-2105005" TO ▲ SOURCE ASSY NOTE	6-5-61	Compton
		MAIN	C7	DELTA 1/16 INC. IN THIS ZONE	6/13/61	Compton
		2-E	C8	Revised Caution Note	6-14-61	
			D	ADD Dwg 372-2105010 "Rods & B/A	11/1/62	

APPROVED BY A.E.C. 25 APRIL 1960

ORIGINAL

QUANTITY	PART NO.	DESCRIPTION	STOCK SIZE	MATERIAL OR VENDOR	MATERIAL SPECIFICATION	FINISH
		ASSEMBLY				NONE
1	372-2105 020	CORE SHROUD, CENTER BUNDLE & PERIPHERAL BUNDLE ASSEMBLIES				
▲	372 2105018-11	DUMMY SOURCE				
1	372 2105016-9	SOURCE ASSY ▲				
6	372-2105010-9	PERIPHERAL BUNDLE ASS'Y				
1	372-2105009-9	SHROUD ASS'Y				
1	372-2105009	CENTER BUNDLE ASS'Y				

AS BUILT

LIST OF MATERIAL

CALC WT	PART NUMBER	NEXT ASSY APPLICATION	USED ON	QTY REQD
372-2105005	372-2105002	PM3A		1
372-2105005	372-2105002	PM-1		1

UNLESS OTHERWISE SPECIFIED: DIMENSIONS ARE IN INCHES; DIMENSIONS ARE AFTER PLATING; TOLERANCES OF: FRACTIONS ± | DECIMALS ± | ANGLES ±; NOTED; RMS FINISH EXCEPT AS NOTED ✓; INTERCHANGEABILITY STATUS: INTERCHANGEABLE, REPLACEABLE, UNCONTROLLED

APPROVALS — DATE: AF-AEC 334 9-20; ENGR: AD 3-7-62; DESIGN: [illegible] 3/7/62; DRAFTING: [illegible]; MFG: [illegible]; QUALITY CONTROL: [illegible]

PM-1 NUCLEAR POWER PLANT CONTRACT: AT(30-1)-2949

CORE INSTL.
PM-1 REACTOR CORE

SCALE 1/2 ENDITEM

THE GLENN L. MARTIN COMPANY
BALTIMORE, MARYLAND
NUCLEAR DIVISION

D E 372-2105005 SHEET
CODE 96997

1 372-2105005 372-0X/60 372-0215/00

DATE	APPROVAL	ZONE	REVISIONS DESCRIPTION	DATE	APPROVAL
		7-D	A1		
		6-D	A1		
		5-B	A1		
		5-A	A1		
		4-A	A1		
		4-B	A1		
		3-D	A1		
		2-D	A1		
		1-D	A1		
9/20		1-C	A1		
		1-B	B1		
		1-A	B1		
		2-A	B1		
		3-A	B1		
		4-A	B1		
		5-A	B1		
		6-A	B1		
		7-A	B1		
9/20		7-B	B1		
		7-C	C1		
		7-C	C1		
		7-B	C1		
		6-B	C1		
		6-C	C1		
		5-C	C1		
		4-C	C1		
		3-C	C1		
		2-C	C1		
		1-C	C1		
9/20		1-C	C1		

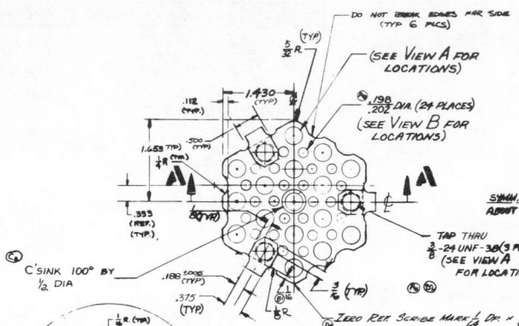

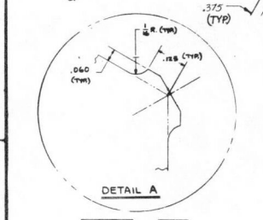

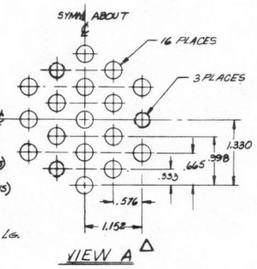

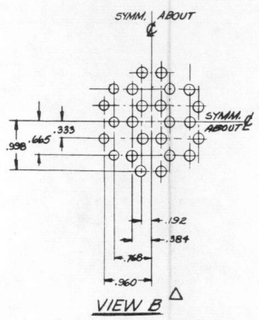

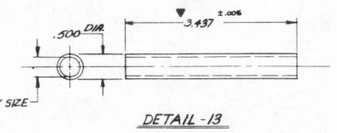

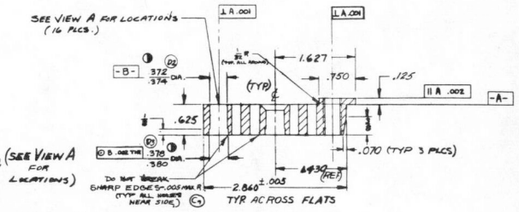

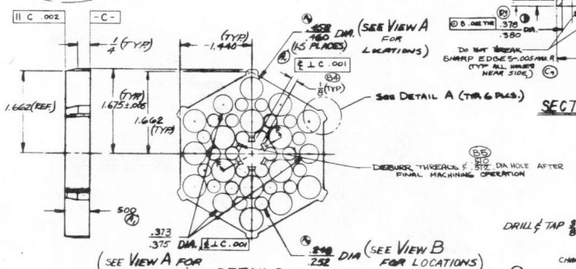

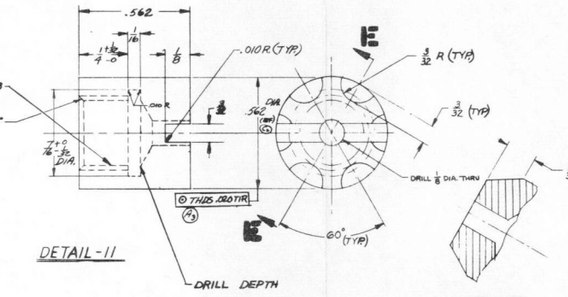

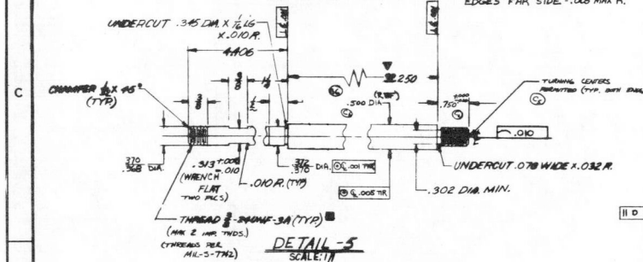

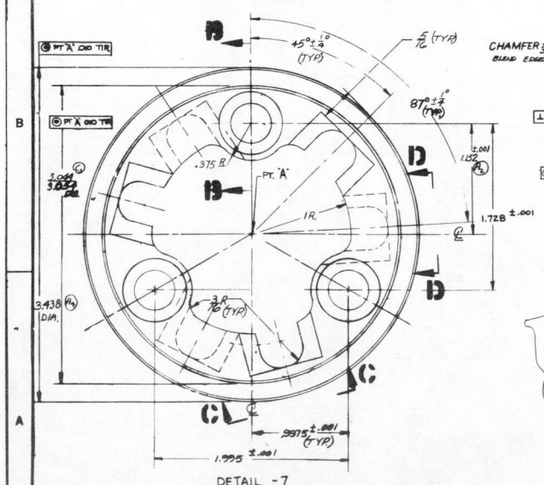

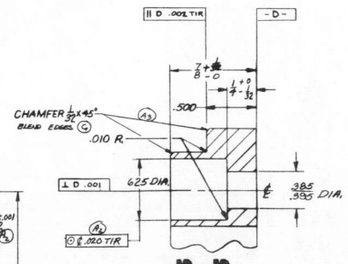

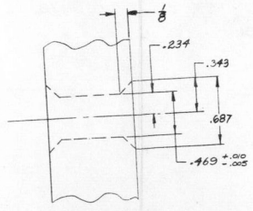

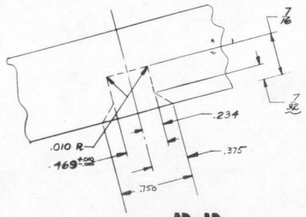

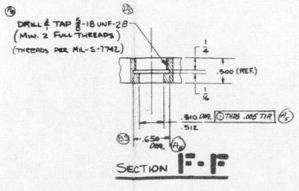

NOTES:

1. DECIMAL TOLERANCE ± .010 UNLESS OTHERWISE NOTED.
2. HOLE LOCATIONS SHOWN IN VIEW A, VIEW B, TO BE WITHIN .005 OF TRUE POSITION.
3. DIMENSIONS INDICATED ARE SUBJECT TO CONFIRMATION BY MFG. DEVELOPMENT TESTS.
4. GEOMETRIC AND POSITIONAL TOLERANCE SYMBOLS ARE PER MIL-STD-8A.
5. BREAK ALL SHARP EDGES .010 - .020 EXCEPT AS NOTED
6. MANUFACTURE DETAILS 5-8-13 IN SETS OF THREE WITH DIM. INDICATED MATCHING WITHIN .001.
7. THESE COMPONENTS SHALL MEET THE FOLLOWING MATERIAL CONSTITUENT LIMITATIONS:
   COBALT = .05 % BY WEIGHT MAX.
   COBALT + TANTALUM: .15 % BY WEIGHT MAX.
   CARBON: .08 % BY WEIGHT MIN.
8. THREAD DIAMETERS ON OPPOSITE ENDS OF DETAIL-3 SHALL ESTABLISH 6 FOR THAT PART
9. MFG. ALL COMPONENTS PER MARTIN SPEC. MN 7890.
10. NO METAL STAMPS OR MARKINGS SHALL BE PERMITTED ON ANY SECTIONS UNLESS NOTED OR SPECIFIC PRIOR APPROVAL WAS OBTAINED FROM THE PURCHASER.

APPROVED BY A.E.C. 25 APRIL 1960

D E 372-2105002 SHEET

D E 372-2105006 SHEET

AS BUILT

QUANTITY	PART NO.	DESCRIPTION	STOCK SIZE	MATERIAL SPECIFICATION
-13		SPACER	5/16 O.D. x .120 WALL x 3 1/2	STL. STEEL TUBING ASTM 304
-11		NUT	3/4 DIA. x 1	STL. STEEL RND. BAR ASTM 304
-7		PICK-UP PLATE	3 1/2 DIA x 1	STL. STEEL RND. BAR ASTM 304
-5		SUPPORT ROD	.500 DIA x 39	STL. STEEL RND. BAR ASTM 304
-3		GRID PLATE	.625 THK x 3 1/2 x 3 1/2	STL. STEEL PLATE ASTM 304
-1		ORIFICE PLATE	1/4 x 3 1/2 x 3 1/2	STL. STEEL PLATE ASTM 304

372-2105006-13	372-2105003		
-11			
-7			
-5			
-3			
372-2106006-1	372-2105002		

PM-1 NUCLEAR POWER PLANT — CONTRACT AT(49)-5(2558)

CORE DETAILS
CENTER BUNDLE
PM-1 REACTOR CORE

THE EARTH COMPANY
SALTSBURG, MARYLAND
NUCLEAR DIVISION

D E 372-2105006 SHEET

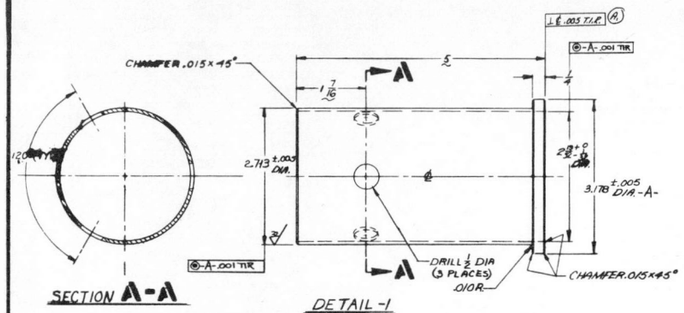

SECTION A-A

DETAIL -1

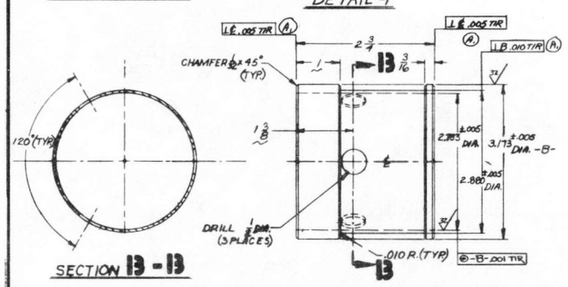

SECTION B-B

DETAIL -3

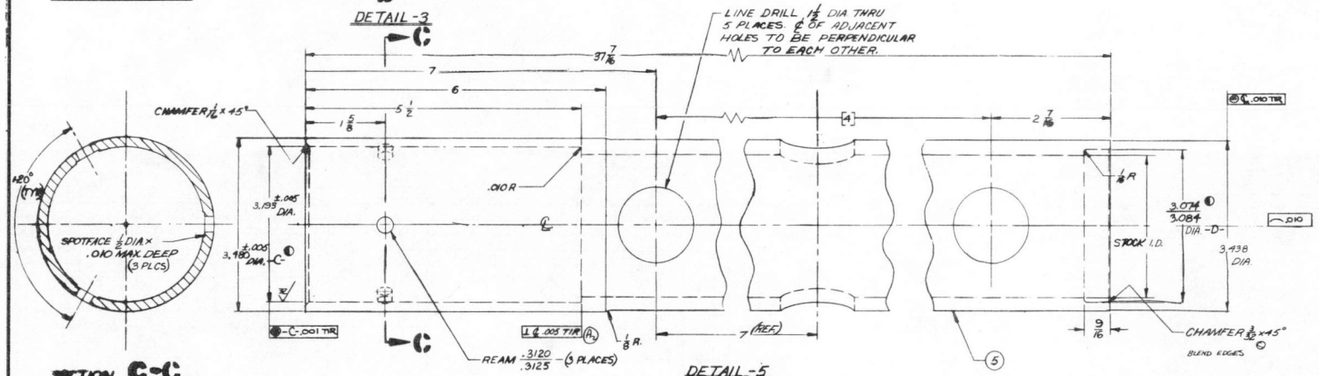

SECTION C-C

DETAIL -5

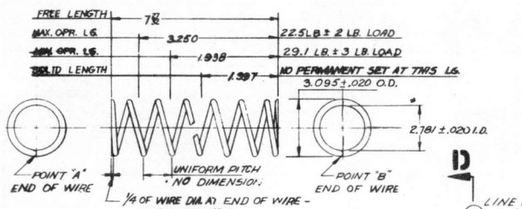

DETAIL -7 (SEE NOTES)
NO SCALE

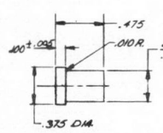

DETAIL -11

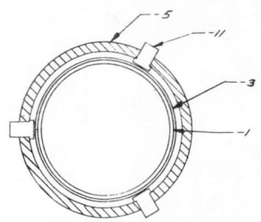

SECTION D-D

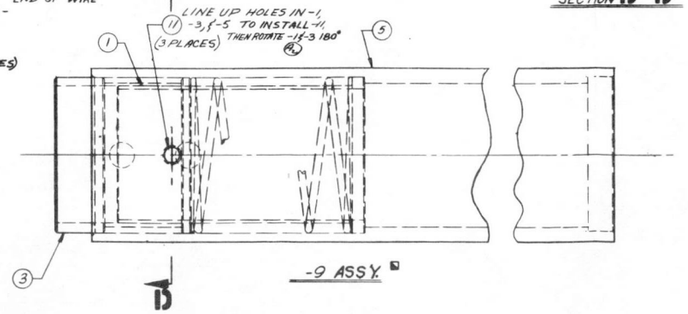

-9 ASS'Y.

REVISIONS				
SYMBOL	ZONE	REV	DESCRIPTION	DATE
9/21	ITEM	A	ADDED [redacted]	
		B	REVISED SHEET 2	
10/1	ITEM	B	STOCK WAS ¼ DIA.	
9/21	ITEM	C	¼ EXPANSION WAS ⅛ ADDED "SHEET 2"	
		C1	DELETED "ASSEMBLY"	
		C2	ADDED NOTE 7	
		C3	ADDED NOTE 9	
		C4		
11/4	ITEM	D.	N/A WAS 372 2105002	
4/12		E.	ADDED 372 SF 373758	
		E1	DELETED 372 SF 373758	
		E2	ADDED 372 2105004	
		E3	P.C. 4778 INC. IN ENG.	

(C) 7. NO METAL STAMPS OR MARKINGS SHALL BE PERMITTED ON ANY SECTIONS UNLESS NOTED OR SPECIFIC PRIOR APPROVAL HAS BEEN OBTAINED FROM THE PURCHASER.

THE FOLLOWING NOTES ARE APPLICABLE TO DETAIL -7 COIL

1. FOR MATERIAL & WIRE DIA. SEE L/M
2. SPRING RATE 5 #/IN. ± 10%.
3. HAND OF WINDING OPTIONAL
4. TOTAL NO. OF COILS 9 ± ½ COIL (NO. OF COILS TO BE COUNTED FROM POINT "A" TO POINT "B")
5. BOTH ENDS CLOSED & GROUND SQUARE WITH SPRING AXIS TO WITHIN ½ DEGREE. (AFTER FORMING & GRINDING THE END COILS, THE WIRE DIAMETRICALLY OPPOSITE THE END OF THE WIRE SHALL HAVE BEEN REDUCED TO ⅓ THE WIRE DIAMETER)
6. HEAT TREAT AFTER COILING TO 220,000 PSI ULTIMATE TENSILE STRENGTH.

(B) 6. THE BASIC ASSY SHALL BE TESTED BY DEPRESSING -3 COLLAR UNTIL -7 SPRING IS AT MIN. OPERATING LENGTH AND THEN RELEASING GRADUALLY, A MIN. OF 10 TIMES. THERE SHALL BE NO EVIDENCE OF STICKING OR BINDING BEARE, BURING, OR AFTER THE TEST.

(C) 5. ℄ OF DETAIL -5 SHALL BE ESTABLISHED BY DIA'S :C- & -D-

(A) 4. THE FOLLOWING SHALL BE USED AS REQUIRED FOR LUBRICATION AT ASSY. OF CLOSE FITTING PARTS: COLLOIDAL GRAPHITE (DISPERSED IN ALCOHOL OR PURE WATER) AS MFD. BY APPROVED VENDORS.

(A) 2. GEOMETRIC AND POSITIONAL TOLERANCE SYMBOLS ARE PER MIL STD-8A

1. BREAK ALL SHARP EDGES .010-.020

GEN'L NOTES:

APPROVED BY A.E.C. 25 APRIL 1960

E 372-2105007

E 372-2105007

AS BUILT

3	-11	1	PIN	(B) .125 DIA x 1 3/8	S/S BAR	ASTM 304
1	-7	1	SPRING	.157 DIA x .100 LG.	INCONEL X	AMS 5699
1	-5	1	TUBE	3/8 O.D. x .300 WALL = .40	S/S TUBING	ASTM 304
1	-3	1	COLLAR	3/8 O.D. x .500 WALL = .5	S/S TUBING	ASTM 304
1	-1	1	SLEEVE	3/8 O.D. x .500 WALL = .7	S/S TUBING	ASTM 304
		-9	HOLD DOWN ASSY			

LUBRICANT — SEE NOTE 4 — DAG-154 (OR EQUIV.)

PART NUMBER	NEXT ASSY	USED ON APPLICATION	QTY REQ'D	INTERCHANGEABILITY STATUS
372-2105007-9	372-2105004-5	PM-3A	1	0
372-2105004-5	372-2105003-5	PM-1	1	0

PM-1 NUCLEAR POWER PLANT CONTRACT AT(30-1)-2380

DETAILS - HOLD DOWN CENTER BUNDLE

PM-1 REACTOR CORE

THE MARTIN COMPANY BALTIMORE, MARYLAND NUCLEAR DIVISION

E 372-21

DETAIL "C"
SCALE: NONE
HOLE LOCATION - 18 PLACES (SEE NOTE 4)

DETAIL "B"
TYPICAL 3 PLACES

TYPICAL 12 PLACES
-7 (PRESS FIT INTO -3 UNTIL BOTTOMED)
-15 (PRESS FIT INTO -3 (-7)
STAKE -3 BOTH SIDES TO RETAIN -15
-11 (PRESS FIT INTO -3 UNTIL BOTTOMED)
-17 (PRESS FIT INTO -3 (-11) STAKE -3 ONE SIDE TO RETAIN -17

DETAIL "A"
TYPICAL 3 PLACES

-18 (PRESS FIT INTO -3 UNTIL BOTTOMED)
-21 (PRESS FIT INTO -3 (-18) STAKE -3 ONE SIDE TO RETAIN -21
12 PLACES

D-D SHOWN
E-E SHOWN
F-F ROTATED 180°

LOCATE SERIAL NO. (AS SUPPLIED BY PURCHASER) IN THIS AREA, USE ¼ HIGH CHARACTERS, .005 - .010 DEEP. NO ROUGH EDGES OR BURRS PERMITTED.

PLAN VIEW

SEE DETAIL "C" FOR HOLE LOCATION (18 PLACES)
SEE DETAIL "D" FOR ALIGNMENT PIN LOCATIONS
SPOTFACE 1¼ DIA. × ⅛ CSK. R. × 38.750 DIMENSION (12 PLACES.) (SEE NOTE 5.)
SPOTFACE 1½ DIA. × ⅛ CSK. R. × 38.760 DIMENSION (6 PLS.) (SEE NOTE 5)
2 DIA. TOOLING HOLES IN -5 PERMISSIBLE AS SHOWN DURING FABRICATION. 6 PLACES AT 60° ON 6 DIA. B.C.

DETAIL "D"
SCALE: NONE
ALIGNMENT PIN LOCATIONS
-7 (3 PLACES), -11 (3 PLACES), -18 (12 PLACES)

PART NO.	DIM. "A"
-7	25/32
-11	37/32
-13	1 5/8

DETAIL -7-11-13

DETAIL -15, -17, -21

PART NO.	DIM. "L"
-15	.600
-17	.750
-21	1.020

DETAIL -5

DETAIL -3

C-C

DETAIL -1

D-D

ORIGINAL
APPROVED BY AEC
25 APRIL 1960

GEOMETRIC AND POSITIONAL TOLERANCE SYMBOLS ARE PER MIL-STD-8A.
7. ALL WELDS SHALL BE VISUALLY & LIQUID PENETRANT INSPECTED AFTER FABRICATION. WELDING & INSPECTION PROCEDURES, TECHNIQUES, & MATERIALS SHALL BE IN ACCORDANCE WITH MARTIN SPEC. NO. MM-2005 ▷ .003 WELD PENETRATION REQ'D IN ALL FINAL WELDS.
8. ALL COMPONENTS SHALL BE MANUFACTURED IN ACCORDANCE WITH MARTIN SPEC. NO. MM-7990 B
9. ALL WELDED ASSYS SHALL BE FULLY ANNEALED AFTER WELDING.
10. LOCATION "A" FOR -11 PIN SHALL BE DRILLED IN -19 WELDED ASSY BEFORE ANY OTHER HOLES. THIS LOCATION & THE THEOR. CENTER OF -19 ASSY PLAN VIEW ESTABLISH "X" AXIS. "Y" AXIS SHALL BE PERPENDICULAR TO "X" AXIS THRU THEOR CENTER. ALL REMAINING HOLES SHALL BE DRILLED WITH RESPECT TO "X" & "Y" AXES.
11. ALL WELDS SHALL BE MADE USING 308 STAINLESS STEEL WELD ROD.
12. CENTERLINE OF -19 ASSEMBLY SHALL BE ESTABLISHED BY DIA B, AT -5 SPIDER LEVEL, AND DIA A
13. ALL COMPONENTS SHALL MEET THE FOLLOWING MATERIAL CONSTITUENT LIMITATIONS:
a) COBALT: .05 WGT % MAX.
b) COBALT + TANTALUM: .15 WGT % MAX.
c) CARBON: .03 WGT % MAX.
14. THE FOLLOWING SHALL BE USED AS REQUIRED FOR LUBRICATION AT ASSY OF CLOSE FITTING DOWELS.
a) COLLOIDAL GRAPHITE (DISPERSED IN ALCOHOL OR PURE WATER) AS MFD BY APPROVED VENDORS. C1

5. SPOTFACES SHALL BE COPLANAR WITHIN .003.
6. HOLE LOCATIONS SHOWN SHALL BE WITHIN .001 OF THEOR. POSITION WITH RESPECT TO THEOR CENTER OF -19 ASSY AND X-Y AXIS AS ESTABLISHED IN NOTE 10
2. BREAK ALL SHARP EDGES .010 - .020 R
4. DECIMAL DIMENSION TOLERANCE ± .010 UNLESS OTHERWISE NOTED.

Notes:

ZONE	STR	DESCRIPTION	DATE	APPROVAL
		1/16 MAX. ASSY. ADDED PLUG TO CAV. R. BOTTOMS 60° ADDED MAT'L TO RADIUS		
		REVISED DETAIL -3		
		REVISED -5, .600 WAS .625		

ZONE	STR	DESCRIPTION	DATE	APPROVAL
		REVISED STOCK SIZE -19-3, ADDED DIA. ADDED NOTES 7, 8 & 9, ADDED D DETAIL		
		ADDED DETAIL -3, -15, -17, -21, ADDED SCALE NOTE		
9/10	12	ST. WAS .625 MIN. MAX. TO CAV. R. REMOVED NOTE 3; REVISED NOTE 12. REVISED 3 (.125 DIA. ON) & B DIMENS	5/23/60	W. KRUEGLE
11/8	2	6-2340	6-2340	GUILLIAN
		2.5 DIA. WAS 2.5x2.6		
		.24 STK THK WAS .19 STK THK		
		ADDED NOTE 14, DELETED REFERENCE TO MM		
		ADDED NOTE 13		
		-3 STOCK WAS .7	2 DEC 60	TWCH
9/6/61	2	ADDED PM-3A	6-12-61	TWCH / LLS
9/6/61	2	ADDED PM-3A	6-12-61	LLS
9/6/61	2	SHEET 2 ADDED, SEE CONTINUATION SHEET 2	6-12-61	CHENAULT

DETAIL -19 WELDED ASSY

SEE DETAIL "A" FOR DETAIL MACHINING INFO.
SEE DETAIL "B" FOR INSTL OF -7, -11
LOCATION "A" (REF)
PRELIMINARY MACHINE CUT (AEC)
CHAMFER ⅛ × 45°
⅛ DIA HOLE ⅜ DEEP, C'BORE .375 DIA. .375 DEEP × ⅛ CSK. R.
LOCATION "A" (REF)
PRELIMINARY MACHINE CUT (BMI)
CHAMFER ⅛ × 45°
CSK 90° × ⅞ DIA. (3 PLACES)
¾ (.750) DIA. HOLE (3 PLACES)
SEE NOTE 5
19
-1
-3
-5
-9

A-A

(15) NO METAL STAMPS OR MARKINGS SHALL BE PERMITTED ON ANY SECTIONS UNLESS NOTED OR PRIOR SPECIFIC APPROVAL HAS BEEN OBTAINED FROM THE PURCHASER.

CONTINUATION OF NOTES:

QUANTITY	PART NO.	DESCRIPTION	STOCK SIZE	MATERIAL OR VENDOR	MATERIAL SPECIFICATION	FINISH
		LUBRICANT	SEE NOTE 14	Dag-154 (OR EQUIV)		
12	-21	LOCK PIN	M/F AB-5			
3	-17	LOCK PIN	M/F AB-5			
3	-15	LOCK PIN	M/F AB-5			
12	-18	ALIGNMENT PIN	M/F AB-14			
3	-11	ALIGNMENT PIN	M/F AB-14			
3	-7	ALIGNMENT PIN	M/F AB-14			
1	-5	BOTTOM SPIDER	25 DIA × 2	5/8 PLATE	ASTM 347	
1	-3	MOUNTING RING	22 13/16 ID x 1/8 x 7 3/16 LG	3/8 RING	ASTM 347	
1	-1	CYLINDER	22 13/16 ID x ½ x 37 LG	3/8 RING	ASTM 347	
	-19	WELDED ASSY.				NONE
	-9	SHROUD ASSY.				

AS BUILT

LIST OF MATERIAL — PM-1 NUCLEAR POWER PLANT — CONTRACT AT (11-1)-1345

PART NUMBER	USED ON	APPLICATION	QTY REQD	INTERCHANGEABILITY STATUS
372-2105009-9	PM-3A	1	0	INTERCHANGEABLE
372-2105009-3	PM-1	1	0	REPLACEABLE
372-2105009	PM-3A	1	0	UNCONTROLLED

UNLESS OTHERWISE SPECIFIED: DIMENSIONS ARE IN INCHES; TOLERANCES ARE AFTER PLATING; FRACTIONS ± DECIMALS ± ANGLES ±; NOTED. RMS FINISH EXCEPT AS NOTED

DEPT	ISSUE	SHT
M. JOYCE	594	8-3-60
		5-7-60
		6-12-61
		6-12-61
		6-12-61

CORE SHROUD ASSY
PM-1 REACTOR CORE
SCALE NONE

THE MARTIN COMPANY
BALTIMORE, MARYLAND
NUCLEAR DIVISION

E 372-2105009 SHEET 1 OF 2

E 372-2105009 SHEET 1 OF 2

E 372-2105009 SHEET 1 OF 2

REVISIONS					
	ZONE	DESCRIPTION	DATE	APPROVED
A1				
A2				
A3				
A4				
A5				
A6				
A7				

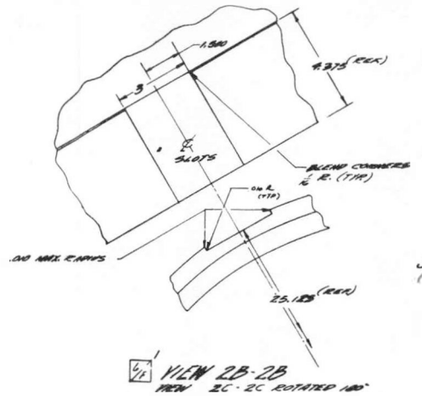

1/11 VIEW 2B-2B
VIEW 2C-2C ROTATED 180°

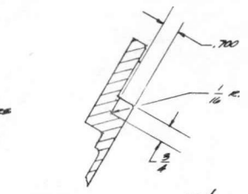

SECTION 2A-2A 4/E
(TYP 6 PLCS)

312 2105009 (2) E

AS BUILT

QUANTITY /DASH NO.	PART NO.	LOC	DESCRIPTION	STOCK SIZE	MATERIAL OR VENDOR	MATERIAL SPECIFICATION	FINISH
FOR EACH ASSY			LIST OF MATERIAL				
FOR EACH DASH NO. QTY.							

UNLESS OTHERWISE SPECIFIED
DIMENSIONS ARE IN INCHES AND ARE AFTER PLATING.
TOLERANCES ON DECIMALS
.X ±.1 .XX ±.03 .XXX ±.010
ANGLES ±1°
MACHINED SURFACES ✓
REF. MIL-STD-16
MIL-I-8500 STATUS
INTERCHANGEABLE
REPLACEABLE
UNCONTROLLED

DRAWN BY: [illegible] DATE: 5-31 12/1/59
CHECKED
STRESS ENGR.
MT. ENGR.
MFG. ENGR.
PROJ. ENGR.
QA [illegible]
ENGINEER JP McM-G
CONT. REP.

THE MARTIN COMPANY BALTIMORE, MARYLAND

CORE SHROUD ASSY
MK1 REACTOR CORE

CALC. WT. | DASH NUMBER | NEXT ASSY | USED ON | FINAL ASSY | TEST | QTY. REQD | APPLICATION

CODE IDENT NO. 38597 | SIZE E | 312-2105009

SCALE 3/4 | SHEET 2 of 2

12. THE ALIGNMENT STRUCTURE SHALL BE LOADED AGAINST THE SPACER DURING THE FINAL DRILLING AND PINNING OPERATION TO PROVIDE ZERO CLEARANCE BETWEEN THE SPACER AND UPPER GRID
11. NO METAL STAMPS OR MARKINGS SHALL BE PERMITTED ON ANY SECTIONS UNLESS NOTED OR PRIOR SPECIFIC APPROVAL HAS BEEN OBTAINED FROM PURCHASER.

10. ALL FUEL TUBES SHALL HAVE FREE LATERAL MOTION AT UPPER GRID PLATE ~~LOWER~~ AFTER FINAL ASSY
9. DECIMAL TOLERANCE ±.010 UNLESS OTHERWISE NOTED.
8. THE FOLLOWING SHALL BE USED AS REQD FOR LUBRICATION AT ASSY OF CLOSE FITTING DOWEL PINS:
   a. COLLOIDAL GRAPHITE DISPERSED IN ALCOHOL OR PURE WATER AS MFG. BY APPROVED VENDORS.
7. MFG. PER MARTIN SPEC. MAN-7890
6. ☆ DIM SHOWN IN DETAIL B MUST BE CHECKED AFTER ASSY IS COMPLETE EXCEPT FOR INSERTION OF CONTROL ROD. ACTUAL LOCATION OF PARTS INDICATED IN DETAIL B MUST BE AS SHOWN WITH ±.005 TOLERANCE ON THE TRUE DISTANCE BETWEEN ANY GUIDE RAIL LOCATION AND EITHER ALIGNMENT STRUCTURE HOLE LOCATION.
5. TUBES (372-2105013-7, 372-2105013-9) SHALL BE EXPANDED INTO THE LOWER GRID (372-2105012) BY A PROCESS, AS APPROVED BY THE PURCHASER, WHICH WILL PROVIDE THE FOLLOWING:
   a. AN INSIDE DIA. OF .2653±.002 ON THE 372-2105013-9 FUEL ELEMENTS
   b. A MIN. OF 500 LBS FORCE TO PULL THE TUBE FREE FROM THE GRID
   c. SHARP EDGES AT THE INLET I.D., MAX. R. .005 ∮ FLUSH WITH SURFACE WITHIN .005.
   d. LINE TO LINE CONTACT OVER A MIN OF 80% OF EXPANDED AREA, WITH A MAX. GAP OF .001 ALLOWED IN THE VOID REGION.
   e. THE TUBE EXPANSION PROCESS SHALL NOT IMPAIR THE BOND INTEGRITY OF THE FUEL TUBES.
   f. THE PROCESS SHALL CONTROL LOCATION OF THE FUEL RELATIVE TO THE LOWER GRID WITHIN THE DIMENSION SHOWN.

CONTINUATION OF NOTES

5. (CONTINUED)
   g. 90 ± FIXITY OF THE ELEMENT TO LOWER GRID JOINT. (THIS REQUIREMENT APPLICABLE TO 013-9 FUEL ELEMENT ONLY.)

4. 372-2105013-9 ELEMENTS TO BE PLACED NEXT TO THE CONTROL ROD CHANNEL SHALL BE BOWED .020 TO .030 PRIOR TO ASSEMBLY. THE TUBES SHALL BE EXPANDED INTO THE GRID SO THAT THE BOW IS IN THE DIRECTION AWAY FROM THE CONTROL ROD CHANNEL.

13. A MAXIMUM BOW OF .032 IN THE DIRECTION INDICATED IS ALLOWED ON THE LOWER GRID PLATE (372-2105012) AFTER ROLL EXPANSION OF ALL ELEMENTS.

372-2105015-5 SPACER

372-2105011 GRID

EE SHOWN
FF SIMILAR
GG SIMILAR

372-2105016

A-A

29

B-B

30 (REF) FUEL LENGTH

DRILL AND REAM .1874/.1867 DIA HOLE. X 1 1/16 DEEP.

.250

(TYP) .093

DEFORM EDGE OF PART WITH ∮ DIA. 7/8 BAR (3rd SERIES ALLOY) SO AS TO INCASE PINS IN HOLES. NO VISUAL EVIDENCE OF CRACKING ALLOWED AFTER ASSEMBLY.

372-2105015-5

-19

372 2105 013-9

372 2105 012

THESE PLANES TO BE ESTABLISHED AT GUIDE RAIL LOCATIONS

SEE NOTE 13

.265 +.003 -.004 (REF)

372 2105 015-1

TORQUE TO 150 in-lbs

4.125 (TRUE DIM)

SEE DETAIL A

PLANE -A-

C-C
TYP. 3 PLCS

DETAIL A

D-D

ASSEMBLED LOCATIONS OF GUIDE RAILS (372-2105014-1, -3, ∮-5) IN PLANE A SHALL BE WITHIN .003 OF INDICATED DIMENSIONS.

.330±.002 (TYP)

3.900±.002

HOLE LOCATIONS IN ALIGNMENT STRUCTURE (372-2105015-1)

SYM	DESCRIPTION	DATE	APPROVAL
(7-D)	F, 372-2105013-9 ELEMENTS AND TUBES		
6-B, 5-B	F, ADDED BOWING ALLOWANCE IN LOWER GRID		
5-B	F, ADDED LOCATING SLOTS FOR EXPANSION CHECK PLUGS	7/6/61	THC

372-2105010-9 372-2105005 PM-1A
372-2105010-9 372-2105006 PM-1

6	A5-11	PIN		
12	372-2105013-39	POISON ELEMENT ASSY.		
3	372-2105015-5	SPACER		
1	372-2105016	CONTROL ROD		
1	372-2105014-5	GUIDE RAIL		
1	372-2105014-3	GUIDE RAIL		
1	372-2105014-1	GUIDE RAIL		
3	372-2105015-1	SLEEVE		
1	372-2105018-3	ALIGNMENT STRUCTURE		
1	372-2105011	UPPER GRID		
3	372-2105013-19	POISON ELEMENT ASSY		
121	372-2105013-9	FUEL ELEMENT ASSY		
1	372-2105012	LOWER GRID		
5	372-2105013-7	DUMMY ELEMENT ASSY		
1	-29	CORE STRUCTURE ASSY		NONE
	-19	CORE TUBES ASSY		NONE

LUBRICANT — SEE NOTE 8 — DAG-154 (OR EQUIV.)

AS BUILT

CUSTOMER APPROVAL					
DATE	SIGN	ZONE	SYM	DESCRIPTION	DATE	APPROVAL
		2-D	A,	ADDED HOLES TO ∮ TO ALIGN WITH ∮ ON ADDED SERIAL NO., ADDED TRUE DIM.		
		6-D	A,	CORRECT PATTERN OF CONTROL ROD CHANNEL		
		7-F	A,	ADDED NOTES 8 & 9 (A), REVISED NOTE 5 C & G	11/21/60	W. ERMELLE
		7-F	A,	ADDED ∮ LOCATE TO ELEMENTS		
		4-D	B,	ADDED NEOLUBE TO 372-2105013-9		
9/20	TW	7-E	B1	REVISED NOTE 5 G		
9/20	TW	4-D	B,	REVISED NOTE, ADDED 1 1/2 DIM.	6-27-61	W. ERMELLE
			C,	ROLL FIELD 2 1/16 TO INCREASE 372-2105013-9 SLEEVE & ELIMINATE LOWER GRID PINNING		
			C,	REVISE NOTE 8, ELIMINATE NEOLUBE		
11/20	TW		C,	ROLL FIELD AT LOWER END		
			C,	ADDED NOTE 11 (12)		THC

4. b. PREVENT COUNTER-CLOCKWISE ROTATION OF 372-2105015-3 RELATIVE TO 372-2105014-1, -3, ∮-5. FOR SUGGESTED METHOD SEE DETAIL A.
4. a. USING 3/16 DIA. STAINLESS STEEL ROD (300 SERIES ALLOY) PLACED PERPENDICULAR TO AXIS OF DETAIL 372-2105014-1, DEPRESS OUTER SURFACE OF 372-2105015-3 1/16 INTO CORRESPONDING GROOVE IN 372-2105014-1. TYPICAL FOR DETAILS 372-2105014-3 ∮ -5
3. ① SURFACES-B- TO LIE IN PLANE-A- WITHIN .001
2. ⊖ DENOTES LOCATION OF DUMMY ELEMENT TUBES
1. ▲, ✱ DENOTES LOCATION OF POISON ELEMENT TUBES

GEN'L. NOTES:

A5-11

372 2105 014-1

372-2105016

372 2105 013-19

372 2105 013-39

372 2105 014-3

372 2105 014-5

372 2105 011

372 2105 013-29

LOCATE CODED SERIAL NO. IN THIS AREA. (SEE NOTE BELOW)

1 3/4 TYP

LOCATE SERIAL NO. (AS SUPPLIED BY PURCHASER) WITH 3/16 HIGH CHARACTERS .005-.010 DEEP. NO ROUGH EDGES OR BURRS PERMITTED. THE SERIAL NO. SHALL ALSO BE INDICATED BY AN APPROVED CODING SYSTEM USING VARIOUS GROUPINGS & NUMBER OF THROUGH HOLES APPROX. 3/16 DIA. AND LOCATED IN THE AREA SHOWN.

B-B

ORIGINAL
APPROVED BY AEC
25 APRIL 960

372-2105010 SHEET

372-2105010 SHEET

372-2105010 SHEET

PM-1 NUCLEAR POWER PLANT CONTRACT: AT(30-1)2345

PERIPHERAL BUNDLE

PM-1 REACTOR CORE

THE MARTIN COMPANY BALTIMORE, MARYLAND NUCLEAR DIVISION

372-2105010

SCALE FULL

372-0193/3Y
372-0194/3Y

LTR	DATE	BY	SYM	DESCRIPTION	CHKD	APPD
			A	REVISED / ADDED HOLE LOCATIONS		
			A1	ADDED / MOVED DIM. / NOTE		
			A2	REVISED DIMENSIONS		
	9/20		A3	ADDED NOTES, REVISED NOTES 2&5	9/24	
			A4	REVISED PART NOS. SHEET 2		
			A5	REVISED NOTE 1 & TOLER. 2 PL. DIA.		
			B	3-D SHEET WAS 7/16 THK		
			B1	DWG. SHEET WAS 7/16 THK		
			B2	DWG WAS .003		
			B3	ADDED NOTE "FAR SIDE - .008 MAX R."		
			B4	REVISED PLANE VIEW, INCLUDE SHEETS B-4, B-8, & C-C, AND ITEM 10 TO DETAIL C		
	9/20		B5	ADDED CHAMFER NOTE		
			B6	ADDED NOTE 7		
	4/14		C	REVISED PARTS LISTING	4-20	
			C1	WAS PN "A" REC. 4/12 INC. NUMB.		
			C2			

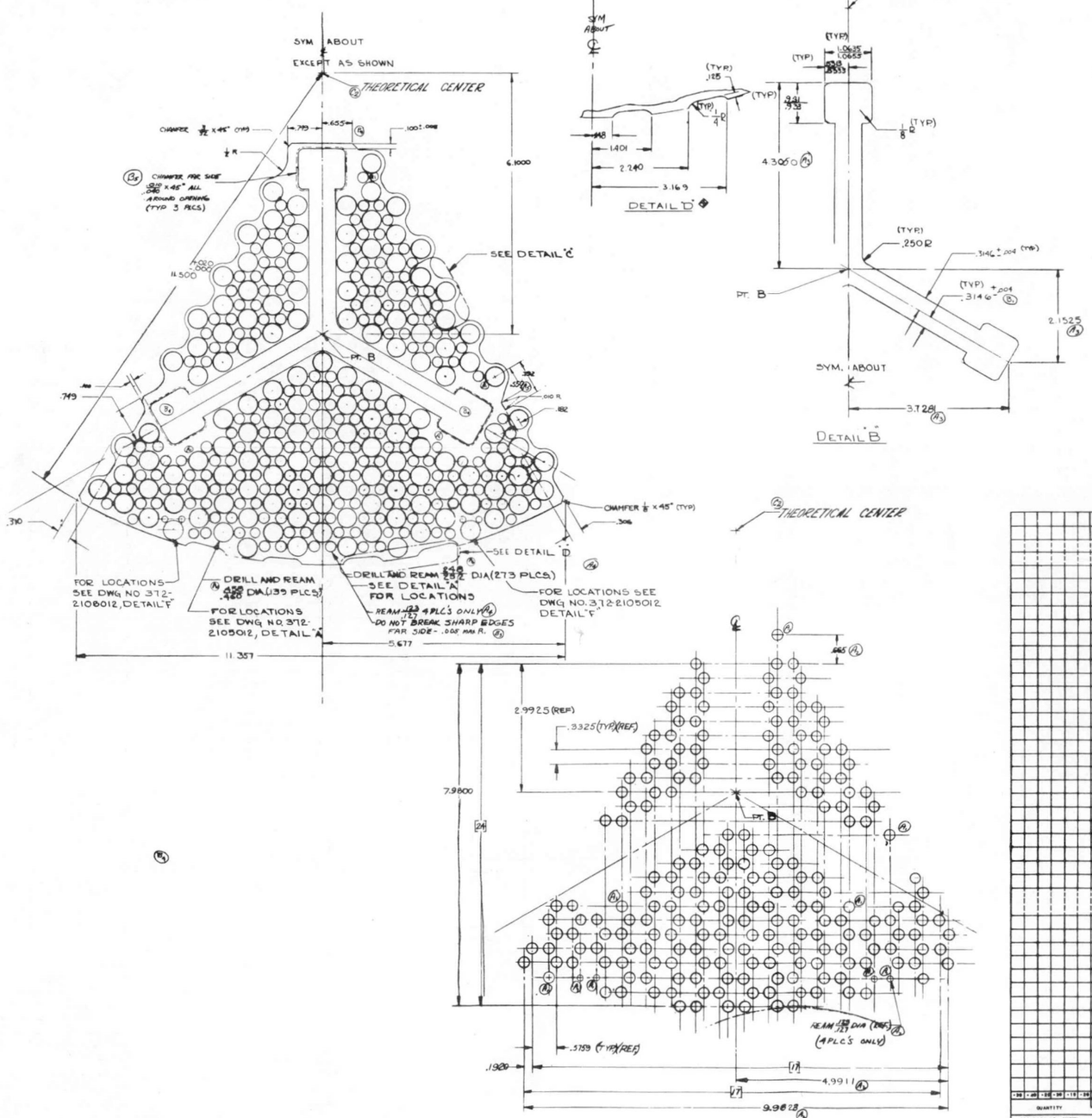

7. NO METAL STAMPS OR MARKING SHALL BE PERMITTED ON ANY SECTIONS UNLESS NOTED OR PRIOR SPECIFIC APPROVAL HAS BEEN OBTAINED FROM THE PURCHASER.
6. MFG. PER MARTIN SPEC. MN-7890
5. THE FOLLOWING MATERIAL CONSTITUENT LIMITATIONS SHALL BE MET:
COBALT: .05 WGT % MAX.
COBALT + TANTALUM: .15 WGT % MAX.
CARBON: .03 WGT % MIN.
4. HOLE LOCATIONS SHALL BE WITHIN .005 OF TRUE POSITION.
3. GEOMETRIC AND POSITIONAL TOLERANCE SYMBOLS ARE PER MIL-STD-8A.
2. BREAK ALL SHARP EDGES .010-.020 EXCEPT AS NOTED
1. UNLESS OTHERWISE SPECIFIED, DECIMAL TOLERANCES AS FOLLOWS:
DIM. SHOWN IN THOUSANDTHS OF AN INCH (X.XXX): ±.010
DIM. SHOWN IN TEN-THOUSANDTHS OF AN INCH (X.XXXX): ±.0005

NOTES:

ORIGINAL
APPROVED BY AEC
25 APRIL 1960

C E 372-2105011

AS BUILT

C E 372-2105011

C E 372-2105011

QUANTITY	PART NO.	DESCRIPTION	STOCK SIZE	MATERIAL OR VENDOR	MATERIAL SPECIFICATION	FINISH
		UPPER GRID	10 3/4 X 11 3/4	STL. STEEL PLATE	ASTM 304 ▼5	NONE

LIST OF MATERIAL — PM-1 NUCLEAR POWER PLANT CONTRACT AT(30-1)-2345

CALC WT	PART NUMBER	NEXT ASSY	APPLICATION
372-2105011	372-2105010	PM3A	
372-2105011	372-2105010	PM-1	

UNLESS DIMENSIONS ARE IN INCHES. DIMENSIONS ARE AFTER PLATING. TOLERANCES ON FRACTIONS ± 1/64 | DECIMALS ± .01 | ANGLES ± 1/2°
RMS FINISH 125 EXCEPT AS NOTED
INTERCHANGEABILITY STATUS: INTERCHANGEABLE / MATCHABLE / NON-INTERCHANGEABLE

FINAL ASSY	REV	QTY REQD
1	0	
	0	

DRAWN	DATE
CHKD	3-60
ENGR	3-60
APPD	3-60
MFG	3-60

UPPER GRID CORE SEGMENT PM1 REACTOR CORE

THE MARTIN COMPANY BALTIMORE, MARYLAND NUCLEAR DIVISION

C E 372-21
SHEET

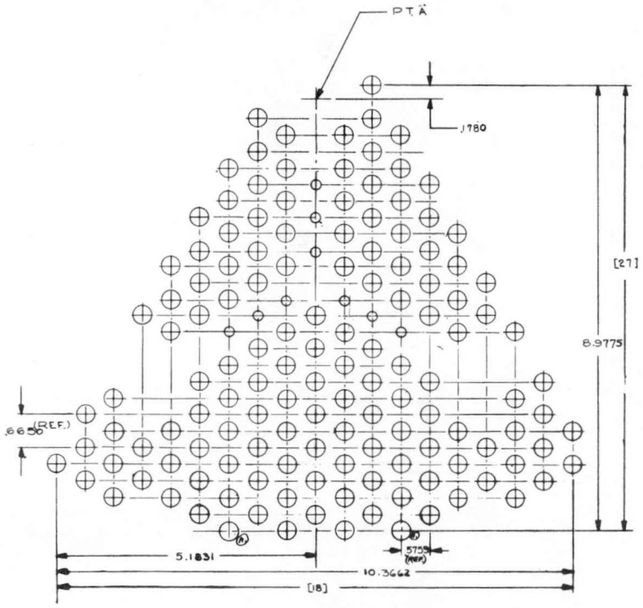

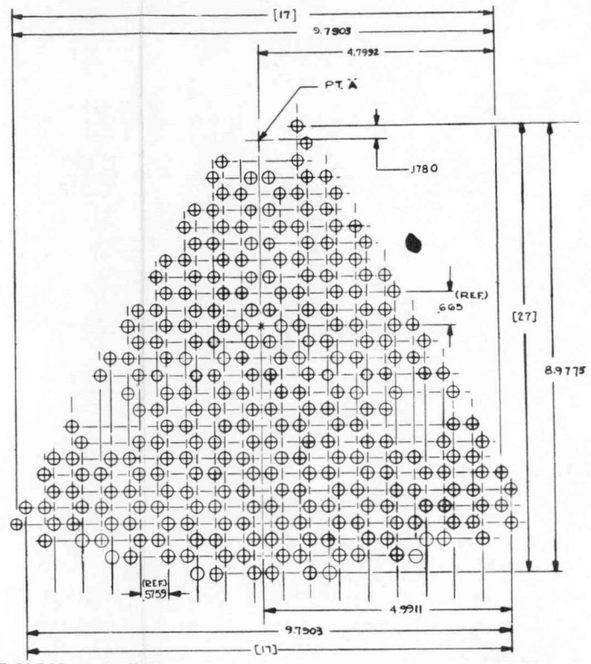

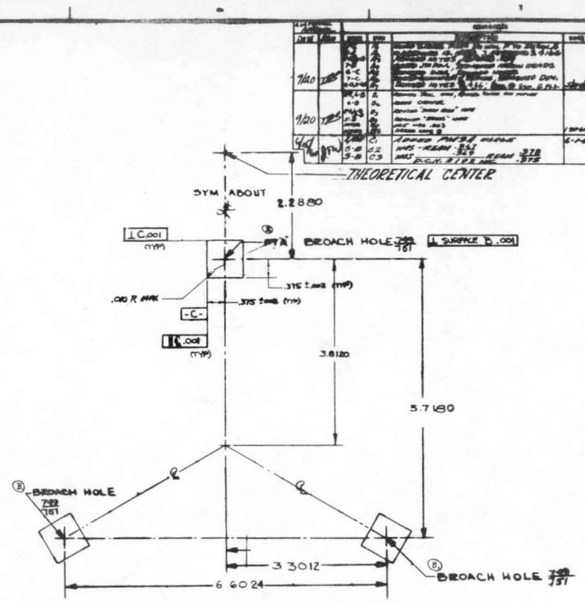

DETAIL C

⑦ T. MFG. PER MARTIN SPEC. MN 78390.

⑥ 6. THIS COMPONENT SHALL MEET THE FOLLOWING MATERIAL CONSTITUENT LIMITATIONS:
COBALT: .05 WGT % MAX
COBALT + TANTALUM: .15 WGT % MAX
CARBON: .03 WGT % MIN.

5. UNLESS OTHERWISE SPECIFIED, DECIMAL TOLERANCES ARE AS FOLLOWS:
DIM. SHOWN IN THOUSANDTHS: ±.010
DIM. SHOWN IN TEN-THOUSANDTHS: ±.0005

4. ⑦ DIMENSIONS INDICATED ARE SUBJECT TO CONFIRMATION BY ⑦ MFG. DEVELOPMENT TESTS.

3. BREAK ALL SHARP EDGES .010 - .020 ⑥ EXCEPT AS NOTED.

2. ⑥ HOLE LOCATIONS SHALL BE WITHIN .005 ⑥ OF TRUE POSITION.

1. GEOMETRIC AND POSITIONAL TOLERANCE SYMBOLS ARE PER MIL-STD-8A.

NOTES:

ORIGINAL
APPROVED BY A.E.C.
25 APR. 1960

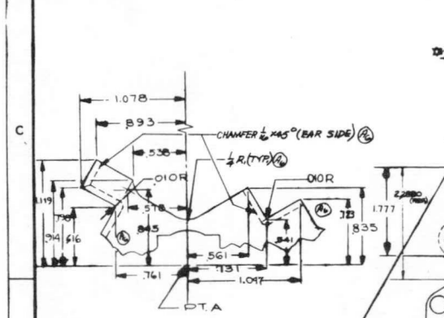

DETAIL E
SCALE 2:1

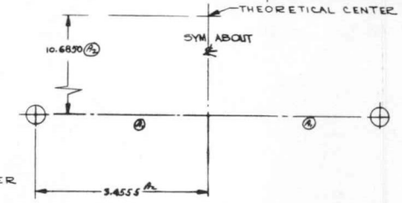

DETAIL B

DETAIL F

DETAIL D
SCALE 2:1

⑥ 8. NO METAL STAMPS OR MARKINGS SHALL BE PERMITTED ON ANY SURFACE ⑦ UNLESS NOTED OR APPROVED. SPECIFIC APPROVAL HAS BEEN OBTAINED FROM THE PURCHASER.

CONTINUATION OF NOTES:

AS BUILT

QUANTITY	PART NO.	DESCRIPTION	STOCK SIZE	MATERIAL OR VENDOR	MATERIAL SPECIFICATION	FINISH
		LOWER GRID	3/4 X 12 X 11	CORROSION RESISTING STEEL PLATE	ASTM 304 ⑥ ⑦	NONE

LIST OF MATERIAL

PWR NUCLEAR POWER PLANT CONTRACT AT (30-1)-23-5

372-2105012	372-2105010	PM3A	1	0	
372-2105012	372-2105010	PM-1	0		

LOWER GRID
CORE SEGMENT
PM-1 REACTOR CORE

THE MARTIN COMPANY
BALTIMORE, MARYLAND
NUCLEAR DIVISION

C E 372-2105012 SHEET

C E 372-2105012 SHEET

E 372-2105012 SHEET

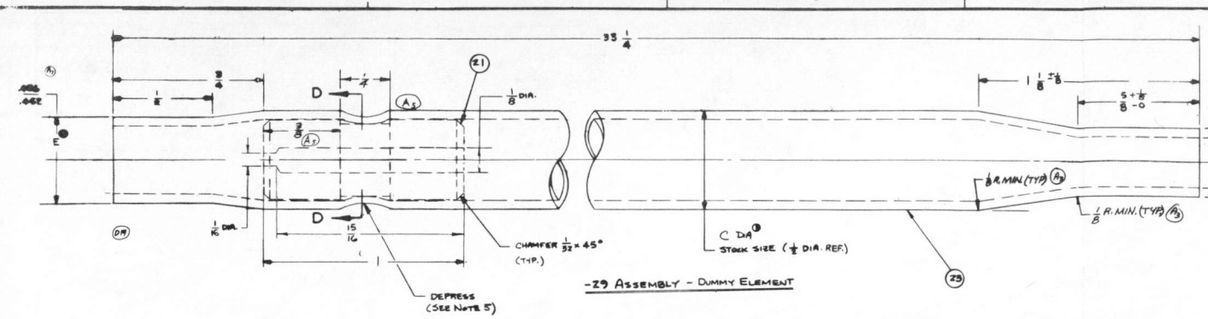

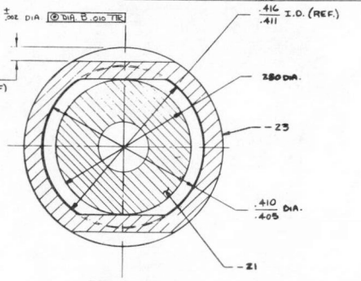

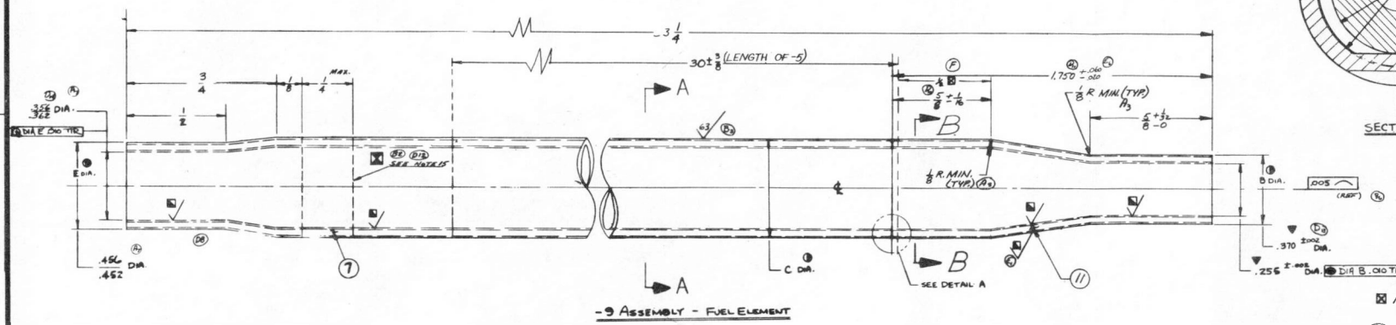

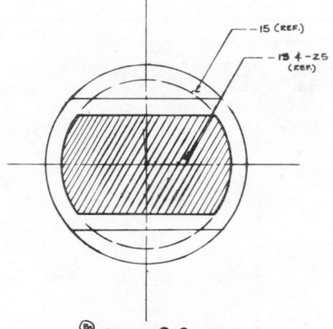

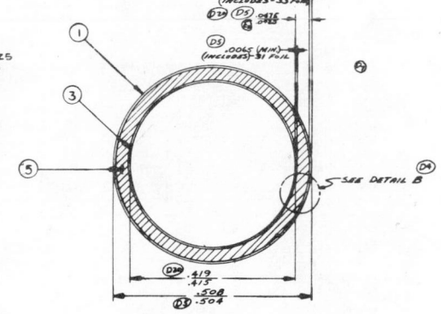

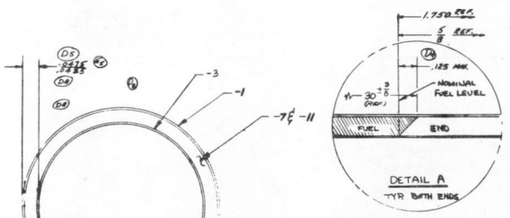

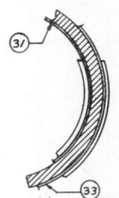

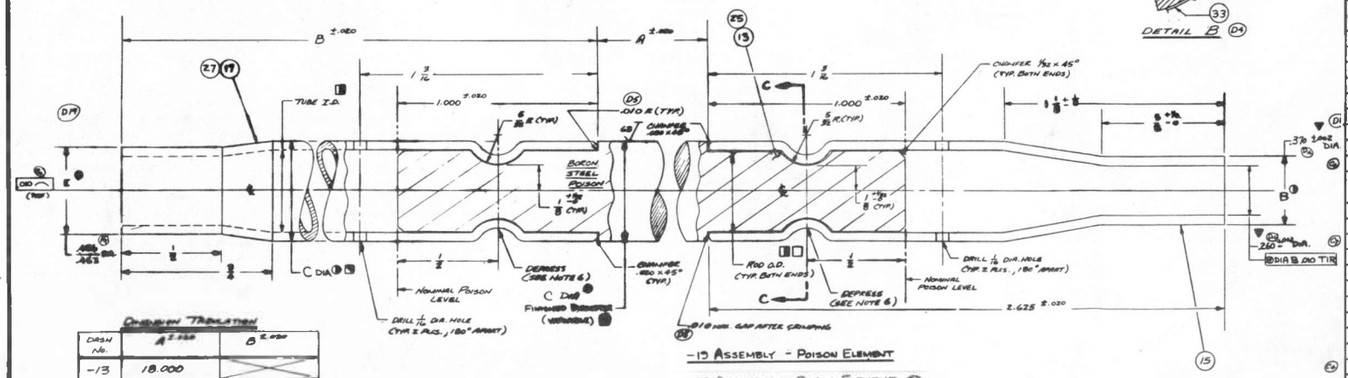

DASH No.	A ±.020	B ±.020
-13	18.000	
-25	28.000	
-17		12.625
-27		2.625

CUSTOMER TRANSLATION

DATE	DWN	REVISIONS DESCRIPTION	DATE	APPROVED
4/6/61	JW	ADDED DETAIL A, REMOVED .005 MIN.		TRC
		5 1/2 WAS 4 1/2		
		7TH PLACE WAS ILLEGIBLE		
7/6/61	JW	REVISED IDENTIFICATION & LOCATION	26 JUNE 61	TRC
		.005 (MIN) WAS .362/.366		
		370 WAS .362/.366		
		.005 WAS .362/.366		
		REMOVED		
		ADDED DETAIL B	27 JUNE 61	TRC
		NOTE 10 & 11 REVISED		
		ADDED NOTE 12		
		.010 WAS 1/16 DIA.		
		.010 WAS .005		
		ADDED NOTE 13	29 JUNE 61	TRC
		ADDED NOTE 14		
		ADDED NOTE 15	1 JULY 61	TRC

DATE	DWN	REVISIONS DESCRIPTION	DATE	APPROVED
10/21	JW	NOTES 2 THRU 6 REVISED NOTES 1,2,3,6,7, & 13 RESPECTIVELY.	10-18-60	RBS
5/11	JW	ADDED DETAILS - 31 AND - 33	5-11-61	MYER
		REVISED WIDTH, PLATE		
		REVISED NOTE 13 & 7 ADDED		
		NOTED DETAIL "B"		
		ADDED DIM. (.004 WAS .005; .3125 WAS .313; .125 WAS .126; .010 WAS .02 R, .010 WAS .002		
		REVISED -31 PIN		
		DIMS. .2345 .2355 WAS .2295 .2305 REMOVED		

DATE	DWN	REVISIONS DESCRIPTION	DATE	APPROVED
		ADDED NOTE 16		
		ADDED NOTE 17		
		ADDED NOTE 18		
9/60	JW	ADDED RADIUS REVISED NOTES 1&7		
		3/8 WAS 1/2 CORRECTED PICTURE WORK		W.R.RUSH
4/61	JW	ADDED .304		
7/61	JW	REV. NOTE 10. REM. Δ Symbol 4 PLS.		
		REVISED NOTE 6		TRC

1. DIAMETER C ON ALL ELEMENTS (AS INDICATED) SHALL BE CONCENTRIC WITH ℄ ESTABLISHED BY DIAMETERS B & E WITHIN .010 TIR FOR FUEL ELEMENTS (-9) & WITHIN .020 TIR DUMMY & ORGANIC POISON ELEMENTS (-29 & -39).
2. DETAILS -13 & -25 END DIAMETERS SHALL BE CONCENTRIC WITH C DIAMETER .004 TIR.
3. MACHINE END DIAMETERS OF DETAILS -13 & -25 (POISON ROD) TO PRESS FIT INTO INNER DIAMETER OF DETAILS -15, -17, & -27 RESPECTIVELY WITH .0001 TO .002 INTERFERENCE.
4. ALL COMPONENTS SHALL BE MFG TO THE FOLLOWING APPLICABLE MASTER SPECIFICATIONS:
   A) FUEL ELEMENT: MN-7231
   B) POISON ELEMENT: MN-7232
   C) DUMMY ELEMENT: MN-7230
5. USING 3/8 DIA 5/8 ROD (300 SERIES ALLOY) PLACED ⊥ AXIS OF -29 ASSY, DEPRESS OUTER SURFACE OF -23 1/16 INTO CORRESPONDING GROOVE IN -21. TYPICAL 2 PLCS. 180° APART.
6. USING 5/16 DIA 5/8 ROD (300 SERIES ALLOY) PLACED ⊥ AXIS OF -19 ASSY, DEPRESS OUTER SURFACE OF -15 & -17 TUBES 1/16 INTO CORRESPONDING GROOVES IN -13 ROD. REPEAT THIS PROCEDURE FOR -39 ASSY, USING -15 & -27 TUBES & -25 POISON ROD.
7. DETAILS -15, -17, -21, -23, & -27 SHALL COMPLY WITH THE FOLLOWING MATERIAL CONSTITUENT LIMITATIONS: COBALT: .05 WGT % MAX
   COBALT + TANTALUM: .15 WGT % MAX
   CARBON: .03 WGT % MAX.
8. [illegible]
9. [illegible]
10. DIM INDICATED SUBJECT TO CONFIRMATION BY MFG. DEVELOPMENT TESTS.
11. TUBE ENDS TO BE SQUARE & PARALLEL WITHIN .005 TIR.
12. POSITIONAL & GEOMETRIC TOLERANCES PER MIL STD 8-A.
13. THE NOMINAL C DIA. WILL BE SPECIFIED BY THE PURCHASER AFTER THE ACTUAL POISON CONTENT OF THE -13 & -25 MATERIAL IS DETERMINED ANALYTICALLY. (SEE MN-7232.) DIA. SPECIFIED WILL BE FROM .470 - .500 WITH A TOLERANCE OF ±.0005.
14. SURFACE FINISH OF THE BEAD ENDS (-7 & -11) I.D., AS CAUSED BY THE REDUCING OPERATION, SHALL BE TO STANDARDS APPROVED BY THE PURCHASER.
15. SUITABLE FUEL ELEMENT IDENTIFICATION MARKINGS, AS APPROVED BY THE PURCHASER, SHALL BE LOCATED IN THIS AREA. NO OTHER STAMPS OR MARKINGS SHALL BE PERMITTED ON ANY SURFACES UNLESS PRIOR SPECIFIC APPROVAL HAS BEEN OBTAINED FROM THE PURCHASER.
16. STOCK SIZES INDICATED TO BE DETERMINED BY MANUFACTURER.
17. BREAK ALL SHARP EDGES .010 - .020 R UNLESS OTHERWISE NOTED.
18. A DIA. INCREASE OF .005" IS ALLOWABLE BETWEEN THE FUEL AREA AND THE SEALED PORTION OF THE END CAP (TYP BOTH ENDS OF FUEL ELEMENT.)

NOTES CONTINUED:

16. THE NOMINAL FUEL LOADING IN EACH -9 ELEMENT SHALL BE 40.13 GRAMS U235. THE NOMINAL POISON LOADING IN EACH -19 ELEMENT SHALL BE .255 GRAMS BORON-10, AND THE NOMINAL POISON LOADING IN EACH -39 ELEMENT SHALL BE .383 GRAMS [illegible]

GEN'L. NOTES:

APPROVED BY AEC 24 APRIL 1961

AS BUILT

QUANTITY	PART NO.	NOMENCLATURE	MATERIAL OR VENDOR	SPECIFICATION	DCS
	-33	OUTER FOIL	S/S SHEET	ASTM 240 TYPE 347 OR MN-7231	NONE
	-31	INNER FOIL	S/S SHEET	ASTM 240 TYPE 347 OR MN-7231	NONE
1	-27	TUBE	5/8 TUBE	ASTM 249 TYPE 347 OR MN-7231	
1	-25	POISON ROD	5/8 ROLLED	ASTM 744 GR 347 OR MN-7232	NONE
	-23	TUBE	S/S TUBE	ASTM 249 TYPE 347 OR MN-7231	NONE
1	-21	PLUG	1/4 BAR	ASTM 276 TYPE 347 OR MN-7231	
1	-17	TUBE	3/4 TUBE	ASTM 249 TYPE 347 OR MN-7231	
1	-15	TUBE	5/8 TUBE	ASTM 249 TYPE 347 OR MN-7231	
1	-19	POISON ROD	5/8 ROLLED	ASTM 744 GR 347 OR MN-7232	
1	-11	END	S/S SHEET	ASTM 240 TYPE 347 OR MN-7231	
1	-7	END	S/S SHEET	ASTM 240 TYPE 347 OR MN-7231	
1	-5	CORE TUBE	S/S TUBE	ASTM 249 TYPE 347 OR MN-7231	
1	-3	INNER CLAD	S/S TUBE	ASTM 249 TYPE 347 OR MN-7231	
1	-1	OUTER CLAD	S/S TUBE	ASTM 249 TYPE 347 OR MN-7231	NONE
	-39	POISON ELEMENT ASS'Y.			
	-29	DUMMY ELEMENT ASS'Y.			
	-19	POISON ELEMENT ASS'Y.			
	-9	FUEL ELEMENT ASS'Y.			

PM-1 NUCLEAR POWER PLANT CONTRACT: AT(30-1)-2345

DRAWN	TRACED	DESIGNED	CHECKED	ENGINEER
4/6/61	4/6/61	4/6/61	4/6/61	4/6/61

PM-1 CORE ELEMENTS
FUEL - POISON - DUMMY

THE BARTH COMPANY
BALTIMORE, MARYLAND
NUCLEAR DIVISION

SCALE NOTED

F 372-2105013 SHEET

F 372-2105013 SHEET

E 372-2105013 SHEET

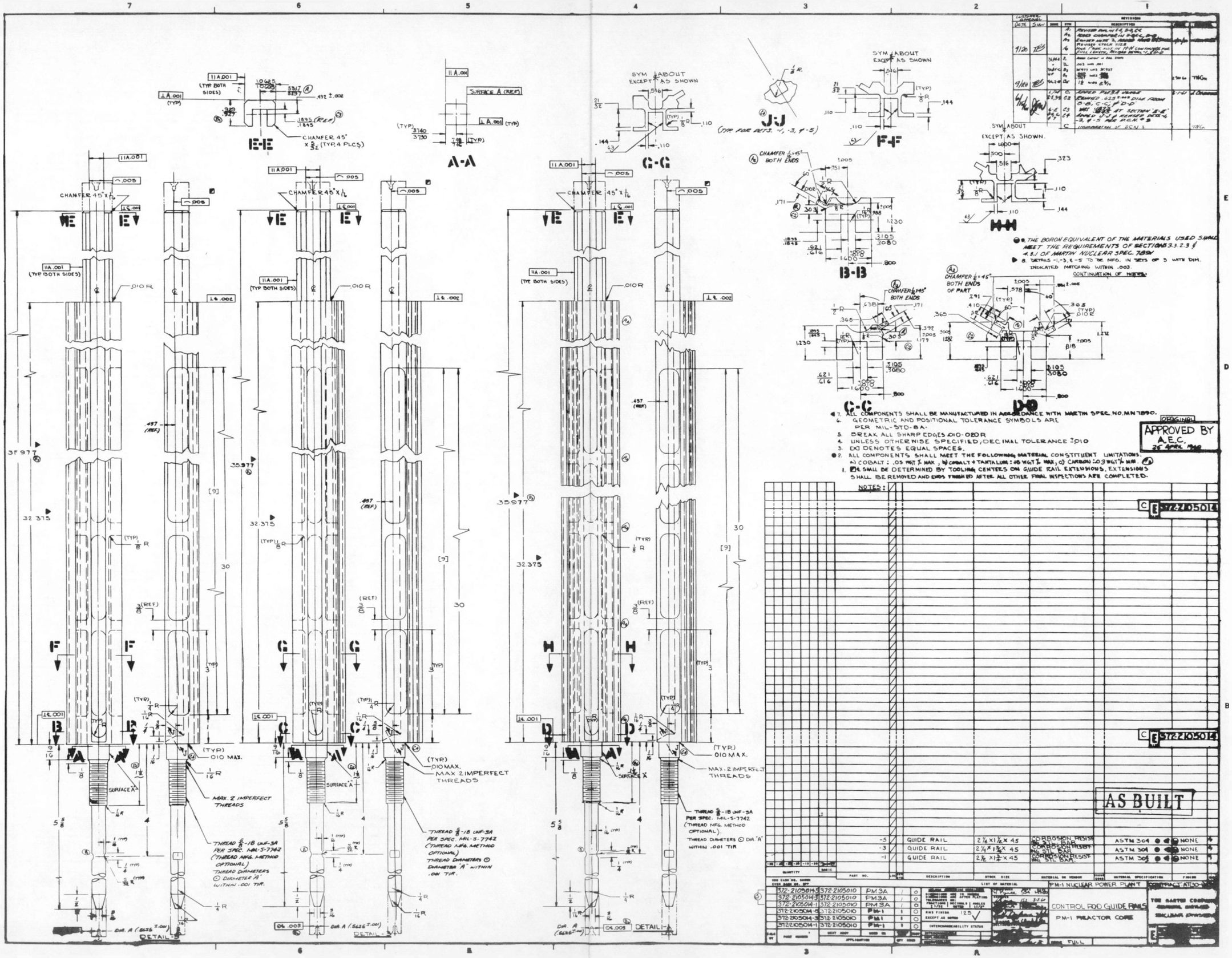
E-E
A-A
G-G
J-J
F-F
H-H
B-B
C-C
D-D
DETAIL "B"
DETAIL "C"
DETAIL "D"
CHAMFER .45° X 5/32 (TYP 4 PLCS)
CHAMFER 45° X 1/16
11A.001
(TYP BOTH SIDES)
.010 R
32.375
35.977
30
(TYP) 010 MAX.
MAX. 2 IMPERFECT THREADS
THREAD 5/8-18 UNF-3A PER SPEC. MIL-S-7742 (THREAD MFG. METHOD OPTIONAL) THREAD DIAMETERS © DIAMETER 'A' WITHIN .001 TIR.
SURFACE A
SURFACE X
DIA. A (.5626 +.001 -.000)
Ø.003 Ⓜ
SYM ABOUT EXCEPT AS SHOWN
(TYP) 1/8 R
.144
.110
.323
.516
.600
.500
.751
.171
.365
.978
.410
.291
.638
.392
1.230
1.272
.621
.616
.3105
.3080
1.6000
.800
.457 (REF)
CHAMFER 1/2 x 45° BOTH ENDS OF PART
CONTINUATION OF NOTES
APPROVED BY A.E.C. 25 APRIL 1960
ORIGINAL
AS BUILT
NOTES:
7. ALL COMPONENTS SHALL BE MANUFACTURED IN ACCORDANCE WITH MARTIN SPEC. NO. MN 7890.
6. GEOMETRIC AND POSITIONAL TOLERANCE SYMBOLS ARE PER MIL-STD-8A.
5. BREAK ALL SHARP EDGES .010-.020 R
4. UNLESS OTHERWISE SPECIFIED, DECIMAL TOLERANCE ±.010
3. (X) DENOTES EQUAL SPACES.
2. ALL COMPONENTS SHALL MEET THE FOLLOWING MATERIAL CONSTITUENT LIMITATIONS: a) COBALT: .05 WGT % MAX, b) COBALT + TANTALUM: .10 WGT % MAX, c) CARBON: .03 WGT % MIN.
1. (E) SHALL BE DETERMINED BY TOOLING CENTERS ON GUIDE RAIL EXTENSIONS. EXTENSIONS SHALL BE REMOVED AND ENDS FINISHED AFTER ALL OTHER FINAL INSPECTIONS ARE COMPLETED.
8. THE BORON EQUIVALENT OF THE MATERIALS USED SHALL MEET THE REQUIREMENTS OF SECTIONS 3.3.2.3.4 & 3.1 OF MARTIN NUCLEAR SPEC. 7891
9. DETAILS -1, -3, & -5 TO BE MFG. IN SETS OF 3 WITH DIM. INDICATED MATCHING WITHIN .003
-5 GUIDE RAIL 2 1/4 X 1 1/2 X 45 CORROSION RESIST MATL BAR ASTM 304 NONE
-3 GUIDE RAIL 2 1/4 X 1 3/4 X 45 CORROSION RESIST MATL BAR ASTM 304 NONE
-1 GUIDE RAIL 2 1/2 X 1 1/2 X 45 CORROSION RESIST MATL STL BAR ASTM 304 NONE
372-2105014-5 372-2105010 PM 3A
372-2105014-3 372-2105010 PM 3A
372-2105014-1 372-2105010 PM 3A
372-2105014-5 372-2105010 PM-1
372-2105014-3 372-2105010 PM-1
372-2105014-1 372-2105010 PM-1
PM-1 NUCLEAR POWER PLANT
CONTROL ROD GUIDE RAILS
PM-1 REACTOR CORE
THE MARTIN COMPANY NUCLEAR DIVISION
372-2105014
372-2105015
AS BUILT

7/20	TBS	5-D	B			
		5-E	B			
7/20	TBS	6-B	B			
			B			
9/20	TBS		C			
		6-D	C			
		6-C	C			
		6-C	C			
			C			
4/21/61	[illegible]		C			
		5-E	C			

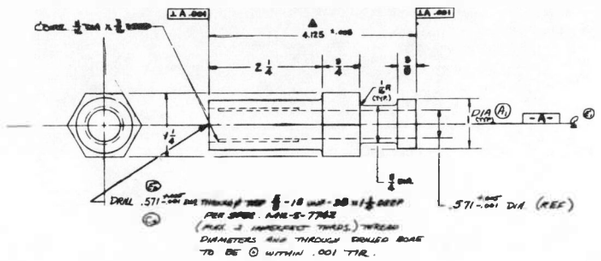

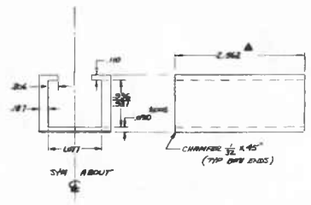

DETAIL -5

DETAIL -1
EXCEPT AS NOTED, ALL DIMS. SHALL BE Ø WITHIN .010 TIR.

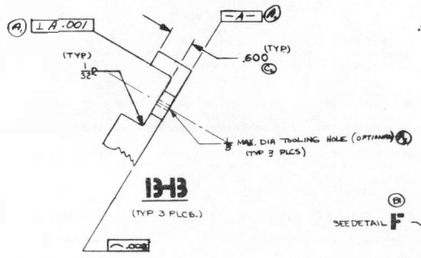

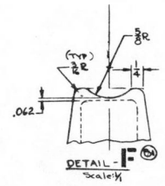

DETAIL -F
Scale 1/1

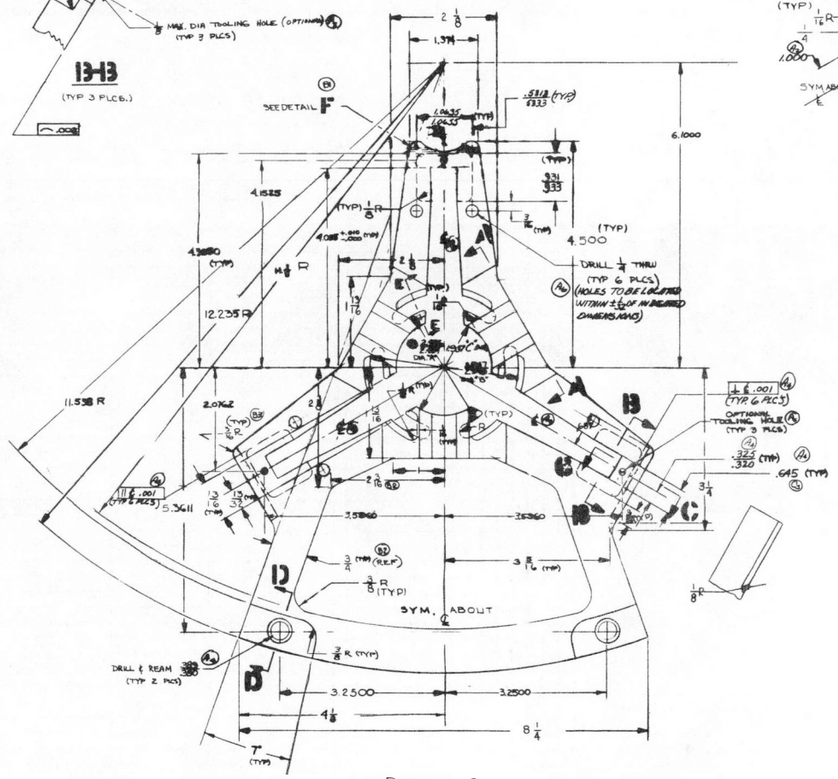

DETAIL -3

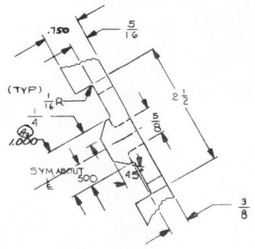

A-A
TYP 3 PLACES

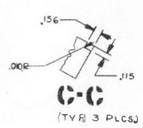

C-C
(TYP 3 PLCS.)

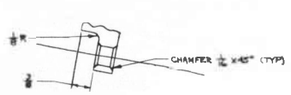

D-D

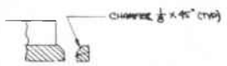

E-E

(C4) 8. NO METAL STAMPS OR MARKINGS SHALL BE PERMITTED ON ANY SECTIONS UNLESS NOTED OR FRAME SPECIFIC APPROVAL HAS BEEN OBTAINED FROM THE PURCHASER.

(4) 7. FIT OF THE -3 DETAIL WITH THE GUIDE TUBE ASSY (372-2105009-29) IN ALL THREE ORIENTATIONS SHALL BE ASSURED THROUGH THE USE OF A SUITABLE INSPECTION FIXTURE AND APPROVED BY THE PURCHASER.

(1) 6 MANUFACTURE PER MARTIN SPEC. MTN 1000.

5. BREAK ALL SHARP EDGES .010 - .020 R.

(C2) 3. UNLESS OTHERWISE SPECIFIED, DECIMAL TOLERANCES ARE AS FOLLOWS:
DIM SHOWN IN THOUSANDTHS : ± .010
DIM SHOWN IN TEN-THOUSANDTHS : ± .0005

(5) 2. DETAILS -1 (-5 TO BE MFG IN SETS OF THREE WHEN DIM. INDICATED ▲ MATCHING WITHIN .001

(3) (6) 1. DIA 'A' & DIA 'B' EACH CONCENTRIC ABOUT DETAIL -1 CENTER .001 TIR. DIA 'C' CONCENTRIC ABOUT DETAIL -3 CENTER .010 TIR.

NOTES:

APPROVED BY A.E.C. 25 APRIL 1960

372-2105015 SHEET

372-2105015 SHEET

AS BUILT

QUANTITY	PART NO.	DESCRIPTION	STOCK SIZE	MATERIAL OR TRADE NAME	SPEC NUMBER	MATERIAL SPECIFICATION	FINISH	REVISION
	-5	SPACER	1 1/2 x 1 1/2 x 4 1/2 Lg	S/S BAR		ASTM 304		(C5)
	-3	ALIGNMENT STRUCTURE	12 x 12 x 5/8 (04)	S/S PLATE		ASTM 304		
	-1	LOCK SLEEVE	1 1/4 HEX x 5 Lg	S/S BAR		ASTM 304		

LIST OF MATERIAL

CALC WT	PART NUMBER	NEXT ASSY APPLICATION	USED ON	QTY REQD	TEST
	372-2105015-5	372-2105010	PM3A	3	0
	372-2105015-3	372-2105010	PM3A	1	0
	372-2105015-1	372-2105010	PM3A	3	0
	372-2105065-5	372-2105010	PM-1	3	0
	372-2105065-3	372-2105010	PM-1	1	0
	372-2105015-1	372-2105010	PM-1	3	0

UNLESS OTHERWISE SPECIFIED: DIMENSIONS ARE IN INCHES. TOLERANCES ON FRACTIONS | DECIMALS | ANGLES ± 1/32 | ± .010 | ± 1°. MATED. RMS FINISH 125 EXCEPT AS NOTED. INTERCHANGEABILITY STATUS: INTERCHANGEABLE, REPLACEABLE, NONCONTROLLED.

PM-1 NUCLEAR POWER PLANT

CONTRACT AT(30-1)-2349

LOCK SLEEVE & ALIGNMENT STRUCTURE

PM-1 REACTOR CORE

THE MARTIN COMPANY BALTIMORE, MARYLAND NUCLEAR DIVISION

SCALE FULL

DWG E 372-2105015 SHEET

CODE 38081

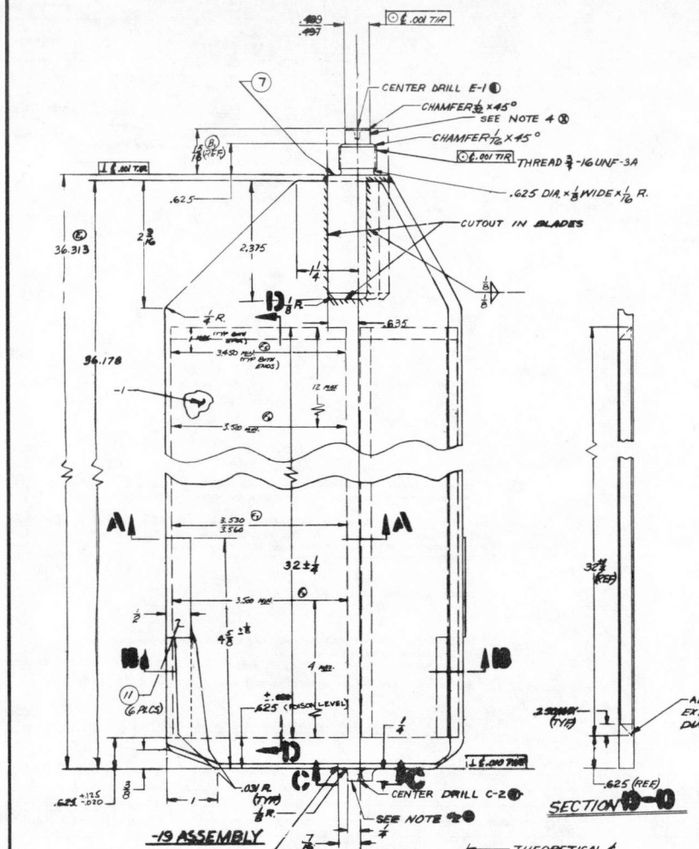

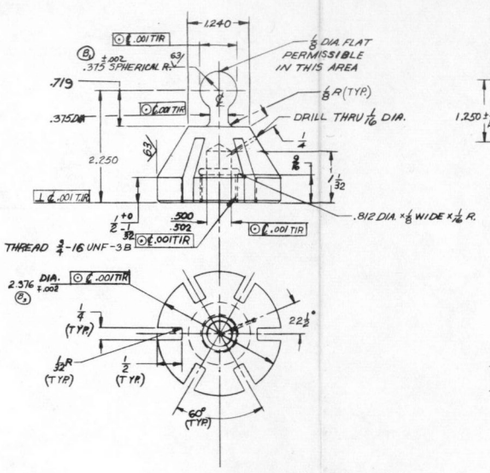

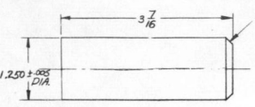

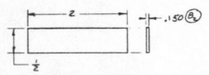

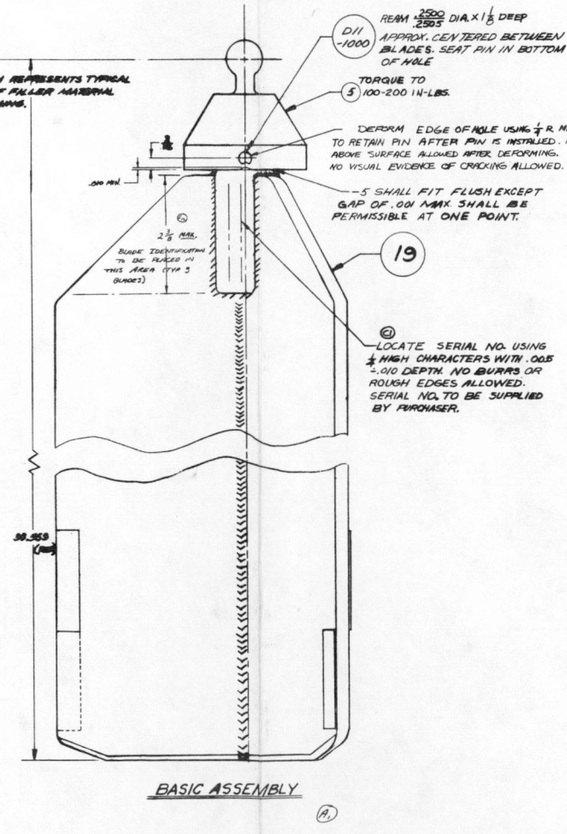

NOTES:

1. ● THESE CENTERS TO BE LOCATED ON TRUE CENTERLINE AS ESTABLISHED AFTER WELDING OF BLADES ℄-7
2. ● THIS LUG TO BE GROUND OFF FLUSH WITH BOTTOM OF CONTROL ROD AFTER FINAL INSPECTION OF ASS'Y BY PURCHASER.
3. DECIMAL TOLERANCE ±.010 UNLESS OTHERWISE NOTED.
4. ● THIS END TO BE MACHINED TO TRUE ℄ AS ESTABLISHED BY NOTE 1.
5. ● THEORETICAL ℄'S ARE DEFINED BY THREE PLANES ANGULARLY SPACED AT EXACTLY 120° ANGULAR ALIGNMENT OF THE ROD BLADES IS DETERMINED BY THE DIMENSION FROM THESE THEORETICAL ℄'S. (SEE SECTION B-B.)
6. ▲ CHAMFER IN THIS AREA TO BE MACHINED AFTER LUG IS GROUND OFF PER NOTE 2. AFTER LUG IS GROUND OFF SEAL WELD BOTTOM OF CONTROL ROD (SEE SECTION C-C.)
7. ■ BRAZE WITH COAST METALS N.P. OR EQUIVALENT AS APPROVED BY PURCHASER. BRAZING PROCESS & SAMPLES TO BE PER NOTE 8. BRAZE PROCESS SHALL GIVE 100% PENETRATION.
8. ANNEAL -19 AFTER WELDING.
9. CONTROL RODS TO BE FABRICATED TO MARTIN NUCLEAR SPEC. 7893. EACH BLADE OF THE CONTROL ROD SHALL CONTAIN FROM 752.5 TO 757.7 GMS B_4C. THE EUROPIUM CONTENT PER CONTROL ROD SHALL AVERAGE 790 GMS MIN PER BLADE, AVERAGED OVER 3 BLADES.
10. BREAK ALL EDGES OF CONTROL ROD ASS'Y .020 TO .040 R.
11. * STOCK SIZE OF THESE PARTS TO BE DETERMINED BY MANUFACTURER.
12. ● INERT ARC WELD FULL LENGTH OF BLADE, USING TYPE 348 FILLER ROD AS REQ'D. TO DIMENSIONS SHOWN - WELD ZONE SHALL NOT EXTEND INTO (-1) POISON MATERIAL. WELDS SHALL BE FREE FROM POROSITY AND TUNGSTEN INCLUSIONS WITH NO EVIDENCE OF DEFECTS WHEN EVALUATED BY VISUAL AND LIQUID PENETRANT METHODS. WELDING PROCESSES TO BE PER NOTE 9.
13. ALL DIMENSIONS APPLY AFTER FINAL HEAT TREAT PROCESS.
14. THE FOLLOWING SHALL BE USED AS REQUIRED FOR LUBRICATION AT ASS'Y OF CLOSE FITTING PINS, THREADS, OR DOWELS:
    COLLOIDAL GRAPHITE DISPERSED IN ALCOHOL OR PURE WATER AT MFGR.'S APPROVED VENDORS. (12)
15. ● -11 WEAR PADS AND -5 CAP SHALL BE AGE HARDENED ACCORDING TO A PURCHASER APPROVED SPECIFICATION AT 1040 ± 10 °F TO PROVIDE AN ULTIMATE TENSILE STRENGTH OF FROM 150,000 TO 170,000 PSI WITH A MINIMUM ELONGATION OF 15% IN 2" OR 4 x DIA. TEST BARS ARE REQUIRED. (12)

CUSTOMER APPROVAL		REVISIONS			
DATE	SIGN	ZONE	SYM	DESCRIPTION	DATE	APPROVAL
9/16/60	[illegible]	4-A	A	REVISED THE RELEASE TO AEC	3/18/60	T.W. Cox
		8/M	A1	REMOVED PRELIMINARY NOTE		
		8/M	A2	ELIM. COMMERCIAL MIX. Eu_2O_3		
		6-3	A3	WAS 5/16, NOW .3105 ± .003; WAS .370 MIN. NOW .375 MIN.		
		7&7A	B1	ADDED REF. TO 1/16 DIAM., ADDED TOLERANCE		
9/19/60	[illegible]	7-D	B2	.150 WAS .140	9/22/60	W. BETHUNE
		7-E	B3	2.376 DIA WAS 2.360 DIA	9/22/60	T.W. COX
9/19/60	[illegible]	7-C	C1	ELIM. WORDING LOCATE PINS RUNOUT .005-.010 WAS .010 MAX.	9/23/60	L.A. BENJAMIN
		8/M	C2	1/16 WAS 1/16 ± .2439 DIA WAS 3 DIA		
11/1/60	[illegible]	NOTE 9	D1	ELIM. NOTE 9	2/28/61	T.W. COX
		2	D2	ADD NOTE 15, NOTES 12 & 14		

CUSTOMER APP.		REVISIONS			
DATE	SIGN	ZONE	SYM	DESCRIPTION	DATE	APPROVAL
11/24/60	[illegible]	7-E	E1	3C 313 WAS 3C 303	11/24/60	T.W. COX
12/16/60	[illegible]	7-F, 7-G, 7-H	F1	ADDED PIN 3.4 LOCATE	6-1-61	[illegible]
		7-G	F2	REVISED NOTE 15, LIST OF MATERIAL & A-A PER EC 42		
		NOTE 15	F3	REVISED NOTE 15		T.W. COX
		NOTE 14	F4	ADDED NOTE 14		
12/16/60	[illegible]	7-E	F1	ADDED DWG. AND PIN NUMBERS	12-16-60	T.W. COX
		7-D	F2	ADDED 1.150 MIN.		
		7-D	F3	ADDED .1375/.1350		
		7-B	F4	ADDED .5 R & .781 (REF)		
		7-A	F5	ADDED .281/.280 & .266/.260		T.W. COX

												LUBRICANT		DAG-154 (or Equiv.)	
			1				D11-1000					DOWEL PIN		PIC DEGUSSA CORP. FOR ROCKWELL U.S.A.)	(OR EQUIVALENT)
12	2								-13			COVER	14	5/5 PLATE	ASTM 347 (See NOTE 9)
		3							-11			PAD	1/4 DIA x 2 1/2	17-4 PH 5/5 BAR	AMS 5643
			1						-7			STUD	1 1/4 DIA x 5	5/5 RND BAR	ASTM 347
				1					-5			CAP	2 1/2 DIA x 3	17-4 PH 5/5 BAR	AMS 5643
1									-3			CORE FRAME & COVER	14	5/5 PLATE	ASTM 347 (See NOTE 9)
1									-1			CORE (POISON)	14	Sintered Powder Disperion in Type 304L Powder	SEE NOTE 9
	1								-39			BLADE ASSY.			
		3							-29			BRACKET ASSY.			
			1						-19			WELDED ASS'Y			
												CONTROL ROD ASS'Y			

-39	-29	-19	-5	-1	QUANTITY
			BASIC		

000 DASH NO. SHOWN / EVEN DASH NO. OFF	PART NO.	LOCATION	DESCRIPTION	STOCK SIZE	MATERIAL OR VENDOR	ASTM NO.	MATERIAL SPECIFICATION	FINISH	SCALE
			LIST OF MATERIAL						

UNLESS OTHERWISE SPECIFIED: DIMENSIONS ARE IN INCHES. DIMENSIONS ARE AFTER PLATING. TOLERANCES ON: FRACTIONS ± 1/32, DECIMALS ± .005, ANGLES ± 1°. RMS FINISH EXCEPT AS NOTED 125. INTERCHANGEABILITY STATUS: INTERCHANGEABLE / REPLACEABLE / UNCONTROLLED.

CALC WT	PART NUMBER	NEXT ASSY	USED ON	ASSY QTY	TEST QTY	REQD
	372-2105016	372-2105010	PM-1	1	0	
	372-2105016	372-2105010	PM-1	1	0	

APPLICATION

ORIGINAL
APPROVED BY A.E.C
25 APRIL 1960

AS BUILT

PM-1 NUCLEAR POWER PLANT CONTRACT AT(30-1)

CONTROL ROD ASS'Y
PM-1 REACTOR CORE

THE GLENN L. MARTIN COMPANY
BALTIMORE, MARYLAND
NUCLEAR DIVISION

SCALE NONE

SIZE E 372-2105016 REV

SHEET

REVISIONS						
ZONE	LTR	DESCRIPTION	DATE	APPROVED
	A	RELEASED ISSUE, PER E ORDER [illegible]	7/20	[illegible]
	B	REVISED SPACER, NOTE 5 & SHEET 2	7/20	[illegible]
	C	ADDED NOTE 6, REVISED NOTE 4	10/26	[illegible]
	D	ADDED TEMPERATURE, NOTE 8 & NOTE 6, DIMENSIONAL NOTE 9 & 10	1/26	[illegible]
	E	ADDED MAT'L SPEC CHANGE PER REV. E ORDER NOTE 1 & ADDED NOTE 7 PER ECN 42	4/1/26	[illegible]
	F	CHANGED NOTE 4 & 7 PER ECN 43	6/26	[illegible]

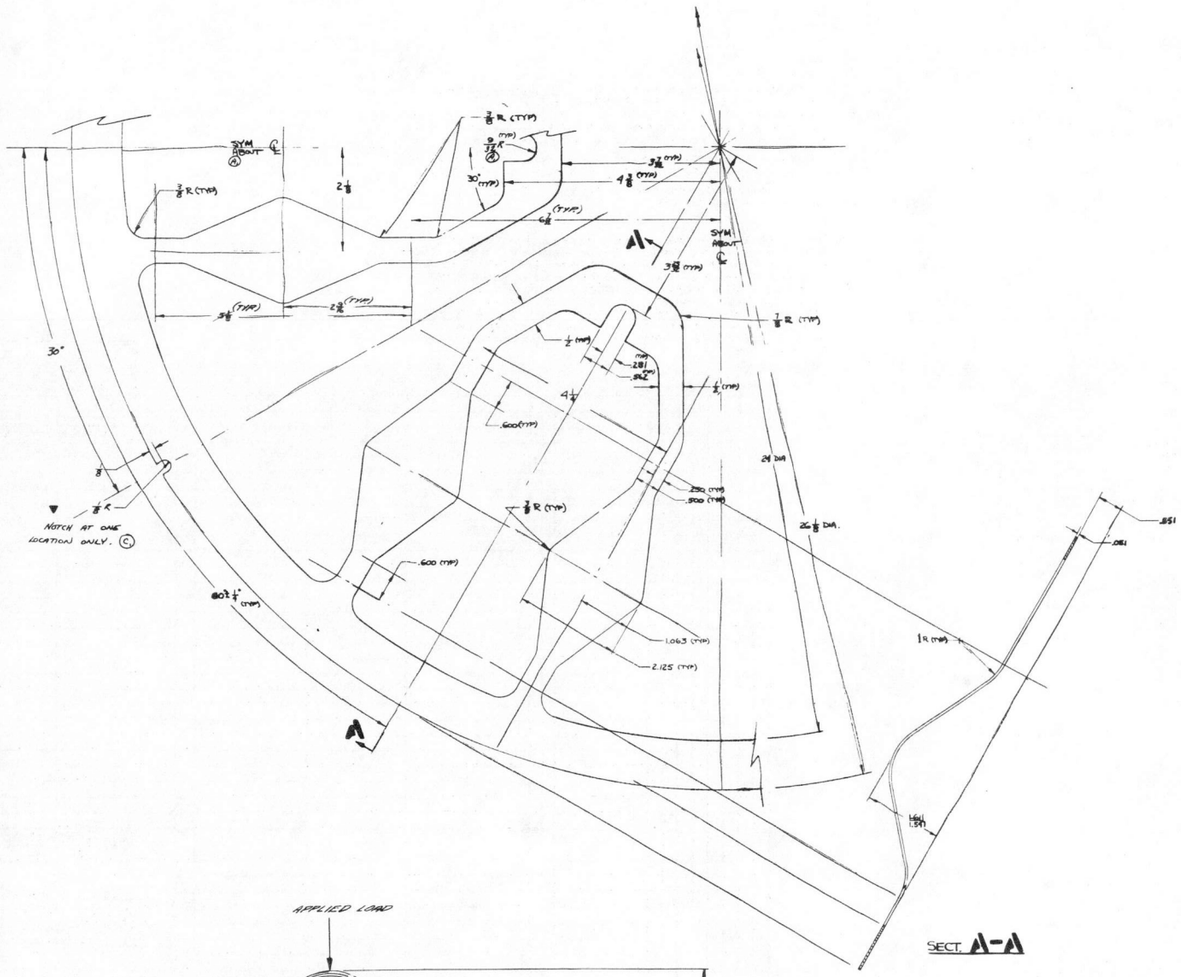

(8) TEST SCHEMATIC

NOTES:

(12) 7. AFTER FABRICATION, AREAS HAVING FORMED BENDS SHALL BE INSPECTED BY FLUORESCENT PENETRANT INSPECTION.

(C) 6. TWO SPRINGS SHALL BE STACKED FOR TESTING AND FINAL ASSEMBLY IN 372-2105008 UPPER SKIRT. THE VARIANCES IN SPRING OUTSIDE DIAMETERS SHALL BE MATCHED WHEN STACKING.

(A) 5. NO METAL SHAPES OR MARKINGS SHALL BE PERMITTED ON ANY SURFACES UNLESS NOTED OR PRIOR SPECIFIC APPROVAL HAS BEEN OBTAINED FROM THE PURCHASER.

(8)(C) 4. AFTER MANUFACTURING AND INSPECTION, MATCHED SPRING SETS SHALL BE TESTED IN ACCORDANCE WITH TEST SCHEMATIC. MEASURE SPRING RATE USING 80# PRELOAD AND .250 DEFLECTION. RATE SHOULD BE 340 ± 12% #/IN. SPRING SET SHALL NOT BE DEFLECTED MORE THAN .500 RESULTS OF TESTS SHALL BE SUBMITTED TO MARTIN NUCLEAR ENGINEERING DEPT.

3. DECIMAL TOLERANCES ± AND UNLESS OTHERWISE NOTED.

(C) 2. SPRINGS TO BE MANUFACTURED AS A MATCHED PAIR AS DISTINGUISHED BY NOTCHES.

(12) 1. AFTER FORMING, SPRINGS SHALL BE AGED PER AMS 5542 TO THE FOLLOWING MINIMUM REQUIREMENTS: .2% YIELD STRENGTH PSI – 150,000 ULTIMATE TENSILE STRENGTH PSI – 185,000

ORIGINAL
APPROVED BY A.E.C.
25 APR 1960

D E 372-2105017 SHEET

D E 372-2105017 SHEET

QUANTITY	PART NO.	DESCRIPTION	STOCK SIZE	MATERIAL OR VENDOR	MATERIAL SPECIFICATION	FINISH
-30 -40 -25 -30 -15 -20 -5 -10 BASIC		SPRING	.28 (.28 x .051	INCONEL "X" (ONE PIECE) & ALL ANNEALED	AMS 5542	AS BUILT

LIST OF MATERIAL

ODD DASH NO. SHOWN
EVEN DASH NO. OFF

CALC WT	PART NUMBER	NEXT ASSY APPLICATION	USED ON	QTY REQD
	372-2105017	372-2105004-7	PM-2A	2
	372-2105047	372-2105004-7	PM-1	2

FINAL ASSY TEST

UNLESS OTHERWISE SPECIFIED DIMENSIONS ARE IN INCHES. DIMENSIONS ARE AFTER PLATING. TOLERANCES: FRACTIONS 1/32, DECIMALS .XX ±.02, .XXX ±.010, ANGLES ±1/2°
RMS FINISH EXCEPT AS NOTED ✓
INTERCHANGEABILITY STATUS
INTERCHANGEABLE
REPLICABLE
UNCONTROLLED

SPECIFICATIONS	REV'D	DATE
TITLE		
DRAWING	183	10/26
STYLE/SIZE/FORM		
MATERIAL		
SPECIAL REQUIREMENTS		
SPECIFICATION REVISIONS		

Bill Hopkins 3/6/26
Chas L. Hall 3/6/26
Robert Hall 3/6/26
SCALE FULL SIZE

PM-1 NUCLEAR POWER PLANT
CONTRACT: AT(30-1)-2348

SPRING, HOLD DOWN, UPPER SKIRT
PM-1 REACTOR CORE

THE MARTIN COMPANY
BALTIMORE, MARYLAND
NUCLEAR DIVISION

DOC E 372-2105017 SIZE SHEET
CODE 30697

372-0795/09

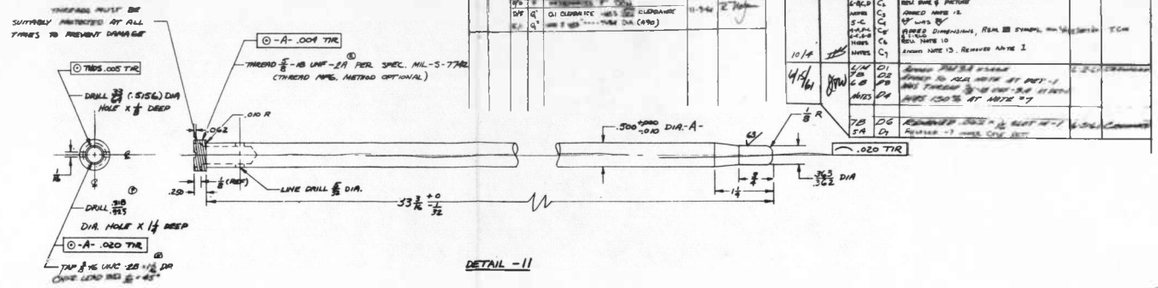

DETAIL -11

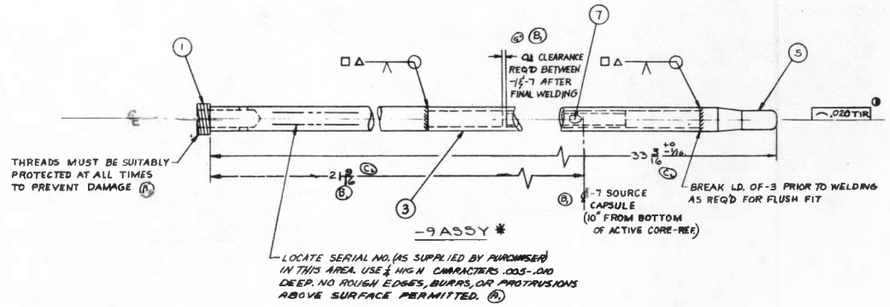

-9 ASSY *

NOTES :-

(A) 14. LUBRICATE ALL THREAD BEARING AREAS WITH COLLOIDAL GRAPHITE (DISPERSED IN ALCOHOL OR PURE WATER) AS MFG. BY APPROVED VENDORS.

(C7) △13 THE -9 SOURCE SHALL BE USED FOR THE INITIAL 372-2105005 ASS'Y ONLY. THE -11 DUMMY SOURCE SHALL BE USED FOR SUBSEQUENT 372-2105005 ASS'YS OR AS SPARE PARTS FOR EITHER THE INITIAL OR SUBSEQUENT ASS'YS.

(C) 12. NO METAL STAMPS OR MARKINGS SHALL BE PERMITTED ON ANY SECTIONS, UNLESS NOTED OR PRIOR SPECIFIC APPROVAL HAS BEEN OBTAINED FROM THE PURCHASER.

11. ALL EXTERNAL DIMENSIONS SHALL BE RECHECKED AFTER COMPLETION OF THE -9 ASSY.

(B)

*10. THE SOURCE CAPSULE(-7) SHALL CONTAIN A POLONIUM-BERYLLIUM (Po-Be) NEUTRON SOURCE. A SOURCE STRENGTH OF 15 CURIES IS REQUIRED AT REACTOR START-UP. THE DESIGN SOURCE STRENGTH AT THE REQUIRED DELIVERY DATE TO THE PURCHASER SHALL BE SPECIFIED IN THE ORDERING DATA. THE SOURCE SHALL BE DESIGNED TO WITHSTAND A MAX. TEMPERATURE OF 1250 °F. OUTER CASE SHALL BE FABRICATED FROM ASTM 304L MATERIAL. INNER CASE MATERIAL IS OPTIONAL (AS REQUIRED TO MEET TEMPERATURE LIMITATIONS). FINAL MATERIAL SELECTED AND DIMENSIONS NOT SPECIFIED SHALL BE SUBMITTED TO AND APPROVED BY THE CONTRACTOR PRIOR TO FABRICATION.

(B) (C)

NOTES (CONT.) :-

▼ 9. DETAILS -1, -3 & -5 SHALL HAVE MATERIAL CONSTITUENT LIMITATIONS AS FOLLOWS: COBALT: .05 WGT % MAX., (COBALT + TANTALUM: .15 WGT % MAX.); (A4) CARBON: .03 WGT % MIN.;

(B) & (C) OF -9 ASSY SHALL BE ESTABLISHED BY DIA'S -A- & -B- ON DETAILS -1 & -5, RESPECTIVELY.

□ 7. (A4) INERT ARC WELD — 105 % MINIMUM PENETRATION REQUIRED. WELD PROCEDURE & SAMPLES TO BE APPROVED BY PURCHASER. ALL WELDS SHALL BE VISUALLY AND LIQUID PENETRANT INSPECTED AFTER FABRICATION. WELDING AND INSPECTION PROCEDURES, TECHNIQUES AND MATERIALS SHALL BE IN ACCORDANCE WITH MARTIN SPEC. NO. MN-2005.

6. HELIUM LEAK CHECK AFTER WELDING. PROCEDURE TO BE SUBMITTED TO MARTIN CO. FOR APPROVAL. CHAMBER SHALL BE FILLED WITH HELIUM DURING FINAL WELDING AND THEN LEAKED CHECKED AT 14 PSI Δ P. MAX PERMISSIBLE LEAK RATE TO BE 10^{-9} STD CC/SEC.

(A4) △ 5. AFTER WELDING, MACHINE WELD REGION IF REQUIRED, TO MAINTAIN TUBE DIA. .500 +.000 -.010.

4. ALL PARTS SHALL BE MFG. TO MEET THE REQUIREMENTS OF MARTIN SPEC. MN 7890.

3. DECIMAL DIMENSION TOLERANCE ±.010 UNLESS OTHERWISE NOTED.

2. BREAK ALL SHARP EDGES .010 -.020 R EXCEPT AS NOTED

1.

(C7)

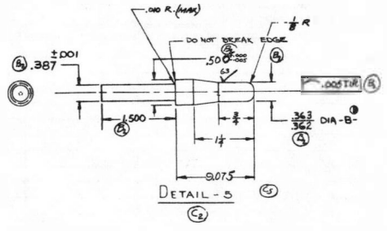

DETAIL -5 (C2)

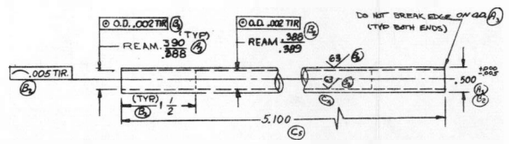

DETAIL -3

THIS DETAIL SHALL BE SUFFICIENTLY STRAIGHT AS TO ALLOW THROUGH PASSAGE OF A PLUG (B) .3870 DIA (MIN) BY 2.1 LONG.

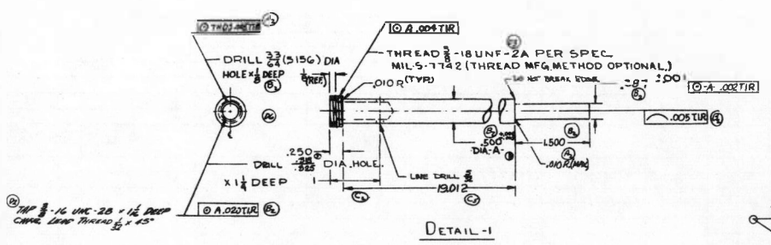

DETAIL -1

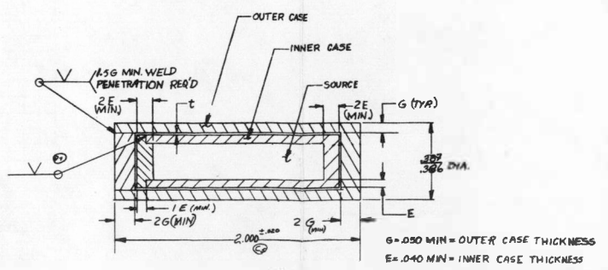

G = .030 MIN = OUTER CASE THICKNESS
E = .040 MIN = INNER CASE THICKNESS
t = .001 MAX. = RADIAL CLEARANCE

DETAIL -7 (A)

APPROVED BY AEC 25 APRIL 1960

AS BUILT

QUANTITY	PART NO.	DESCRIPTION	STOCK SIZE	MATERIAL OR VENDOR	MATERIAL SPECIFICATION	FINISH	REV
1	-11	DUMMY SOURCE	3/8 DIA x 36 LG	S/S RND BAR	ASTM 304 ▼	NONE	(C)
1	-7	SOURCE CAPSULE				*	
1	-5	GUIDE STUD	1/2 DIA X 12 LG	CORROSION RESISTING STL. BAR	ASTM 347 ▼	NONE	4/2
1	-3	CAPSULE CASE	3.00 DIA x .134 WALL x 6 LG	CORROSION RESISTING STAINLESS STEEL TUBING	ASTM 347 ▼	NONE	8/4
1	-1	LOCK STUD	1/2 DIA X 2.2 LG	CORROSION RESISTING STL. BAR	ASTM 347 ▼	NONE	5/4

LIST OF MATERIAL

372-2105018-11	372-2105005	PM-3A	△	0	
372-2105018-9	372-2105005	PM-3	1	0	
372-2105018-11	372-2105005	PM-1	△	0	
372-2105018-9	372-2105005	PM-1	1	0	

PM-1 NUCLEAR POWER PLANT CONTRACT AT(30-1)-1594

SOURCE (PRIMARY) PM-1 REACTOR CORE

THE MARTIN COMPANY BALTIMORE, MARYLAND NUCLEAR DIVISION

E 372-2105018

372-075/86

372-075/04 372-075/03 372-075/00

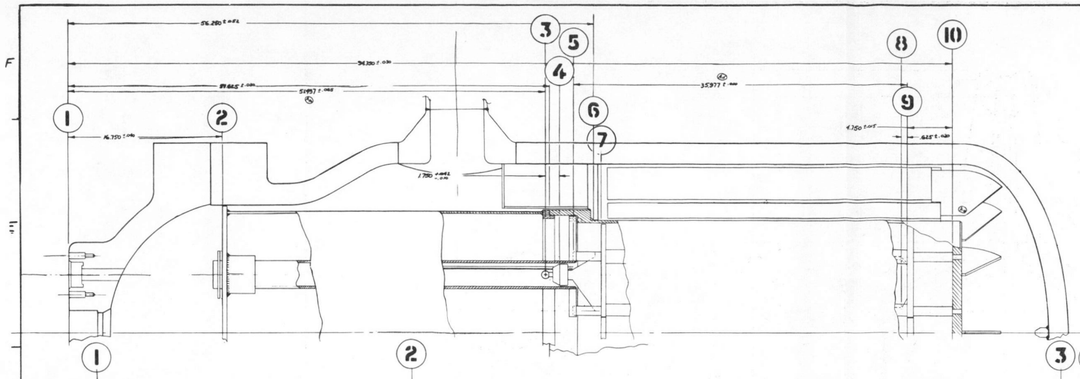

CONFORMS TO ATTRIBUTE		REVISIONS			
QA'S	C-M'S	ZONE	SYM	DESCRIPTION	DATE	APPROVED
			A	ZONES 7 & 8		
			A_1	ADD "ON ASSY" ; ADD "ON ASSY"		
			A_2	MOUNTING PAD THICKNESS "A" ; "A" AND "B"		
			A_3	54-10.447 / 53.60 NOM ; 54.2378 to 54.278		
			A_4	ADD 1.625		
			A_5	ADD 1.625		
			A_6	ADD .007		
			A_7	CHANGE "NOM" TO "EQUAL SPACE"		
			A_8	DIM .472		
			A_9	.750 DIM .250		
		E-6	A_{10}	REMOVE THICK DIMENSION		
		E-6	A_{11}	ADD .750 DIM		
			A_{12}	.250 DIM .500		
			A_{13}	ADDED .75 DIM, REVISED DIMENSION		
			A_{14}	.625 DIM .625		
		F-8	A_{15}	32.777 DIM 32.927		
		F-8	A_{16}	21.937 DIM 21.987	12 JUNE 64	12 JUNE 64
				ADD D	11/66	11/66

STATION 1
POINT 1 A. TRUE PILOT ℄ VS. THEOR. ℄ .035 Ⓔ
B. ACTUATOR ℄ VS. PILOT ℄ .005 Ⓔ

STATION 2 GUIDE TUBE I.D. LOCATION, UPPER END
POINT 1 A. RADIAL CLRNC., SKIRT ASSY VS. VESSEL CNTR. DIA .0095
B. GUIDE TUBE HOLE LOCATIONS VS. SKIRT ASSY CENTER .001
C. RADIAL CLRNC. TUBE O.D. VS. SKIRT HOLES .006 DIAM .007 Ⓔ
D. CONCENTRICITY, TUBE O.D. VS. TUBE I.D. .005" TIR DIA. .0025

STATION 3 CONTROL ROD PICKUP BALL LEVEL
POINT 1 EXPECTED MISALIGNMENT, ACTUATOR ROD ℄
A. PILOT LOCATION FROM STATION 1 .0035
B. ACTUATOR DEFLECTION AT MAX. EXTENSION DUE TO .001 TIR ℄ MOUNTING FLANGE TO PILOT ℄ .010 Ⓔ
C. MAX. EXPECTED FIXED RUNOUT (ENERGIZED CONDITION) OF ACTUATOR CLAMP CENTER PER TRADCO DWG. 574-10745 1-21-66 , INCLUDES .005 OFFSET AT PILOT HOLE ℄ PERPENDICULARITY OF ACT. BODY FLANGE TO ACT. ARMATURE HSG. .0214 Ⓔ
D. DEFLECTION DUE TO PRESSURE VESSEL HEAD .025
POINT 2 MAX. POSSIBLE MISALIGNMENT, ACT. ROD ℄
A. SUM OF A, B, D. ABOVE .0385
B. MAX. RUNOUT ACT. ℄ DUE TO MFG. TOLERANCES .0387 Ⓐ
POINT 3 CONTROL ROD PICKUP BALL CENTER AT POSITION OF MAX ACT. ROD BENDING — PROJECTION OF LINE BETWEEN STA 4 PT 2 ℄ STA 8 PT 3.

STATION 4 CONTROL ROD GUIDE RING LEVEL
POINT 1 PROJECTION OF CONTROL ROD ℄ DETERMINED BY STA 7 PT 3 ℄ STA 8 PT 2.
POINT 2 DETERMINED BY GUIDE RING VS. GUIDE TUBE CLEARANCE
POINT 3 MAX. DEFLECTION OF CONTROL ROD GUIDE RING BEFORE ASSEMBLY OF GUIDE TUBE (PROJECTION OF LINE BETWEEN STA 7 PT 4 ℄ STA 8 PT 2)

STATION 5 UPPER ALIGNMENT STRUCTURE LEVEL
POINT 1 PROJECTION OF CORE SHROUD ℄ BETWEEN STA 6 PT 1 ℄ STA 10 PT 1
POINT 2 ALIGNMENT STRUCTURE LOCATION (PT 1 = PREVIOUS)
A. LOCATION OF SHROUD CENTER W/RESP TO DIA 'A' ON SHROUD .001
B. ALIGNMENT PIN LOCATION W/RESP TO CORE SHROUD ℄ .001
C. CLRNC, ALIGNMENT PINS VS. STRUCTURE INSERTS .0015 DIA
D. ALIGNMENT STRUC. HOLES W/RESP TO STATIC CENTER .001
POINT 3 GUIDE TUBE LOWER POSITIONING (PT 2 = PREVIOUS)
A. CONCENTRICITY, TUBE I.D. VS TUBE O.D. (MAT'L A) .0025
B. CLRNC, STRUC CENTERING DIA VS. GUIDE TUBE O.D. .0065 DIA .0065 Ⓔ
C. CONCENTRICITY, CENTERING DIA TO STRUC. CENTER .0005
POINT 4 GUIDE RAIL POSITIONING (PT 2 = PREVIOUS)
A. GUIDE RAIL SOCKET POSITION VS. ALIGNMENT STRUC. CENTER .002
B. CLRNC, GUIDE RAIL SOCKET VS. GUIDE RAIL .0035
C. GUIDE RAIL SLOT CENTER VS. REAME SURFACES OF RAIL ENDS. .005

STATION 6 VESSEL ORIFICE PLATE LEVEL
POINT 1 CLRNC, CORE SHROUD VS. ORIFICE PLATE .005 DIAM .0035 Ⓔ

STATION 7 UPPER GRID LEVEL
POINT 1 INTERSECTION OF BUNDLE ℄ PROJECTED BETWEEN STA 5 PT 4 ℄ STA 10 PT 2
POINT 2 MINIMUM DISTANCE THAT CONTROL ROD CAN MOVE FROM BUNDLE ℄ BEFORE CONTACTING UPPER GRID .110 Ⓐ
POINT 3 CONTROL ROD PLAY MAX DESIGN ALLOWABLE FROM BUNDLE ℄ TO CLRNC UPPER GRID .094 Ⓐ
POINT 4 MAX DISPLACEMENT OF CONTROL ROD AT UPPER GRID LEVEL (FROM PT 1) .195 Ⓐ

STATION 8 CONTROL ROD WEAR PAD LEVEL
POINT 1 INTERSECTION OF BUNDLE ℄ BETWEEN STA 10 PT 2 ℄ STA 5 PT 4
POINT 2 MAX MOVEMENT OF CONTROL ROD ABOUT BUNDLE ℄ .075
POINT 3 MAX MOVEMENT OF CONTROL ROD ABOUT BUNDLE ℄ .049

STATION 9 LOWER GRID LEVEL

STATION 10 BUNDLE LOCATION
POINT 1 A. OFFSET OF CORE SHROUD BOTTOM DUE TO CLRNC ORIFICE PLATE VS. CORE SHROUD .0035
B. OFFSET OF CORE SHROUD BOTTOM DUE TO PERPENDICULARITY OF SHROUD ℄ ORIFICE PLATE W/RESP TO VESSEL ℄ = .004
POINT 2 (PT 1 = PREVIOUS)
A. OFFSET OF BUNDLE ℄ DUE TO CLRNC. BETWEEN AND RELATIVE POSITIONS OF GUIDE RAILS ℄ CORE SHROUD HOLES. .009

A J 372-2105015

B J 372-2105015

LETTERED DIMENSIONS:
Ⓐ A=.024 MINIMUM CLEARANCE BETWEEN CONTROL ROD AND UPPER GRID ASSUMING MAX CONTROL ROD DEFORMATION (UPPER GRID MISALIGNMENT.
Ⓑ B=.062 +.002 -.000 CLEARANCE BETWEEN CONTROL ROD GUIDE RING, AND GUIDE TUBE I.D.
C=.202 MAX MISMATCH BETWEEN ACTUATOR LATCH ℄ ℄ CONTROL ROD BALL ℄ AT BALL PICK-UP.
D=.066 MAX. ACTUATOR ROD BENDING. THIS BENDING ~~DEFLECTION~~ TO ZERO AS CONTROL ROD IS WITHDRAWN 30 INCHES.
Ⓔ E=.260 MAX OFFSET OF CONTROL ROD PICKUP BALL FROM THEORETICAL ℄ BEFORE SKIRT ASSY WITH GUIDE TUBE IS ASSEMBLED OVER CORE.

AS BUILT

CALC WT	DASH NUMBER	NEXT ASSY	FINAL ASSY
Ⓑ	387-2105 000	PM-1	1
Ⓐ	575-2105 000	PM-1	1

ASSD ON APPLICATION

PM-1 NUCLEAR PLANT — 372-2105-01

ALIGNMENT STUDY

PM-1 REACTOR CORE

THE BABCOCK COMPANY BARBERTON, OHIO NUCLEAR DIVISION

J 372-2105015 SHT

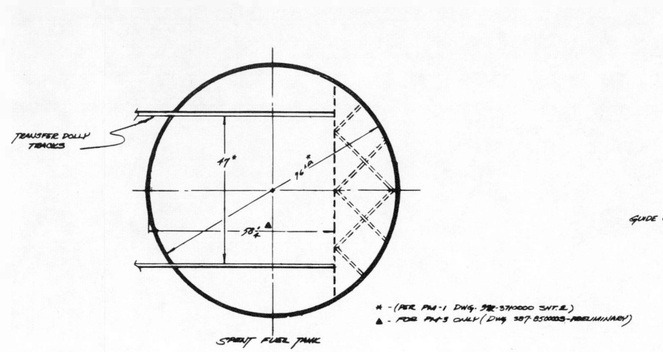
TRANSFER DOLLY TRACKS
47°
14"
33½ ▲
STARLIT FUEL TANK
H - (REF. FIG-1, DWG. 372-5710000 SHT. 2)
▲ - FOR FIG-3 ONLY (DWG. 387-8510005-PRELIMINARY)

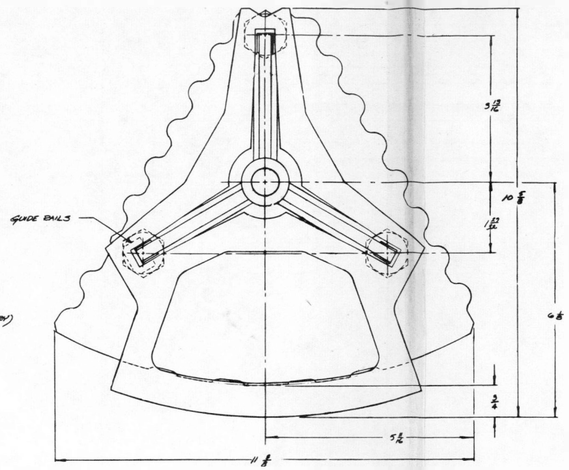
GUIDE RAILS
5 13/16
10 5/8
1 13/16
6 5/8
3/4
5 1/16
11 3/8

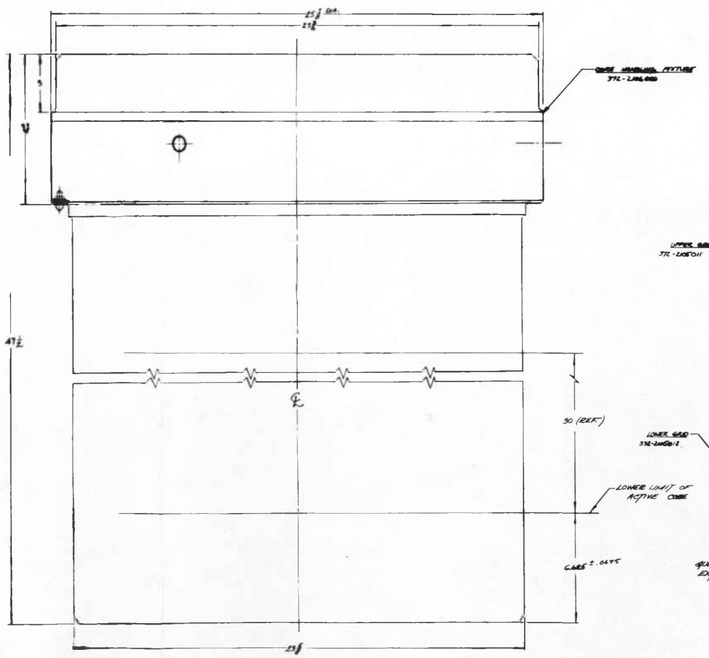
CORE SAMPLING FIXTURE 372-1240000
5
47½
50 (REF.)
LOWER LIMIT OF ACTIVE CORE
CORE ≈ 0495
CORE SAMPLING - 372-1207000

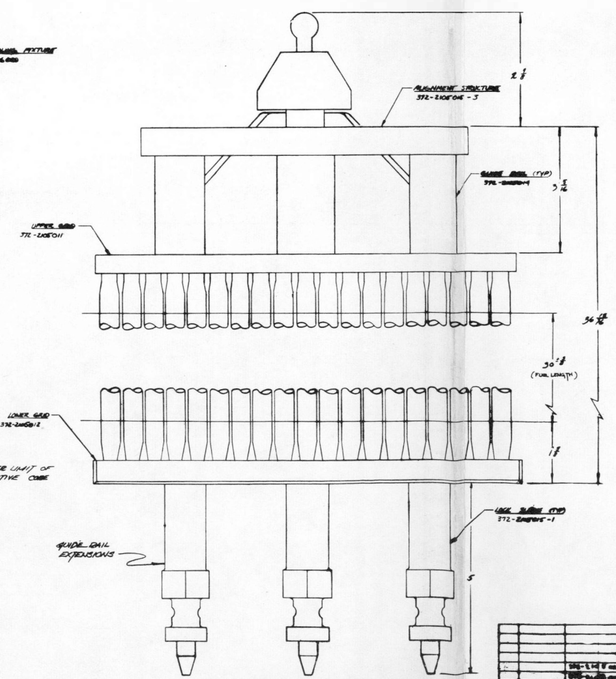
ALIGNMENT STRUCTURE 372-2105040 - 3
GUIDE RAIL (TYP) 372-2105041
UPPER GRID 372-2105011
LOWER GRID 372-2105012
GUIDE RAIL EXTENSIONS
LOCK BUSHING (TYP) 372-2105042 - 1
5 1/2
34 7/8
30 1/8 (FUEL LENGTH)
1 1/8
5
PERIPHERAL BUNDLE - 372-2105020

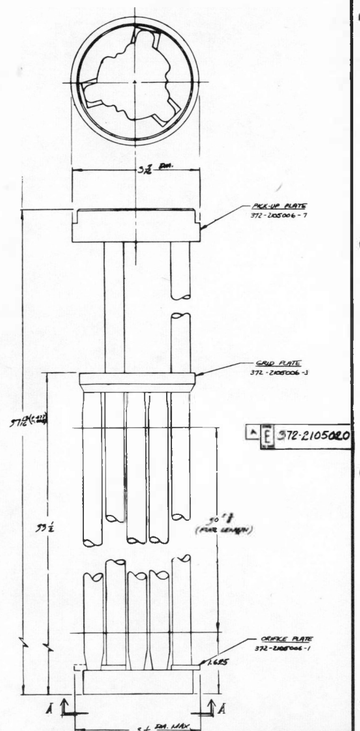
5 1/2 DIA.
PICK-UP PLATE 372-2105016 - 7
GRID PLATE 372-2105006 - 3
372-2105020
37 1/2
50 1/8 (FUEL LENGTH)
GUIDE PLATE 372-2105044 - 1
4 SPS
5 1/2 DIA. MAX.
372-2105080
VIEW A-A
AS BUILT
CENTER BUNDLE - 372-2105015